Expanding the understanding of peptidoglycan turnover in *Chlamydiae*: biosynthesis, degradation and recycling

Dissertation

zur

Erlangung des Doktorgrades (Dr. rer. nat.)

der

Mathematisch-Naturwissenschaftlichen Fakultät

der

Rheinischen Friedrich-Wilhelms-Universität Bonn

vorgelegt von

Jula Reuter

aus

Bad Neuenahr

Bonn, August 2022

Angefertigt mit Genehmigung der Mathematisch-Naturwissenschaftlichen Fakultät
der Rheinischen Friedrich-Wilhelms-Universität Bonn

1. Gutachterin: Prof. Dr. Tanja Schneider
2. Gutachterin: Priv.-Doz. Dr. Christiane Dahl

Tag der Promotion: 30.11.2022
Erscheinungsjahr: 2023

Table of contents

		p.
	Abbreviations	5
	Register of tables	7
	Register of figures	8
1.	**Introduction**	**11**
1.1.	The *Chlamydiae* phylum - *Chlamydia* and *Chlamydia*-like organisms	11
1.2.	Chlamydial intracellular lifestyle and developmental cycle	14
1.3.	Chlamydial cell envelope	17
1.4.	Chlamydial persistence	18
1.5.	Cell division and peptidoglycan turnover in *Chlamydia*	20
1.5.1.	Biosynthesis of peptidoglycan precursors in *Chlamydia*	22
1.5.2.	Assembly of the septal peptidoglycan ring in *Chlamydia*	24
1.5.3.	The chlamydial amidase AmiA	26
1.5.4.	NlpC/P60 domain-containing proteins	27
1.6.	Chlamydia as human pathogen	28
1.7.	Aim of the thesis	32
2.	**Materials and Methods**	**33**
2.1.	*In silico* methods and online tools	33
2.2.	Chemicals and Reagents	34
2.3.	Cultivation of bacterial and mammalian cells	34
2.3.1.	Media preparation and additives	34
2.3.1.a.	Media used for cultivation of bacteria	35
2.3.1.b.	Medium used for cultivation of mammalian cells	35
2.3.1.c.	Antibiotics, tested compounds and media additives	36
2.3.2	Used organisms	37
2.3.2.a.	*E. coli* strains used for plasmid propagation and subcloning	37
2.3.2.b.	*E. coli* strains used for recombinant protein production	38
2.3.2.c.	*E. coli* mutant strains used in complementation assays	38
2.3.2.d.	*Chlamydia* strains	39
2.3.2.e.	Mammalian cell line	39
2.3.3.	Bacteriological methods	39
2.3.3.a.	Preparation of chemically competent *E. coli*	39
2.3.3.b.	Heat shock transformation of chemically competent *E. coli*	40

		p.
2.3.4.	Mammalian cell culture and chlamydial propagation	40
2.3.4.a.	Solutions used in mammalian cell culture and microscopy	41
2.3.4.b.	Cultivation of Hep2 cells	41
2.3.4.c.	Subcultivation and splitting of Hep2 cells	41
2.3.4.d.	Permanent culture of Hep2 cells	41
2.3.4.e.	Propagation and strainkeeping of *C. trachomatis* D/UW-3/CX	42
2.3.4.f.	Permanent culture of *C. trachomatis* D/UW-3/CX	43
2.4.	Molecular methods	43
2.4.1.	Isolation of genomic DNA from bacteria	43
2.4.2.	Polymerase chain reaction (PCR)	43
2.4.3.	Agarose gel electrophorese for DNA separation	46
2.4.4.	Purification of DNA fragments and plasmids	46
2.4.5.	Photometric determination of DNA concentration	46
2.4.6.	Molecular cloning	47
2.4.6.a.	Restriction of DNA with endonucleases	47
2.4.6.b.	Ligation of an insert into a plasmid	47
2.4.6.c.	In-Fusion cloning	47
2.4.6.d.	PCR-based site directed mutagenesis	48
2.4.7.	Sequencing	48
2.4.8.	Expression vectors	48
2.5.	Biochemical methods	50
2.5.1.	Recombinant protein production and purification	50
2.5.1.a.	Protein purification of by His_6-tag affinity chromatography	51
2.5.1.b.	Protein purification by *Strep*-tactin affinity chromatography	52
2.5.2.	Quantification of recombinant protein with Bradford reagent	53
2.5.3.	Protein analysis by SDS-PAGE	54
2.5.4.	Preparation and Remazol staining of *E. coli* peptidoglycan sacculi	54
2.5.5.	*In vitro* assays using purified recombinant protein	55
2.5.5.a.	MraY *in vitro* activity assay	55
2.5.5.b.	Testing putative inhibitors of MraY *in vitro* activity	55
2.5.5.c.	Analysis of *in vitro* activity towards lipid II	56
2.5.5.d.	Remazol dye release assay	56
2.5.5.f.	Analysis of *in vitro* activity of YkfC	57
2.5.5.e.	Analysis of substrate specificity of YkfC	57

		p.
2.5.5.g.	Testing putative inhibitors of YkfC *in vitro* activity	58
2.5.6.	Thin layer chromatography (TLC)	58
2.5.6.a.	TLC for the detection of lipids	59
2.5.6.b.	TLC for the detection of peptides	59
2.5.7.	High performance liquid chromatography and mass spectrometry (HPLC-MS)	59
2.6.	Complementation assays using *E. coli* mutant strains	60
2.6.1.	Complementation of an DapD- and Mpl-deficient *E. coli* mutant	60
2.6.2.	Complementation of an MepS-deficient *E. coli* mutant	61
2.7.	Investigation of the antichlamydial effect of compounds in a cell culture based *C. trachomatis* D/UW-3/CX infection model	62
2.7.1	Preparation of Hep2 host cells for cell culture based experiments	62
2.7.2.	Alamar Blue cell viability assay	62
2.7.3.	Determination of a compound's minimal inhibitory concentration (MIC) against *Chlamydia* infection	63
2.7.3.a.	Determination of the MIC against a productive *Chlamydia* infection	63
2.7.3.b.	Determination of the MIC against a *Chlamydia* infection in a penicillin G-induced persistent state	64
2.7.4.	Evaluation of cell culture based experiments by fluorescence microscopy	64
3.	**Results**	**66**
3.1.	Analysis of novel compounds in a *Chlamydia* cell culture infection model	66
3.1.1.	Analysis of the antichlamydial effect of novel candidate compounds	66
3.1.2.	Analysis of cytotoxicity for inhibitors of bacterial peptidoglycan (PG) precursor biosynthesis	71
3.2.	Analysis of the antichlamydial effect of MraY inhibitors	73
3.2.1.	Muraymycin inhibits *C. pneumoniae* MraY activity *in vitro*	74
3.2.2.	Effect of muraymycins on a productive *Chlamydia* infection model	76
3.2.3.	Effect of muraymycin D2 on a progressed productive and a persistent *Chlamydia* infection model	79
3.3.	Novel aspects of AmiA activity	83
3.3.1.	Analysis of an *E. coli* AmiA mutant lacking the autoinhibitory domain	83
3.3.2.	*In silico c*omparison of the active sites of AmiA from *C. pneumoniae* and *C. trachomatis*	86
3.3.3.	*C. trachomatis* AmiA shows no DD-CPase activity on lipid II	87
3.4.	Analysis of chlamydial PG recycling	90
3.4.1.	*In silico* analysis of putative chlamydial YkfC homologs in *Bacillus*	90

		p.
3.4.2.	Recombinant *C. trachomatis* YkfC ($YkfC_{Ctr}$) shows catalytic activity on PG-derived tripeptide	97
3.4.3.	$YkfC_{Ctr}$ shows substrate specificity for PG-derived peptides	100
3.4.4.	$YkfC_{Ctr}$ shows activity on *B. subtilis* PG-derived peptides	104
3.4.5.	$YkfC_{Ctr}$ *in vitro* activity is inhibited by chloroacetone and E-64	105
3.4.6.	$YkfC_{Ctr}$ *in vitro* activity is not inhibited by α-X-chalcones	107
3.4.7.	*In silico* analysis of putative NlpC/P60 peptidases from *Chlamydia*-like organisms	108
3.4.8.	$YkfC_{Ctr}$, $NlpC/P60_{Ela}$ and $NlpC/P60_{Sne}$ act as tripeptide peptidases in *E. coli*	112
3.4.9.	Recombinant *B. subtilis* YkfC does not show *in vitro* activity on lipid II	117
4.	**Discussion**	**118**
5.	**Summary**	**149**
6.	**References**	**150**
	Danksagung	**180**

Abbreviations

Amino acids are abbreviated according to the IUPAC amino acid single letter or three letter code. Nucleotide abbreviations are in accordance to the IUPAC nucleotide code.

(*v*/*v*)	Volume/volume percent
(*w*/*v*)	Weight/ volume percent
A	Absorbance
AB	Aberrant body
ADP	Adenosine diphosphate
AHT	Anhydrotetracycline
ATP	Adenosine triphosphate
BLAST	Basic Local Alignment Search Tool
BSA	Bovine serum albumin
C_{55}-P	Undecaprenyl phosphate, Bactoprenol lipid carrier
CC	Candidate compound
CHAPS	3-[(3-Cholamidopropyl)-dimethylammonio]-1-propansulfonat
CHA	Chloroactone
Cpn	*Chlamydiae pneumoniae*
CPZ	Caprazamycin
Ctr	*Chlamydiae trachomatis*
DAPI	4′,6-Diamidin-2-phenylindol
DD-CPase	DD-Carboxypeptidase
DMEM	Dulbecco’s modified Eagles Medium
DMM	n-Dodecyl-β-D-maltoside
DMSO	Dimethylsulfoxide
DNA	Deoxyribonucleic acid
dNTPs	Deoxynucleotide triphosphate
DTT	Dithiothreitol
EB	Elementary body
Eco	*Escherichia coli*
EDTA	Ethylendiamintetraacetate
Ela	*Estrella lausannensis*
GlcNAc	N-acetylglucosamine
HBSS	Hank’s balanced salt solution
HPLC	High performance liquid chromatography
IC_{50}	Inhibitory concentration at which 50% of the target is not affected

IFN γ	Interferon gamma
IPTG	Isopropyl β-d-1-thiogalactopyranoside
LB	Lysogeny broth
Lipid I	Undecaprenyl-pyrophosphoryl-MurNAc-pentapeptide
Lipid II	Undecaprenyl-pyrophosphoryl-MurNAc-GlcNac-pentapeptide
LPS	Lipopolysaccharide
MS	Mass spectrometry
mDAP	meso-diaminopimelic acid
MIC	Minimal inhibitory concentration
MOMP	Major outer membrane protein
MRY	Muraymycine
MurNAc	N-acetylmuramic acid
NA	Nutrient (broth) agar
no.	number
OD_{600nm}	Optical light scattering at 600 nm
ORF	Open reading frame
p.	page
PAGE	Polyacrylamide gel electrophoresis
PBP	Penicillin binding protein
PenG	Penicillin G
PG	Peptidoglycan
pI	Post infection
RB	Reticular body
RBB	Remazol brilliant blue
RNA	Ribonucleic acid
SDS	Sodium dodecyl sulfate
SEDS	Shape, Elongation, Division and Sporulation
Sne	*Simkania negevensis*
STI	Sexual transmitted infection
TAE	Tris-acetate-EDTA buffer
TB	Terrific broth
Tris	Tris (hydroxymethyl) diamine
UDP	Uridine diphosphate
YT	Yeast extract tryptone broth

Register of tables

No.		p.
2.1	Online tools and their applications in this work.	33-34
2.2	Media composition for cultivation of *E. coli.*	35
2.3	Composition of DMEM used for cultivation of mammalian cells.	36
2.4.	Antibiotics, tested compounds and media additives.	36
2.5	Primers used in this work.	44-46
2.6	Expression vectors used in this work.	48-50
2.7	Conditions determined for purification of recombinant proteins.	50-51

Register of figures

No.		p
1.1.	The *Chlamydia* developmental cycle.	15
1.2.	Model of PG biosynthesis and degeneration at the cell division site in *Chlamydia*.	23
1.3	Model of the secondary structure of the NlpC/P60 protein superfamily domain.	28
3.1.	Alamar Blue cell viability assay for the treatment of mammalian Hep2 cells with novel antimicrobial candidate compounds.	67
3.2.	Fluorescence microscopic analysis of the effect of candidate compounds CC3, CC4, CC6 and CC7 on a productive *Chlamydia* infection model and on Hep2 host cells.	69
3.3.	Alamar Blue cell viability assay for treatment of mammalian Hep2 cells with inhibitors of bacterial MraY.	72
3.4.	Alamar Blue cell viability assay for treatment of mammalian Hep2 cells with inhibitors of bacterial MurJ.	73
3.5.	Effect of muraymycin D2 and its derivates on the enzymatic activity of recombinant $MraY_{Cpn}$.	75
3.6.	Fluorescence microscopic analysis of the effect of muraymycins on a productive *Chlamydia* infections model.	77
3.7.	Fluorescence microscopic analysis of the effect of muraymycin D2 on a progressed productive and a persistent *Chlamydia* infection model.	80
3.8.	3D *in silico* models and growth kinetics of $AmiA_{Eco}$, $AmiA_{Eco}$_ΔA148-S191 and $AmiA_{Cpn}$.	84
3.9.	*In vitro* activity of the *E. coli* AmiA mutant $AmiA_{Eco}$_ΔA148-S191 on PG sacculi.	85
3.10.	Primary sequence alignment and comparison of 3D *in silico* models of $AmiA_{Cpn}$ and $AmiA_{Ctr}$.	86
3.11.	*In vitro* activity of $AmiA_{Ctr}$.	88
3.12.	Comparative analysis of the genomic context of the gene encoding the putative PG recycling peptidase YkfC in *Chlamydia*.	91
3.13.	Primary sequence alignment of $YkfC_{Bce}$, $YkfC_{Ctr}$, and $YkfC_{Cpn}$.	93
3.14.	Comparison of 3D *in silico* overall structure models of $YkfC_{Bce}$, $YkfC_{Ctr}$, and $YkfC_{Cpn}$.	95
3.15.	Comparison of 3D *in silico* models of the active site models from $YkfC_{Bce}$, $YkfC_{Ctr}$ and $YkfC_{Cpn}$.	96
3.16.	Purification and *in vitro* activity of recombinant $YkfC_{Ctr}$.	97
3.17.	Analysis of the *in vitro* activity of recombinant $YkfC_{Ctr}$.	98
3.18.	MS analysis of $YkfC_{Ctr}$ *in vitro* activity on peptides derived from *E. coli* PG by $CwlC_{Bsu}$ digestion.	101

3.19.	Substrate specificity of $YkfC_{Ctr}$.	102
3.20.	MS analysis of $YkfC_{Ctr}$ *in vitro* activity on peptides derived from *B. subtilis* PG by $CwlC_{Bsu}$ digestion.	104
3.21.	Effect of cysteine peptidase inhibitors on the enzymatic activity of $YkfC_{Ctr}$.	106
3.22.	Effect of different α-X-chalcone derivates on the enzymatic activity of $YkfC_{Ctr}$.	107
3.23.	Primary sequence alignment of $YkfC_{Bce}$ and $NlpC/P60_{Ela}$.	108
3.24.	Comparison of 3D *in silico* models of $YkfC_{Bce}$ and $NlpC/P60_{Ela}$.	109
3.25.	Primary sequence alignment of $YkfC_{Bce}$ and $NlpC/P60_{Sne.}$	110
3.26.	Comparison of 3D *in silico* models of $NlpC\_A2_{Tva}$ and $NlpC/P60_{Sne}$.	111
3.27.	*In vivo* complementation of the *E. coli dapD*$^-$ Δ*mpl* mutant using different chlamydial NlpC/P60 proteins.	113
3.28.	*In vivo* complementation of the *E. coli* Δ*mepS* mutants using different chlamydial NlpC/P60 proteins.	115
3.29.	*In vitro* activity of $YkfC_{Bsu}$ on PG precursor lipid II (mDAP type).	117
4.1.	Comparison of 3D *in silico* models of $AmiA_{Eco}$, $AmiA_{Cpn}$ and $AmiA_{Ctr}$.	130
4.2.	Primary sequence alignment of the NlpC/P60 domain found in proteins of *Bacillus*, *Chlamydia* and *Chlamydia*-like organisms.	141
4.3.	Proposed model of the PG turnover process at the division site in *Chlamydia.*	143

1. Introduction

In Europe, chlamydiae occur primarily as causative agents of sexually transmitted infections (STIs). *Chlamydia trachomatis* infection is commonly regarded as the most frequent cause of female infertility in industrialized countries (Akande *et al*., 2010) and is considered an underdiagnosed, widely spread STI in Germany (Stock *et al*., 2001; Griesinger *et al*., 2007). High prevalence of urogenital chlamydial infection is mainly due to the fact that this bacterium remains undetected - and this on several levels. First of all, public awareness of STIs beyond HIV is not very pronounced in Germany, as a recent nationwide health and sexuality survey shows that while 71.1 % of the participants named HIV/AIDS when asked which STIs they were aware of, chlamydial infection was only mentioned by 15.6 % of the female and 7.8 % of the male participants (Matthiesen *et al.*, 2021). Secondly, the majority of urogenital chlamydial infections initially remains asymptomatic, and thus go undetected even in younger age groups, who were found to be generally better informed about STIs (Skaletz-Rorowski *et al*., 2021; Matthiesen *et al*., 2021). Last but not least, chlamydiae are specialized in remaining as inconspicuous as possible on a cellular level. *C. trachomatis*, as all known members of the *Chlamydiae* phylum, is highly adapted to an obligate intracellular lifestyle. Chlamydiae are equipped to manipulate their host cells in order to take full advantage of this habitat while at the same time being able to hide from their host cell's immune recognition. The following introductory chapters provide the background for this work's research, covering chlamydial phylogeny (1.1.), lifestyle (1.2.), cell envelope (1.3.) and persistence (1.4.), as well as the interplay of cell division and peptidoglycan turnover in *Chlamydia* (1.5.), and the organism's role as a human pathogen (1.6.).

1.1. The *Chlamydiae* phylum - *Chlamydia* and *Chlamydia*-like organisms

The closest free-living bacterial relatives of *Chlamydiae* known to date are members of the phyla *Verrucomicrobia*, *Lentisphaerae*, and *Kiritimatiellaeota* and together with the *Planctomycetes*, these groups form the PVC superphylum (Wagner & Horn, 2006; Rivas-Marín & Devos, 2018). It is estimated that the last common ancestor of all chlamydiae had adopted an intracellular lifestyle 1-2 billion years ago (Kamneva *et al*., 2012; Subtil *et al*., 2014) and since then phylum-level diversity has grown. Besides the *Chlamydiaceae* family, which includes human pathogen *C. trachomatis,*

the first chlamydial species described by researchers (von Prowazek & Halberstadter, 1907), the *Chlamydiae* phylum includes lineages that are found within protists, such as amoebae, and in diverse animal hosts (Horn, 2008; Taylor-Brown *et al.*, 2015). Molecular diversity surveys suggest the existence of hundreds of chlamydial families (Lagkouvardos, *et al*. 2014; Collingro *et al*., 2020) of which only six are currently available as laboratory cultures in suitable host cells (Taylor-Brown *et al*., 2018; Collingro *et al*., 2020). In order to distinguish between 'classical' human pathogenic *Chlamydia* of the *Chlamydiaceae* family and more recently identified environmental chlamydial lineages, the latter are referred to collectively as *Chlamydia*-like organisms.

The *Chlamydiaceae* family includes several well-known pathogens which are able to infect a diverse array of vertebrates (Bachmann *et al*., 2014; Elwell *et al*., 2016). Among these organisms are *C. trachomatis* and *Chlamydia pneumoniae*, the major chlamydial species that infect humans and can cause a broad spectrum of diseases with varying severity (see chapter 1.6. '*Chlamydia* as a human pathogen'). While *C. trachomatis* exclusively infects humans, *C. pneumoniae* has a diverse host range and has been found in horses, reptiles, amphibians, and also marsupials (Bodetti *et al*., 2002; Hotzel *et al.*, 2001; Wardrop *et al*., 1999). The finding of animal genotypes of *C. pneumoniae* in humans suggests the possibility of interspecies transmission (Cochrane *et al*., 2005), but direct evidence for zoonosis is currently missing (Cheong *et al.*, 2019). Another human pathogenic member of the *Chlamydiaceae* is *Chlamydia psittaci* which primarily infects birds, but may also cause pneumonia in humans after zoonotic transmission (Knittler & Sachse, 2015).

Chlamydia-like organisms are not a phylogenetically coherent group; rather, the term refers to a variety of chlamydiae occurring in diverse environments, as members of various microbiomes, and in a wide host range (Collingro *et al*., 2020; Köstelbacher *et al*., 2021). Recently, chlamydial lineages that dominate microbial communities in deep marine sediments were described, which may even indicate a possible environmental impact of these species (Dharamshi *et al.*, 2020). Like *Chlamydia*, all known members of *Chlamydia*-like organisms are obligat intracellular and depend on eukaryotic host cells. While the natural host/s of some species remains unidentified (Taylor-Brown *et al*., 2018), some *Chlamydia*-like organisms are reported to play a role as emerging animal and/or human pathogens (Taylor-Brown *et al.*, 2015).

Members of the *Simkaniaceae* and *Parachlamydiaceae* families are capable of growing in a range of cells from amoebae to human pneumocytes (Casson *et al*., 2006; Vouga, *et al*., 2017a), making them putative opportunistic human pathogens with reported cases of respiratory tract infections (Friedman *et al*., 2006; Lamoth *et al*., 2011). *Waddlia chondrophila* of the *Waddliaceae* family, which was first described in samples of bovine abortion tissues, has also been reported in association with miscarriage and adverse pregnancy outcomes in humans (Baud *et al*., 2007; 2014).

The key characteristic of all *Chlamydiales* is an obligate intracellular lifestyle with a biphasic developmental cycle, which is described in chapter 1.2. As well-adapted parasitic and thus minimal bacteria, chlamydiae are able to acquire resources from their host cell. As a result, the chlamydial genome decreased in size compared to free-living bacteria, economizing on costly metabolic pathways which have become non-essential in this lifestyle. While the genome of Gram-negative model organism *Escherichia coli* K12 (substrain MG1655) has a size of 4.6 mega base pairs (Mb) (Riley *et al*., 2006), the genomes of human pathogenic *C. trachomatis* (strain D/UW-3/CX) and *C. pneumoniae* (strain CWL029) are reduced to 1.0 Mb and 1.2 Mb, respectively (Stephens *et al*., 1998; Kalman *et al.*, 1999).
Due to their small genome size, many bacterial metabolic pathways are incomplete or do not exist at all in *Chlamydiaceae* and consistently they became auxotrophic for most amino acids, cofactors and for purine and pyrimidine nucleotides and dependent on scavenging metabolic intermediates from their eukaryotic host cells (Omsland *et al*., 2014; Mehlitz *et al*., 2017). The extent to which *Chlamydiaceae* rely on their host for energy production has not yet been fully clarified, as shown here by the example of glycolysis. Sequencing of the *C. trachomatis* genome revealed an almost complete set of glycolytic enzymes, lacking only hexokinase, the first enzyme of the pathway responsible for converting glucose to glucose-6-phosphate (Stephens *et al*., 1998). This lack is compensated for by the ability of *Chlamydia* to take up glucose-6-phosphate directly from the host cell (Schwöppe *et al*., 2002; Mehlitz *et al*., 2017). Despite these abilities, it seems that *C. trachomatis* is not fully independent in terms of energy production, beyond the uptake of glucose-6-phosphate, and relies on scavenging host cell-derived ATP and NAD^+ (Mehlitz *et al*., 2017). Additionally, a recent study found that glycolytic enzymes of the eukaryotic host cell are enriched in

the vicinity of intracellular *Chlamydia* and may also play a role in enabling chlamydial growth (Ende & Derré, 2020).

Compared with *Chlamydiaceae*, the genomes of *Chlamydia*-like organisms tend to be less reduced, although the genome sizes also differ within representatives of this group. The genome size of *W. chondrophila* (strain WSU86-1044) is 2.1 Mb (Bertelli *et al*., 2010), that of *Simkania negevensis* (strain Z) is 2.5 MB, while that of *Parachlamydiaceae acanthamoebae* (strain UV-7) amounts to 3.1 Mb (Collingro *et al*., 2011). *Chlamydiaceae* and *Chlamydia*-like organisms share a common core genome, which was originally thought to consist of 560 genes (Collingro *et al*., 2011), however, the characterization of previously unknown chlamydial lineages reduced this number to 340 genes (Collingro *et al*., 2020). Chlamydial core genes with a known function are mainly housekeeping genes and genes coding for components involved in the highly conserved intracellular lifecycle, such as a T3SS secretion system for the release of effector proteins that manipulate the host cell, homologs to ATP/ADP translocases, a glucose-6-phosphate transporter, and a master transcription factor involved in governing the chlamydial developmental cycle (Collingro *et al*., 2011; 2020). While the basic chlamydial biology is conserved within the *Chlamydiae* phylum, the larger genetic repertoire of *Chlamydia*-like organisms indicates that they, while still being fully dependent on an eukaryotic host cell, have retained a higher metabolic potential. Hence, these organisms are able to adapt to less homeostatic growth niches and thus to a wider host range compared to *Chlamydiaceae* (Taylor-Brown *et al*., 2015; Collingro *et al*., 2020).

1.2. Chlamydial intracellular lifestyle and developmental cycle

Chlamydiae go through a complex developmental cycle that is unique and astonishing for bacteria with such a reduced genome size. In its course, chlamydial cells alternate between two cell forms, both of which have a round morphology but differ in their metabolism: extracellular elementary bodies (EBs) and intracellular reticular bodies (RBs) (Moulder, 1991; Abdelrahman & Belland, 2005).

In their EB form, chlamydiae can survive outside their eukaryotic host cells, as EBs are resistant to osmotic and chemical stress due to a rigid cell surface consisting of cross-linked outer membrane proteins (Newhall, 1987; Hatch, 1996). EBs show low metabolic activity and cannot replicate, but are infectious due to their ability to attach to and invade host cells (Abdelrahman & Belland, 2005). They are taken up by endocytosis and are therefore located in a vacuole enclosed by the host cell's

membrane which is named chlamydial inclusion. As soon as contact with the host is established, chlamydiae use a type III secretion system (T3SS), that is part of the chlamydial core genome (Collingro *et al*., 2011), to deliver effector proteins into the inclusion membrane and the host cytoplasm (Dai & Li, 2014). One of the tasks performed by these effector proteins is to remodel the inclusion's surface so that it escapes the host cell's lysogenic pathway and is instead transported to the vicinity of nucleus by the host cell's microtubule trafficking system (Bastidas *et al*., 2013; Grieshaber *et al*., 2006). Further effects are the inhibition of apoptosis triggering processes and the redirecting of the intracellular vesicle transport (Elwell *et al*., 2016). The conditions inside the chlamydial inclusion are largely unknown, although it has been suggested for *C. trachomatis* that parameters such as pH and sodium,

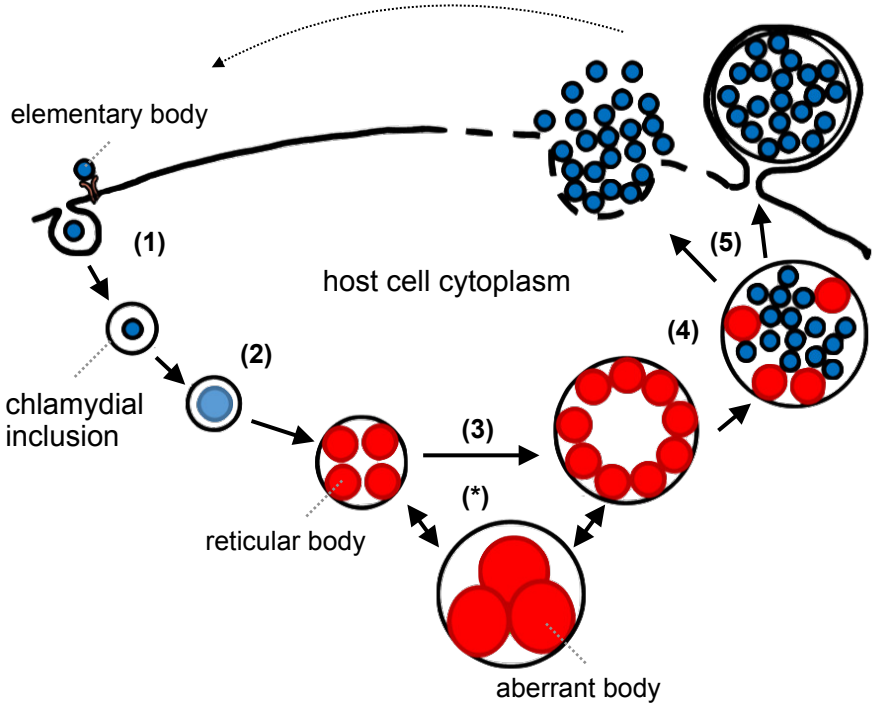

Fig. 1.1. The *Chlamydia* developmental cycle. At the beginning of the early stage of chlamydial infection, **(1)** a chlamydial elementary body (EB) enters the eukaryotic host cell by endocytosis. During all following intracellular steps chlamydiae are located within the inclusion. **(2)** The EB differentiates to a reticular body (RB) and chlamydial replication is initiated. **(3)** RBs continue to replicate and the inclusion grows. In the late infection stage, **(4)** RBs re-differentiate to EBs. **(5)** Chlamydiae leave the host cell either by lysis or extrusion and released EBs might infect novel host cells. **(*)** Under stressing conditions, the development can become temporally interrupted and chlamydial persistence occurs. In this state chlamydial cells do not replicate and might show as enlarged aberrant bodies, but can revert to RBs once the stress factor is removed. (Figure modified from Brockett & Liechti, 2021).

potassium, and calcium concentration appear to correspond to the host cell's cytosol (Grieshaber *et al.*, 2002). In order to allow expansion of the inclusion required for bacterial growth, chlamydiae are able to obtain lipids from host membrane systems (Capmany & Damiani, 2010).

The developmental cycle of human pathogen *C. trachomatis*, as shown in figure 1.1, has been extensively studied and stands exemplary for other members of the *Chlamydiaceae*. The exact duration of one cycle of chlamydial development, which is characterized by temporally distinct patterns of gene expression correlating with the chlamydial growth stages (Belland *et al*., 2003), differs depending on the chlamydial species and the type of host cell. Intracellular steps of chlamydial development take place exclusively within the inclusion and thus, as described above, in an environment in which chlamydiae can draw on resources from the host cell and are protected from osmotic stress. *C. trachomatis* infection starts with the attachment of an EB to the surface of the eukaryotic host cell, followed by the release of pre-packed chlamydial effector proteins, which ensure that the inclusion is established as an optimal niche for the pathogen (Elwell *et al*., 2016). About six to eight hours after internalization of usually a single EB into the host cell, its transition into a highly metabolically active RB occurs, which is then able to replicate (Moulder, 1991; Abdelrahman & Belland, 2005; Elwell *et al*., 2016). EBs of *C. trachomatis* are shown to undergo a polarized cell division process with similarities to the budding procedure of members of the *Planctomycetes* (Abdelrahman *et al*., 2016). The chlamydial replication process is unique, as their genomes lack tubulin-like homolog FtsZ, the central organizer of the bacterial divisome (Weiss, 2004). Instead, actin-like homolog MreB is thought to coordinate the chlamydial division complex, a machinery which is inextricably linked with components of the chlamydial peptidoglycan biosynthesis pathway (Gaballah *et al.*, 2011; Ouellette *et al*., 2012; 2020) (see chapter 1.5. 'Cell division peptidoglycan turnover in *Chlamydia'*).

For *C. trachomatis*, the peak of RB replication is reached at 18 - 24 hours post infection (hpI) (Nicholson *et al*., 2003) and due to the increase in chlamydial biomass the inclusion grows until it occupies a significant portion of the host cell cytoplasm. Subsequently, at 24 to 72 hpI, the majority of RBs starts to asynchronously re-differentiate back into the EB form (Moulder, 1991; Nicholson *et al*., 2003). Finally, chlamydiae are released into the extracellular space either by lysis of the host cell or,

alternatively, by releasing the inclusions in a vesicle called extrusion from the intact host cell (Moulder, 1991; Hybiske & Stephens, 2007). While remaining RBs cannot survive the extracellular osmotic condition, EBs are adapted to it and might start the next cycle of infection in new host cells (Moulder, 1991; Hybiske & Stephens, 2007).

1.3. Chlamydial cell envelope

Chlamydiae are Gram-negative bacteria, however, due to their intracellular lifestyle the composition of their cell envelope differs from free-living bacteria. In the latter, a rigid cell wall is needed to maintain the cell shape, to provide stability, and to protect the cell from osmotic lysis. To this end, a peptidoglycan (PG) sacculus encloses the cell, a tightly woven meshwork of linear glycan chains cross-linked by peptide bridges (Höltje, 1998; Scheffers & Pinho, 2005). In Gram-negative organisms, an outer membrane forms the cell's surface, so the PG layer is located in the periplasmic space between outer and cytoplasmic membrane (Gupta, 2011).

In chlamydiae, osmotic stability and rigidity of extracellular EBs is maintained by a high amount of inter- and intramolecular cystine bonds between proteins of the outer membrane (Newhall, 1987; Hatch, 1996). After entering the host cell, inside the inclusion, chlamydiae have to restore membrane fluidity to allow replication. To this end, the degree of protein cross-linking in the outer membrane is reduced during differentiation from EB to RB (Newhall, 1987). One of the cysteine-rich proteins is OmpA, which makes up 61% of all outer membrane proteins in *C. trachomatis* EBs (Caldwell *et al*., 1981) and is also known as major outer membrane protein (MOMP). While the genome of *Chlamydia* encode a single MOMP, the outer membranes of *Simkania* and *Waddlia* contain a large number of different MOMP-like proteins in high abundance (Aistleitner *et al*., 2015). In addition to membrane proteins, the chlamydial outer membrane is formed by genus-specific lipopolysaccharide (LPS). Bacterial LPS typically consists of a hydrophobic membrane anchor, named lipid A, a non-repeating core oligosaccharide, and a distal polysaccharide (Raetz *et al*., 2007). *Chlamydia* LPS is truncated in comparison, as it only consists of a trisaccharide core linked to lipid A (Rund *et al*., 1999; Kosma, 1999). Due to alterations in its lipid A structure, endotoxin activity of chlamydial LPS is reduced compared to LPS common to other Gram-negative species (Heine *et al*., 2007; Yang *et al*., 2019).

For intracellular chlamydiae which proliferate inside an inclusion within a host cell, an isotonic environment where they are protected from osmotic stress, maintaining a stabilizing PG sacculus becomes obsolete. Indeed, a stepwise rationalization of the energy cost-intensive PG synthesis pathway during adaptation to a small host range can be observed in these bacteria (Klöckner *et al*., 2018). *Protochlamydia*, but not *Simkania*, maintains a modified PG sacculus (Pilhofer *et al*. 2013), and there is evidence for a cell wall in *Waddlia* (Jacquier *et al*., 2015a). In *Chlamydia*, however, PG is reduced to a narrow and transient ring that occurs at the septum of dividing RBs (Liechti *et al*., 2014; 2016). In the case of *Waddlia*, localization of PG-binding proteins also indicates the existence of a septal PG ring (Frandi *et al*., 2014; Jacquier *et al*., 2015b), whereas the structure of septal PG in *Protochlamydia* is unknown. Since spatially and temporally limited occurrence of PG in *Chlamydia* goes along with a reduced generation of immunostimulatory PG-derived fragments, this adaption to their intracellular lifestyle might confer a pathogenic advantage. Nonetheless, the fact that *Chlamydia* retains complex pathways for PG synthesis and degradation despite its reduced genome size suggests that this turnover process is essential for chlamydial development.

1.4. Chlamydial persistence

In addition to the two states described above in the section on the biphasic lifecycle (chapter 1.2. ‘Chlamydial intracellular lifestyle and developmental cycle’), chlamydiae may also outlast stressful times by going into distinct states of persistence. The states of persistence are physiologically distinct from EBs and RBs and can be assigned to the different kind of stressors to which chlamydiae react by temporarily interrupting their development but remaining viable. Once the stressing conditions cease, chlamydiae can rapidly resume their normal replication and generation of infectious particles (Tamura & Manire, 1968; Panzetta *et al*., 2018). The phenomenon was first described in a study analyzing the response of *C. psittaci* to penicillin, which found the chlamydial cells enlarged in the antibiotic’s presence, while normal morphology was restored after its removal (Matsumoto & Manire, 1970).

Persisting states of chlamydiae with varying phenotypes as a temporary response to different stressors have been described in cell culture models (Hogan *et al*., 2004), and there is evidence for their occurrence in *in vivo Chlamydia* infections of humans

and pigs (Borel *et al.*, 2008; Pospischil e*t al.*, 2009). Frequently, but not necessarily, these states are accompanied by the appearance of enlarged chlamydial cell forms, named aberrant bodies (ABs), which can transit back into EBs when favorable conditions are restored (fig. 1.*) (Panzetta *et al*., 2018). However, AB formation as a stress response is not limited to *Chlamydiaceae*, as aberrant phenotypes have been observed under different experimental conditions *in vitro* for *Chlamydia*-like organisms, such as *W. chondrophila, S. negevensis,* and *Estrella lausannensis* (Scherler *et al*., 2020; Vouga *et al*., 2017b; de Barsy *et al*., 2014).
Transition of an chlamydial infection into a persisting state can be induced by a variety of non-bactericidal stimuli, including presence of the cytokine interferon gamma (IFN-γ) that induces tryptophan starvation, deprivation of nutrients (i.e., iron, amino acids, glucose), co-infection with viruses, heat shock and antibiotic treatment (Hogan *et al*., 2004; Panzetta *et al*., 2018). Depending on the kind of stress factor, different transcriptional responses are triggered in chlamydiae, indicating that the resulting chlamydial persistence phenotypes vary (Panzetta *et al*., 2018).

In terms of treatment of chlamydial infections, the observation that persistence can occur as a response to cell wall targeting antibiotics has been of particular importance. Due to residence within an osmotically-stable niche, an environment that allows *Chlamydia* to lack a stabilizing PG cell wall (Liechti *et al*., 2014; 2016), chlamydiae are protected from bactericidal effects of PG-targeting compounds that occur in free-living bacteria. However, various studies have shown that septal PG synthesis must run smoothly in order to enable chlamydial cell division, as the mechanisms of both processes appear to be inextricably linked (Ouellette *et al*., 2012; 2020; Jacquier *et al*., 2014; 2015b; Cox *et al*., 2020; Liechti, 2021). Hence, treatment of chlamydiae with antibiotics that interfere with PG assembly induces a persisting state in which cell replication is halted (Klöckner *et al*., 2018). *Chlamydia* is susceptible to β-lactam antibiotics such as penicillin, which bind to the transpeptidase domain of bacterial penicillin binding proteins (PBPs). PBPs catalyze the final step of PG assembly, the polymerization of its periplasmic meshwork. *Chlamydia* expresses two homologs of high-molecular-weight PBPs (PBP2, PBP3) (Barbour *et al*., 1982), whose roles in the chlamydial division process will be the subject of the next chapter (1.5. ‘Cell division and peptidoglycan turnover in *Chlamydia*’). When *Chlamydia* is

exposed to the β-lactam antibiotic in cell culture, RBs turn into enlarged ABs, as they continue to grow and replicate chromosomal DNA while halting cell division (Matsumoto & Manire, 1970; Lambden *et al*., 2006). This condition occurs as long as the drug is present, after its removal a recovery period is initiated. In *C. trachomatis*, it has been observed that penicillin-induced ABs asynchronously converted back to RBs during this phase by a budding-resembling process (Matsumoto & Manire, 1970; Skilton *et al*., 2009). Consistent with results obtained in cell culture models, transition into a viable non-infectious state with occurrence of an AB form as a response to treatment with β-lactam amoxicillin was observed for genital *Chlamydia muridarum* infection in mice (Phillips-Campbell *et al*., 2014). Taken together, their ability to enter into an inert state as a response to treatment with PG synthesis-targeting antibiotics allows chlamydiae to avoid effects which these compounds would otherwise have on their developmental process. Thus, classical cell wall targeting antibiotics, like β-lactams, are not suitable for treatment of *Chlamydia* infection. Furthermore, even antibiotics that do not induce a persistence state themselves might be impaired in their effectivity by the phenomenon. In order to clear infection, some compounds depend on their target to be metabolically active and therefore may become ineffective when they find the chlamydiae in a state of persistence.

In this work, muraymycin, a substance which affects upstream steps in bacterial PG precursor synthesis (Tanino *et al*., 2011), was tested for its effect on a productive *C. trachomatis* infection in a cell culture model to see if it would halt chlamydial development similar to antibiotics targeting periplasmic PG assembly. In addition, to investigate a possible effect on *Chlamydia* in a persisting state, the compound was tested in an *in vitro* penicillin G-induced persistence model (Klöckner 2016; Brunke 2018).

1.5. Cell division and peptidoglycan turnover in *Chlamydia*

Among the genes abandoned by *Chlamydia* is *ftsZ* coding for the central organizer of the bacterial division site (Bi & Lutkenhaus, 1991). Instead of multiplying by a binary fission process coordinated by FtsZ, *Chlamydia* appear to divide by an MreB-dependent polarized budding mechanism (Abdelrahman *et al*., 2016; Ouellette *et al*., 2020). In rod-shaped bacteria like *E. coli*, actin-like homolog MreB regulates assembly of the PG biosynthesis machinery at sites of cell wall growth (Doi *et al.*,

1988). However, in cell-wall less and round *Chlamydia* cells, MreB is thought to act as the central coordinator of cell division along with the actin-binding protein RodZ (Ouellette *et al*., 2012; 2020; Kemege *et al*., 2015). It is known that RodZ acts as the transmembrane anchor for cytoplasmic MreB filaments in *E. coli* (Morgenstein *et al*., 2015) and the chlamydial RodZ homolog was shown to interact with septal MreB in *C. trachomatis* (Kemege *et al*., 2015). Two recent studies strongly support the hypothesis that MreB functionally replaces the central division organizer FtsZ in *Chlamydia* (Gaballah *et al*., 2011; Ouellette *et al*., 2012). In the first one, MreB was observed to form a ring at the septum of polarized dividing *C. trachomatis* cells that resembled the FtsZ ring at the septum of *E. coli* cells dividing by binary fission (Lee *at al*., 2020). The second study found that co-expression of MreB and RodZ of *C. trachomatis* could restore division in an *E. coli* mutant in which *mreB* was deleted and FtsZ activity was suppressed (Ranjit *et al*., 2020).

Polarized division in *Chlamydia* is hypothesized to go as follows: First the RB enlarges and its outer membrane becomes polarized with MOMP and LPS being present at opposite cell poles. Subsequently, the MOMP-enriched pole expanses asymmetrically, leading to formation of a nascent budding daughter cell, and finally mother and daughter cell separate (Abdelrahman *et al*., 2016). As mentioned above, the cell division process is closely interlinked with the occurrence of a narrow PG band at the septum of *Chlamydia* (Liechti *et al*., 2014; 2016; Liechti, 2021) (chapter 1.3. 'Chlamydial cell envelope'). Although the precise mechanisms by which this septal PG ring participates in the chlamydial cell division have yet to be determined, it appears to play a role in the process. Strong evidence for this association comes from the observation that treatment with inhibitors of PG synthesis stops cell division in *Chlamydia* (Barbour *et al*., 1982; Jacquier *et al*., 2015b; Klöckner *et al.*, 2018; Cox *et al*., 2020; Liechti, 2021) (chapter 1.4. 'Chlamydial persistence'). In order for the PG ring to conform its shape to the dividing septum during daughter cell budding and septation, both PG synthesis and degradation must occur in a coordinated manner. In accordance with its role as a chlamydial division organizer, MreB is likely to orchestrate the septal PG assembly (Liechti *et al*., 2016; Liechti, 2021). MreB of *C. pneumoniae* was shown to interact with enzymes of the lipid II synthesis process (MurF, MurG and MraY) *in vitro*, suggesting that it is able to tether cytoplasmic PG precursor synthesis to the division site (Gaballah *et al*., 2011).

While synthesis of PG precursor molecules (section 1.5.1) and assembly of the septal PG ring (section 1.5.2) are relatively well characterized in *Chlamydia*, the process of chlamydial PG degradation it is not fully understood. Even less is known about what happens to its breakdown products, which have the potential to become a risk for *Chlamydia*, since their release can trigger the host cell's immune response and thus the bacterium's eradication by the immune system. In order to gain further insight into chlamydial PG degradation and the fate of PG-derived peptides, two enzymes were closely examined in this work: AmiA, a PG hydrolyzing amidase which is functionally characterized in *Chlamydia* and *Waddlia* (Klöckner *et al*., 2014; Frandi *et al*., 2014) (section 1.5.3.) and a previously uncharacterized *C. trachomatis* protein, which might play a role in chlamydial PG turnover due to a conserved NlpC/P60 domain (section 1.5.4).

1.5.1. Biosynthesis of peptidoglycan precursors in *Chlamydia*

Bacterial PG is a biopolymer made up by a tight network of linear glycan chains cross-linked by peptide bridges. Its backbone consists of β-1,4-linked disaccharides of N-acetylglucosamine (GlcNAc) and N-acetylmuramic acid (MurNAc), linked by a β-1,4-bond and harboring a pentapeptide side chain on the lactoyl group of the MurNAc unit (Höltje 1998; Schleifer & Kandler, 1972). The pentapeptide side chain contains L- and D-amino acids and one dibasic acid which allows peptide cross-linking to fortify the network. In Gram-negative bacteria, this dibasic moiety is typically meso-diaminopimelate (mDAP), whereas in Gram-positive bacteria L-Lys usually takes this role (Schleifer & Kandler, 1972; Vollmer *et al*., 2008a).

In bacteria, PG biosynthesis begins in the cytoplasm with the formation of the soluble precursor UDP-MurNAc-pentapeptide, catalyzed by the enzymes Mur A-F which, with the exception of MurB and MurD, have been shown to be functionally conserved in *Chlamydia* (McCoy *et al*., 2003; Hesse *et al*., 2003; McCoy & Maurelli 2005; Patin *et al*., 2009; 2012) (fig. 1.2.a). In the first step, transferase MurA adds enolpyruvate to N-acetylglucosamine (GlcNAc) which is reduced to N-acetylmuramic acid (MurNAc) by MurB (McCoy *et al*., 2003; van Heijenoort, 2001). Subsequently, five amino acids are added to the sugar unit to generate the peptide side chain. The pentapeptide sequence most common in known PG structures of Gram-negative bacteria is L-Ala-γ-D-Glu-mDAP-D-Ala-D-Ala (Schleifer & Kandler, 1972; Vollmer *et al*., 2008a).

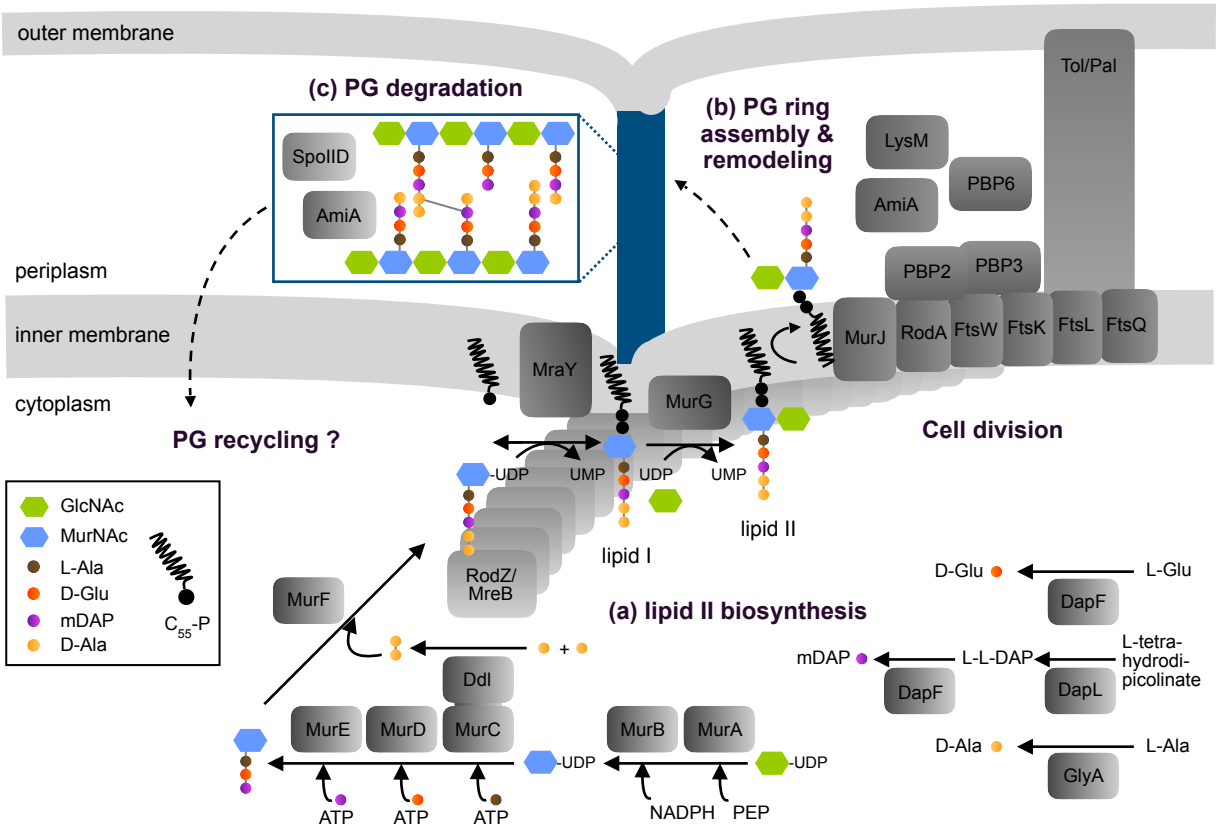

Fig. 1.2. Model of PG biosynthesis and degeneration at the cell division site in *Chlamydia*. While a cell wall is missing in *Chlamydia*, a PG ring is synthesized at the septum of dividing cells (Liechti *et al*., 2014). In the absence of the division organizer FtsZ, PG synthesis and cell division are orchestrated by the actin-like protein MreB in combination with RodZ (Ranjit *et al*., 2020). **(a)** PG synthesis in *Chlamydia* starts in the cytoplasm with the formation of the PG building block lipid II (reviewed in Klöckner *et al*., 2018; Ouellette *et al*., 2020): First, UDP-MurNAc-pentapeptide is assembled by enzymes Mur A-F, which, with the exception of MurB and MurD, have been shown to be functionally conserved. The peptide stem consists of L-Ala, D-Glu, mDAP and D-Ala. The enantiomers D-Glu and D-Ala are thought to be generated by racemase activity of GlyA and DapF, while mDAP is synthesized via an aminotransferase pathway that involves bifunctional DapF in its final step. Newly synthesized UDP-MurNAc-pentapeptide is bound to the membrane carrier C_{55}-P by MraY to generate lipid I, which is transformed to lipid II by addition of GlcNAC by MurG. Finally, lipid II is translocated across the inner membrane, probably by the flippase MurJ. **(b)** In the periplasm, lipid II is incorporated into the PG meshwork in a process involving components of the divisiome. The cell division proteins FtsI (PBP3), FtsK, FtsL, FtsQ, and FtsW, AmiA, and the Tol-Pal system required to control the outer membrane division in free-living bacteria are conserved in *Chlamydia* (reviewed in Ouellette *et al*., 2020). While PG assembly has not yet been fully elucidated, the enzyme pairs RodA-PBP2 and FtsW-PBP3 may act as transpeptidase-glycosyltransferase complexes to assemble the PG ring (indicated in blue) (Liechti, 2021). *C. pneumoniae* expresses three enzymes that act as DD-carboxypeptidases and could play a role in the remodeling of PG: PBP6, AmiA and a LysM protein (reviewed in Klöckner *et al*., 2018). **(c)** Two PG degradation enzymes are known in *Chlamydia*. The amidase AmiA which, in *C. pneumoniae*, also act as a lipid II DD-carboxypeptidase (Klöckner *et al*., 2014) and the dual functioning lytic transglycosylase and muramidase SpoIID (Jacquier *et al*., 2019). To date, little is known about possible *Chlamydia* recycling enzymes which could re-provide PG degradation products for synthesis.

Structural analysis of *C. trachomatis* muropeptides obtained from cell culture found a L-Ala/L-Gly-γ-D-Glu-mDAP-D-Ala sequence in the stem peptide (Packiam *et al*., 2015). In addition to its ability to acquire amino acids from its host cell, *Chlamydia* possess enzymes to generate amino acid stereoisomers γ-D-Glu (Liechti *et al*., 2018) and D-Ala (De Benedetti *et al.*, 2014) as well as the amino acid mDAP (McCoy *et al*., 2006), which cannot be provided by their mammalian host (Pillai *et al*., 2006; Cox *et al*., 2000) (fig. 1.2.a).

The first amino acid of chlamydial PG stem peptide is added to MurNAc by activity of MurC, which is fused with D-Ala ligase Ddl (Hesse *et al*., 2003; McCoy & Maurelli, 2005). The next amino acids added are D-Glu and mDAP, in two enzymatic steps catalyzed by MurD and MurE, respectively (Patin *et al*., 2009; Klöckner *et al*, 2018). Finally, a D-Ala-D-Ala dipeptide, generated by the Ddl domain of the *Chlamydia* MurC/Ddl fusion protein (McCoy & Maurelli, 2005), is added to the UDP-MurNAc-tripeptide by MurF (Patin *et al*., 2012).

After the stem peptide is completed, UDP-activated MurNAc pentapeptide is linked to an membrane carrier, undecaprenyl phosphate (C_{55}-P), to form the precursor lipid I. This reversible step is catalyzed by the integral membrane protein MraY. As the last cytoplasmic step of PG synthesis, membrane-associated MurG adds another sugar unit (GlucNAc) to lipid I, producing the final PG building block lipid II. Both enzymes, MraY and MurG, are functionally conserved in *Chlamydia* (Henrichfreise *et al*., 2009). Lipid II is translocated across the inner membrane into the periplasm by an integral membrane protein with flippase activity. In *Chlamydia*, this step might be catalyzed by the transporter MurJ, which is conserved in the chlamydial genome and was shown to act as a lipid II flippase in free-living Gram-negative bacteria (Sham *et al*., 2014).

1.5.2. Assembly of the septal peptidoglycan ring in *Chlamydia*

Inside the periplasm, newly synthesized lipid II building blocks are linked to form the PG meshwork (fig. 1.2.b). This process requires PG synthases capable of displaying glycosyltransferase activity to join the disaccharide moiety of lipid II into long glycan strands and transpeptidase activity to crosslink the peptide stems of two lipid II molecules (Egan *et al*., 2015). The *Chlamydia* genome encodes two high molecular weight PBPs, PBP2 and PBP3 (FtsI), which are predicted to act as monofunctional PG transpeptidases (class B PBPs) (Ouellette *et al*., 2012; Klöckner *et al*., 2018).

Since their activity depends on the presence of mDAP and D-Ala-D-Ala moieties in the stem peptides, cross-linking of the PG meshwork can be modulated by enzymes which cleave the terminal D-Ala from the pentapeptide side chains (Ghosh *et al*., 2008). In *C. pneumoniae*, three enzymes with DD-carboxypeptidase *in vitro* activity on lipid II are characterized: a low molecular weight PBP (PBP6), a LysM-domain containing protein (Cpn0902) and an amidase with dual function (AmiA) (Otten *et al*., 2015; Klöckner *et al*., 2014).

Notably, while homologs of PG transpeptidases are conserved in *Chlamydia*, classical bacterial PG glycosyltransferases, which are bifunctional PBPs harboring PG transpeptidase and PG glycosyltransferase domains (class A PBPs) (Egan *et al*., 2015), are missing. However, the chlamydial PG biosynthetic gene cluster includes a set of protein homologs named SEDS (shape, elongation, division and sporulation) (Henrichfreise *et al*., 2016) which were shown to make up a novel class of PG glycosyltransferases (Meeske *et al*., 2016). Since SEDS proteins RodA and FtsW interact with class B PBP2 and PBP3, respectively, it was hypothesized that they are specialized transpeptidase-glycosyltransferase pairs executing PG synthesis at different subcellular sites in free-living bacteria (Meeske *et al*., 2016). Consistent with this, FtsW in complex with its cognate monofunctional transpeptidase was shown to act as PG synthase to produce septal PG during cell division in *Staphylococcus* (Taguchi *et al*., 2019).

At first glance, it may seem surprising that two pairs of enzymes with apparently redundant tasks, RodA-PBP2 and FtsW-PBP3, are conserved in *Chlamydia*. However, current studies suggest that these two transpeptidase-glycosyltransferase pairs are involved at different stages of PG ring assembly and therefore may function independently during chlamydial division. PBP2 activity has been observed to be necessary for the PG ring to expand (Liechti, 2021) and for polarized division to be initiated in *C. trachomatis* (Cox *et al*., 2020). PBP3 comes into play later, its activity seems to play less of a role in the budding process than in enabling the formation of the nascent daughter cell (Cox *et al*., 2020). Cox and colleagues as well as Liechti hypothesized in their studies that the chlamydial PG synthases regulate the organization of the PG ring in order to allow for its expansion and contraction, processes that appear to be essential to maintain polarized cell division in *Chlamydia* (Cox *et al*., 2020; Liechti, 2021).

1.5.3. The chlamydial amidase AmiA

The N-acetylmuramoyl-L-alanine amidases of *E. coli* (AmiA, B and C) are periplasmic enzymes involved in the splitting of septal PG necessary for daughter cell separation during cell division (Uehara & Bernhardt, 2011). They hydrolyze PG by cleaving the amide bond between the MurNAc unit of the glycan strand and L-Ala, the first residue of the peptide side chain (Vollmer *et al*., 2008b). Catalytic activity of AmiA, AmiB, and AmiC is zinc-dependent and in their active sites three zinc coordinating residues are conserved together with a fourth glutamic acid residue, that is predicted to act as a general base catalyst (Lupoli *et al*., 2009; Rocaboy *et al*., 2013). While *E. coli* relies on all three cell division amidases for proper cell separation, only AmiA is conserved in minimal chlamydiae. AmiA homologs of *Chlamydia* and *Waddlia* have been shown to possess amidase activity and to support daughter cell separation in *E. coli* triple amidase knockout mutants (Klöckner *et al*., 2014; Frandi *et al*., 2014).

In order to avoid uncontrolled destruction of the cell wall, PG hydrolytic activity of these amidases must be tightly regulated in free-living bacteria. In particular activity of AmiA, since this enzyme appears to be distributed throughout the periplasm of *E. coli*, while AmiC was shown to localize almost exclusively at the division septum (Bernhardt & de Boer, 2003). All three cell division amidases in *E. coli* possess only low basal *in vitro* activity due to an autoinhibitory α-helix domain, which occludes the enzymes' active sites and keep them in an 'off' state (Yang *et al*., 2012). They are activated by interaction with the septal ring factors EnvC and NlpD, which stimulates a conformational change within the enzymes, thereby releasing the regulatory α-helix from the active sites (Yang *et al*., 2012). EnvC activates AmiA and AmiB, while NlpD promotes AmiC activity (Uehara *et al*., 2010). This regulatory mechanism ensures that the activity of the amidases is restricted to the site of cell division in *E. coli*. AmiA homologs in chlamydiae lack an autoinhibitory domain and are by default active enzymes (Klöckner *et al*., 2014; Frandi *et al*., 2014). Consistent with this, chlamydial genomes neither encode homologs of EnvC and NlpD nor of the division proteins FtsE and FtsX, that are required to recruit AmiA to the division plane in *E. coli* (Yang *et al*., 2011). So far it remains elusive whether chlamydiae maintain mechanisms to regulate amidase activity and/or recruit AmiA to the division site. In *Waddlia*, AmiA was found throughout the periplasm with a possible enrichment at the division site in

deeply constricted cells (Frandi *et al*., 2014), while localization of AmiA in *Chlamydia* is still unknown.

AmiA from *C. pneumoniae* was shown to possess dual activity on PG precursor lipid II *in vitro*, acting as amidase and DD-carboxypeptidases (Klöckner *et al*., 2014; Klöckner, 2016). The latter function is penicillin sensitive and was assigned to an SxxK motif that is conserved among PBPs (Klöckner *et al*., 2014; Gosh *et al*., 2008). The ability to use lipid II as a substrate has not been tested for *W. chondrophila* AmiA (Frandi *et al*., 2014) and it is currently unknown whether the dual activity is specific to AmiA of *C. pneumoniae* or whether it is also a feature of other chlamydial AmiA homologs.

1.5.4. NlpC/P60 domain-containing proteins

Proteins of the NlpC/P60 superfamily are widely represented in various bacteria and involved in the processing of compounds of the bacterial cell envelope, mainly its PG layer. The occurrence of this superfamily is not restricted to the bacterial kingdom as proteins with NlpC/P60 domains have been found in certain eukaryotes, viruses and archaea (Anantharaman & Aravind, 2003). NlpC/P60 enzymes are predominantly involved in the degradation of bacterial PG by cleaving the linkage between γ-D-Glu and mDAP (or Lys) of its stem peptide (Anantharaman & Aravind, 2003; Xu *et al*., 2015). In addition, NlpC/P60 enzymes identified in *Bacillus* have been shown to possess γ-D-Glu-mDAP peptidase activity towards poly-γ-glutamate, a *Bacillus*-specific polymer of the cell surface and towards fragments of PG pentapeptide (Schmidt *et al*., 2001; Fukushima *et al*., 2018). While some of these hydrolases are able to digest both, PG and poly-γ-glutamate (Fukushima *et al*., 2018), the NlpC/P60 domain-containing protein YkfC has narrow substrate specificity and is unlikely to cleave one of these cell envelope polymers (Xu *et al*., 2015). Instead, YkfC has been shown to specifically hydrolyze PG-derived peptides and is thought to play a role in bacterial PG recycling (Xu *et al*., 2015).

The structural core of the NlpC/P60 domain has a prototypical papain-like fold and active site which harbors three conserved residues, namely a Cys-His dyad and a third polar residue (Anantharaman & Aravind, 2003; Xu *et al*., 2010). The domain consists of segregated α- and β-elements: three N-terminal α-helices are followed by five β-strands (fig. 1.3) (Anantharaman & Aravind, 2003). The second α-helix is

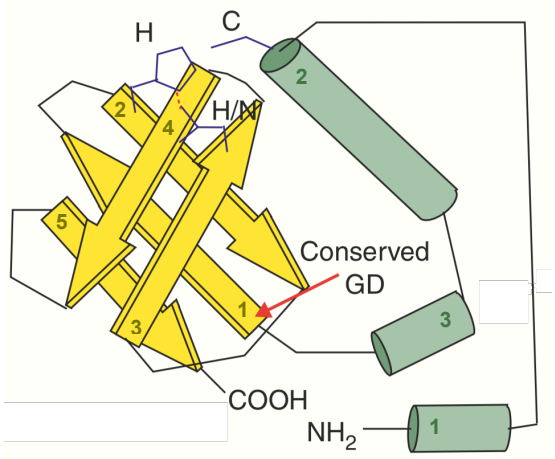

Fig. 1.3. Model of the secondary structure of the NlpC/P60 protein superfamily domain. The model is based on *in silico* analysis of predicted secondary structures and sequence conservation profile among members of this protein superfamily. Yellow arrows represent β-strands and green cylinders represent α-helices. (Figure from Anantharaman & Aravind, 2003).

conserved in all known NlpC/P60 proteins and is associated with the active site, since the cysteine residue of the catalytic dyad occurs at its extreme amino terminus. The catalytic histidine and conserved polar residue are located on the second and third of the β-strands, respectively, in close proximity to cysteine with which they form the active site. The catalytic cysteine likely acts as a nucleophile that attacks the peptide bond of the substrate, with histidine acting as the base and then the acid catalyst for the proton transfers in sequential steps. The conserved polar residue is thought to be involved in orienting the catalytic histidine correctly in the active site (Anantharaman & Aravind, 2003). In addition to the residues of the active site, a glycine, which is often followed by an aspartate, is characteristically conserved at the first β-strand of the NlpC/P60 domain (Anantharaman & Aravind, 2003). Here, a putative NlpC/P60 domain-containing protein was found to be encoded in the genomes of representatives of *Chlamydia* and *Chlamydia*-like organisms. Based on analysis of the predicted protein structure and in particular the architecture of the NlpC/P60 domain as well as its biochemical characterization, it was investigated whether this enzyme might play a role in the chlamydial PG turnover process.

1.6. *Chlamydia* as a human pathogen

Within *Chlamydiae*, the most common and well-known human pathogenic species are members of the *Chlamydiaceae*, mainly *C. trachomatis* and *C. pneumoniae*. Historically, chlamydiae were first recognized by modern medicine as the causative agent of trachoma, an infectious disease of the human eye (von Prowazek & Halberstadter, 1907). It is caused by *C. trachomatis* serovars A to C, transmitted directly by smear infection and possibly also by flies that have come into contact with

discharge from eyes of infected individuals (Cook, 2008; Last *et al*., 2020). Over the course of time, repeated or long-lasting infection causes the cornea to become scarred which ultimately results in its opacity (Cook, 2008). Trachoma is the leading infectious cause of blindness worldwide and in 2020 was still a public health problem in 46 countries with its occurrence being inextricably linked with economic deprivation (WHO, 2020). In Europe, trachoma has been eradicated due to high living and hygiene standards (Burton & Mabey, 2009). However, urogenital infection with *C. trachomatis* serovars D to K remains the most commonly reported sexually transmitted infection (STI) in this region (ECDC, 2021).

On a global level, too, *C. trachomatis* is also one of the most common causative agents of curable STIs, second only to the protozoan *Trichomonas vaginalis* (Rowley *et al*., 2019). However, since it is estimated that as many as 70-80 % of women and up to 50 % of men with chlamydial urogenital infection are asymptomatic (Stamm, 1999), the number of cases might be underestimated. Urogenital infection with *C. trachomatis* is transmitted exclusively by sexual intercourse. In addition, if a pregnant person is infected, vertical transmission of chlamydiae to the newborn can occur during birth, and may lead to conjunctivitis or pneumonia in infants (Darville, 2005). Adult urogenital *C. trachomatis* infection is associated with genital tract syndromes, including inflammation of the urethra, the cervix or the epididymis (Malhotra *et al*., 2013). However, it often causes minimal or no symptoms, remains subclinical, and therefore goes unnoticed. Left untreated, the chlamydial infection has the potential to become chronic, with repeated cycles of productive infection and persistence. It has been estimated that without treatment up to 50 % of infected women continue to be infected for over a 1 year (Geisler, 2010). Chlamydial infection can ascend from the cervix to the upper reproductive tract (i.e., uterus, oviducts), where it may results in pelvic inflammatory disease (PID), a polymicrobial infection caused primarily by *C. trachomatis* and *Neisseria gonorrhea* (Haggerty & Ness, 2006; Wiesenfeld *et al*., 2012). Prolonged exposure of the oviducts to *C. trachomatis* promotes damage to epithelial cells and scarring, which may result in tubal factor infertility and, should conception occur, increased susceptibility to ectopic pregnancy, as well as premature pregnancy termination (Menon *et al*., 2015; Xia *et al*., 2020; Rours *et al*., 2011).

C. trachomatis infection of the upper genital tract can be treated with the macrolide azithromycin and the tetracycline doxycycline (Savaris *et al.*, 2017). However, asymptomatic infection might evade detection and often goes untreated. In addition, antibiotic treatment does not prevent against reinfection. In order to circumvent these problems in treatment, numerous attempts have been made in recent years to develop an antichlamydial vaccine. Recently, a phase 1 clinical trial of a vaccine against *C. trachomatis* was successfully completed for the first time (Abraham *et al*., 2019). This vaccine uses an engineered version of the chlamydial MOMP, comprising heterologous immunorepeats from *C. trachomatis* serovars D to G, as the antigen (Abraham *et al*., 2019). In animal models, it was shown to elicited protection against vaginal shedding of *C. trachomatis*, while experimental data to investigate wether it is associated with protection in the upper genital tract is currently lacking. However, by reducing chlamydial transmission, this type of vaccine could help to reduce the number of newly occurring genital infections (De la Maza *et al*., 2021).

Another member of *Chlamydiaceae* affecting human health is *C. pneumoniae,* which is a widespread respiratory pathogen responsible for community-acquired pneumonia. It is likely to be transmitted between humans via aerosols and infects the upper and lower respiratory tract, where it can cause sinusitis and pharyngitis in addition to pneumonia and bronchitis (Grayston et al., 1993; Burillo & Bouza, 2010). Like *C. trachomatis* genital infection, respiratory tract infection with *C. pneumoniae* often goes asymptomatic, but has the potential to become chronic. It might contribute to the development of asthma, as the respiratory tract microbiome has been suggested to underlie the development of this disease (Huang & Boushey, 2015) with *C. pneumoniae* being among the bacteria discussed to play a role in its pathogenesis (Webley & Hahn, 2017). In addition, while lung epithelial cells and alveolar macrophages are initially infected, the infection can spread to blood monocytes and monocyte-derived macrophages, by which the bacterium may be systemically disseminated throughout the body (Herweg & Rudel, 2016; Di Pietro *et al*., 2019). *C. pneumoniae* is discussed to be potentially linked to atherosclerotic processes and development of Alzheimer’s Disease, as it has been detected in atherosclerotic lesions (Di Pietro *et al*., 2013) and in brain tissue samples of patients suffering from Alzheimer’s Disease (Dreses-Werringloer *et al.*, 2005).

The insidiousness of *Chlamydia* is rooted in its ability of asymptomatic infection. But how does this pathogen manage to evade an inflammatory host response? On the one hand, due to its ability to go into a persistent state, the organism can endure the stressing conditions caused by an immune response for an extended period of time. In addition, *Chlamydia* also seems to have found a way to stay under the host immune system's radar and thus avoiding an immune response. For this kind of survival strategy, the chlamydial PG metabolism might be a contributing factor. Besides a potential role in the chlamydial replication and energy recovery, this work focuses on how enzymes involved in the chlamydial PG turnover process might help to minimize the release of immunostimulatory degradation products and thus reduce the risk of alerting the host cell's immune system.

1.7. Aim of the thesis

This work's overall goal was to gain insight into the role of peptidoglycan (PG) turnover in chlamydiae, in terms of their lifecycle, immune evasion and energy recovery.

The first aim was to study the interplay between PG biosynthesis and the chlamydial lifecycle by testing antimicrobial compounds such as muraymycin with predicted targets in PG precursor lipid II synthesis against productive and persistent *C. trachomatis* infection in cell culture experiments. Complementary cytotoxicity analyses were intended to assess possible detrimental effects towards the mammalian host cells of *Chlamydia.* In addition, biochemical analyses were planned to identify chlamydial targets on a molecular level.

Remodeling of the PG ring during chlamydial cell division is a critical process as the uncontrolled release of PG degradation products may impede immune evasion of the intracellular pathogen. The second aim of this work was to gain deeper insight into the role of cell division amidase AmiA in this process. To this end, comparative analyses on AmiA homlogs from model organism *E. coli* and the human pathogens *C. pneumoniae* and *C. trachomatis* were planned that focused on autoinhibitory mechanisms and dual enzymatic activity.

Little is known about the chlamydial pathway for PG recycling that may help to reduce the release of immunostimulatory degradation products and contribute to energy recovery in chlamydiae. This work aimed to identify new components of the chlamydial PG machinery that may catalyze uncharacterized steps in PG ring recycling using a combination of complementary *in silico*, biochemical, and *E. coli* surrogate host experiments.

2. Materials and Methods

2.1. *In silico* methods and online tools

Online tools and bioinformatic software used in this work are listed in table 2.1.

Table 2.1. Online tools and their applications in this work.

Tool	Application	Weblink	Reference(s)/ Source
BLAST (Basic Local Alignment Search Tool)	Searching for regions of similarity between biological sequences	https://blast.ncbi.nlm.nih.gov/Blast.cgi	Altschul *et al.*, 1990
Clustal Omega	Sequence alignment	https://www.ebi.ac.uk/Tools/msa/clustalo/	Sievers *et al*., 2011; Madeira *et al*., 2022
In-Fusion Cloning Primer Design Tool	Primer design for In-Fusion cloning	https://www.takarabio.com/learning-centers/cloning/primer-design-and-other-tools	Takara Bio Europe (Sweden)
InterPro	Protein domain database	https://www.ebi.ac.uk/interpro/	Blum *et al*., 2021
KEGG	Kyoto Encyclopedia of Genes and Genomes	https://www.kegg.jp	Kanehisa & Goto, 2000
Magellan V. 6.5	Plate reader software used in readout of Bradford assay	Software	Tecan Trading AG, (Switzerland)
Phyre2	Homology-based 3D protein modelling	http://www.sbg.bio.ic.ac.uk/~phyre2/html/page.cgi?id=index	Kelley *et al*., 2015
PrediSi	Prediction of signal peptides	http://www.predisi.de	K. Hiller, Institute for Microbiology, University of Braunschweig, 2003
Prism-09	Statistical analysis	Software	GraphPad Software, LLC (USA)
QuickChange Primer Design tool	Primer design for site-directed mutagenesis	https://www.agilent.com/store/primerDesignProgram.jsp	Agilent Technologies (USA)

Table 2.1. Online tools and their applications in this work.

Tool	Application	Weblink	Reference(s)/ Source
SignalP-06	Prediction of signal peptides and the location of their cleavage sites	https://services.healthtech.dtu.dk/service.php?SignalP	Nielsen, 2019
Snap Gene Viewer V5.3.2	Sequence analysis	(free software) https://www.snapgene.com/snapgene-viewer/	Insightful Science, GSL Biotech LLC (USA)
Sparkcontrol Magellan V1.2.25	Plate reader software used in readout of Alamar Blue assays and for growth curves in complementation assays	Software	Tecan Trading AG, (Switzerland)
TMHMM-2.0	Prediction of transmembrane helices in proteins	https://services.healthtech.dtu.dk/service.php?TMHMM-2.0	Krogh *et al.*, 2001
UniProt	Curated protein database	https://www.uniprot.org	Bateman *et al.*, 2021
UCSF Chimera	Visualization and analysis of protein structures	https://www.cgl.ucsf.edu/chimera/	Pettersen *et al.*, 2004
Zen2 (blue edition)	Evaluation of microscopy	Software	Carl Zeiss Microscopy GmbH, (Germany)

2.2. Chemicals and Reagents

If not specified otherwise, all used chemicals and reagents were HPLC grade or higher and were purchased from Sigma-Aldrich, Merck Millipore or Carl Roth.

2.3. Cultivation of bacterial and mammalian cells

2.3.1. Media preparation and additives

All media used for cultivation of bacteria were sterilized by autoclaving at 121 °C for 20 minutes. For solid media, 1.5 % (*w/v*) agar-agar was added pre-autoclaving. Heat-sensitive additives were sterile filtered and added post-autoclaving.

2.3.1.a. Media used for cultivation of bacteria

The composition of media utilized in this work to cultivate bacteria are listed in table 2.2. Lysogeny broth or agar plates were prepared following the LB-Miller formula and used for liquid and solid cultivation of *Escherichia coli.* For recombinant protein production in *E. coli,* either terrific broth (TB) for autoinduction, 2 × yeast extract-tryptone broth (2xYT), or LB without NaCl were used. Salt-free LB was supplemented post-autoclaving with sterile filtered cosolvents in an iso-osmotic concentration of 342 mM (Otten *et al*., 2015). For complementation assays with *E. coli* mutant strains, either TB or nutrient broth were used.

Table 2.2. Media composition for cultivation of *E. coli.*

Medium	Composition	pH
Lysogeny broth (LB) (Bertani, 1951)	10 g/l tryptone, 5 g/l yeast extract, 10 g/l NaCl	7.2
Nutrient broth	5 g/l tryptone, 3 g/l yeast extract	7.2
Terrific broth (TB) (Tartoff & Hobbs, 1987)	medium: 12 g/l tryptone, 24 g/l yeast extract, 4 g/l glycerol phosphate buffer solution: 0.17 M KH_2PO_4, 0.72 M K_2HPO_4 (autoclave separately, after autoclaving add 100 ml buffer solution to 900 ml TB, to make a total volume of 1000 ml)	7.2
Terrific broth (TB) for autoinduction (Studier, 2005)	composition similar to TB additives: 10 mM $MgSO_4$, 10 mM $MgCl_2$, 0.55 g/l glucose monohydrate, 2.1 g/l lactose monohydrate	7.2
2× yeast extract-tryptone broth (2xYT) (Miller, 1972)	16 g/l tryptone, 10 g/l yeast extract, 5 g/l NaCl	7.5

2.3.1.b. Medium used for cultivation of mammalian cells

To grow mammalian Hep 2 cell line in cell culture, Dulbecco's Minimum Essential Medium (DMEM) high Glucose, GlutaMAX supplement with pyruvate medium was prepared under sterile conditions according to the composition shown in Table 2.3. For cell viability assays and MIC determinations, gentamicin and amphotericin B were omitted and the medium was referred to as MIC-DMEM.

Table 2.3. Composition of DMEM used for cultivation of mammalian cells.

Component	Aliquots	Final concentration
Dulbecco's Minimum Essential Medium (DMEM) high Glucose, GlutaMAX supplement, pyruvate (Thermo Scientific)	500 ml	-
MEM Non Essential Amino Acids (100x) (Thermo Scientific)	5 ml	1x
MEM Vitamins Solution (100x) (Thermo Scientific)	5 ml	1x
Gibco Amphotericin B (250 µg/ml) (Thermo Scientific)	5 ml	2.5 µg/ml
Gibco Gentamicin sulfate (50 mg/ml) (Thermo Scientific)	0.5 ml	50 µg/ml
Fetal bovine serum (Thermo Scientific), heat inactivated according to manufacturer's instructions	50 ml	-

2.3.1.c. Antibiotics, tested compounds and media additives

Compounds used as media additives in this work are listed in table 2.4.

Table 2.4. Antibiotics, tested compounds and media additives.

Substance	Solvent	Stock concentration; storage conditions	Final concentration	Source
Ampicillin sodium salt	H_2O	10 mg/ml; - 20 °C	100 µg/ml	Ratiopharm
Anhydrotetracycline (AHT)	Dimethylformamide	1 µg/ml; - 20 °C, dark	200 ng/ml	IBA Lifesciences
Candidate compounds (CC1-10)	DMSO	1 mg/ml; room temperature, dark	1 - 128 µg/ml	-
Caprazamycin derivate CPZ2	DMSO	1 mg/ml, 10 mg/ml; - 20 °C	1 - 128 µg/ml	S. Ichikawa, Hokkaido University
Chlormaphenicol	EtOH	100 mg/ml; - 20 °C	34 µg/ml	Sigma-Aldrich
Ciprofloxacin hydrochloride	H_2O	0.1 mg/ml; - 20 °C	1 µg/ml	Fargon
Cycloheximide	HBSS	0.1 mg/ml; - 20 °C	0.0012 mg/ml	Sigma-Aldrich
Isopropyl β-D-1-thiogalactopyranoside (IPTG)	H_2O	1 M, - 20 °C	1 mM	Thermo Scientific
Kanamycinsulfate	H_2O	10 mg/ml; - 20 °C	100 µg/ml	Carl Roth

Table 2.4. Antibiotics, tested compounds and media additives.

Substance	Solvent	Stock concentration; storage conditions	Final concentration	Source
Muraymycin D2, Muraymycin derivates	DMSO	1 mg/ml, 10 mg/ml; - 20 °C	1 - 128 µg/ml	S. Ichikawa, Hokkaido University
MurJ-Inhibitors	DMSO	1 mg/ml; - 20 °C	1 - 128 µg/ml	T. Schneider, University of Bonn
Penicillin G sodium salt (PenG)	H_2O	10 mg/ml; - 20 °C,	100 U/ml	Carl Roth
α-X-Chalcones	DMSO	1 mg/ml, 10 mg/ml; - 20 °C	40 µM	S. Amslinger, University of Regensburg

2.3.2. Used organisms

2.3.2.a. *E. coli* strains used for plasmid propagation and subcloning

E. coli NEB5a (DH5α)

For plasmid propagation, subcloning and permanent storage of expression vectors, the commercial available *E. coli* NEB5a (DH5α) strain (genotype: *fhuA2Δ_(fhuA2 Δ(argF-lacZ)U169 phoA glnV44 Φ80Δ (lacZ)M15 gyrA96 recA1 relA1 endA1 thi-1 hsdR17*) (New England Biolabs) was used.

E. coli NEB DH10 β

For propagation and subcloning of large plasmids, the commercial available *E. coli* NEB DH10 β strain (genotype: *Δ(ara-leu) 7697 araD139 fhuA ΔlacX74 galK16 galE15 e14- φ80dlacZΔM15 recA1 relA1 endA1 nupG rpsL (Str^R) rph spoT1 Δ(mrr-hsdRMS-mcrBC)*) (New England Biolabs) was used.

E. coli W3110

For genomic DNA isolation, the *E. coli* W3110 strain (genotype: F$^-$ lambda$^-$ IN(rrnD-rrnE)1 rph-1) (Leibniz Institute DSMZ-German Collection of Mircoorganisms and Cell Cultures) was used. This strain was also used for peptidoglycan sacculi preparation.

2.3.2.b. *E. coli* strains used for recombinant protein production

E. coli C43(DE3)

The *E. coli* C43(DE3) strain (genotype: *F– ompT gal dcm hsdS$_B$(r$_B$$^-$ m$_B$$^-$)(DE3*)) (Wagner *et al*., 2008) was used for transmembrane, cyto- and periplasmic protein production.

E. coli JM83

The *E. coli* JM83 strain (genotype: *rpsL ara Δ(lac-proAB) Φ80dlacZΔM15*) (Leibniz Institute DSMZ-German Collection of Mircoorganisms and Cell Cultures) was used for periplasmic protein production.

2.3.2.c. *E. coli* mutant strains used in complementation assays

E. coli AT980 *dapD* deficient, *mpl* deletion mutant

An *E. coli* mutant strain deficient for DapD and Mpl was kindly generated for this work by D. Mengin-Lecreulx (Institute for Integrative Biology of the Cell, Université Paris-Saclay, France). Two previously described *E. coli* strains were used to construct this mutant: *E. coli* AT980 and *E. coli* MLD2502. *E. coli* AT980 (genotype: *dapD2*, *λ*$^-$, *e14*-, *relA1*, *spoT1*, *thiE1*) is deficient for DapD and requires mDAP as a medium supplement for growth (Bukhari & Taylor, 1971; Park *et al.*, 1998). *E. coli* MLD2502 is a strain derived from BW25113 (genotype: lacI^q, rrnB$_{T14}$, *ΔlacZ*$_{WJ16}$, *hsdR514*, *ΔaraBAD*$_{AH33}$, *ΔrhaBAD*$_{LD78}$) that carries an additional deletion of the chromosomal *mpl* gene (Δ*mpl*::Cm^R) (Hervé *et al*., 2007). The *E. coli* double mutant strain used in this work was constructed by transduction of the Δ*mpl*::Cm^R mutation into the AT980 strain by phage P1 transduction (Miller, 1972).

E. coli JW2163-3 *mepS* deletion mutant (Baba *et al*., 2006)

E. coli JW2163-3 (genotype: *Δ(araD-araB)567*, *ΔlacZ4787*(::rrnB-3), *λ*$^-$, *Δspr-732::kan*, *rph-1*, *Δ(rhaD-rhaB)568*, *hsdR514*) was received from the Keio *E. coli* mutant strain collection (Baba *et al.*, 2006). This strain carries a knockout mutation of the chromosomal *mepS* gene (*Δspr-732::kan; mepS* was formally known as *spr*). An *E. coli mepS* deletion mutant is phenotypically characterized by its inability to grow in in low osmolarity medium at high temperature (Hara *et al.*, 1996).

2.3.2.d. *Chlamydia* strains

Chlamydia pneumoniae GiD

In this work, DNA from *C. pneumoniae* GiD (kindly provided by the Hegemann group, Funktionelle Genomforschung der Mikroorganismen, University of Düsseldorf) was used for cloning of *C. pneumoniae* genes. Bioinformatic research was conducted using the genome of the reference strain *C. pneumoniae* CWL029 (Kalman *et al*., 1999). The sequence of the cloned genes is consistent with that of the corresponding genes in *C. pneumoniae* CWL029 strain and gene locus tags are used tantamount to each other.

Chlamydia trachomatis D/UW-3/CX

The type strain *C. trachomatis* D/UW-3/CX is an agent of human urogenital infection. It was propagated using the mammalian Hep2 cell line and was used in cell culture assays to analyze the effect of antimicrobial compounds. Bioinformatic research was conducted using the genome of *C. trachomatis* D/UW-3/CX (Stephens *et al*., 1998) and DNA from this strain (kindly provided by H. Bühl, Henrichfreise group) was used for cloning of *C. trachomatis* genes.

2.3.2.e. Mammalian cell line

Hep2 subclone B cell line

Hep2 cells are adherent epithelial carcinoma cells derived via HeLa contamination. This cell line carries a silent copy of Human Papillomavirus. In this work, Hep2 cells were used as host cells for propagation of *Chlamydia trachomatis* D/UW-3/CX.

2.3.3. Bacteriological methods

E. coli strains were cultivated in liquid or solid Lysogeny broth (LB; for composition see tab. 2.2) at 37 °C, unless stated otherwise. Liquid cultures were shaken vigorously to enable proper aeration, growth was determined by measuring optical light scattering (OD_{600nm}) at 600 nm wavelength. Permanent cultures of *E. coli* strains were created my mixing fresh overnight liquid culture with sterile glycerol in a 1:1 ratio (*v*/*v*) and were stored at - 70 °C.

2.3.3.a. Preparation of chemically competent *E. coli*

In order to prepare chemically competent cells for heat shock transformation, 20 ml of LB were inoculated at 1% (*v*/*v*) with an overnight culture of the respective *E. coli* strain to be transformed. The cells were grown under shaking to an OD_{600nm} of 0.4 at 37 °C and then harvested by centrifugation at 4000 x g for 15 minutes. Cell harvest and all subsequent steps were conducted at 4 °C using pre-cooled solutions and reaction tubes. The cell pellet was carefully resuspended in 8 ml sterile 0.1 M $CaCl_2$ solution and the suspension was incubated for 20 minutes on ice. Afterwards cells were pelleted again as described and carefully resuspended in 2 ml sterile 0.1 M $CaCl_2$ solution containing 15 % glycerol (*v*/*v*). After incubation for 30 minutes on ice, 50 µl aliquots of the chemically competent cells were stored at - 70 °C.

2.3.3.b. Heat shock transformation of chemically competent *E. coli*

For heat shock transformation, chemically competent cells (see 2.3.3a) were thawed on ice and mixed with 10 - 100 ng plasmid DNA. After 30 minutes incubation on ice, the heat shock was performed at 42 °C for 90 seconds. Immediately after the heat shock, cells were incubated on ice for 2 minutes before adding 950 µl of fresh LB. Cells were then incubated under shaking for 1 hour at 37 °C before being plated on a selective agar plate and incubated overnight.

2.3.4. Mammalian cell culture and chlamydial propagation

2.3.4.a. Solutions used in mammalian cell culture and microscopy

Hank's balanced salt solution (HBSS)

Isotonic HBSS (Gibco, Thermo Scientific) was used to wash and transport cells and to prepare reagents used in mammalian cell culture.

Trypsin solution

Trypsin solution was used to dissociate adherent cells. Trypsin 0.5 % (10x) with EDTA (Gibco, Thermo Scientific) was aliquoted into 2.5 ml samples in 50 ml tubes and stored at - 20 °C. A trypsin working solution was prepared by adding HBSS to the aliquots to a final volume of 50 ml and then stored at 4 °C.

Cycloheximide stock solution

Cycloheximide is an inhibitor of eukaryotic protein biosynthesis. Its addition to the cultivation medium enhances the release of ATP from the mammalian host cells which may then be utilized by *Chlamydia.* The compound was dissolved in HBSS to produce a 0.1 mg/l stock solution which was aliquoted into 0.36 ml samples and stored at - 20 °C.

Saccharose-phosphate-glutamic acid (SPG) buffer

SPG buffer was used to store chlamydial elementary bodies at - 70 °C. To prepare SPG buffer, the following components were dissolved in double-distilled water: 220 mM saccharose, 3.82 mM KH_2PO_4, 10.8 mM Na_2HPO_4 x 2 H_2O and 4.36 mM glutamic acid x H_2O. The buffer was then sterilized and stored at 4 °C.

2.3.4.b. Cultivation of Hep2 cells

Hep2 cells were cultivated in 15 ml DMEM (for composition see 2.3.1.b.) in 75 cm^2 coated cell culture flasks (Greiner) and incubated at 5 % (*v*/*v*) CO_2 at 37 °C. Growth and confluency of the cell monolayer were checked regularly by light microscopy.

2.3.4.c. Subcultivation and splitting of Hep2 cells

It took about 2-4 days for Hep2 cells to develop a confluent monolayer in 15 ml DMEM in 75 cm^2 cell culture flasks. After this period, cells from two flasks were split into fresh cultivation medium. For this purpose, DMEM was removed from the monolayer which was then rinsed with 10 ml HBSS. Cells were detached from the flask by adding 5 ml trypsin working solution. Once complete detachment of the monolayer was achieved, trypsin was inactivated by adding 5 ml DMEM (which contains FKS). Cells were pelleted by centrifugation at 42 x g for 10 minutes at 4 °C. Subsequently, the cell pellet was gently resuspended in 3.5 ml DMEM and new flasks with 15 ml fresh DMEM were seeded with 0.6 ml of the cell suspension. Subsequently, the Hep2 cells were regrown to a confluent monolayer, which was then used either for the next round of splitting or for infection with *C. trachomatis* D/UW-3/CX (see section 2.3.4.e.).

2.3.4.d. Permanent culture of Hep2 cells

To generate permanent cryopreserved cultures of Hep2, cells from two 75 cm^2 cell culture flasks were detached and harvested as described in section 2.3.4.c. The cells were resuspended in DMEM supplemented with 5 % (*v*/*v*) DMSO at a concentration of 3 to 6 x 10^6 cells/ml. The cell suspension was aliquoted into 1 ml samples in cryotubes and frozen to - 70 °C at a cooling rate of 1 °C/min using an isopropanol mammalian cell line freezing container (Mr. Frosty by Nalgene).
In order to reinoculate Hep2 cells from the permanent culture, a 1 ml aliquot was rapidly thawed at 37 °C and resuspended in 10 ml DMEM pre-warmed to 37 °C. To remove DMSO, cells were centrifuged at 105 x g for 10 minutes at room temperature and the resulting pellet was resuspended in pre-warmed 1 ml DMEM. The Hep2 cell suspension was used to inoculate two 75 cm^2 cell culture flasks with 15 ml pre-warmed DMEM each. The cells were then grown to a confluent monolayer.

2.3.4.e. Propagation and strainkeeping of *C. trachomatis* D/UW-3/CX

To continuously cultivate *C. trachomatis* D/UW-3/CX, chlamydial elementary bodies (EBs) were harvested from infected Hep2 host cells and used to infect new cells. The monolayers from two flasks with infected Hep2 cells were mechanically detached with a cell scraper and the cells were transferred into an aerosol-proof tube containing 3 mm diameter glass beads. The glass beads were used to mechanically lyse the host cells by vigorous vortexing for 30 seconds. Afterwards the lysate was centrifuged at 1497 x g for 10 minutes at 4 °C to remove host cell debris. The supernatant containing the chlamydial EBs was collected and was used either to infect new host cells or to set up permanent *Chlamydia* cultures (see section 2.3.4.f.).
To infect new host cells, two 75 cm^2 cell culture flasks in which Hep2 cells had been grown to a confluent monolayer were prepared as follows. First, the old medium was removed from the cells and 8 ml DMEM per flask was added, then 6 ml of the EB-containing supernatant was added for infection. After incubation at 37 °C and 5 % (*v*/*v*) CO_2 for 3 hours, the medium in each of the two flasks was changed to 15 ml DMEM with 0.0012 mg/ml cycloheximide (see section 2.3.4.a.).

2.3.4.f. Permanent culture of *C. trachomatis* D/UW-3/CX

C. trachomatis D/UW-3/CX EBs harvested from Hep2 cells as described in section 2.3.4.e. were used to generate permanent cultures. For this purpose, the lysate, cleared from host cell debris, was centrifuged again for 30 minutes at 4 °C and maximum speed in order to pellet the EBs. The pellet was then resuspended in 1 ml sterile SPG buffer (for composition see 2.3.4.a.) and stored in cryotubes at - 70 °C. The EB stocks could be used to re-infect host cells by thawing them and adding 0.1 ml to a 75 cm^2 cell culture flasks containing confluent Hep2 cells.

2.4. Molecular methods

2.4.1. Isolation of genomic DNA from bacteria

Genomic DNA from *C. pneumoniae* GiD was kindly provided by the Hegemann group (Funktionelle Genomforschung der Mikroorganismen, University of Düsseldorf). Genomic DNA from *C. trachomatis* D/UW-3/CX isolated with the DNeasy Blood & Tissue Kit (Quiagen) was kindly provided by H. Bühl (Henrichfreise group).
Genomic DNA from *E. coli* W3110 was isolated using the GenElute Bacterial Genomic DNA Kit (Sigma-Aldrich) according to the manufacturer's instructions.

2.4.2.Polymerase chain reaction (PCR)

The polymerase chain reaction (PCR) (Mullis *et al*., 1986) allows for exponential amplification of specific DNA sequences and is based on the ability of oligonucleotide primers to specifically bind denatured DNA strands. PCR is a cyclic, temperature-mediated sequence of DNA strand denaturation, primer annealing, and polymerase-mediated 5'-3' elongation of the DNA sequence framed by the primers.
The primers used in this work to amplify DNA for sequencing and cloning are listed in table 2.5. PCR was conducted using a C1000 Thermal Cycler (BioRAd). For cloning purposes, genomic DNA or plasmids served as templates and the Phusion High-Fidelity DNA-Polymerase (New England Biolabs) was used. To proof successful cloning, cell material served as template, which was picked from a selective agar plate, resuspended in 10 µl H_2O and lysed at 95 °C for 5 minutes. In this case the KAPA2G FastReadyMix with Dye (PeqLab/Roche) was used. For both purposes, PCR was performed according to the respective manufacturer's instructions

regarding the buffer system, the primer concentration and the determination of the annealing temperature.

Tab. 2.5. Primers used in this work.

Name	Sequence 5' -> 3'	nt	notes
IBA2_seq_for	GAG TTA TTT TAC CAC TCC CT	20	sequencing pASK_IBA vectors (IBA Lifescience)
IBA2_seq_rev	CGC AGT AGC GGT AAA CG	17	sequencing pASK_IBA vectors (IBA Lifescience)
pBAD24_seq_for	CTG TTT CTC CAT ACC CGT T	19	sequencing primer pBAD24 vectors (Coli Genetic Stock Center)
pBAD24_seq_rev	GCC AGG CAA ATT CTG TTT T	19	sequencing primer pBAD24 vectors (Coli Genetic Stock Center)
cpn0245_pBAD24_for	GAG GAA TTC ACC ATG AAA CAC TAC CTA TCA TTT TCT CCT	39	Cloning of *cpn0245* (*ykfC*$_{Cpn}$) into pBAD24+
cpn0245_pBAD24_rev	TCA TCC GCC AAA ACA TTA CAG AAA GGC TTT TCT TTT TCT	39	Cloning of *cpn0245* (*ykfC*$_{Cpn}$) into pBAD24+
ct127_pBAD24_for	GAG GAA TTC ACC ATG CCG CAC CAA GTC TTA TTG TCT CCT	39	Cloning of *ct127* (*ykfC*$_{Ctr}$) into pBAD24+
ct127_pBAD24_rev	TCA TCC GCC AAA ACA TCA AAA GAA GGC TTT TCT ATT TTT	39	Cloning of *ct127* (*ykfC*$_{Ctr}$) into pBAD24+
ELAC_2173_for	GAG GAA TTC ACC ATG AGT TCT GTC GGG CAG ATG T	34	Cloning of ELAC_2173 (*nlpC/P60*$_{Ela}$) into pBAD24+
ELAC_2173_rev	TCA TCC GCC AAA ACA TCA GTT GGT GGA CAG TCT CTT	36	Cloning of ELAC_2173 (*nlpC/P60*$_{Ela}$) into pBAD24+
SNE_A23160_for	GAG GAA TTC ACC ATG ACC TAT TTT GTC CCA AAA GTT TCA A	40	Cloning of SNE.A23160 (*nlpC/P60*$_{Sne}$) into pBAD24+
SNE_A23160_rev	TCA TCC GCC AAA ACA TTA CGA GAG GAA TCG TCG GAC T	37	Cloning of SNE.A23160 (*nlpC/P60*$_{Sne}$) into pBAD24+
mepS_pBAD24_ins_for	GAG GAA TTC ACC ATG GTC AAA TCT CAA CCG ATT TTG AG	38	Cloning of *b2175 (meps*$_{Eco}$) into pBAD24+
mepS_pBAD24_ins_rev	TCA TCC GCC AAA ACA TTA GCT GCG GCT GAG AAC CC	35	Cloning of *b2175 (meps*$_{Eco}$) into pBAD24+
T7	TAA TAC GAC TCA CTA TAG GG	20	sequencing pET vectors (Novagen)

Name	Sequence 5' -> 3'	nt	notes
T7term	TGC TAG TTA TTG CTC AGC GG	20	sequencing pET vectors (Novagen)
Cpn0245XmaI52bfor	GCG CGC CCC GGG AAA CAC TAC CTA TCA TTT TCT CC	35	Cloning of *cpn0245* (*ykfC*$_{Cpn}$) into pET52b+ using XmaI
Cpn0245EagI52brev	GCG CGC CGG CCG TTA CAG AAA GGC TTT TCT TTT TC	35	Cloning of *cpn0245* (*ykfC*$_{Cpn}$) into pET52b+ using EagI
CT127XmaI52bfor	GCG CGC CCC GGG CCG CAC CAA GTC TTA TT	29	Cloning of *ct127* (*ykfC*$_{Ctr}$) into pET52b+ using XmaI
CT127EagI52brev	GCG CGC CGG CCG TCA AAA GAA GGC TTT TCT ATT TTA G	37	Cloning of *ct127* (*ykfC*$_{Ctr}$) into pET52b+ using EagI
CT268XmaI52bfor	GCG CGC CCC GGG AGG GGT ATC AGA TCT TCA AAC	33	Cloning of *ct268* (*amiA*$_{Ctr}$) into pET52b+ using XmaI (C. Otten, Henrichfreise lab)
CT268EagI52brev	GCG CGC CGG CCG TTA TTT ATG CAC TTT TTT TGC TC	35	Cloning of *ct268* (*amiA*$_{Ctr}$) into pET52b+ using EagI (C. Otten, Henrichfreise lab)
CPN_0245_C173A_for	AGT CTG GAA AAG CCG GGT GTT GAT GCT TCG GGA TTT ATC A	40	CxA mutagenesis of *cpn0245* (*ykfC*$_{Cpn}$) (Bühl, 2019)
CPN_0245_C173A_rev	TGA TAA ATC CCG AAG CAT CAA CAC CCG GCT TTT CCA GAC T	40	CxA mutagenesis of *cpn0245* (*ykfC*$_{Cpn}$) (Bühl, 2019)
CT_127_C172A_for	ACA GCT TCC TCG TAA TGG TGT AGA TGC TTC GGG GTA TAT TC	41	CxA mutagenesis of *ct127* (*ykfC*$_{Ctr}$)
CT_127_C172A_rev	GAA TAT ACC CCG AAG CAT CTA CAC CAT TAC GAG GAA GCT GT	41	CxA mutagenesis of *ct127* (*ykfC*$_{Ctr}$)
EL_C193A_for	GCA CAA GAC CGG AAG CAT CCA CTC CCC TGA AAG G	34	CxA mutagenesis of *ELAC_2173* (*nlpC/P60*$_{Ela}$)
ELA_C193A_rev	CCT TTC AGG GGA GTG GAT GCT TCC GGT CTT GTG C	34	CxA mutagenesis of *ELAC_2173* (*nlpC/P60*$_{Ela}$)
SNE_C151A_for	TCA TCC GCC AAA ACA TTA CGA GAG GAA TCG TCG GAC T	37	CxA mutagenesis of *SNE.A23160* (*nlpC/P60*$_{Sne}$)
SNE_C151A_rev	AAG AAG TCC CGA GGC ATC CAC TCC TTG ACA GGT CC	35	CxA mutagenesis of *SNE.A23160* (*nlpC/P60*$_{Sne}$)
AmiAEc_ΔADfor	CTA ACC GTG GGG CAA GTA GTC TGA CGC TCG	30	ΔA148-S191 mutagenesis of *b2435* (*amiA*$_{Eco}$) (M. Brunke, Henrichfreise lab)

Name	Sequence 5' -> 3'	nt	notes
AmiAEc_ΔADrev	CGA GCG TCA GAC TAC TTG CCC CAC GGT TAG	30	ΔA148-S191 mutagenesis of *b2435* (*amiA*$_{Eco}$) (M. Brunke, Henrichfreise lab)

2.4.3. Agarose gel electrophorese for DNA separation

Agarose gel electrophoresis was used to identify and purify DNA fragments. DNA samples were loaded onto a gel, which was subjected to an electric field, causing the DNA to migrate to the cathode due to its negatively charged phosphate backbone. Since shorter DNA fragments can move faster through the pores of the gel than longer fragments, the DNA fragments are separated according to their size. By using a marker composed of DNA fragments of known size, the size of the separated DNA fragments was assessed.

To prepare the gel, 1 % (*w*/*v*) agarose was solved in 60 ml of 1x TAE buffer (40 mM Tris-HCl, 1 mM EDTA, 0.11 % (*v*/*v*) acetic acid, pH 8.3). To visualize DNA after electrophoresis, 1 µL of GelRed nucleic acids stain 10,000x solution (Biotium) was added during gel preparation. Samples were mixed with 6x DNA gel loading dye (Thermo Scientific) and loaded into the wells of the agarose gel. The GeneRuler 1 kb DNA Ladder (Thermo Scientific) was used as a marker for determining DNA size. Gel electrophoresis was conducted in 1x TAE buffer at 80-100 V for 60 minutes. After the electrophoresis, the GelRed stained DNA was visualized using UV light.

2.4.4. Purification of DNA fragments and plasmids

The GeneJET gel extraction kit (Thermo Scientific) was used to purify DNA fragments from the agarose gel after electrophoresis or to desalt and purify DNA fragments during the cloning process according to the manufacturer's instructions. The GeneJET Plasmid Miniprep Kit (Thermo Scientific) was used to isolate plasmid DNA from *E. coli* cells according to the manufacturer's instructions.

2.4.5. Photometric determination of DNA concentration

The amount of purified DNA fragments or plasmids in a sample was determined by measuring its absorbance at 260 nm using a spectrophotometer (NanoPhotometer, Implen).

2.4.6. Molecular cloning

Molecular cloning of DNA fragments into a vector was performed either by restriction digestion and ligation (see sections 2.4.6.a & b) or using the in fusion cloning kit (see section 2.4.6.c). The QuickChange Lightning (QCL) Site-Directed Mutagenesis Kit (see section 2.4.6.d) was used to insert mutations within a gene in a controlled manner. An overview of constructed expression vectors is given in table 2.6.

2.4.6.a. Restriction of DNA with endonucleases

To clone a DNA fragment amplified from genomic DNA into a plasmid, both the DNA fragment and the purified plasmid were separately digested with type II restriction endonucleases (New England Biolabs). The restriction enzymes were chosen prior to the construction of the PCR primers (tab. 2.5) so that the DNA fragment was framed by the respective recognition sites. DNA digestion with endonuclease was performed according to the manufacturer's instructions in a 50 µl reaction containing approximately 1 µg DNA (either insert or plasmid), 1x CutSmart Buffer (New England Biolabs) and 10 U of each restriction enzyme (New England Biolabs). The reaction was incubated at 37 °C for 60-90 minutes and then stopped by DNA purification using the GeneJET Gel Extraction Kit (see section 2.4.4.).

2.4.6.b. Ligation of an insert into a plasmid

After the DNA restriction und purification (see section 2.4.6.b.), DNA fragments were inserted into a plasmid restricted with the same enzymes by using a T4 DNA-ligase (Thermo Scientific). Ligation was performed according to the manufacturer's instructions in a 20 µl reaction containing 10-100 ng of insert and plasmid at a ratio of 3:1, 1x T4 DNA ligation buffer (Thermo Scientific) and 5 U T4 DNA ligase (Thermo Scientific). The reaction was incubated at room temperature for 10-20 minutes. Then either *E. coli* DH5α or *E. coli* DH10 β (see section 2.3.2.a.) were transformed with the ligated plasmid as described in section 2.3.3.b. Successful molecular cloning was confirmed by PCR as described in section 2.4.2.

2.4.6.c. In-Fusion cloning

To clone a DNA insert from one expression vector into another, the In-Fusion HD Cloning Kit by Clontech (Takara Bio Europe) was used. Insert and plasmids were

amplified and linearized by PCR with primers designed with the manufacturers' online tool (tab. 2.1). After amplification, the PCR products were purified with the GeneJET Gel Extraction Kit (see section 2.4.4.). The purified DNA was used to clone the insert into the plasmid using the In-Fusion HD Cloning Kit according to the manufacturer's instructions. Subsequently, *E. coli* DH5α (see section 2.3.2.a.) was transformed with the reaction product as described in section 2.3.3.b.

2.4.6.d. PCR-based site directed mutagenesis

Site-directed mutagenesis was performed to to generate mutants of recombinant proteins by introducing mutation into a gene in a controlled manner. For this purpose, the QuickChange Lightning Site-Directed Mutagenesis Kit (Agilent Technologies) was used according to the manufacturer's instructions. Mutagenesis was accomplished by PCR using a plasmid carrying the gene of interest as template and primers both containing the mutation and designed using the manufacturer's online tool (see table 2.1). Subsequently, *E. coli* DH5α (see section 2.3.2.a.) was transformed with the PCR product as described in section 2.3.3.b

2.4.7. Sequencing

The Sanger sequencing service provided by GATC (GATC Biotech) was used to confirm correct insertion of the gene of interest into the respective plasmid.

2.4.8. Expression vectors

The expression vectors used in this work are listed in table 2.6.

Table 2.6. Expression vectors used in this work.

Name	Encoded construct	Features	Reference/ Source
pASK-IBA2C	-	CamR, TetO/TetP, MCS, OmpA, C-terminal Strep-tag II	IBA Lifesciences
pASK-IBA2C_nlpC/P60$_{Ela}$	NlpC/P60$_{Ela}$ (ELAC_2173)	IBA2C derivate	N. Jacquier, University of Lausanne

Name	Encoded construct	Features	Reference/ Source
pASK-IBA2C_nlpC/P60$_{Sne}$	NlpC/P60$_{Sne}$ (SNE.A23160)	IBA2C derivate	N. Jacquier, University of Lausanne
pASK-IBA2C_amia$_{Eco}$	AmiA$_{Eco}$	IBA2C derivate	A. Klöckner (Klöckner, 2016)
pASK-IBA2C_amia$_{Eco}$_ΔA148-S191	AmiA$_{Eco}$ A148-S191 deletion mutant	IBA2C derivate	this work
pASK-IBA2C_envC$_{Eco}$	EnvC$_{Eco}$	IBA2C derivate	A. Klöckner (Klöckner, 2016)
pBAD24	-	AmpR, Arabinose pBAD promotor	Coli Genetic Stock Center (Yale, USA)
pBAD24_ykfC$_{Cpn}$	YkfC$_{Cpn}$ (Cpn0246)	pBAD24 derivate	this work
pBAD24_ykfC$_{Cpn}$C173A	YkfC$_{Cpn}$ (Cpn0246) C173A mutant	pBAD24 derivate	this work
pBAD24_ykfC$_{Ctr}$	YkfC$_{Ctr}$ (Ct127)	pBAD24 derivate	this work
pBAD24_ykfC$_{Ctr}$C172A	YkfC$_{Ctr}$ (Ct127) C172A mutant	pBAD24 derivate	this work
pBAD24_nlpC/P60$_{Ela}$	NlpC/P60$_{Ela}$ (ELAC_2173)	pBAD24 derivate	this work
pBAD24_nlpC/P60$_{Ela}$C193A	NlpC/P60$_{Ela}$ (ELAC_2173) C193A mutant	pBAD24 derivate	this work
pBAD24_nlpC/P60$_{Sne}$	NlpC/P60$_{Sne}$ (SNE.A23160)	pBAD24 derivate	this work
pBAD24_nlpC/P60$_{Sne}$C153A	NlpC/P60$_{Sne}$ (SNE.A23160) C153A mutant	pBAD24 derivate	this work
pBAD24_mepS$_{Eco}$	MepS$_{Eco}$	pBAD24 derivate	this work
pET-52b(+)	-	AmpR, T7, MCS, N-terminal Strep-tag II	Novagen
pET52b_ykfC$_{Cpn}$	YkfC$_{Cpn}$ (Cpn0246)	pET52 derivate	this work
pET52b_ykfC$_{Ctr}$	YkfC$_{Ctr}$ (Ct127)	pET52 derivate	this work
pET52b_ykfC$_{Ctr}$C172A	YkfC$_{Ctr}$ (Ct127) C172A mutant	pET52 derivate	this work
pET52b_amiA$_{Ctr}$	AmiA$_{Ctr}$ (Ct268)	pET52 derivate	this work

Name	Encoded construct	Features	Reference/ Source
pPR-IBA1	-	AmpR, T7, MCS, C- terminal Strep-tag II	IBA Lifesciences
pPR-IBA1_mraY$_{Cpn}$	MraY$_{Cpn}$ (Cpn0900)	IBA1 derivate	I. Löckener (Henrichfreise lab, University Bonn)
VLL-002_mraY$_{Cpn}$	*cpn0900* / MraY$_{Cpn}$	AmpR, T7, C-terminal His$_6$-tag	B. Henrichfreise (Henrichfreise *et al.*, 2009)

2.5. Biochemical methods

2.5.1. Recombinant protein production and purification

For protein production, 1-2 colonies of a freshly transformed *E. coli* production strain bearing the appropriate expression vector (tab. 2.6) were picked from a selective agar plate and grown overnight in 50 ml selective LB or TB autoinduction medium (for compositions see tab. 2.2) under vigorous shaking. Overnight cultures were used to inoculate 4 l of the appropriate selective production medium at 2 % (*v*/*v*) and incubated at 37 °C and 130 rpm to ensure good aeration. For production of recombinant MraY$_{Cpn}$, these parameters were changed to 30 °C and 110 rpm based on the protocol of Schneider and colleagues (Schneider *et al.*, 2009). As shown in table 2.7, expression conditions differed depending on the construct to be produced with regard to production strains, media, type of induction and incubation temperature and time. Despite performing expression screens, not all constructs could be successfully produced for purification in this work.

Table 2.7. Conditions determined for purification of recombinant proteins.

Construct	*E. coli* production strain	Production medium	Induction methode	Incubation conditions
MraY$_{Cpn}$	C43(DE3)	2 x 2 l 2xYT medium	1 mM IPTG at OD_{600nm} = 0.6	25 °C, 16 hours, 110 rpm
AmiA$_{Eco}$	JM83	2 x 2 l salt-free LB medium with 342 mM mannitol (Otten *et al.*, 2015)	200 ng/ml AHT at OD_{600nm} = 0.6	30 °C, 4 hours, 110 rpm

Construct	*E. coli* production strain	Production medium	Induction methode	Incubation conditions
$AmiA_{Eco}$_ ΔA148-S191	JM83	2 x 2 l salt-free LB medium with 342 mM mannitol (Otten *et al*., 2015)	200 ng/ml AHT at OD_{600nm} = 0.6	30 °C, 4 hours, 110 rpm
$EnvC_{Eco}$	JM83	2 x 2 l salt-free LB medium with 342 mM saccharose (Otten *et al*., 2015)	200 ng/ml AHT at OD_{600nm} = 0.6	30 °C, 4 hours, 110 rpm
$AmiA_{Ctr}$	C43(DE3)	4 x 1 l TB autoinduction medium (Studier, 2005)	autoinduction	30 °C, 20 hours, 110 rpm
$YkfC_{Ctr}$	C43(DE3)	4 x 1 l TB autoinduction medium (Studier, 2005)	autoinduction	30 °C, 20 hours, 110 rpm
$YkfC_{Ctr}$ C172A	C43(DE3)	4 x 1 l TB autoinduction medium (Studier, 2005)	autoinduction	30 °C, 20 hours, 110 rpm
$YkfC_{Cpn}$	C43(DE3)	4 x 1 l TB autoinduction medium (Studier, 2005)	autoinduction	30 °C, 20 hours, 110 rpm

After incubation, cells were harvested by centrifugation for 20 minutes at 7550 × g and 14 ºC. The resulting cell pellet was utilized for purification of recombinant protein by affinity chromatography. With the exception of recombinant $MraY_{Cpn}$, which was purified via His_6-tag (see section 2.5.1.a.), recombinant protein was purified via *Strep*-tactin (see section 2.5.1.b.).

2.5.1.a. Protein purification of by His_6-tag affinity chromatography

Purification of recombinant *C. pneumoniae* MraY ($MraY_{Cpn}$)

The recombinant transmembrane protein $MraY_{Cpn}$ was purified via a C-terminal His_6-tag as described by Henrichfreise and colleagues (Henrichfreise *et al*., 2009) based on the protocol of Schneider and colleagues (Schneider *et al.*, 2009) with minor changes. Harvested cell pellets of 4 l production culture were washed in 200 ml of 25 mM Tris-HCl, pH 8, and resuspended in 30 ml of the same buffer containing 2 mM 2-mercaptoethanol, 150 mM NaCl, 30 % (*v*/*v*) glycerol, and 1 mM $MgCl_2$ (buffer A). Subsequently, 1 U/ml benzonase was added and $MgCl_2$ concentration was increased to 3 mM. The cell suspension was sonicated and centrifuged at 31850 × g at 4 ºC for 30 minutes. The pellet was resuspended in 10 ml buffer A supplemented with

17.8 mM n-dodecyl-β-D-maltoside (DDM) and incubated on ice. After 50 minutes of incubation, the mixture was centrifuged (at 31850 × g for 30 minutes at 4°C) to separate membrane debris from solubilized membrane protein. The supernatant (S1) was collected and stored at - 20 °C, while the pellet was resuspended in 10 ml buffer A supplemented with 21.5 mM DDM and incubated for 30 minutes on ice. The mixture was centrifuged (at 31850 × g for 30 minutes at 4 °C) and the supernatant (S2) was collected.

Both supernatants (S1, S2) were further purified by using His_6-tag affinity chromatography. Each supernatant was incubated under gentle shaking at 4 °C with 1.5 ml of Ni-NTA agarose (Macherey-Nagel) which was previously washed twice with 10 ml of buffer A. After 3 hours of incubation, mixtures were loaded on columns for affinity chromatography and each rinsed first with 7.2 ml of buffer A and then with 7.2 ml of washing buffer (buffer A supplemented with 3.9 mM DDM and 10 mM imidazole). Recombinant protein was eluted by sequential adding 3 x 0.5 ml elution buffer 1 (buffer A with 3.9 mM DDM and 100 mM imidazole), elution buffer 2 (buffer A with 3.9 mM DDM and 200 mM imidazole) and elution buffer 3 (buffer A, with 3.9 mM DDM, 300 mM imidazole), respectively. Eluates were collected separately and stored at - 70 °C.

2.5.1.b. Protein purification by *Strep*-tactin affinity chromatography

Purification of recombinant AmiA ($AmiA_{Eco}$, $AmiA_{Eco}$ ΔA148-S191) and EnvC ($EnvC_{Eco}$) from *E. coli*

Recombinant $AmiA_{Eco}$, $AmiA_{Eco\Delta}$A148-S191, and $EnvC_{Eco}$ were purified via a C-terminal Strep-tag II by affinity chromatography using a 50 % Strep-tactin matrix (IBA Lifescience) following manufacturer's instructions for purification of periplasmic protein with slight modifications. Cell pellets harvested from 4 l of production culture were washed with 200 ml of 100 mM Tris-HCl, pH 8. Then pellets were resuspended in 20 ml of the same buffer containing 500 mM saccharose and 1 mM EDTA (buffer P) which was supplied with EDTA free Pierce proteinase inhibitor Mini tablets (Thermo Scientific). Cell suspensions were mixed with 1 mg/ml lysozyme, 1 U/mL benzonase and 2.5 mM $MgCl_2$ and incubated on ice. After 45 minutes of incubation, suspension were sonicated and centrifuged at 31850 × g at 4 ºC for 30 minutes. After centrifugation, the supernatant was loaded onto a column containing 1 ml of *Strep*-

Tactin Sepharose (IBA Lifescience) which had been pre-equilibrated with buffer A. Afterwards the column was washed six times with buffer W (100 mM Tris-HCl, pH 8, containing 150 mM NaCl and 1 mM EDTA). Recombinant protein was eluted by adding six times 0.5 ml of buffer E (100 mM Tris-HCl, pH 8, with 150 mM NaCl and 1 mM EDTA and 2.5 mM desthiobiotin). Eluates were collected separately, supplemented with 30 % (*v*/*v*) glycerol and stored at - 20 °C.

Purification of recombinant *C. pneumoniae* YkfC ($YkfC_{Cpn}$), *C. trachomatis* AmiA ($AmiA_{Ctr}$) and YkfC ($YkfC_{Ctr}$, $YkfC_{Ctr}$ C172A)

Recombinant $YkfC_{Cpn}$, $AmiA_{Ctr}$, $YkfC_{Ctr}$, and $YkfC_{Ctr}$ C172A were purified via an N-terminal Strep-tag II by affinity chromatography using *Strep*-tactin XT Sepharose (Merck) as matrix. Cell pellets harvested from 4 l of production culture were washed in 200 ml of 25 mM MOPS, pH 7.2, and resuspended in 40 ml of the same buffer containing 1 M NaCl and 1 mM $MgCl_2$ (buffer A). The cell suspensions was supplemented with 2 µg/ml polymyxin B, 1 mM phenylmethyl sulfonyl fluoride (PMSF) and 1 U/ml benzonase. Cells were broken by sonication, mixed with 0.5 % CHAPS and incubated at 4 ºC with gentle shaking. After 1 hour of incubation, the suspension was centrifuged for 1 hour at 310500 × g at 4 º C. The supernatant was loaded onto a *Strep*-tactin XT Sepharose column which had a bed volume of 1 ml and had been pre-equilibrated with buffer A. After the passage was complete, the column was washed 5 times with buffer B (25 mM MOPS, pH 7.2, containing 500 mM NaCl, 2 mM $MgCl_2$, 10 % (*v*/*v*) glycerol). Recombinant protein was eluted by adding six times 0.5 ml of buffer C (25 mM MOPS, pH 7.2, supplemented with 300 mM NaCl, 2 mM $MgCl_2$, 10 % (*v*/*v*) glycerol and 50 mM desthiobiotin). Eluates were dialysed against 2 x 1 l dialysis buffer (25 mM MOPS, pH 7.2, 150 mM NaCl, 2 mM $MgCl_2$, 10 % (*v*/*v*) glycerol and 2 mM dithiothreitol (DTT) (Pharma Biotech)) at 4 ºC overnight. For $YkfC_{Ctr}$ inhibitor screens, DTT was omitted from the buffer. After dialysis, eluates were aliquoted and stored at - 70 ºC.

2.5.2. Quantification of recombinant protein with Bradford reagent

The concentration of recombinant purified protein was determined using Bradford reagent (Bradford, 1976) containing Coomassie Brilliant Blue G250, a dye which interacts with positively charged amino acid residues and thereby exhibits an

absorbance shift to 595 nm. Bradford reagent (BioRad) was diluted 1:5 in water and 200 µl of the dilution were mixed with 10 µl of protein sample in a 96-well Greiner plate and incubated for 10 minutes at room temperature and protected from light. For quantification, a bovine serum albumin standard was prepared and treated similar to the sample. After the incubation, absorbance was measured at 595 nm using a Tecan infinite M200 plate reader and the Magellan V.6.5 software (Tecan) (tab 2.1).

2.5.3. Protein analysis by SDS-PAGE

Sodium dodecyl sulfate polyacrylamide gel electrophoresis (SDS-PAGE), a method developed by Laemmli (Laemmli, 1970) allows to determine presence and purity of purified protein. In this work, protein analysis by electrophoresis was performed using 4-12 % gradient polyacrylamide GenScript ExpressPlus pre-cast gels (GenScript) with running buffer and conditions following the manufacturer's instructions. For protein denaturation, samples were incubated at 95 °C for 5 minutes with NuPAGE LDS sample buffer (Thermo Scientific) and 5 mM dithiothreitol (DTT) (Pharma Biotech), which served as reducing agent to break intramolecular dissulfide linkages. After gel electrophoresis, the gel was stained with PageBlue protein staining solution (Thermo Scientific) and subsequently washed with water for destaining. The size of protein bands was estimated visually by comparison to a molecular weight maker (PageRuler Plus Prestained protein ladder; Thermo Scientific).

2.5.4. Preparation and Remazol staining of *E. coli* peptidoglycan sacculi

The preparation and Remazol staining of *E. coli* peptidoglycan (PG) sacculi was performed according to a protocol by Uehara and colleagues with slight modifications (Uehara *et al*., 2010). 4 l of LB were inoculated 1 % (*v*/*v*) with an overnight culture of *E. coli* W3110 (see section. 2.3.2.a.) and incubated at 37 °C under shaking until an OD_{600nm} of 0.6 was reached. Cells were harvested via centrifugation for 15 minutes at 11,160 x g and 4 °C. The pellet was resuspended in 40 ml PBS buffer (16 mM Na_2HPO_4, 4 mM KH_2PO_4, 115 mM NaCl, pH 7,4) and the suspension poured into 160 ml boiling 5 % (*w*/*v*) SDS in PBS. After the mixture was boiled with stirring for 30 minutes, it was incubated overnight at room temperature. The suspension was then centrifuged at 30,137 x g for 30 minutes and the pellet washed three times with 100 ml H_2O before being resuspended in 4 ml PBS containing bovine pancreatic α-

chymotrypsin at a final concentration of 0.3 mg/ml. The suspension was incubated overnight at 37 °C. Thereafter, α-chymotrypsin was again added to a final concentration of 0.6 mg/ml and the incubation continued for 3 hours at 37 °C. Then 1 ml of 5 % (*w*/*v*) SDS in PBS was added and the mixture incubated for 2 hours at 95 °C.

Afterwards PG sacculi were harvested by centrifugation at 29,680 x g for 30 minutes and the pellet was washed three times with 2 ml H_2O before being resuspended in 2 ml of PBS containing α-amylase from *Aspergillus oryzae* at a final concentration of 0.2 mg/ml. After 2 hours incubation, the amylase-treated sacculi were washed three times with 2 ml H_2O and then resuspended in 20 mM Remazol Brilliant Blue (RBB) dissolved in 4 ml 0.25 M NaOH and incubated at 37 °C overnight. The suspension was then neutralized by the addition of 487.2 µl of 1M HCl. The stained PG sacculi were harvested by centrifugation at 29,680 x g for 30 minutes and and repeatedly washed with H_2O until the supernatant was clear. The pelleted RBB-PG sacculi were frozen at - 70 °C, lyophilized in a lyophilizer (Martin Christ GmbH), and then stored at - 20 °C.

2.5.5. *In vitro* assays using purified recombinant protein

2.5.5.a. MraY *in vitro* activity assay

Henrichfreise and colleagues showed the ability of recombinant purified $MraY_{Cpn}$ to produce lipid I *in vitro* (Henrichfreise *et al*., 2009). Based on their protocol, an *in vitro* assay was performed both to verify purification of active recombinant $MraY_{Cpn}$ and to study the effect of potential inhibitors of chlamydial MraY on this reaction (see section 2.5.5.b). Two substrates are needed for $MraY_{Cpn}$ to generate lipid I *in vitro*: lipid carrier C_{55}-P and 'crude substrate' containing UDP-MurNAc-pentapeptide (mDAP type). The latter was prepared from *Bacillus cereus* DSM2302 and kindly provided by I. Bodenstein (Schneider group, University Bonn). Since concentration of recombinant $MraY_{Cpn}$ and 'crude substrate' could not be precisely determined, pre-tests were carried out to determine an optimal ratio between enzyme and substrate. The optimized reaction was carried out in a final volume of 50 µl. For substrate preparation, 2.5 nmol C_{55}-P (Larodan) were dried in solvent resistant tubes and subsequently solved in triton X-100 (with a final concentration of 0.43 % (*w*/*v*)) by vortexing for 1 minute. Afterwards 75 mM Tris-HCl, pH 7.5, 6 mM $MgCl_2$, 10 % (*v*/*v*)

DMSO and 'crude substrate' were added and the reaction was started by adding recombinant $MraY_{Cpn}$. The reaction mixtures was incubated at 30 °C for 90 minutes. After the incubation, lipid reaction products were extracted and analyzed by thin layer chromatography (TLC) ('TLC lipids') as described in section 2.5.6.a.

2.5.5.b. Testing putative inhibitors of MraY *in vitro* activity

Putative inhibitors of chlamydial MraY were tested for their effect in the enzyme's *in vitro* activity assay described in section 2.5.5.a. The compounds were added prior to starting the reaction by adding recombinant $MraY_{Cpn}$. Putative inhibitors tested in this work were muraymycin and its derivates, which were kindly provided by S. Ichikawa (Center for Research & Education on Drug Discovery, Hokkaido University, Japan).

2.5.5.c. Analysis of *in vitro* activity towards lipid II

To analyze enzymatic activity of recombinant purified protein on the PG precursor molecule lipid II, 2 nmol lipid II (mDAP type) were dried in solvent resistant tubes and subsequently solved in the reaction mixture by vortexing for 3 minutes. The reaction was started by adding the enzyme to be analyzed and subsequently incubated overnight at 37 ° C. To analyze *in vitro* activity of $AmiA_{Ctr}$ towards lipid II, the reaction contained 50 mM Tris-HCl buffer, pH 8.5, 150 mM NaCl, 2 mM $MgCl_2$, 0.02 mM ZnCl, triton X-100 in a final concentration of 0.1 % (*v/v*) and 4 µM enzyme. For *Chlamydia* $YkfC_{Ctr}$, composition of the reaction is described in section 2.5.5.f. To analyze *in vitro* activity of *Bacillus* $YkfC_{Bsu}$ towards lipid II, the reaction contained 50 mM MOPS buffer, pH 7.5, triton X-100 in a final concentration of 0.1 % (*v/v*) and 2 µM enzyme. After incubation, lipid II was extracted for analysis by TLC ('TLC lipids') as described in section 2.5.6.a.

2.5.5.d. Remazol dye release assay

To test recombinant purified protein for hydrolytic activity on PG, isolated RBB-stained PG sacculi from *E. coli* W3110 (see section 2.5.4.) were used as substrate. Assays were carried out in a final volume of 100 µl containing 1.25 µg of RBB-stained PG sacculi. To detect activity of AmiA from *C. trachomatis* or *E. coli*, the reaction also contained 7 µM of protein, 50 mM Hepes buffer pH 7.5 and 2 % (*v*/*v*) DMSO. To investigate activity of *C. trachomatis* YkfC, 4 µM protein, 50 mM MOPS pH 7.5,

150 mM NaCl and 2 mM $MgCl_2$ were added. Each reaction was incubated overnight at 37 °C. Subsequently, insoluble material was removed by centrifugation for 10 min at 21000 × g and 4 °C. Hydrolytic activity releases remazol dye into the supernatant, while no activity leaves the PG sacculi intact, leaving the supernatant colorless. To detect remazol, the supernatant was measured at 595 nm using a spectrophotometer (NanoPhotometer, Implen).

2.5.5.e. Analysis of *in vitro* activity of YkfC

In order to analyze peptidase activity of recombinant purified YkfC of *C. trachomatis* ($YkfC_{Ctr}$), the protein was tested for its *in vitro* activity using L-Ala-γ-D-Glu-mDAP tripeptide (Tri-DAP; InvivoGen) as substrate. To optimize the assay, different pH values of the reaction were tested (50 mM MES buffer for pH 5.5 and 6.5; 50 mM MOPS buffer for pH 7.5; 50 mM CHES buffer for pH 9.5). The standard $YkfC_{Ctr}$ *in vitro* assay in this work was carried out in a final volume of 25 µl containing 50 mM MOPS buffer pH 7.5, 150 mM NaCl, 2 mM $MgCl_2$, 0.5 mM substrate and lastly 2 µM enzyme solved in dilution buffer. Adding the enzyme started the reaction which was subsequently incubated at 37 ºC for 2 hours. It was terminated by incubation for 5 minutes at 100 ºC, followed by centrifugation for 5 minutes at 17000 x g. The supernatant was collected and 20 µl were analyzed by TLC for the detection of peptides (‘TLC peptides’, section 2.5.6.b).

2.5.5.f. Analysis of substrate specificity of YkfC

Activity of $YkfC_{Ctr}$ was tested on different substrates to analyze its specificity. In order to test potential substrates, the *in vitro* assay was carried out as described in section 2.5.5.e. Each reaction had a final volume of 25 µl containing 1 mM of the respective substrate solved in H_2O and 2 µM enzyme. After 2 hours of incubation at 37 ºC, the supernatants were collected and analyzed in a TLC system for peptide detection (‘TLC peptides’, section 2.5.6.b.).

For lipid II as a substrate, the procedure was adjusted as follows: The total reaction volume was increased to 50 µl and contained triton X-100 in a final concentration of 0.1 % (*v/v*). For substrate preparation, 4 nmol lipid II (mDAP type) were dried in solvent resistant tubes and subsequently solved in the reaction mixture (lacking the enzyme) by vortexing for 3 minutes. The reaction was started by adding the enzyme

and incubated overnight at 37 ºC. It was terminated by incubation for 5 minutes at 100 ºC, followed by centrifugation for 5 minutes at 17000 x g. The supernatant was collected and divided into two samples, each with a volume of 20 µl, which were analyzed separately. One sample was analyzed using the TLC system for peptide detection (‘TLC peptides’, section 2.5.6.b.) Lipid II was extracted from the other sample for analysis on a TLC system for lipid detection (‘TLC lipids’, section 2.5.6.a.). To test PG-derived peptides as potential substrates, mixtures of peptides derived from *E. coli* or *B. subtilis* PG were kindly provided by R. Kluj (Mayer lab, Department of Microbiology/Organismic Interactions, University of Tübingen). For the generation of these substrates, PG from both species was digested with recombinant *B. subtilis* amidase CwlC, as described by Walter and colleagues (Walter *et al*., 2021). The peptide mixtures were incubated with recombinant $YkfC_{Ctr}$ following the enzyme’s standard *in vitro* assay (see section 2.5.5.f.). Reaction products were analyzed by mass spectrometry performed by R. Kluj (see section 2.5.7.).

2.5.5.g. Testing putative inhibitors of YkfC *in vitro* activity

Different inhibitors were tested for their effect towards *in vitro* γ-D-Glu-mDAP peptidase activity of $YkfC_{Ctr}$. Chloroactenone, iodoacetamide, phenylmethylsulfonyl fluoride (PMSF) and E-63 were purchased from Merck. Derivates of the of α,β-unsaturated carbonyl compound α-X-chalcone were kindly provided by S. Amslinger (Institute of Organic Chemistry, University of Regensburg). Inhibitors were solved in H_2O to generate 1 mM stock solutions. The $YkfC_{Ctr}$ *in vitro* assay with tripeptide as the substrate was carried out as described in section 2.5.5.f. with the following modification: Instead of starting the reaction by adding the enzyme, $YkfC_{Ctr}$ was pre-incubated with the inhibitor for 15 minutes at room temperature, prior to adding the substrate to start the reaction. The subsequent steps were continued as described above and reaction products were analyzed in a TLC system for peptide detection (‘TLC peptides’, section 2.5.6.b.).

2.5.6. Thin layer chromatography (TLC)

Thin layer chromatography (TLC) was used to analyze reaction products of *in vitro* assays with purified recombinant protein. HPTLC alumina silica gel 60 plates (Merck Millipore) were used for all TLC analyses. Depending on which components were to

be detected, two systems with different mobile phases and staining methods were used. The first allowed visualization of lipids and was used to either detect production of lipid I by recombinant *C. pneumoniae* MraY or to analyze enzymatic activity towards lipid II ('TLC lipids', section 2.5.6.a.). The second system enabled analysis of peptidase activity of recombinant enzymes by detecting peptides and amino acids ('TLC peptides', section 2.5.6.b.).

2.5.6.a. TLC for the detection of lipids

To detect either production of lipid I or hydrolytic activity towards lipid II, the reactions of the respective *in vitro* assays were terminated and centrifugation for 5 minutes at 17,000 x g. Subsequently the supernatant was collected. Lipids were extracted into the organic phase by adding n-butanol/pyridine acetate (1:4 (*v/v)*, pH 4.2) in a ratio of 1:1 (*v/v*) to the supernatant followed by vortexing for 3 minutes. Phases were separated by centrifugation at 17,000 x g for 5 minutes and the organic phase was spotted on a silicate plate. Based on the method by Rick (Rick *et al*., 1998), chloroform-methanol-water-ammonia (88:48:10:1) was used as mobile phase. To visualize lipid II, TLC plates were stained by engulfing them in phosphomolybdic acid stain (2.5 % (*w/v*) phosphomolybdic acid, 1 % (*w/v*) ceric-sulfate solved in 6 % (*v/v*) sulfuric acid), followed by drying and heating at 120 °C using a hot plate.

2.5.6.b. TLC for the detection of peptides

In order to visualize peptides and amino acids to investigate peptidase activity of purified recombinant protein, reaction products of *in vitro* assays were analyzed by TLC. Terminated reactions were centrifuged by 17000 x g for 5 minutes and 20 µl of the supernatant were spotted on a silicate plate. TLC was performed using 2-butanol-pyridine-ammonia-water (39:34:10:26) as mobile phase and separation was visualized by spraying the dried plate with ninhydrin stain (0.2 % (*w/v*) ninhydrin, 0.5 % (*v/v*) acetic acid solved in 99.8 % p.A ethanol). Since staining may take some time, it is advisable to store the plates overnight completely protected from light before evaluating them.

2.5.7. High performance liquid chromatography and mass spectrometry (HPLC-MS)

In order to investigate activity of recombinant purified $YkfC_{Ctr}$ on peptides derived from *E. coli* or *B. subtilis* PG, reaction products of the *in vitro* assay (section 2.5.5.f) were analyzed by high performance liquid chromatography (HPLC) combined with mass spectrometry (MS). HPLC-MS was kindly performed by R. Kluj (Mayer lab, Department of Microbiology/Organismic Interactions, University of Tübingen) using an electrospray ionisation (ESI) time of flight mass spectrometer (MS) (microTOF II, Bruker Daltonics) connected with an UltiMate 3000 HPLC (Dionex). Soluble components in 5 µl samples were separated on a reversed-phase C18 column (Gemini 5 µm C18 110 Å 150 mm × 4.6 mm; Phenomenex) in an UltiMate 3000 HPLC (Dionex) by applying a 30-min linear gradient of 0-40 % acetonitrile (buffer A: 100 % acetonitrile) at a flow rate of 0.2 ml/min. Before each run, the column was pre-equilibrated with 0.01 % formic acid/0.05 % ammonium formate, followed by the linear gradient to 100 % acetonitrile. After each run, the column was rinsed for 12.45 minutes with 60 % acetonitrile and subsequently re-equibrilated for 12.45 minutes with 0.01 % formic acid/0.05 % ammonium formate. The mass-to-charge rations of the separated samples were analyzed by MS, operating in negative ion mode with a mass range of 120-1000. Extracted ion chromatograms for PG-derived tripeptide (3P; theoretical mass $[M-H]^-$ = 389.167), tetrapeptide (4P; $[M-H]^-$ = 460.204), mDAP ($[M-H]^-$ = 189.087) and mDAP-Ala ($[M-H]^-$ = 260.124) were obtained within an error range of ± 0.02.

2.6. Complementation assays using *E. coli* mutant strains

2.6.1. Complementation of an DapD- and Mpl-deficient *E. coli* mutant

To test chlamydial proteins for their ability to degrade PG-derived L-Ala-y-D-Glu-mDAP tripeptide *in vivo*, an *E. coli* AT980 mutant strain, deficient for DapD and with a deletion of the *mpl* gene (see section 2.3.2.c) was used. It is hereinafter referred to as *E. coli dapD*$^-$ Δ*mpl* mutant. To avoid activity of the *E. coli* peptidase MpaA, the complementation assay was performed in terrific broth (TB) (tab. 2.2), since the transcriptional regulator PgrR diminishes expression of MpaA under nutrient-rich growth conditions (Uehara & Park, 2003; Shimada *et al.*, 2013).

Cells of the *E. coli dapD*$^{-}$ Δ*mpl* mutant strain were transformed by heat shock (see section 2.3.3.b.) with pBAD24+ expression vectors harboring the constructs of interest (tab. 2.6.). For each construct, three colonies of the appropriate transformed mutant strain were separately picked and each inoculated in 5 ml of LB medium containing 200 µg/ml mDAP (Fluka), 100 µg/ml ampicillin and 34 µg/ml chloramphenicol. Cultures were grown at 37 °C under vigorous shaking for 16 hours. Subsequently, 150 µl of each culture were diluted in 5 ml of TB medium containing 200 µg/ml mDAP, 100 µg/ml ampicillin and 0.4 % (*w*/*v*) L-arabinose. Fresh cultures were grown at 37 °C under vigorous shaking. Once cells reached an OD_{600nm} of 1, 1 ml of each culture was harvested by centrifugation at 26,000 x g and 4 °C for 15 minutes. Cell pellets were washed twice, each time being resuspended in 1 ml TB, followed by centrifugation (26,000 x g, 4 °C, 15 minutes). Finally, pellets resuspended in 1 ml of TB were diluted 1:3 in TB medium. The cell suspensions were each loaded into a well on a 96-well Greiner plate. Each well was prepared with 100 µl TB containing 200 µg/ml ampicillin and 0.8 % (*w*/*v*) L-arabinose supplemented with 80 µM tripeptide (Tri-DAP; InvivoGen). By adding 100 µl of cell suspension, medium additives were diluted 1:2 (final concentrations: 100 µg/ml ampicillin, 0.4 % (*w*/*v*) L-arabinose, 40 µM tripeptide). The Tecan Spark 10M plater reader and the SPARKCONTROL Magellan 1.2. software (Tecan) (tab. 2.1) were used to incubate the cells while simultaneously monitoring their growth. The sample-loaded 96-plate was incubated for 6 hours at 37 °C with intermittent shaking every 15 minutes and measuring OD_{600nm} every 30 minutes. To compare the influence of the expressed constructs on the growth of the *E. coli dapD*$^{-}$ Δ*mpl* mutant, the logarithm of the OD_{600nm} values minus the value measured at the starting point of the incubation (referred to as $\Delta \ln OD_{600nm}$ value) was plotted against time.

2.6.2. Complementation of an MepS-deficient *E. coli* mutant

The *E. coli* JW2163-3 strain (see section 2.3.2.c) carries a deletion of the *mepS* gene and is hereinafter referred to as *E. coli* Δ*mepS* mutant. An *E. coli* MepS-deficient strain is characterized by the inability to grow on low osmolarity nutrient broth agar (NA) plates (tab. 2.2) at high temperature (Hara *et al.*, 1996). This mutant strain was used to test for putative PG endopeptidase activity of chlamydial proteins. Since multicopy expression of *E. coli* MepS ($Meps_{Eco}$) was shown to suppress the

phenotypic defects of the mutant (Singh *et al*., 2012), $MepS_{Eco}$ was overproduced as a positive control.

Cells of the *E. coli* Δ*mepS* mutant strain were transformed by heat shock (see section 2.3.3.b.) with pBAD24+ expression vectors harboring the constructs of interest (tab. 2.6). For each construct, three colonies of the appropriate transformed mutant strain were separately picked and each grown in 5 ml of LB medium containing 100 µg/ml ampicillin and 30 µg/ml kanamycin at 30 °C under vigorous shaking for 16 hours. Subsequently, 150 µl of each culture were transferred in 5 ml of nutrient broth containing 100 µg/ml ampicillin and 30 µg/ml kanamycin. Cultures were grown at 30 °C under vigorous shaking and harvested at an OD_{600nm} of 1. For cell harvest, 1 ml of each culture was centrifuged at 26,000 x g and 4 °C for 15 minutes. Cell pellets were resuspended in 1 ml of a 0.9 % (*w*/*v*) NaCl solution and starting from this suspension a 1:10 serial dilution was carried out in 0.9 % (*w*/*v*) NaCl in a 96-well Greiner plate. Dilutions were plated on NA plates containing 0.04 % (*w*/*v*) L-arabinose using a replica plater (Merck). After drying, plates were incubated overnight at 30 °C, 37 °C and 42 °C, respectively.

2.7. Investigation of the antichlamydial effect of compounds in a cell culture based *C. trachomatis* D/UW-3/CX infection model

2.7.1. Preparation of Hep2 host cells for cell culture based experiments

To investigate the cytotoxic effects of compounds on Hep2 cells (see section 2.7.2) and to determine their minimal inhibitory concentration (MIC) against *Chlamydia* infection (see section 2.7.3), Hep2 host cells were prepared as follows. Cells grown in a ell culture flasks were detached by treatment with trypsin as described in section 2.3.4.c and seeded into a flat TC-96-well plate (Sarstedt) with approximately 1250-1750 Hep2 cells diluted in 200 µl DMEM per well (for medium composition see section 2.3.1.b). Cells were grown into a confluent monolayer at 37 °C and 5 % (*v*/*v*) CO_2 for 48 hours. Before the Hep2 cells were used for assays, they were washed twice with 100 µl MIC-DMEM (DMEM without the addition of gentamicin and amphotericin B) per well to remove gentamicin and amphotericin B.

2.7.2. Alamar Blue cell viability assay

The Alamar Blue assay for cell viability (Thermo Scientific) was used to assess the cytotoxic effect of antimicrobial compounds on mammalian Hep2 cells. This assay utilizes resazurin to detect living cells by their reducing power. Resazurin is a non-toxic, cell-permeable compound that is blue in color and virtually non-fluorescent. In living cells, it is reduced to resorufin, a red colored and highly fluorescent compound that can be detected in a fluorescence-based plate reader.

For the cell viability assay, 200 µl of fresh MIC-DMEM per well was added to Hep2 cells that had been grown into a monolayer and prepared as described in section 2.7.1. The compound of interest was added at serially diluted concentrations from 128 µg/ml to 1 µg/ml. Cells were treated with 70 % (*v*/*v*) EtOH and the vehicle control as standards. After treatment, the cells were incubated for 28 hours at 37 °C and 5 % (*v*/*v*) CO_2. Then cells were washed twice with HBSS before adding 100 µl per well of alamarBlue Cell Viability Reagent (Invitrogen, Thermo Scientific) diluted 1:10 in HBSS. After 1-2 hours of incubation at 37 °C and and 5 % (*v*/*v*) CO_2, the supernatant was transferred into a black 96-well plate (Greiner). The assay was evaluated by measuring the supernatant fluorescence at 550 nm excitation and 595 nm emission wavelength using a Tecan Spark 10M plater reader and the SPARKCONTROL Magellan 1.2. software (Tecan) (tab. 2.1). Following the fluorescence readout, the relative proportion of living cells was determined using the values obtained from treatment with EtOH (0 % cell viability) and the vehicle control (100 % cell viability) as standards. The IC_{50} value was determined as the compound concentration at which 50 % of the Hep2 cells were still viable.

2.7.3. Determination of a compound's minimal inhibitory concentration (MIC) against *Chlamydia* infection

For free-living bacteria, the minimum inhibitory concentration (MIC) is defined as the lowest concentration of an antimicrobial compound that inhibits the visible growth of the organism. In the case of obligate intracellular *Chlamydia*, MIC determination is performed by evaluating the effect of a compound on the amount and morphology of chlamydial inclusions as well as its effect on the morphology of chlamydial cells (Donati et al. 2010; Suchland et al. 2003). Kintner and colleagues introduced a cell culture-based assay that allows to study the effect of antimicrobial compounds in a

Chlamydia infection model by using fluorescence microscopy (Kintner *et al*., 2014). Based on this method, an assay was established in the Henrichfreise group that enables the investigation of the effect of compounds on a productive *C. trachomatis* D/UW-3/CX infection in mammalian culture (Klöckner, 2016) (see section 2.7.3.a). In addition, this assay has been extended to include the introduction of penicillin G-induced chlamydial persistence, so that compounds can be tested for their effect on *C. trachomatis* in a persistent state (Brunke, 2018) (see section 2.7.3.b).

2.7.3.a. Determination of the MIC against a productive *Chlamydia* infection

For MIC determination, Hep2 cell monolayers prepared as described in section 2.7.1 were infected with freshly prepared *C. trachomatis* D/UW-3/CX EB-containing lysate (for preparation see section 2.3.4.e). For this purpose, 200 µl of fresh MIC-DMEM and 50 µl of the EB lysate were added per well. This step marked the beginning of the infection and was referred to as 0 hours post infection (hpI). The cells were incubated at 37 °C and 5 % (*v*/*v*) CO_2 to allow the infection to proceed. After for 2 hours of incubation, cells were washed twice with MIC-DMEM to remove free EBs before adding 100 µl medium per well. Test compounds were added at either 2 hpI (‘early application’) or 12 hpI (‘late application’) in a serial dilution ranging from 128 µg/ml to 1 µg/ml. Finally, at 30 hpI, cells were washed twice with 100 µL HBSS per well before treatment with iced methanol for cell fixation. Plates were then stored at - 70 °C until cells were stained and examined by fluorescence microscopy as described in section 2.7.4.

2.7.3.b. Determination of the MIC against a *Chlamydia* infection in a penicillin G-induced persistent state

For MIC determination against *Chlamydia* in a penicillin G-induced persistent state, Hep2 cells were infected with chlamydial EBs as described for MIC determination in an productive infection model (see section 2.7.3.a). At 2 hpI, medium was changed to MIC-DMEM supplied with 100 U/ml penicillin, a concentration shown to be effective to induce a persistent chlamydial condition under the test conditions (Brunke, 2018). The procedure was then carried out as described in section 2.7.3.a.

2.7.4. Evaluation of cell culture based experiments by fluorescence microscopy

To stain both Hep2 and *C. trachomatis* D/UW-3/CX cells for fluorescence microscopic analysis, the Pathfinder *Chlamydi*a Culture Confirmation system by Bio-Rad (Bio-Rad Laboratories) and 4′,6-diamidin-2-phenylindol (DAPI) dye were used. The Pathfinder solution contains fluorescein-conjugated murine monoclonal antibody specific for *Chlamydia* LPS and Evans' blue dye to stain the cytoplasm of Hep2 cells. DAPI dye dissolved in PBS in a concentration of 0.1 mg/ml was used to stain DNA.

The methanol-fixated and frozen cells were thawed and rinsed two times with 100 µl PBS per well. Subsequent dyeing steps were carried out protected from daylight to prevent bleaching of the fluorescent components. The Pathfinder solution was diluted 1:10 in PBS before adding 100 µl to each well and incubating the plate for 30 minutes at 37 °C. After removing the Pathfinder solution, 100 µl PBS and 3 µl DAPI dye were added per well and the plate incubated for one minute. The plates were then washed twice by adding 100 µl of fresh PBS per well for 10 minutes at 4 °C. Finally, cells were covered with 100 µl PBS per well and stored protected from light at 4 °C.

Microscopic evaluation was conducted by using an Axio observer Z.1 fluorescence microscope, the Zen2 (blue edition) software (tab. 2.1) and a HXP 120C type lamp (Carl Zeiss Microscopy GmbH).

3. Results

3.1. Analysis of novel compounds in a *Chlamydia* cell culture infection model

Since obligate intracellular chlamydiae depend on healthy and functional host cells for optimal growth and replication, strategies to analyze putative antichlamydial compounds must not only focus on their effect towards the bacteria but also on their impact on the mammalian host cells. To study the effect of antimicrobial compounds on chlamydiae, the Henrichfreise group uses a cell culture model in which human Hep2 cells are infected with the clinically relevant *C. trachomatis* D/UW-3/CX strain (see section 2.7). In addition to testing antichlamydial effects, cytotoxicity towards non-infected Hep2 cells has to be determined. For this purpose, a resazurin-based microplate cell viability assay called Alamar Blue assay (see section 2.7.2) was used in this work. Preparation of host cells, compound concentration range and incubation time in the cell viability assay were adjusted to the conditions used for testing the antichlamydial effect of the compound of interest. The Alamar Blue Assay uses non-toxic, cell-permeable resazurin, which is reduced to resorufin by the natural reducing power of living cells. Resorufin is a red colored and highly fluorescent compound whose detection in a fluorescence-based plate reader can be used to monitor cell viability. Here, a set of eight novel antimicrobial candidate compounds was analyzed for its antichlamydial activity, and in this process the validity and limitations of the Alamar Blue assay compared to fluorescence microscopic analysis became evident (see section 3.1.1). In addition, the cytotoxicity of antimicrobial compounds already known to inhibit targets inside the bacterial peptidoglycan (PG) precursor biosynthesis was determined (section 3.1.2), as these compounds can serve as tools to elucidate the importance of this process for chlamydial development.

3.1.1. Analysis of the antichlamydial effect of novel candidate compounds

The Alamar Blue microplate assay allows efficient screening for cell viability. It was suggested to use this test system not only for determining cytotoxicity of antimicrobial compounds but also as a tool for measuring chlamydial infection in eukaryotic host cells (Osaka & Hefty, 2013). However, its application is limited by the fact that it fails to detect persistent chlamydial infection by which the host cell's capacity to reduce resazurin is not impaired. Therefore, fluorescence-microscopy is indispensable for reliable analysis of inhibitory effects on chlamydiae (Klöckner, 2016). With this in

mind, the Alamar Blue assay was used as a pre-test for cytotoxicity towards Hep2 host cells prior to fluorescence-microscopy based analysis of chlamydiae.

Eight novel antimicrobial candidate compounds (CC1-CC8) were examined for their antichlamydial activity in this workflow. First, their cytotoxicity towards mammalian host cells was analyzed in the Alamar Blue test system. The determined IC_{50} values ranged between 18 µg/ml and 96 µg/ml and are shown in figure 3.1.

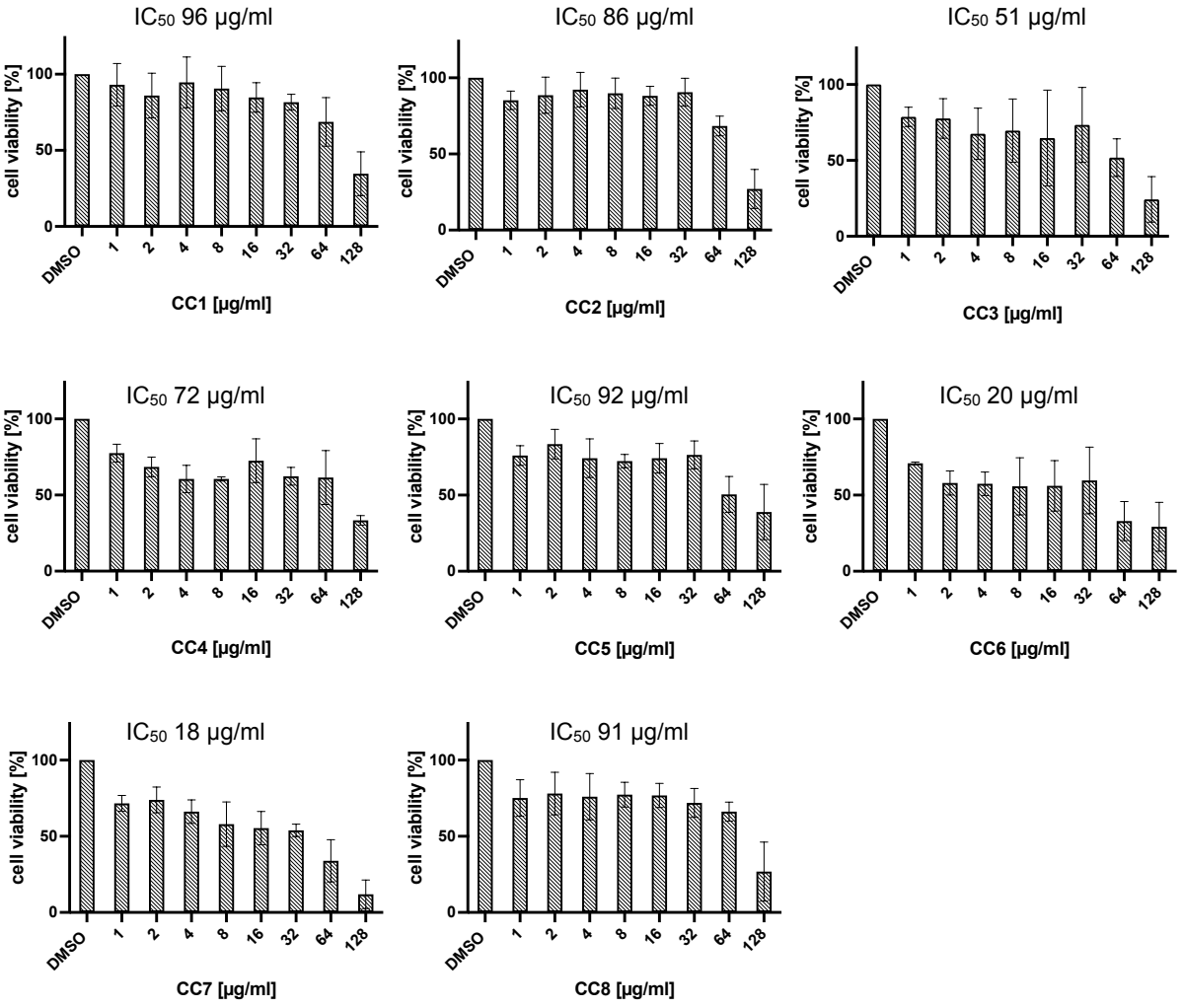

Figure 3.1. Alamar Blue cell viability assay for the treatment of mammalian Hep2 cells with novel antimicrobial candidate compounds. A cytotoxic effect was determined for candidate compound CC1-CC8 as the IC_{50} at 28 hours treatment duration (n=3).

The candidate compounds were then tested in a Hep2 cell culture-based *Chlamydia* infection model, which has been established in the Henrichfreise group to determine the minimum inhibitory concentration (MIC) of compounds against the clinically relevant strain *C. trachomatis* D/UW-3/CX (Klöckner, 2016). For free-living bacteria, the MIC is defined as the lowest concentration of an antimicrobial agent that inhibits visible bacterial growth (Andrews, 2001). For antibiotics that affect chlamydial inclusion formation, the MIC can be determined by analyzing the presence and quantity of inclusions (Donati *et al.,* 2010). Some antimicrobial agents especially PG synthesis-targeting β-lactam antibiotics induce formation of persistent aberrant bodies (ABs) in *Chlamydia* (Kintner *et al*., 2014; Klöckner, 2016). For these agents, the MIC is defined as the lowest concentration that induces the occurrence of abnormal inclusion morphology (Storey & Chopra, 2001), making fluorescence-microscopy analysis essential for antichlamydial MIC determination.

The standard setting for MIC detection in this work covered one round of the widely synchronized biphasic chlamydial life cycle (fig. 3.2.a & b). Hep2 cells were grown to a confluent monolayer prior to infection with *C. trachomatis* D/UW-3/CX. Compounds of interest were added at 2 hours post infection (hpI) in concentrations ranging from 1 µg/ml to 128 µg/ml. As vehicle control, Hep2 cells were treated with DMSO, which served as solvent for the compounds. After 28 hours of incubation in presence of the compound, cells were fixated and stained with three different dyes. A fluorescein-conjugated monoclonal antibody that binds chlamydial lipopolysaccharide (LPS) was used to stain both, chlamydial elementary bodies (EBs) and reticular bodies (RBs). In addition, Evans' blue and DAPI dyes were used to counter-stain host cell cytoplasm and DNA, respectively. The assay was evaluated using fluorescence-microscopy.

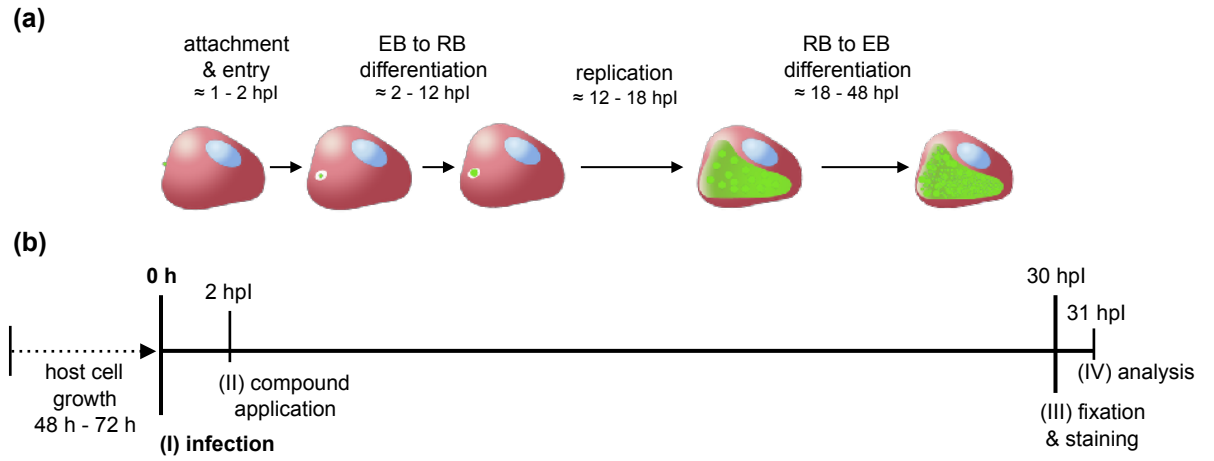

(c) Treatment of *Chlamydia* infected Hep2 cells

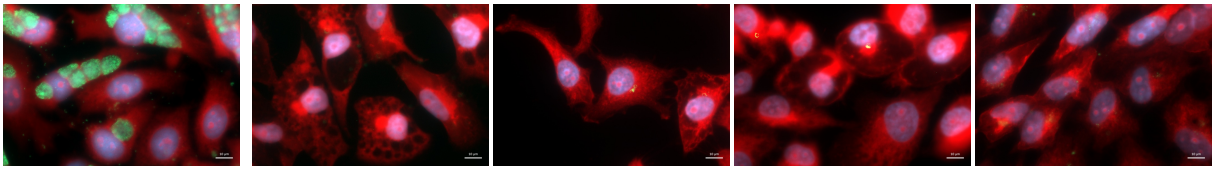

Vehicle control, infected | **CC3** 8 µg/ml | **CC4** 4 µg/ml | **CC6** 4 µg/ml | **CC7** 8 µg/ml

(d) Treatment of uninfected Hep2 cells

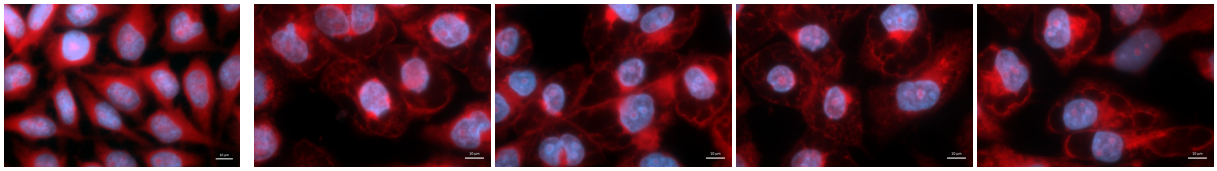

Vehicle control, uninfected | **CC3** 8 µg/ml | **CC4** 4 µg/ml | **CC6** 4 µg/ml | **CC7** 8 µg/ml

Figure 3.2. Fluorescence microscopic analysis of the effect of candidate compounds CC3, CC4, CC6 and CC7 on a productive *Chlamydia* infection model and on Hep2 host cells. Based on the **(a)** different stages of the chlamydial development cycle in a mammalian host cell, **(b)** a workflow for analyzing a compounds effect on a productive chlamydial infection was established (Klöckner, 2016). Hep2 cells were grown for 48-72 hours into a confluent monolayer and infected with *C. trachomatis* D/UW-3/CX (I). The compound of interest was added at 2 hpI (II) and cells were incubated for additional 28 hours. Subsequently, samples were fixed with absolute methanol (-20 °C). Fixated cells were stained with a fluorescein-conjugated monoclonal antibody that binds to chlamydial LPS (green), Evans' blue day staining Hep2 cytoplasm (red) and DAPI dye staining Hep2 nuclei (blue) (III) and analyzed via fluorescence-microscopy (IV). The experimental procedure was used to **(c)** analyze the effect of CC3, CC4, CC6 and CC7 on a productive *Chlamydia* infection in Hep2 cells. Fluorescence-microscopy analysis of the compounds' effect at their minimal inhibitory concentrations (MICs) shows that while all four compounds clear the chlamydial infection, they also alter the Hep2 cytoplasm morphology compared to the vehicle control. The experimental procedure was additionally used to **(d)** analyze the effect of CC3, CC4, CC6 and CC7 on uninfected Hep2 host cells at 28 hours treatment duration. Fluorescence-microscopy analysis shows a change in the Hep2 cell cytoplasm morphology compared to the vehicle control for all four compounds tested. AB: aberrant body, EB: elementary body, RB: reticular body, hpI: hours post infection, scale bar 10 µm.

Four of the eight compounds did not show any significant effect towards *Chlamydia* infection. Even at the highest concentration tested, CC1, CC2, CC5 and CC8 did not alter the chlamydial phenotype observed with vehicle control treatment showed no detectable impact on host cells morphology in concentrations below 128 µg/ml.

The other four compounds showed a different effect on both the host cells and the chlamydial infection. Treatment with CC3, CC4, CC6 and CC7 lead to a complete clearance of the *C. trachomatis* infection (fig. 3.2.c). The formation of chlamydial inclusions was completely prevented at compound concentrations of 4 µg/ml for CC4 and CC7 and 8 µg/ml for CC3 and CC6. However, the fluorescence-microscopic examination unveiled toxic effects of all four compounds at their MICs on the Hep2 cells which lead to alterations of the host cell morphology. This effect occurred not only during treatment of *C. trachomatis* infected Hep2 cells (fig. 3.2.c), but was also observed in the control treatment of uninfected host cells (fig. 3.2.d). The Hep2 cell cytoplasm appeared bloated and, compared to cells in the vehicle controls, the intensity of Evans stain became erratic, resulting in a reticular staining pattern. The treatment also led to the appearance of vacuoles of different sizes in the cytoplasm, which could not be stained with any of the dyes used here.

The damaging effects on host cell morphology at low compound concentrations were not reflected to the same extent in the results of the Alamar Blue cell viability assay, particularly in the case of CC3 and CC4 (fig. 3.1). It seems that despite the observed changes in cytoplasmic morphology, the natural reductive power of Hep2 cells is not seriously affected in the presence of the compounds at their MIC. However, on the basis of this result, it cannot be ruled out that the observed antichlamydial effect of the candidate compounds is caused or at least intensified by their damaging effect on mammalian host cells. The result further underscores the indispensability of fluorescence microscopy not only for analyzing a compound's effect on host-chlamydia interaction, but also as an extension of classical cytotoxicity assay systems such as Alamar Blue to determine direct effects on host cell morphology.

3.1.2. Analysis of cytotoxicity for inhibitors of bacterial peptidoglycan (PG) precursor biosynthesis

The peptidoglycan (PG) biosynthesis is one of the most important bacterial pathways and therefore a promising target for antimicrobial compounds. Until now, only a few clinical prescribed compounds are known which target the membrane-bound steps of the cytoplasmic biosynthesis of the PG precursor lipid II. These steps begin with the integral membrane enzyme MraY, which catalyzes the transfer of the soluble PG precursor UDP-MurNAc pentapeptide to the lipid carrier C_{55}-P, yielding lipid I. Lipid I is subsequently processed to lipid II by the addition of a GlcNAc moiety catalyzed by the glycosyltransferase MurG. Both enzymes, MraY and MurG, are functionally conserved in *Chlamydia* (Henrichfreise *et al*., 2009). The PG building block lipid II is transported by a flippase from the membrane's inner side to its outer side where polymerization to PG takes place. The *Chlamydia* genome encodes three proteins, FtsW, MurJ, and RodA, that might be involved in the flipping of lipid II (Klöckner *et al*., 2018). In this work, the cytotoxicity of MraY and MurJ inhibitors towards mammalian host cells was determined in a preliminary experiment to test their suitability as tools to analyze chlamydial PG synthesis in a cell culture model.

The bacterial enzyme MraY is the target of natural product nucleoside inhibitors like muraymycins and caprazamycins (Tanino *et al*., 2011). Here, muraymycin D2 and its derivates M22, M23, M25, M38, M76, M82, M92, M98 and M100 and the caprazamycin derivate CPZ2 (kindly provided by S. Ichikawa, Center for Research & Education on Drug Discovery, Hokkaido University, Japan) were tested for their effects towards mammalian Hep2 cells (fig. 3.3). For all tested compounds, the determined IC_{50} value was above a compound concentration of 64 µg/ml. Due to their relatively low cytotoxicity, the compounds could be interesting tools to study the effects of MraY inhibition in *Chlamydia*. Therefore, muraymycin D2 and its derivates were analyzed in this work both in a cell culture-based *Chlamydia* infection model and for their effect on the *in vitro* activity of chlamydial MraY (see 3.2. Analysis of the antichlamydial effect of MraY inhibitors).

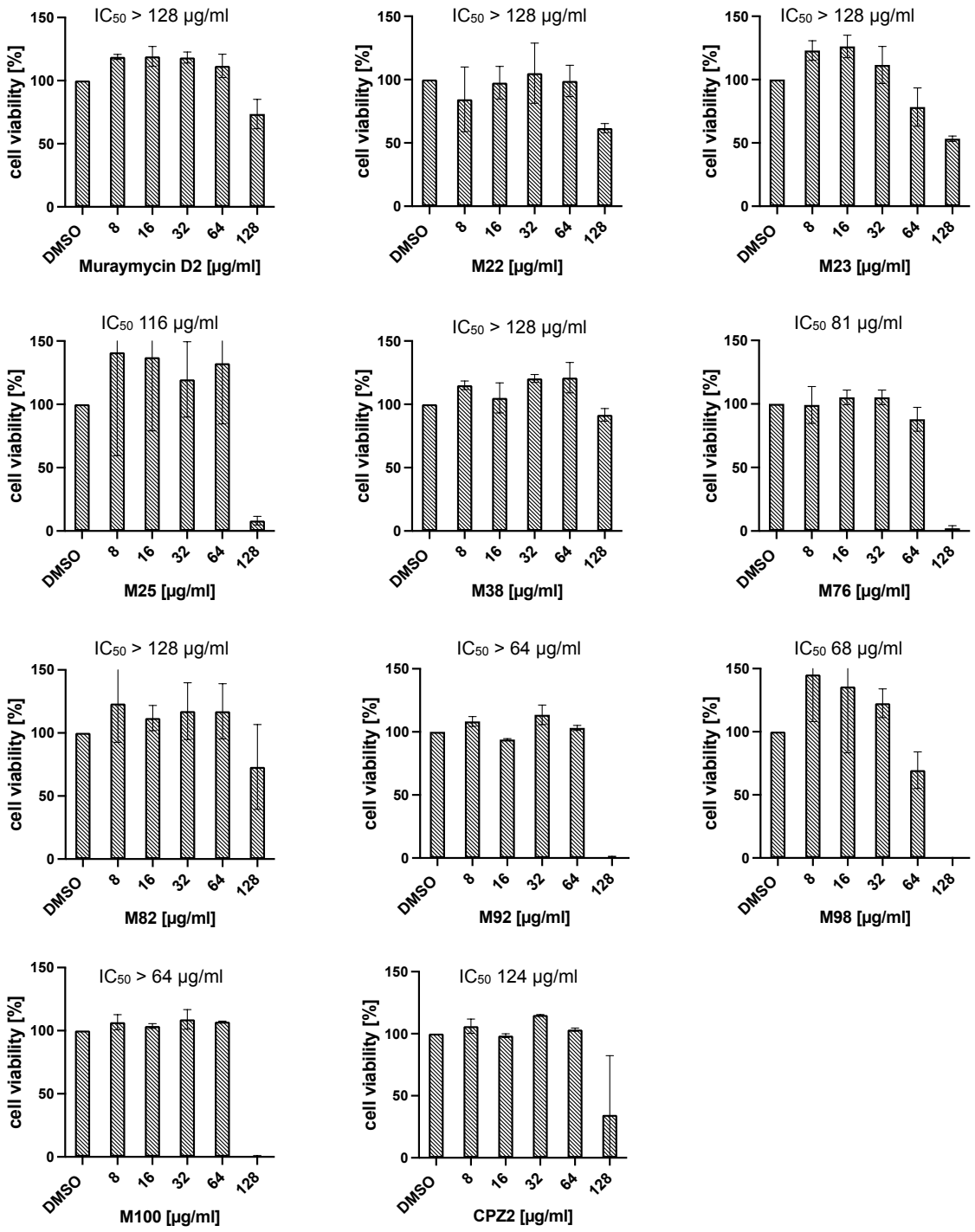

Figure 3.3. Alamar Blue cell viability assay for treatment of mammalian Hep2 cells with inhibitors of bacterial MraY. A cytotoxic effect was determined for muraymycin D2, its derivates M22, M23, M25, M38, M76, M82, M92, M98, M100 and the caprazamycin derivate CA2 as the IC_{50} at 28 hours of treatment duration (n=2).

Despite their reduced genome size, *Chlamydia* retained three proteins, FtsW, MurJ, and RodA that might act as flippases to translocate lipid II across the inner membrane (Klöckner *et al*., 2018). To investigate the role of lipid II export in the *Chlamydia* life cycle, three inhibitors of bacterial MurJ (Inhibitors 1-3; kindly provided

by T. Schneider, Institute for Pharmaceutical Microbiology, University Bonn) were previously tested in the Henrichfreise group for their effect on the *C. trachomatis* infection model in Hep2 cell culture. All three compounds showed an antichlamydial effect with MICs of 32 µg/ml (Inhibitor 1 and 2) and 16 µg/ml (Inhibitor 3) (Klöckner, 2016). In this work, these inhibitors were tested for their cytotoxicity towards the mammalian Hep2 host cells (see fig. 3.4).

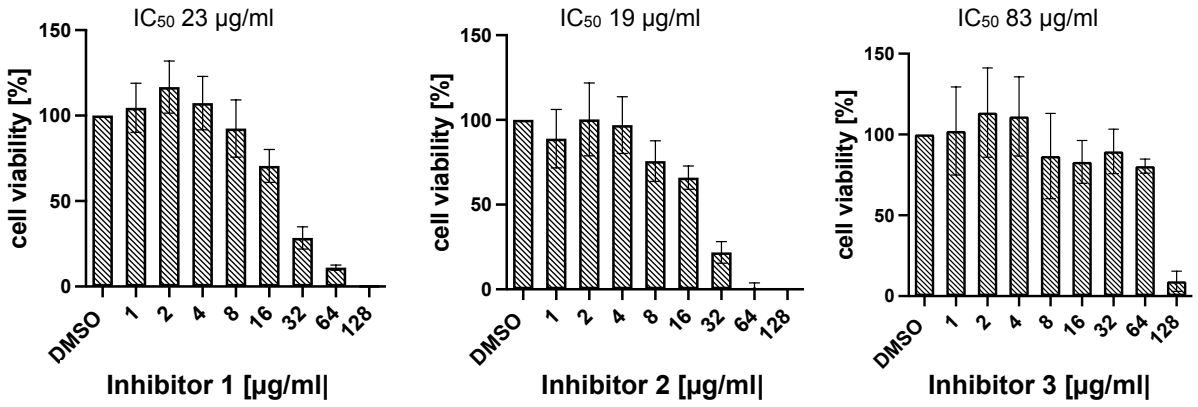

Figure 3.4. Alamar Blue cell viability assay for treatment of mammalian Hep2 cells with inhibitors of bacterial MurJ. A cytotoxic effect was determined for the MurJ Inhibitors 1-3 as the IC_{50} at 28 hours of treatment duration (n=4).

The IC_{50} values determined for the first two compounds, MurJ Inhibitors 1 and 2, were 23 µg/ml and 19 µg/ml, respectively. Since both IC_{50} values are lower than the MIC values of the corresponding compounds, it might be assumed that the previously observed antichlamydial activity results primarily from a disruptive effect on the mammalian host cells. An IC_{50} value of 83 µg/ml was determined for the third tested compound (Inhibitor 3), which is above the MIC of 32 µg/ml determined by Klöckner (Klöckner, 2016). These results suggest that the antichlamydial effect of this MurJ inhibitor may be due to the inhibition of a target within *Chlamydia*, possibly the transport of PG precursor lipid II across the cytoplasmic membrane.

3.2. Analysis of the antichlamydial effect of MraY inhibitors

The integral membrane protein MraY catalyzes the first membrane-bound step of bacterial PG synthesis in which UDP-MurNAc-pentapeptide is transferred to the lipid carrier C_{55}-P, yielding the PG precursor lipid I. This enzyme is the target of the natural product nucleoside inhibitor muraymycin (Tanino *et al*., 2011). A previous study in the Henrichfreise group showed that treatment of a Hep2 cell culture-based *Chlamydia*

infection model with muraymycins exerts a bacteriostatic effect and induces a chlamydial persistent state (Klöckner, 2016). However, whether this antichlamydial effect is due to inhibition of chlamydial MraY or host cell stress during treatment (or a possible combination of both) has not yet been investigated. In order to answer this question, the antichlamydial activity of muraymycin D2 and derivates of this compound (kindly provided by S. Ichikawa, Center for Research & Education on Drug Discovery, Hokkaido University, Japan) was further analyzed in this work. Compounds were tested for their effect on recombinant chlamydial MraY in an *in vitro* activity assay (section 3.2.1) and in a productive and persistent *Chlamydia* cell culture infection model (sections 3.2.2 and 3.2.3). Together with the results of the cytotoxicity assay (section 3.1.2), the fluorescence microscopic analysis of the cell culture-based experiments allowed to assess the effect of these compounds on Hep2 host cells.

3.2.1. Muraymycin inhibits *C. pneumoniae* MraY activity *in vitro*

The ability of chlamydial MraY to synthesize lipid II *in vitro* has been demonstrated in *Chlamydia* (Henrichfreise *et al*., 2009). Due to its ten transmembrane domaines, heterologous overproduction of chlamydial MraY for biochemical characterization is a tedious and elaborate process. Since *Chlamydia* is evolutionary distant from *E. coli* expression strains, attempts to heterologously express and purify chlamydial proteins often face problems like poor solubility, inactive proteins and even toxicity (Otten *et al*., 2015). Based on a protocol for the production of recombinant *S. aureus* MraY by Schneider *et al*. (Schneider *et al*., 2009), Henrichfreise and colleagues were able to establish a method for His-tag purification of heterologusly produced *C. pneumoniae* MraY ($MraY_{Cpn}$) (Henrichfreise *et al*., 2009). However, a known problem with this method is contamination with MraY of the *E. coli* producer strain. Due to a stretch of histidine residues in *E. coli* MraY, it binds to the Ni-NTA column and is unavoidably co-purified in the process. It was shown that host-derived background activity makes up to 41 % of overall detected activity in $MraY_{Cpn}$ *in vitro* activity assays (Henrichfreise *et al*., 2009). In this work, an attempt was made to establish a method for *Strep*-tag purification of $MraY_{Cpn}$ to reduce contamination by *E. coli* MraY, but unfortunately, different attempts to produce *Strep*-tagged $MraY_{Cpn}$ in *E. coli* remained unsuccessful so far.

To gain a first insight into the effect of muraymycin on chlamydial lipid I biosynthesis, the nucleoside inhibitor was tested against the enzymatic activity of $MraY_{Cpn}$ purified via His_6-tag (described in section 2.5.1). In the presence of muraymycin D2, a concentration-dependent inhibition of lipid I production by MraY was observed. At a compound concentration of 0.5 µM, lipid I was no longer be detectable in the assay (fig. 3.5). In addition, complete inhibition of the in vitro production of lipid I was also demonstrated for the muraymycin derivatives M22, M38 and M92 at a concentration of 0.5 µM each and for the derivative M76 at a concentration of 1 µM (fig. 3.5).

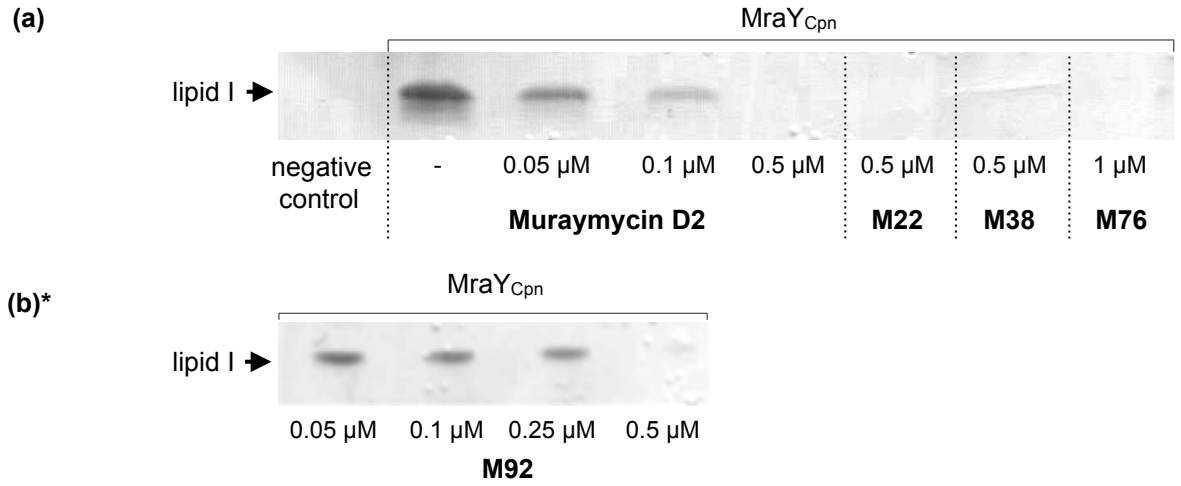

Figure 3.5. Effect of muraymycin D2 and its derivates on the enzymatic activity of recombinant $MraY_{Cpn}$. TLC analysis of the inhibiting effects of muraymycin D2, M22, M38, M76 and M92 on *in vitro* lipid I production. **(a)** & **(b)** Muraymycin D2 inhibits enzymatic activity depending on its concentration with no lipid I detectable at a concentration of 0.5 µM. **(a)** Lipid I production is inhibited in presence of 0.5 µM of the derivates M22 and M38 and 1 µM of derivate M76. **(b)** Derivate M92 inhibits enzymatic activity depending on its concentration with no lipid I detectable at a concentration of 0.5 µM. For the negative control, substrates were incubated with dialysis buffer instead of $MraY_{Cpn}$, the positive control shows $MraY_{Cpn}$ activity in the absence of any inhibitor. *) The assay shown in panel **(d)** was performed in the affiliated master thesis of I. Löckener (Henrichfreise group).

Due to the His-tag purification of the chlamydial MraY, contamination with *E. coli* MraY and thus a contribution of this enzyme to the lipid I production detected in the *in vitro* assay cannot be ruled out. However, as mentioned above, it has been shown that under the assay conditions performed in this work, at least half of the detected enzymatic activity can be attributed to $MraY_{Cpn}$ (Henrichfreise *et al*., 2009). A further indication that the observed lipid I production depends on $MraY_{Cpn}$ activity is the comparison of the *in vitro* activity between $MraY_{Cpn}$ and an active site mutant of this protein. To this end, a $MraY_{Cpn}$D256A mutant was constructed by I. Löckener for the Henrichfreise group based on *in silico* analysis which showed that D256 of $MraY_{Cpn}$

corresponds to D265 in the active site of *Aquifex aeolicus* MraY. In the *A. aeolicus* enzyme, the aspartic acid residue is essential for proper coordinating of a catalytic Mg^{2+} ion and its mutation results in a nearly complete loss of enzymatic activity (Chung *et al*., 2013). In case of chlamydial MraY, *in vitro* lipid I production was clearly reduced for $MraY_{Cpn}$D256A compared to wild type $MraY_{Cpn}$ (I. Löckener, Henrichfreise group, personal communication). It can therefore be assumed that the *in vitro* assay performed in this work is suitable for detecting lipid I production by $MraY_{Cpn}$. Thus, complete inhibition of enzymatic activity of $MraY_{Cpn}$ in this assay by muraymycins suggests that *Chlamydia* MraY is a target of these compounds.

3.2.2. Effect of muraymycins on a productive *Chlamydia* infection model

The *in vitro* data provides evidence that muraymycin is likely to inhibit $MraY_{Cpn}$ activity (see section 3.2.1). A previous study in the Henrichfreise group investigated the effect of muraymycin D2 and derivates of this compound (M22, M23, M24, M25, M38, M76, M82, M92, M98, M100) on a productive *C. trachomatis* infection model in Hep2 cell culture (Klöckner, 2016). The experiment showed that most of these derivates have a bacteriostatic effect and induce a persistent state in *Chlamydia*. Derivate M98 was an exception as treatment with it completely cleared the chlamydial infection (Klöckner, 2016). Since this study was designed to examine the compounds' effect on chlamydial cell morphology, only *Chlamydia* LPS was stained for fluorescence microscopic analysis. Therefore, it is not yet clear whether the antichlamydial activity of muraymycin and its derivatives is due to host cell stress during treatment or to inhibition of chlamydial MraY. To further investigate this question, the effect of muraymycin and its derivatives on Hep2 cells was analyzed in a cytotoxicity assay in this work (see section 3.1.2). In addition, the MICs of muraymycin D2 and its derivates M22, M23, M38, M98 and M100 were determined in a *C. trachomatis* infection model in Hep2 cell culture as the lowest compound concentration that alters chlamydial cell morphology. For this purpose, serially diluted concentrations of muraymycin D2 or its derivates were added to an early and productive chlamydial infection (2 hpI; fig. 3.6.a) and the effect was analyzed by fluorescence-microscopy. This approach allows not only to compare a compound's antichlamydial MIC with its IC_{50} values against the host cells (section 3.1.2, fig. 3.3),

but also to asses the morphology of the Hep2 cells by counterstaining their cytoplasm and nucleus (fig. 3.6.b-f).

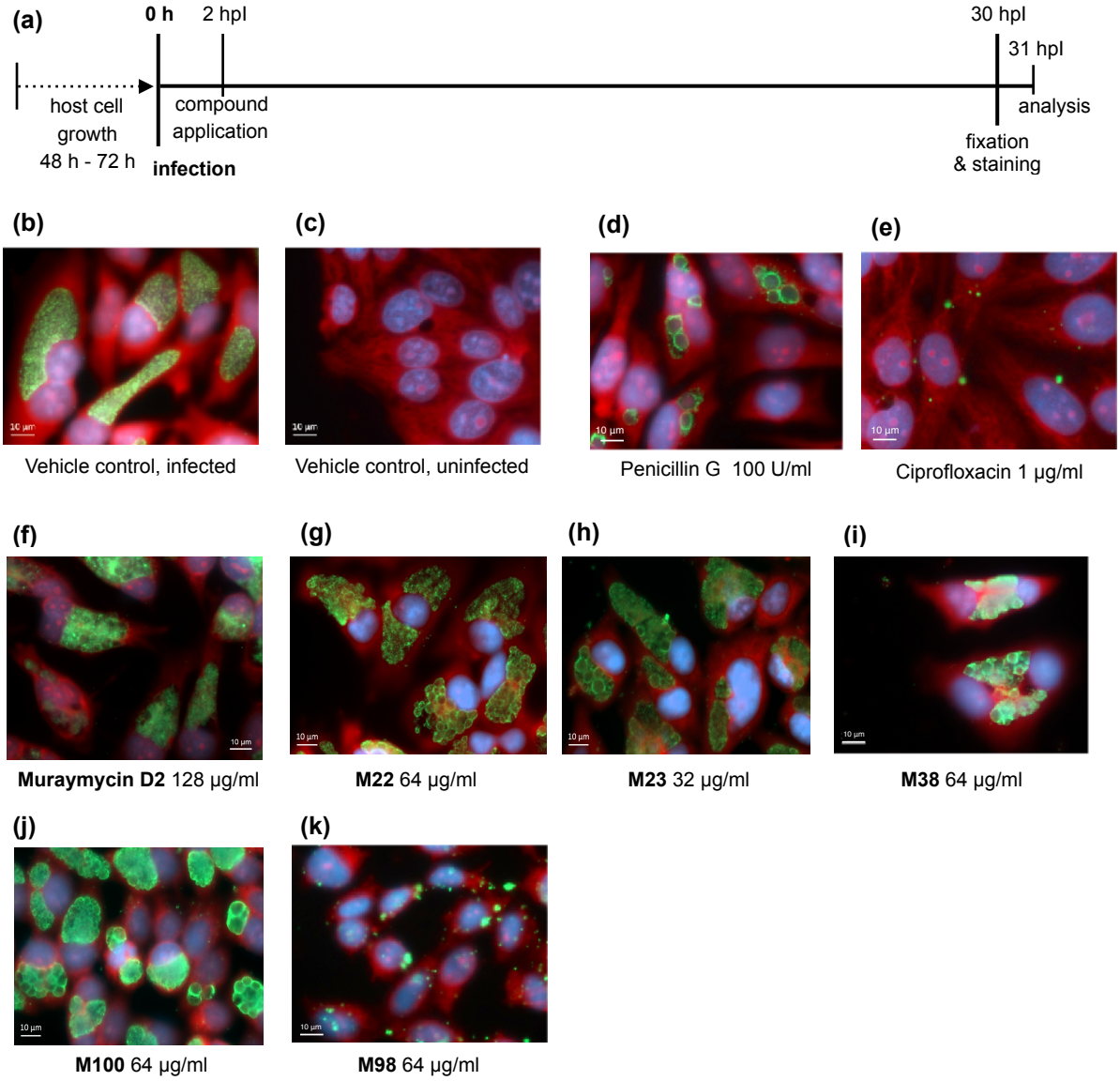

Figure 3.6. Fluorescence microscopic analysis of the effect of muraymycins on a productive *Chlamydia* infections model. The effect of muraymycin D2 and its derivates M22, M23, M38, M98 and M100 was analyzed in a cell culture model. **(a)** Treatment scheme: Hep2 cells were grown into a confluent monolayer and then infected with *C. trachomatis* D/UW-3/CX. Serially diluted concentrations of compounds were added 2 hpl and the cells were fixed and stained for fluorescence microscopic analysis 30 hpl. Microscopy analysis of **(b)** *C. trachomatis* infected and **(c)** uninfected Hep2 cells treated with DMSO as vehicle controls. **(d)** Incubation with β-lactam inhibitor penicillin G (100 U/ml) induced a chlamydial persistent state with enlarged AB formation, while **(e)** incubation with ciprofloxacin (1 µg/ml) cleared the infection. **(f-k)** The effect of muraymycin D2 and its derivates is shown at the respective MIC, the lowest compound concentration which induces an alteration of the chlamydial morphology compared to the vehicle control. Incubation with **(f)** 128 µg/ml muraymycin D2, **(g)** 64 µg/ml M22, **(h)** 32 µg/ml M23, **(i)** 64 µg/ml M38 and **(j)** 64 µg/ml M100 induced a chlamydial persistent state with enlarged AB formation, while incubation with **(k)** 64 µg/ml M98 cleared the infection. AB: aberrant body, green: chlamydial LPS, red: host cell cytoplasm, blue: host cell nucleus, hpI. hours post infection, scale bar 10 µm.

Treatment of the *C. trachomatis* infection with muraymycin D2, M22, M23, M38 and M100 induced a persistent state with the formation of enlarged chlamydial aberrant bodies (ABs) (fig.3.6.f-j) with a phenotype similar to ABs induced by treatment with the β-lactam antibiotic penicillin G (fig. 3.6.d). Muraymycin D2 only showed weak activity towards *C. trachomatis* infection inducing chlamydial persistence at a MIC of 128 µg/ml (fig. 3.6.f). The requirement of such a high compound concentration may be due to the difficulty of accessing a target within the chlamydial cell, which itself resides in an membrane-enclosed inclusion within the host cell's cytoplasm. It is known that muraymycins show antimicrobial activity against Gram-positive bacteria and against an *E. coli* mutant with increased membrane permeability (McDonald *et al*., 2002; Bugg *et al*., 2006). The *in vivo* activity of muraymycins against Gram-positive bacteria can be increased by derivatization. The addition of a lipophilic side chain results in enhanced activity as it allows the compound to better pass the cytoplasmic membrane to reach the active site of MraY (Tanino *et al*., 2011). In contrast to muraymycin D2, the derivatives tested here have an additional lipophilic side chain and their MICs of 64 µg/ml for M22, M23 and M100 and 32 µg/ml for M38 (fig. 3.6.g-k) suggest that this modification could slightly increase their ability to reach their target structure within the chlamydial cell compared to muraymycin D2.

For muraymycin D2, M22, M23, M38 and M100, the MIC value at which detectable antichlamydial activity occurred was below the IC_{50} value of the corresponding compound which was > 128 µg/ml for muraymycin D2, M22, M23 and M38 and > 64 µg/ml for M100 (section 3.1.2, fig. 3.3). In addition, no significant changes of Hep2 cell morphology compared to the infected vehicle control (fig. 3.6.b) were observed during the fluorescence-microscopic analysis for MIC detection. Taken together, the data indicate that the observed chlamydial persistent state results primarily from inhibition of a target within *Chlamydia*. While the *in vitro* enzymatic assay showed that the activity of *Chlamydia* MraY is inhibited by muraymycins (see section 3.2.1), the cell culture experiments indicated that chlamydial development is impaired by this inhibition of the chlamydial PG precursor biosynthesis.

As previously described by Klöckner (Klöckner, 2016), derivative M98 differed in its effect on the *C. trachomatis* infection model. Similar to bactericidal substances such as ciprofloxacin (fig. 3.6.e), M98 induced clearance of chlamydial infection at a MIC of 64 µg/ml (fig. 3.6.k). The bactericidal effect of M98 differs markedly from the

chlamydial phenotypes observed in the case of treatment with muraymycin D2 and the other muraymycin derivatives. This observation might suggest that M98 affects not only the chlamydial PG precursor biosynthesis, but also other processes within the chlamydial cell. However, it cannot be ruled out that the bactericidal effect is due to or enhanced by an an interfering effect of this compound on the host cells, as its IC_{50} value on Hep2 cells was 68 µg/ml.

3.2.3. Effect of muraymycin D2 on a progressed productive and a persistent *Chlamydia* infection model

In the cell culture experiments performed in this work for MIC determination (see sections 3.1.1 and 3.2.2), the compound of interest was added at an early stage of a productive *C. trachomatis* infection (2 hpI). At this point in chlamydial development, EBs are still in the stage of entering the host cell but are neither differentiated to RBs nor replicating. While this experimental setup provides valuable insight into a compound's antichlamydial activity, it cannot provide accurate information about the phase of the chlamydial developmental cycle at which the effect occurs due to the continuous presence of the test compound. Therefore, the cell culture assay used in the Henrichfreise group was extended to study the effect of a test compound on progressed productive as well as persistent *C. trachomatis* infection (Brunke, 2018).
In order to analyze its effect on an established productive *Chlamydia* infection, the compound of interest is applied at 12 hpI (fig. 3.7.b, 'late application'), when RB replication is nearing its peak (Nicholson *et al*. 2003). The observed effect differed depending on whether the compound was applied at an early or late stage of infection. Muraymycin treatment at 2 hpI induced a persistent state with a MIC of 128 µg/ml, but did not affect the number of infected host cells (see section 3.2.2, fig. 3.6.f). In contrast, when it was added at 12 hpI, the number of infected Hep2 host cells decreased (fig. 3.7.e). The observed *Chlamydia* phenotype also differed between the application times. When muraymycin D2 was present while EBs are entering the host cells at 2 hpI, AB formation was induced and *C. trachomatis* devolved into a persistent state. Adding muraymycin to replicating RBs at 12 hpI reduced the number of infected host cells (fig. 3.7.e), but the chlamydial phenotype resembled that of an infection treated with the DMSO vehicle-control (fig. 3.7.d).

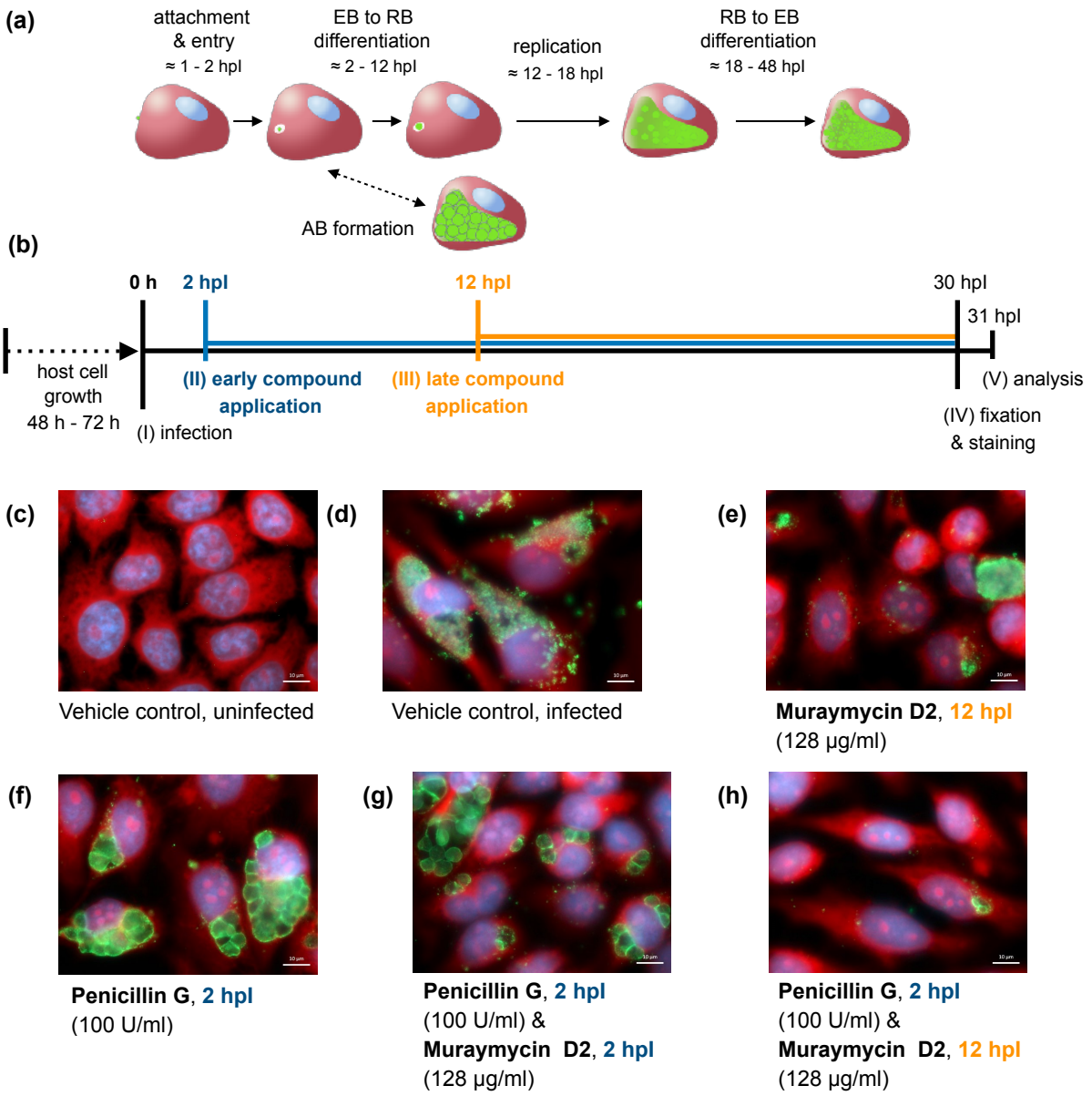

Figure 3.7. Fluorescence microscopic analysis of the effect of muraymycin D2 on a progressed productive and a persistent *Chlamydia* infection model. Based on **(a)** the chlamydial cell cycle, **(b)** a workflow for analyzing persistent chlamydial infection was established (Brunke, 2018). In this model, persistence with AB formation was induced by treatment with 100 U/ml penicillin G. Hep2 cells were grown into a confluent monolayer and then infected with *C. trachomatis* D/UW-3/CX (I). The first time point to add a compound, either penicillin G to induce persistence or muraymycin D2, was 2 hpI (II). The second time point at which muraymycin D2 was added was 12 hpI (III). Infected cells were incubated for a total of 30 hours. Subsequently, samples were fixed, stained (IV) and analyzed via fluorescence-microscopy (V). Panel **(c)** shows infected and uninfected Hep2 cells treated with DMSO as vehicle control. **(d)** Addition of 128 µg/ml muraymycin D2 at 12 hpI to an productive infection without prior treatment reduced inclusion numbers but to a lesser extent compared to its effect on persistent chlamydiae. **(e)** Addition of 100 U/ml penicillin G 2 hpI induced AB formation. **(f)** When muraymycin D2 was added simultaneously with penicillin G at 2 hpI, morphology and numbers ABs were not affected compared to infections treated only with penicillin G. **(g)** When muraymycin D2 (128 µg/ml) was added at 12 hpI to an infection in a penicillin G-induced persistent state, the number of chlamydial inclusions was reduced. AB: aberrant body, EB: elementary body, RB: reticular body, green: chlamydial LPS, red: host cell cytoplasm, blue: host cell nucleus, hpI: hours post infection, scale bar 10 µm.

The cell culture assay can be used not only to assess the effect of a compound on chlamydial replication, but also to study how persistent *Chlamydia* infection responds to treatment. For this purpose, chlamydial AB formation can be induced by addition of the β-lactam antibiotic penicillin prior to addition of the test compound. Here, penicillin G treatment started at 2 hpI (fig. 3.7.b, 'early application') and continued until the cells were fixated. The test compound is subsequently added at 12 hpI to the chlamydial cells in a penicillin G-induced persistent state (fig. 3.7.b, 'late application'). As a control, penicillin G and the compound were added simultaneously. The assay was evaluated by fluorescence-microscopy analysis (fig. 3.7.c-h). As described previously for this assay (Brunke, 2018), treatment with 100 U/ml penicillin G at 2 hpI was sufficient to induce a persistent state in *C. trachomatis* with AB formation (fig. 3.7.f). The number of infected host cells, inclusion size and AB phenotype stayed the same when muraymycin D2 was added simultaneously with penicillin G at 2 hpI (fig. 3.7.g), but changed when the compound was added at 12 hpI to an already established *Chlamydia* infection in an penicillin G-induced persistent state (fig. 3.7.h). Infected Hep2 host cells harboring inclusions were found only sporadically and the inclusion size was reduced compared to a *Chlamydia* infection treated at 2 hpI either with penicillin G alone (fig. 3.7.f) or simultaneously with penicillin G and muraymycin D2 (fig. 3.7.g). The chlamydial cells inside the inclusions exhibited an AB phenotype similar to cells in a penicillin G-induced persistent state (fig. 3.7.f).

These data show that the effect of muraymycin D2 towards the *Chlamydia* infection model differs depending on the time of application. At an early stage of infection, at which EBs are still entering their host cells or have just entered and differentiation into RBs is about to start, treatment with muraymycin D2 induces a persistent state with enlarged AB formation. However, neither the number of infected cells nor the inclusion size are affected by this treatment. At 12 hpI, when chlamydial cells inside the inclusion are completely differentiated into RBs and have started to replicate, the compound's effect becomes more severe. At this time, treatment with muraymycin D2 does not induce a detectable change in chlamydial cell morphology but reduces the number of infected host cells. This observation may indicate that the compound disrupts processes that are critical not only for chlamydial replication but also for survival.

The effect was further enhanced when muraymycin D2 was added to a persistent *Chlamydia* infection. A chlamydial persistent state with formation of enlarged ABs was induced at 2 hpI by adding penicillin G which targets chlamydial PBPs and thus inhibits periplasmic PG assembly (Barbour *et al*., 1982). In this state, chlamydial cells are already showing a stress response to penicillin G treatment and their susceptibility to additional compounds may be increased. When muraymycin D2 was applied at 12 hpI to this cells, the number of infected Hep2 cells decreased. The remaining inclusions were smaller compared to treatment with penicillin G alone. Under this conditions, the compound appears to have a bactericidal effect on the *Chlamydia* infection. This could raise the possibility that muraymycin D2 not only interferes with chlamydial PG precursor biosynthesis by inhibiting MraY, but may also affects another target inside the chlamydial cell. Either inhibition of this additional target or the combined effect of muraymycin D2 on this target as well as on MraY activity might result in a bactericidal effect.

3.3. Novel aspects of AmiA activity

3.3.1. Analysis of an *E. coli* AmiA mutant lacking the autoinhibitory domain

In *E. coli*, three periplamic *N*-acetylmuramoyl-L-alanine amidases (AmiA, B, C) are needed for proper cell separation and are tightly controlled by regulatory factors. In free-living Gram-negative bacteria, the amidase active site is occupied by a conserved α-helix which keeps the enzyme in an inactive state (Yang *et al*., 2012). In order to allow free substrate access to the active site, regulatory factors that interact with the autoregulatory domain are required to initiate conformational change. In *E. coli*, the regulatory factors are LytM domain-containing proteins that specifically activate their respective amidase: AmiA and AmiB are activated by EnvC and AmiC is activated by NlpD (Yang *et al*., 2012). *Chlamydia* conserved only one septal PG hydrolase (AmiA) and does not code for any known regulatory factor. Consistently, chlamydial AmiA lacks an autoinhibitory domain and is unlikely to be autoregulated (Klöckner *et al*., 2014). The importance of the autoregulatory domain for regulation of the amidase activity in free-living bacteria has been shown in previous studies. An amino acid substitution in the autoinhibitory domain of *E. coli* AmiA (E167K) resulted in the same level of *in vitro* activity in dye-release experiments as observed for the wild-type protein in the presence of its activator EnvC (Yang *et al*., 2012). In a cell lysis assay, the *E. coli* AmiAE167K mutant had an effect similar to the autoinhibitory α-helix-deficient *C. pneumoniae* AmiA ($AmiA_{Cpn}$). Both enzymes were shown to be constitutively active in *E. coli* and caused its cell lysis (Klöckner, 2016).

In this work, an *E. coli* AmiA deletion mutant lacking the complete autoinhibitory α-helix (named $AmiA_{Eco}$_ΔA148-S191; fig. 3.8.b) was generated by site directed mutagenesis based on the structure of $AmiA_{Cpn}$ (mutagenesis primers designed by M. Brunke, Henrichfreise group; tab. 2.5). The amino acid sequence to be deleted contains the autoinhibitory α-helix and was chosen based on comparison of the predicted 3D structures of $AmiA_{Eco}$ and $AmiA_{Cpn}$ (fig. 3.8.a & c). All protein structures were predicted using the PHYRE tool (tab. 2.1) based on the crystal structure of *E. coli* AmiC (Rocaboy *et al.*, 2013). The $AmiA_{Eco}$_ΔA148-S191 mutant was tested in a cell lysis assay (fig. 3.8.d). In contrast to wild-type *E. coli* AmiA ($AmiA_{Eco}$) which did not induce lysis when overexpressed without its activator EnvC, overexpression of $AmiA_{Eco}$_ΔA148-S191 alone resulted in cell lysis. Like the autoinhibitory domain-lacking $AmiA_{Cpn}$, $AmiA_{Eco}$_ΔA148-S191 was constitutively active as an amidase.

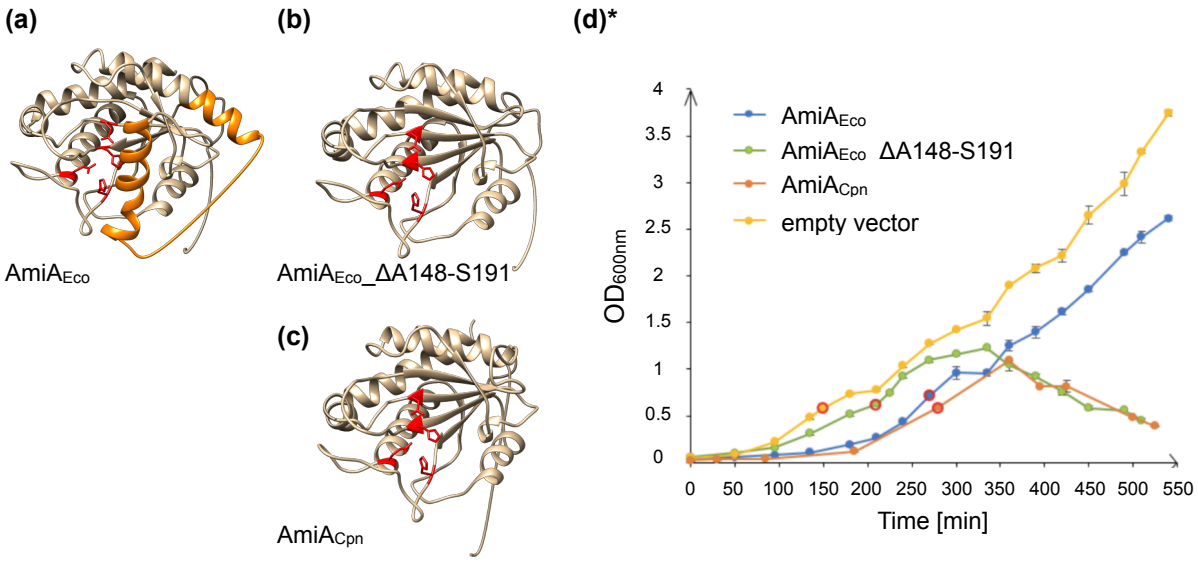

Figure 3.8. 3D *in silico* models and growth kinetics of AmiA$_{Eco}$, AmiA$_{Eco}$_ΔA148-S191 and AmiA$_{Cpn}$. Based on Phyre2 alignment against the crystal structure of *E. coli* AmiC (Rocaboy *et al*., 2013) the 3D structures of **(a)** wild type AmiA$_{Eco}$, **(b)** its autoinhibitory domain-lacking mutant AmiA$_{Eco}$_ΔA148-S191 and **(c)** chlamydial AmiA$_{Cpn}$ were predicted and modeled with the Chimera tool. The autoinhibitory structure of AmiA$_{Eco}$ (shown in orange) was deleted to create AmiA$_{Eco}$_ΔA148-S191. The catalytic residues of the amidase active site are shown in red. **(d)** Growth kinetics of *E. coli* JM83 transformed with different IBA2C+ vector-based constructs encoding AmiA$_{Eco}$, AmiA$_{Eco}$_ΔA148-S191 and AmiA$_{Cpn}$, respectively. Overexpression of the periplasmic proteins was induced at OD$_{600nm}$ = 0.6 (red circles) by adding 200 ng/ml AHT. Overexpression of AmiA$_{Eco}$_ΔA148-S191 and AmiA$_{Cpn}$ resulted in cell lysis, while AmiA$_{Eco}$ showed no basal activity. Error bars indicate ± s.d. (n=3). *) The assay shown in panel **(d)** was performed in the affiliated bachelor thesis of J. Paus (Henrichfreise group).

To further analyze the impact of the autoregulatory domain in *E. coli* AmiA, AmiA$_{Eco}$_ΔA148-S191 was overproduced and purified (see section 2.5.1) and tested for its PG-degrading activity using a remazol brilliant blue (RBB) dye-release assay (see section 2.5.5.d). Previous studies showed that AmiA from both species, *E. coli* and *C. pneumoniae* releases RBB-stained reaction products from the PG sacculi into the supernatant. While AmiA$_{Cpn}$ shows *in vitro* activity in the absence of a regulatory factor (Klöckner *et al*., 2014), AmiA$_{Eco}$ requires the presence of its activator EnvC$_{Eco}$ to hydrolyze PG (Uehara *et al*, 2010). In this work, activity of AmiA$_{Eco}$_ΔA148-S191 was measured in relation to the activity of AmiA$_{Eco}$ activated by EnvC$_{Eco}$ (fig. 3.9). The mutant enzyme was active in the absence of any regulatory factor and displayed 66 % ± 8 % of the lytic activity of wild type AmiA on PG sacculi. Interestingly, activity of AmiA$_{Eco}$_ΔA148-S191 declines to 22 % ± 4 % in presence of EnvC$_{Eco}$. This result indicates that the lytic activity of AmiA$_{Eco}$_ΔA148-S191 on PG is not only independent from the regulatory factor, but is further suppressed if EnvC$_{Eco}$ is present. Loss of the

autoinhibitory structure in AmiAEco_ΔA148-S191 might alter the interaction between the enzyme and the regulatory factor, resulting in a diminishing effect on the enzyme's *in vitro* amidase activity. Taken together, the results underline the importance of the autoinhibitory domain in AmiA for the regulation of amidase activity in free-living bacteria. However, the existence of such a regulatory mechanism can be ruled out in the case of *Chlamydia* AmiA, since the autoinhibitory structure found in *E. coli* AmiA is not present in this enzyme which is active by default. The regulatory mechanism of chlamydial amidase activity during cell division remains to be identified.

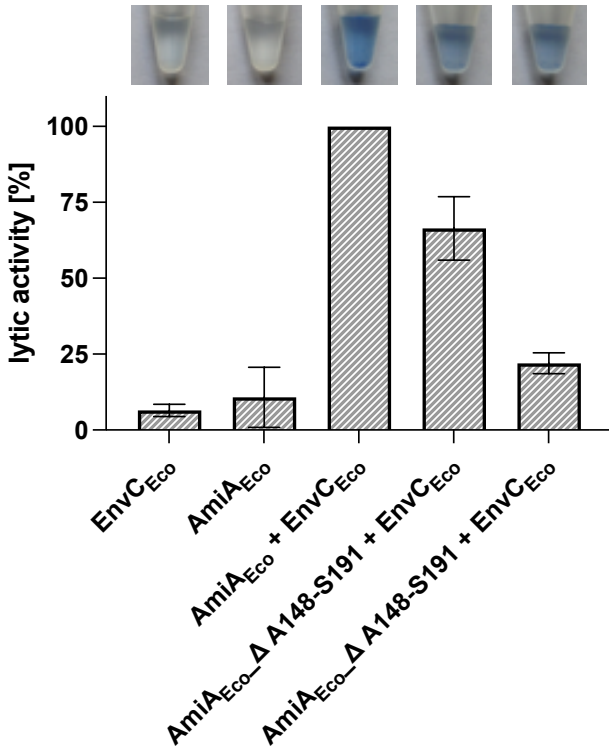

Figure 3.9. *In vitro* activity of the *E. coli* AmiA mutant AmiA$_{Eco}$_ΔA148-S191 on PG sacculi. The activity of the autoinhibitory domain-lacking AmiA$_{Eco}$_ΔA148-S191 on Remazol Brilliant Blue (RBB)-stained PG sacculi was tested in a dye-release assay. Lytic activity on PG releases the RBB stain in the supernatant, turning it blue. The activity was confirmed by measuring the absorbance of the supernatant at 595 nm. Wild type AmiA$_{Eco}$ showed lytic activity in presence of its activator EnvC$_{Eco}$ and the absorbance measured for this sample was set as 100 % lytic activity. The AmiA$_{Eco}$_ΔA148-S191 mutant showed 66 % lytic activity compared to activated wild type AmiA$_{Eco}$. The mutant's activity was reduced to 22 % in presence of EnvC$_{Eco}$. EnvC$_{Eco}$ and AmiA$_{Eco}$ alone showed 6 % and 11 % activity. Error bars indicate ± s.d. (n = 2).

3.3.2. *In silico* comparison of the active sites of AmiA from *C. pneumoniae* and *C. trachomatis*

In contrast to *E. coli* AmiA, *C. pneumoniae* AmiA is a bifunctional enzyme that acts not only as an amidase, but has additional D,D-carboxypeptidase (DD-CPase) activity on lipid II (Klöckner *et al.*, 2014). Both enzymatic activities are independent of each other and the enzyme has two distinct active sites.

(a)

```
AmiACpn     MKLTKYLNTKQLRSMISRLFVRYSLPMSKQLSFFALCVL-GSHPIFAQTPNPPQRVRRSE 59
AmiACtr     MRGIRSSNIRRLSLMIERLCVKPWQPFVNLTLLLLLLTLSSPVSCFADA-AGIPKVSRNE 59
            *:  :  * ::*  **.** *:   *: :   :: * .* .    **::     :* *.*

AmiACpn     VIFIDPGHGGKDQGTASKELHYEEKSLTLSLALTVQSYLKRMGYKPQLTRSSDVYVDLGK 119
AmiACtr     LIVIDPGHGGKDEGTADKELRYKEKTLALSIALSVQGCLRRMGYKTIMTRATDVYVDLSK 119
            :*.*********:***.***:*:**:*:**:**:**. *:*****  :***::******.*

AmiACpn     RVALSNRGQGDVFISIHCNHSSNAAAFGTEVYFYNGKVGSPTRNRMSEVLGKNILAAMEK 179
AmiACtr     RAAIANQNKADVFVSIHCNHSSNTSALGTEIYFYNDKNI--LRTRKSESLGKSILAFMQK 177
            *.*::*:.:.***:*********::*:***:****.*     *.* ** ***.*** *:*

AmiACpn     NGILKSRGLKTANFVVIRDTSMPAVLVETGFLSNSRERAALQDARYRMHVAKGIAEGVHN 239
AmiACtr     NGALRERKVKEGNFAVIRETTMPAVLVETGFLSNSKERAALLDARYRSHLAKGIAEGIHA 237
            ** *:.* :* .**.***:*:***************:***** ***** *:********:*

AmiACpn     FLSGPSFQKPKQNIAKIRKPQIQAN   264
AmiACtr     FILNRQVDKTVSVSSGAKKVHK---  259
            *: . ..:*  .  :  :* :
```

(b)

Figure 3.10. Primary sequence alignment and comparison of 3D *in silico* models of AmiA$_{Cpn}$ and AmiA$_{Ctr}$. (a) Four residues (highlighted in red) are conserved in the amidase active site of chlamydial AmiA. Three zinc-coordinating residues (H67/68, E83 and H136) and a fourth residue, E207 in AmiA$_{Cpn}$ and E205 in AmiA$_{Ctr}$, which is predicted to serve as a general base catalyst (Klöckner *et al.*, 2014). In addition to the amidase active site, the bifunctional enzyme AmiA$_{Cpn}$ contains two motifs that are typically found in PBP DD-CPases: an SxxK (highlighted in light blue) and an SxN motif (highlighted in purple). The third PBP DD-CPases motif (KTG) is missing in chlamydial AmiA (Klöckner *et al.*, 2014). While the SxN motif (highlighted in light blue) is also conserved in AmiA$_{Ctr}$, the SxxK motif found in AmiA$_{Cpn}$ is absent. Instead, there is an SxxK motif (highlighted in magenta) located more C-terminally compared to the AmiA$_{Cpn}$ sequence. **(b)** Differences in the SxxK motif's location are also visible in the predicted 3D structures of the chlamydial amidases. In AmiA$_{Cpn}$, the SxxK motif (purple) is located at the first a-helix distal to the SxN motif (light blue). In AmiA$_{Ctr}$, the SxxK (magenta) and the SxN motif (light blue) lay next to each other. Both 3D models are based on Phyre2 alignment against the crystal structure of *E. coli* AmiC (Rocaboy *et al.*, 2013).

The amidase active site consists of three zinc-coordinating residues (H67, E83 and H136), and a fourth residue (E207) that is predicted to act as a general base catalyst (Klöckner *et al*., 2014; fig. 3.10). The DD-CPase function is penicillin sensitive and was assigned to a penicillin-binding protein motif (Klöckner *et al*., 2014). Penicillin binding proteins (PBPs) with DD-CPase activity found in free-living bacteria are typically acyl-serine transferases containing three motifs, namely SxxK, S(Y)xN, and K(H,R)T(S)G, which are essential for substrate recognition and catalysis (Ghosh *et al,* 2008). Their DD-CPase activity depends on the presence of all three motives (Goffin & Ghuysen, 2002). However, $AmiA_{Cpn}$ contains an SxxK (S96-Y97-L98-K99) and an SxN motif (S140-S141-N142), but lacks a KTG motif (Klöckner, 2014; fig. 3.10). Furthermore, studies with $AmiA_{Cpn}$ active site mutants indicate that the enzyme's penicillin-sensitive DD-CPase activity is exclusively conferred by the SxxK motif and independent of the SxN triad (Klöckner *et al.*, 2014).

The AmiA homolog of *C. trachomatis* ($AmiA_{Ctr}$) shares 59 % overall sequence identity with $AmiA_{Cpn}$. Sequence alignment shows that all four residues of the amidase active site of $AmiA_{Cpn}$ are also conserved in $AmiA_{Ctr}$ (fig. 3.10.a). While the SxN motif found in $AmiA_{Cpn}$ is also conserved in *C. trachomatis* AmiA (S140-S141-N142), the SxxK motif found in $AmiA_{Cpn}$ is absent. The amino acid sequence of $AmiA_{Ctr}$ contains a different SxxK motif (S210-N211-S212-K213) which is located more C-terminally compared to the $AmiA_{Cpn}$ SxxK motif. The difference in the SxxK domain's location is also visible in the predicted protein structures of $AmiA_{Cpn}$ and $AmiA_{Ctr}$ (fig. 3.10.b). Both 3D models were constructed using the PHYRE tool (tab. 2.1) based on the crystal structure of *E. coli* AmiC (Rocaboy *et al.*, 2013). In $AmiA_{Cpn}$, the SxxK motif is located at the first a-helix and distal to the SxN motif, while in in $AmiA_{Ctr}$ both motives are adjacent. As in $AmiA_{Cpn}$, the KTG motif is missing in $AmiA_{Ctr}$.

3.3.3. *C. trachomatis* AmiA shows no DD-CPase activity on lipid II

The *in silico* analysis showed that while the amidase active site is conserved in both $AmiA_{Cpn}$ and $AmiA_{Ctr}$, the SxxK motif responsible for DD-CPase activity of $AmiA_{Cpn}$ (Klöckner *et al.*, 2014) is absent in $AmiA_{Ctr}$ (see section 3.3.2). Instead, an additional SxxK motif was found in $AmiA_{Ctr}$ which is located more C-terminally compared to the SxxK motif in $AmiA_{Cpn}$ (fig. 3.10). To investigate whether the functionality of $AmiA_{Ctr}$ is affected by the altered motif localization, its *in vitro* activity towards PG and lipid II

was examined. For this purpose, $AmiA_{Ctr}$ was heterologously overproduced in *E. coli* and purified (see section 2.5.1). The recombinant enzyme was then tested for its *in vitro* activity in a dye release assay using RBB-stained PG sacculi (section 2.5.5.d) and in an activity assay on lipid II (section 2.5.5.c). In the dye release-assay, $AmiA_{Ctr}$ showed PG-hydrolyzing activity, resulting in the release of RBB-stained reaction products into the supernatant (fig. 3.11.a). Like $AmiA_{Cpn}$, $AmiA_{Ctr}$ lacks an autoinhibitory domain and was shown to be active by default.

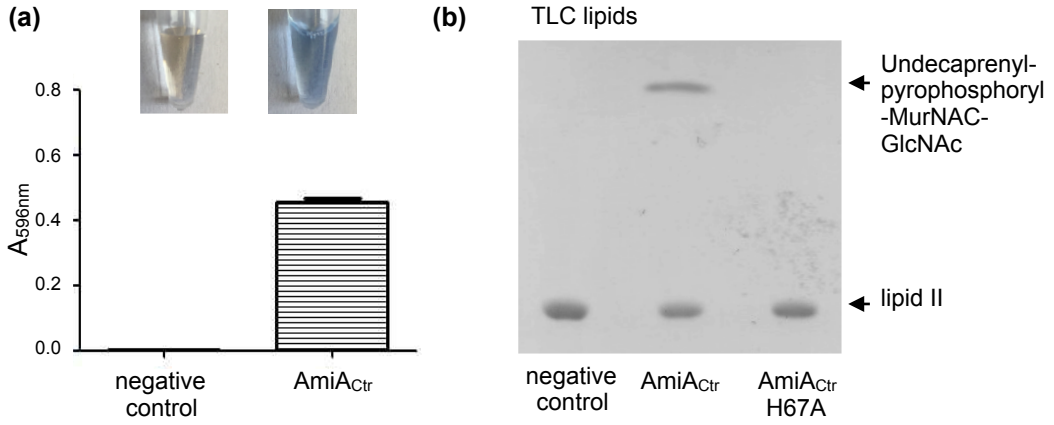

Figure 3.11. *In vitro* activity of $AmiA_{Ctr}$. (a) Dye-release assay and photometric analysis of the reaction products. $AmiA_{Ctr}$ shows hydrolytic activity when incubated with RBB labelled PG, resulting in a blue supernatant. The activity was confirmed by measuring the absorbance of the supernatant at 595 nm. Dialysis buffer served as a negative control. Error bars indicate ± s.d. (n=3). **(b)** *In vitro* activity of $AmiA_{Ctr}$ on the PG precursor lipid II. TLC analysis shows that $AmiA_{Ctr}$, unlike its active site mutant $AmiA_{Ctr}$H67A, exhibits amidase activity on lipid II which leads to an additional undecaprenyl-pyrophosphoryl-MurNAC-GlcNAc band. Neither wild type $AmiA_{Ctr}$ nor the $AmiA_{Ctr}$H67A mutant showed DD-CPase activity on lipid II. Dialysis buffer served as a negative control. Recombinant $AmiA_{Ctr}$H67A was kindly provided by C. Otten (Henrichfreise group).

In addition to PG, its precursor lipid II (mDAP type) was tested as a possible substrate of $AmiA_{Ctr.}$ Reaction products were analyzed by a TLC method that allows visualization of lipids ('TLC lipids'; section 2.5.6.a). Amidase activity on lipid II (undecaprenyl-pyrophosphoryl-MurNAC-(GlcNAc)-pentapeptide), by which its stem peptide is completely cleaved off, would result in the appearance of an additional undecaprenyl-pyrophosphoryl-MurNAC-GlcNAc band. DD-CPase activity, which cleaves the terminal D-Ala residue from the stem peptide, would be detectable via a change in the migration behavior between native lipid II and the resulting tetrapeptide-lipid II. The TLC analysis showed that $AmiA_{Ctr}$ exhibits amidase but no additional DD-CPase activity on lipid II (fig. 3.11.b). As a control, an $AmiA_{Ctr}$ active

site mutant ($AmiA_{Ctr}$H68A) which was kindly provided by C. Otten (Henrichfreise group) was used. This mutant, in which the zinc-coordinating histidine of the amidase active site (fig. 3.10.a) was changed to alanine, had no catalytic activity on lipid II (fig. 3.11.b).

Like $AmiA_{Cpn}$, $AmiA_{Ctr}$ has a conserved amidase active site and was shown to act *in vitro* as a PG hydrolase as well as an amidase on lipid II. Despite the overall high sequence similarity between both chlamydial AmiA homologs, the SxxK motif at position 96-99 in $AmiA_{Cpn}$ (fig. 3.10), which has been shown to be essential for DD-CPase activity in the *C. pneumoniae* enzyme (Klöckner *et al.*, 2014), is missing in $AmiA_{Ctr}$. The SxxK motif found at a more C-terminal position in $AmiA_{Ctr}$ does not appear to be part of a DD-CPase active site, since the enzyme shows no such activity towards lipid II. The results indicate that $AmiA_{Ctr}$, unlike $AmiA_{Cpn}$, is a monofunctional amidase rather than a bifunctional enzyme.

3.4. Analysis of chlamydial PG recycling

3.4.1. *In silico* analysis of putative chlamydial YkfC homologs in *Bacillus*

To gain insight into the mechanism of chlamydial PG recycling, the genomes of two *Chlamydia* species were analyzed for genes encoding proteins with sequences similarities to enzymes associated with cell wall recycling pathways in both the Gram-negative and the Gram-positive model organisms *E. coli* and *Bacillus subtilis*. The result of the screening indicates that PG recycling differs between pathogenic *Chlamydia* and free-living bacteria. Both *s*pecies analyzed, *C. trachomatis* and *C. pneumoniae*, lack homologs of enzymes associated with the PG recycling process in *E. coli* or in *B. subtilis*, with the sole exception of the *B. subtilis* NlpC/P60-cysteine peptidase YkfC ($YkfC_{Bsu}$). $YkfC_{Bsu}$ is a recycling enzyme which specifically cleaves free PG-derived peptides between their γ-D-Glu and mDAP residues (Schmidt *et al*., 2001; Xu *et al*., 2010). Both *Chlamydia* species encode a putative NlpC/P60 peptidase in their genomes that shares 23 % sequence identity with $YkfC_{Bsu}$ in the case of the *C. trachomatis* protein and 29 % sequence identity in the case of the *C. pneumoniae* protein.

In the in *B. subtilis* genome, the gene encoding $YkfC_{Bsu}$ is located in a cluster with other genes associated with PG recycling (fig. 3.12.a). Upstream of *ykfC*, the cluster includes two genes encoding the L,D-carboxypeptidase YkfA and the L-Ala-γ-D-Glu-epimerase YkfB (Schmidt *et al*. 2001). Downstream, *ykfC* is followed by *ykfD* which encodes the oligopeptide transporter protein YkfD. The *B. subtilis ykfABCD* operon appears to be controlled via the promoter of the preceding *dpp* operon (Molle *et al*., 2003) which encodes the D-aminopeptidase DppA and a dipeptide uptake system (DppBCDE) (Cheggour *et al*., 2000; Mathiopoulos *et al*., 1991). Since the genome of pathogenic *Chlamydia* contains only *ykfC* out of all *ykfABCD* genes, there is no gene cluster similar to the *B. subtilis* operon in either *C. trachomatis* or *C. pneumoniae* (fig. 3.12.b & c). In both organisms, a gene coding for an adenylate-kinase, AdK, is located adjacent to the respective gene coding for the putative YkfC homolog. AdK from *C. pneumoniae* has been shown to play an important role in the chlamydial energy metabolism by catalyzing a high-energy phosphoryl transfer reaction between ATP and AMP to generate ADP (Miura *et al*., 2001). Beside the direct proximity to *adK*, the genomic context of the putative YkfC-encoding gene differs between both analyzed *Chlamydia* species. In the *C. trachomatis* genome, *ykfC* (*ct127*) and *adK*

(*ct128*) are arranged in the opposite reading direction to their immediate genomic environment. The genes upstream of *ykfC, ct125* and *ct126*, encode the ribosomal proteins Rl13 and Rs9, respectively. Following *adK* are two genes, *ct129* and *ct130*, which are thought to encode subunits of a GlnPQ ABC-transporter that catalyzes the transport of glutamine and glutamic acid into the cytoplasm of Gram-positive bacteria (Skipp *et al*., 2005; Schuurman-Wolters & Poolman, 2005). In *C. pneumoniae*, the genes coding for AdK (*cpn0244*) and the putative YkfC homolog (*cpn0245*) are also set in the opposite reading direction to their following genes. Next to the putative YkfC homolog, two putative ribosomal proteins, RpsI and RplM, are encoded by *cpn0246* and *cpn0247*. Downstream follow two genes, *cpn0248*, which encodes the putative ABC transporter YcfV with as yet unknown substrate specificity, and *cpn0249*, which encodes a protein with unknown function.

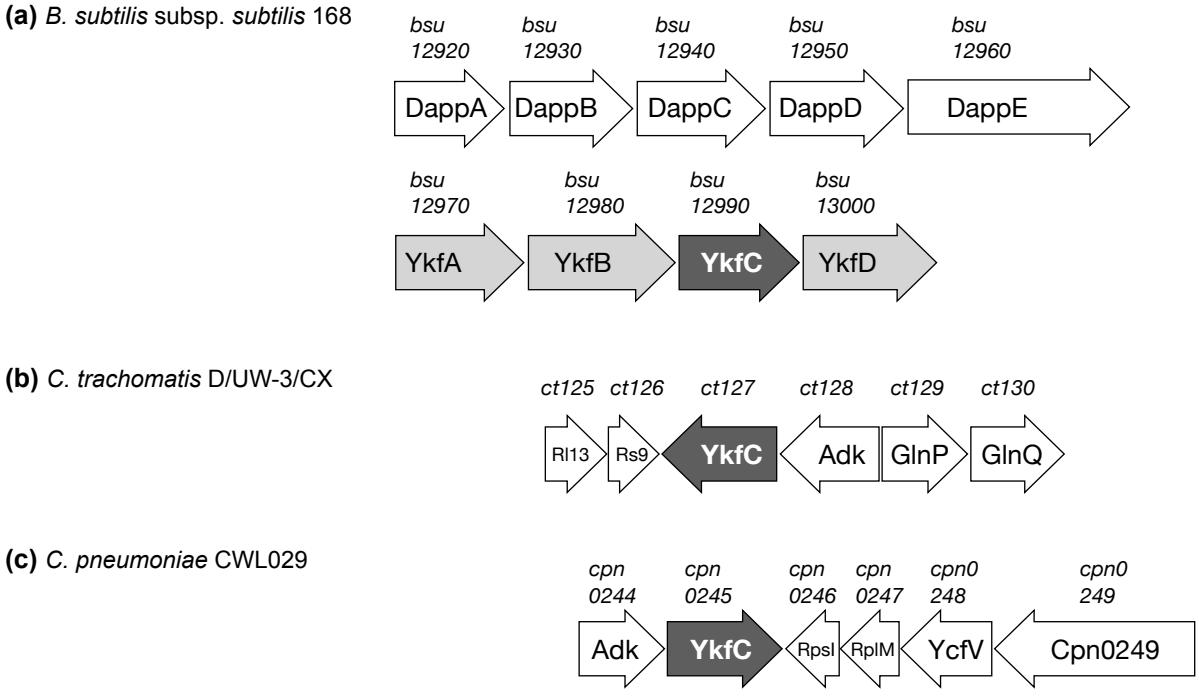

Figure 3.12. Comparative analysis of the genomic context of the gene encoding the putative PG recycling peptidase YkfC in *Chlamydia.* (a) In the genome of *B. subtilis*, *ykfC* (*bsu12990*) is part of the *ykfABCD* cluster which is preceded by the *dpp* operon. In the genomes of the two pathogenic *Chlamydia* species analyzed here, **(b)** *C. trachomatis* and **(c)** *C. pneumoniae*, both the *ykfABCD*-PG recycling gene cluster and the preceding *dpp* operon are missing. Aside from the proximity to a gene encoding AdK, the genomic context of the particular gene encoding a putative YkfC homolog (*ct127* in *C. trachomatis* and *cpn0245* in *C. pneumoniae*) differs in both species.

The biochemical properties of *Bacillus* YkfC have been characterized in *B. subtilis* (Schmidt *et al*., 2001), while the structure of this enzyme was determined by analysis of YkfC from *B. cereus*, which shares 40 % sequence identity with the *B. subtilis* enzyme (Xu *et al.*, 2010). Therefore, the following section focuses on the comparison between the protein structures of the *B. cereus* YkfC ($YkfC_{Bce}$) and the putative chlamydial YkfC proteins from *C. trachomatis* ($YkfC_{Ctr}$) and *C. pneumoniae* ($YkfC_{Cpn}$) which show 25 % and 30 % sequence identity to $YkfC_{Bce}$, respectively.

In silico analysis of the protein structures of $YkfC_{Ctr}$ and $YkfC_{Cpn}$ revealed an overall protein architecture similar to $YkfC_{Bce}$, consisting of two N-terminal SH3b domains, SH3b1 and SH3b2, and a C-terminal NlpC/P60 domain harboring a catalytic triad (Xu *et al.,* 2010) (fig. 3.13). Within the NlpC/P60 peptidase superfamily, the first residue of the catalytic triad is a cysteine which acts as a nucleophile to attack the peptide bond of the substrate. The second residue is a histidine which acts as a base and subsequently as an acid catalyst for the proton transfers in the following steps. The third residue is a polar amino acid which is suggested to serve as an orienting residue for the catalytic histidine (Anantharaman & Aravind, 2003). In all three enzymes analyzed here, $YkfC_{Bce}$, $YkfC_{Ctr}$ and $YkfC_{Cpn}$, this third residue is also a histidine. The active site of $YkfC_{Bce}$ is located at the SH3b1–NlpC/P60 interface, whereas the SH3b2 domain is distal to the active site. Residues from both the SH3b1 and the NlpC/P60 domain form the S2-S1 binding-site cavity. These S1 and S2 sites are complementary in shape and chemical properties to the L-Ala-γ-D-Glu ligand and primarily determine the substrate specificity of YkfC (Xu *et al.,* 2010). Alignment revealed remarkable sequence similarity and conservation of the catalytic triad and the majority of the S1 and S2 sites between the primary sequence of YkfC from *B. cereus, C. trachomatis* and *C. pneumoniae* (fig. 3.13).

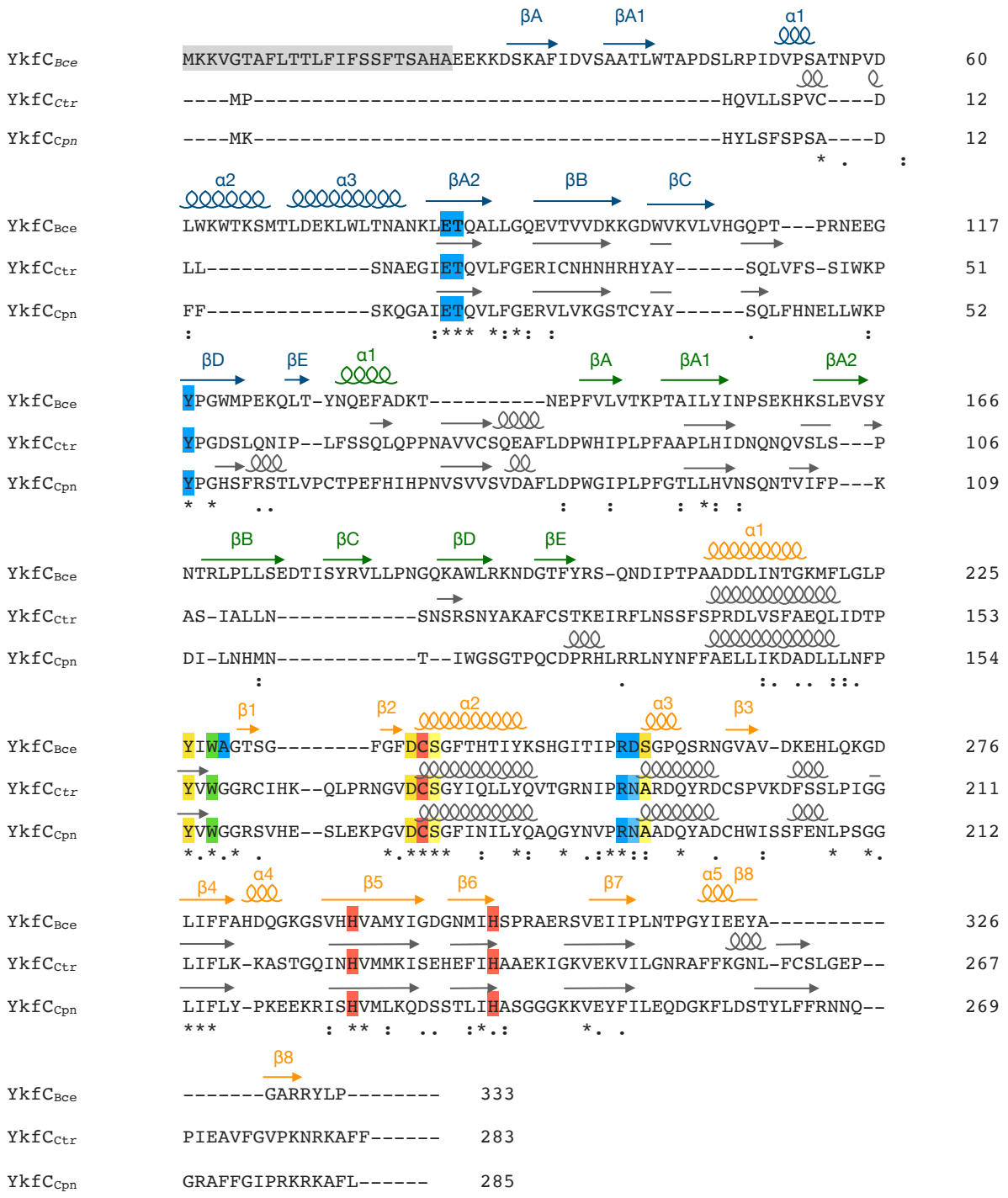

Figure 3.13. Primary sequence alignment of YkfC$_{Bce}$, YkfC$_{Ctr}$, and YkfC$_{Cpn}$. The secondary structure of YkfC$_{Bce}$ (Xu *et al.,* 2010) is shown above the sequence with the Sh3b1 domain in blue, the Sh3b2 domain in green and the NlpC/P60 domain in orange. The *in silico* predicted secondary structures of the *Chlamydia* proteins are shown in grey above the respective sequences. The catalytic triad comprising Cys, His and a polar residue is shown in red. Residues contributing to the S1 and S2 sites essential for substrate recognition in YkfC$_{Bce}$ are highlighted in yellow and blue, respectively, while residues contributing to both sites are highlighted in green. The signal peptide sequence of YkfC$_{Bce}$ is displayed in grey.

In $YkfC_{Bce,}$ five highly conserved residues located in the NlpC/P60 domain primarily contribute to the S1 site that interacts with the γ-D-Glu residue of substrates: Tyr226, Trp228, Asp237, Ser239 and Ser257 (Xu *et al*., 2010) (fig. 3.13 & 3.15; highlighted in yellow). The tyrosine positions the substrate close to the active site's catalytic cysteine and is present in $YkfC_{Ctr}$ and $YkfC_{Cpn}$. The tryptophan contributes to both the S1 and S2 sites and is conserved in $YkfC_{Ctr}$ and $YkfC_{Cpn}$. Likewise, aspartic acid and the first of the two serine residues are conserved. The second serine is changed to alanine in both chlamydial proteins. A similar change of serine at this position to alanine occurs in a YkfC homolog of *Bacillus sphaericus*, whose S1 and S2 binding sites are otherwise identical to $YkfC_{Bce}$ (Xu *et al.*, 2010). Apparently this exchange does not affect the substrate specify since *B. sphaericus* YkfC, similar to as $YkfC_{Bce}$, is a peptidase with a strict specificity for PG-derived peptides (Vacheron *et al.* 1979; Xu *et al*., 2010).

While the γ-D-Glu residue of the substrate interacts with the enzyme's S1 site, its mDAP residue interacts with the S2 binding pocket of YkfC. In $YkfC_{Bce}$, amino acids located in the SH3b1 and the NlpC/P60 domain contribute to the S2 pocket. Residues Glu83, Thr84a and Tyr118 are located in the SH3b1 domain (fig. 3.13 & 3.15; highlighted in blue), with tyrosine being the only one of the three residues that interacts directly with D-Ala through its side chain and is therefore essential for catalysis (Xu *et al*., 2010). All three residues are conserved in $YkfC_{Ctr}$ and $YkfC_{Cpn}$. In the NlpC/P60 domain of $YkfC_{Bce}$, the residues Trp228, Ala229, Arg255 and Asp256 contribute to the S2 site. While tryptophan and arginine are conserved in $YkfC_{Ctr}$ and $YkfC_{Cpn}$, alanine and aspartic acid are changed. In both *Chlamydia* proteins, alanine is replaced with glycine and aspartic acid is changed to asparagine (fig. 3.13). Since the residue at position 256 of $YkfC_{Bce}$ is required to neutralize the positive charge of the free amine of the substrate L-Ala residue, it plays an essential role in substrate specificity. In $YkfC_{Bce}$, this residue is an aspartic acid (Asp256), but its replacement by an aspartate is not uncommon and was also described in other YkfC homologs (Xu *et al*. 2010).

Taken together, conservation of the majority of residues contributing to the $YkfC_{Bce}$ S1-S2 binding site in $YkfC_{Ctr}$ and $YkfC_{Cpn}$ and the conservation of all residues essential to support catalysis indicate a similar substrate specificity and enzymatic activity of *Bacillus* YkfC and the putative YkfC from *Chlamydia*.

While the first 23 residues within the YkfC$_{Bce}$ amino acid sequence are predicted to be a signal peptide for transport into the periplasm (Xu *et al.,* 2010), neither the SignalP-05 nor the PrediSi tool (tab. 2.1) were able to detect a signal peptide in the sequences of YkfC$_{Ctr}$ and YkfC$_{Cpn}$. Interestingly, *B. subtilis* YkfC does not contain a signal peptide either, despite otherwise high sequence identity with YkfC$_{Bce}$ and an analysis of sequence similarities of different YkfC homologs showed that a signal peptide is also absent in proteobacterial and cyanobacterial YkfC homologs (Xu *et al.,* 2010).

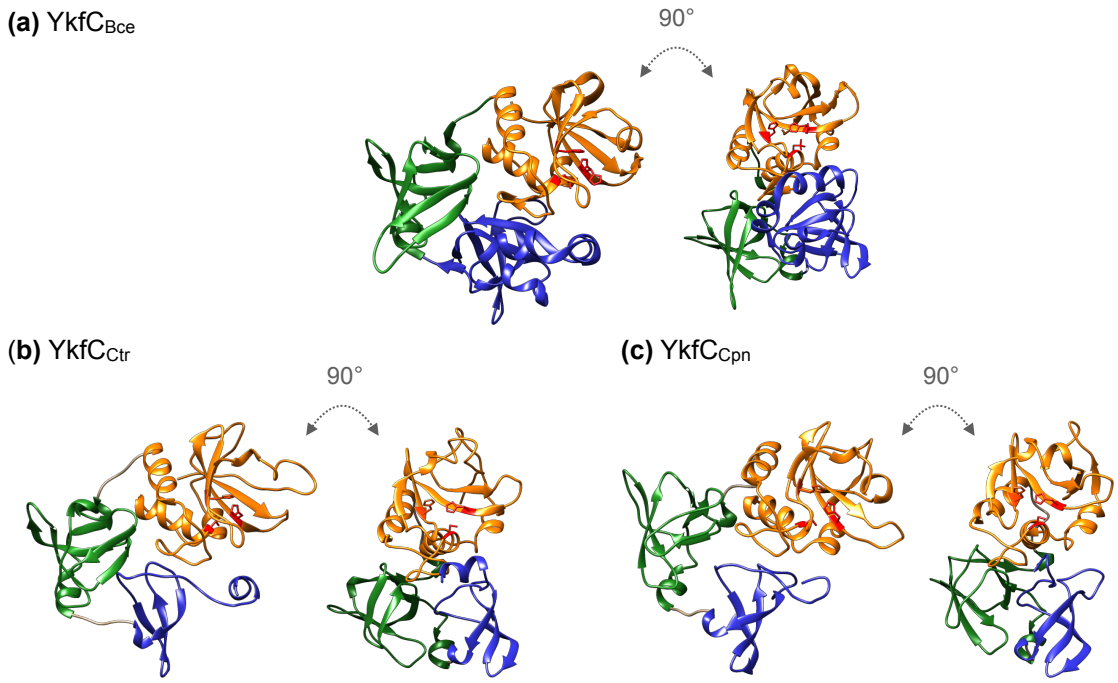

Figure 3.14. Comparison of 3D *in silico* overall structure models of YkfC$_{Bce}$, YkfC$_{Ctr}$, and YkfC$_{Cpn}$. Based on Phyre2 alignment against the protein structure of **(a)** YkfC$_{Bce}$ (Xu *et al.,* 2010) the protein structures of **(b)** YkfC$_{Ctr}$ and **(c)** YkfC$_{Cpn}$ were predicted and modeled with the Chimera tool. The Sh3b1 domain is highlighted in blue, the Sh3b2 domain in green and the NlpC/P60 domain in orange. The catalytic triad comprising Cys, His and a polar residue is shown in red.

Sequence similarity of YkfC$_{Ctr}$ and YkfC$_{Cpn}$ with YkfC$_{Bce}$ allowed 3D *in silico* modeling using the Phyre2 tool (tab. 2.1). The resulting protein structures were visualized using Chimera (tab. 2.1) and compared to the crystal structure of YkfC$_{Bce}$ (Xu *et al.,* 2010) (fig. 3.14). In accordance with the similarities in the primary sequence, 3D modeling shows that both N-terminal SH3b domains and the C-terminal NlpC/P60 domain, which contains the catalytic triad, are conserved in the *Chlamydia* proteins. The secondary structure of the NlpC/P60 domain typically consists of three α-helices and

five β-strands. The catalytic triad's conserved cysteine is located at the extreme N-terminus of the second α-helix and the two conserved catalytic histidine residues are situated at the second and third β-strands, respectively (Anantharaman & Aravind 2003). This conformation of the NlpC/P60 domain is not only conserved in $YkfC_{Bce}$, but also predicted for the active sites of $YkfC_{Ctr}$ and $YkfC_{Cpn}$ (fig. 3.14). As mentioned above, in addition to the conservation of the active site catalytic triad, residues important for substrate interaction of the S1 and S2 site are present in both chlamydial YkfC proteins. Comparison of the 3D models shows that these residues are accessible in the binding-site cavity in $YkfC_{Ctr}$ and $YkfC_{Cpn}$, as shown for $YkfC_{Bce}$ (Xu *et al.,* 2010) (fig. 3.15).

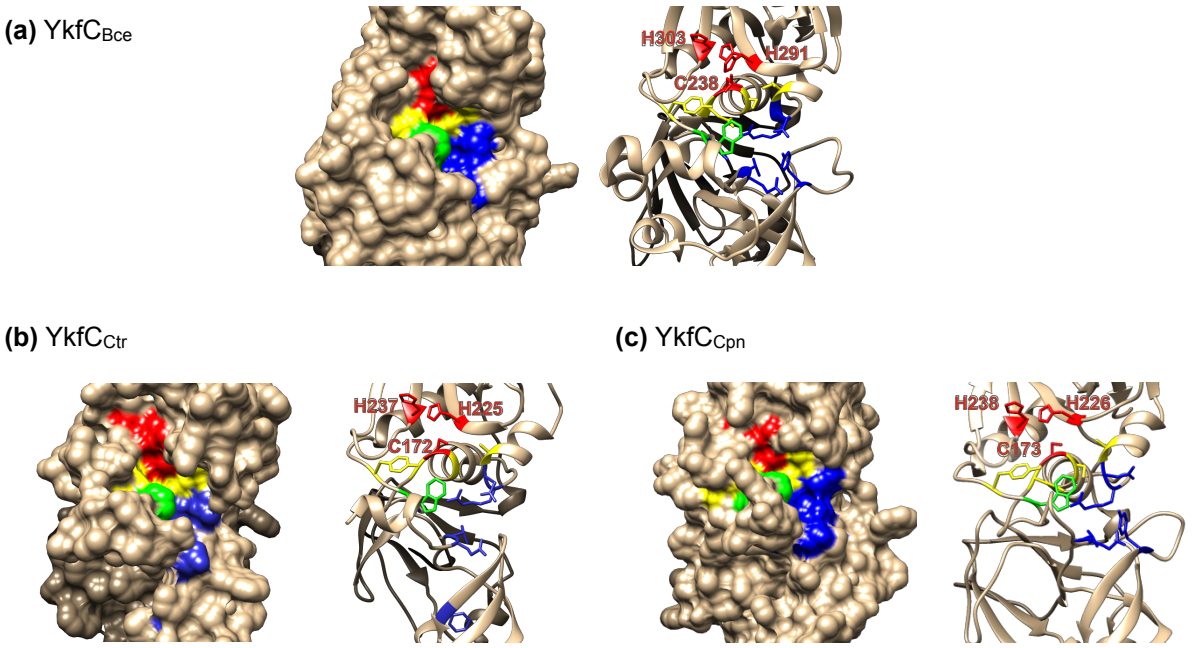

Figure 3.15. Comparison of 3D *in silico* models of the active site in $YkfC_{Bce}$, $YkfC_{Ctr}$ and $YkfC_{Cpn}$. Based on Phyre2 alignment against the structure of the active site of **(a)** $YkfC_{Bce}$ (Xu *et al.,* 2010) the 3D structure of the active site of **(b)** $YkfC_{Ctr}$ and **(c)** $YkfC_{Cpn}$ was predicted and modeled with the Chimera tool. The Cys-His-His catalytic triad is shown in red, residues contributing to the S1 and S2 sites essential for substrate recognition in $YkfC_{Bce}$ are highlighted in yellow and blue, respectively. Residues contributing to both sites are highlighted in green.

Taken together, the observed similarities in the primary sequence, the predicted overall protein structure, and particularly the active site architecture of *C. trachomatis* and *C. pneumoniae* YkfC to *B. cereus* YkfC allow the identification of these proteins as orthologs.

3.4.2. Recombinant *C. trachomatis* YkfC ($YkfC_{Ctr}$) shows catalytic activity on PG-derived tripeptide

To analyze the biochemical properties of the *Chlamydia* YkfC ortholog, $YkfC_{Ctr}$ and $YkfC_{Cpn}$ were heterologously overexpressed in *E. coli*. For this purpose, the corresponding genes, *ct127* and *cpn0245*, were cloned into a pET52b expression vector (tab. 2.6), to create recombinant proteins carrying an N-terminal Strep-tag II. Following production in *E. coli* Bl21, $YkfC_{Ctr}$ was purified with high yield after dialysis (1 mg of recombinant protein per 2 l culture) (see section 2.5.1). Recombinant $YkfC_{Ctr}$ has a calculated molecular weight of 34,1 kDa and showed a band at approximately 35 kDa in SDS PAGE analysis (fig. 3.16.a). In the case of $YkfC_{Cpn}$, purification was not successful as the recombinant protein appeared to aggregate in inclusion bodies. For this reason, further *in vitro* analyses in his work focused on $YkfC_{Ctr}$.

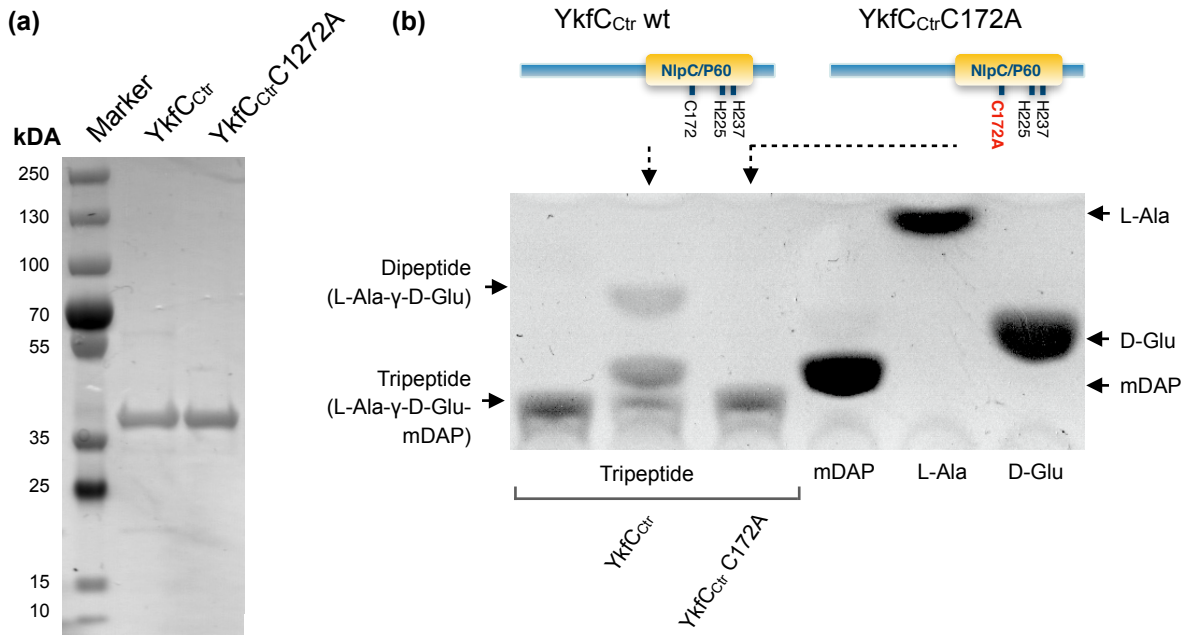

Figure 3.16. Purification and *in vitro* activity of recombinant $YkfC_{Ctr}$. (a) $YkfC_{Ctr}$ and its active site mutant $YkfC_{Ctr}C172A$ were analyzed by SDS-PAGE. **(b)** *In vitro* peptidase activity was analyzed by TLC using L-Ala-γ-D-Glu-mDAP tripeptide as a substrate. Activity is detectable by an equivalent migration distance of the reaction product and the mDAP migration control. $YkfC_{Ctr}$, but not its active site mutant $YkfC_{Ctr}C172A$, released mDAP from the tripeptide. L-Ala-γ-D-Glu-mDAP tripeptide and the amino acids L-Ala, γ-D-Glu, and mDAP served as additional migration controls.

As a control, an active site mutant of $YkfC_{Ctr}$, named $YkfC_{Ctr}C172A$, in which the catalytic triad's cysteine was changed to alanine, was overproduced and purified as described for wild type $YkfC_{Ctr}$. The mutant protein showed a band at approximately

35 kDa in SDS PAGE analysis (fig. 3.16.a). Incubation of the recombinant proteins with PG-derived L-Ala-γ-D-Glu-mDAP tripeptide (section 2.5.5.e), followed by product analysis by thin-layer chromatography (`TLC peptides'; section 2.5.6.b) showed that wild type $YkfC_{Ctr}$ was capable to release mDAP, while $YkfC_{Ctr}$C172A had no catalytic activity on the tripeptide (fig. 3.16.b).

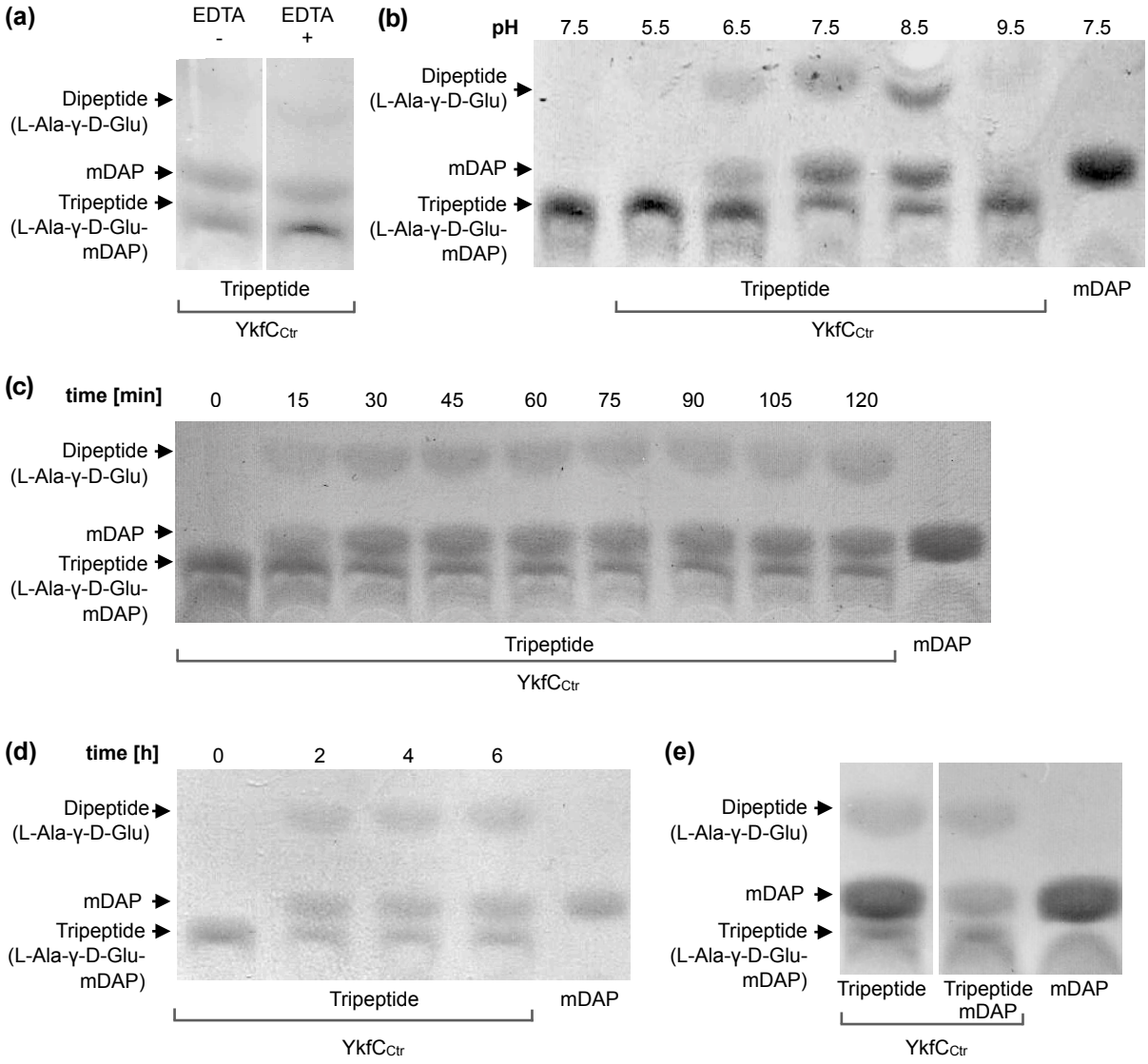

Figure 3.17. Analysis of the *in vitro* activity of recombinant $YkfC_{Ctr}$. *In vitro* peptidase activity of $YkfC_{Ctr}$ was analyzed by TLC using L-Ala-γ-D-Glu-mDAP tripeptide as a substrate. Activity is detectable by an equivalent migration distance of the reaction product and the mDAP migration control. **(a)** $YkfC_{Ctr}$ activity was not decreased in presence of the chelator EDTA (10 mM). **(b)** The chlamydial YkfC homolog showed the highest activity between pH 7.5 and 8.5. Acidic conditions appear to be unfavorable, as shown by the complete loss of activity at pH 5.5. **(c)** $YkfC_{Ctr}$ was able to release mDAP from the tripeptide 15 minutes after the reaction was started by addition of the enzyme. The highest substrate turnover under the experimental conditions tested was observed after 120 minutes of incubation. The enzyme's activity was not affected by **(d)** either prolonged incubation times of 4 and 6 hours **(e)** or the presence of the reaction product mDAP.

To rule out a possible contamination of heterologously produced YkfC$_{Ctr}$ by the zinc-dependent peptidase MpaA of the *E. coli* producer strain, an enzyme that is also able to release mDAP from tripeptide, the metal chelator EDTA was added to the assay. Consistent with the results observed for the YkfC$_{Ctr}$C172A mutant, which showed no background activity, the addition of EDTA did not detectably affect substrate turnover (fig. 3.17.a), confirming high purity and the absence of interfering host peptidases in the protein purification.

To further explore the ability of YkfC$_{Ctr}$ to hydrolyze tripeptide, additional assays were performed to analyze the pH and time dependence. The pH optimum for *in vitro* activity of the enzyme was between 7.5 and 8.5 (fig. 3.17. b) and thus close to the postulated pH value of 7.3 within the *C. trachomatis* inclusion (Grieshaber, 2002). For this reason, all of the following assays were performed in MOPS buffer at pH 7.5. The experiments showed that activity of YkfC$_{Ctr}$ was time-dependent and cleavage of the substrate could already be observed after 15 minutes of incubation (fig. 3.16. c). It should be noted that after longer incubation times of 4 and 6 hours, neither complete turnover of the tripeptide nor an inhibitory effect of the resulting products was observed (fig. 3.17. d). The inability of YkfC$_{Ctr}$ to fully convert the amount of substrate provided could be explained by the fact that the commercially available L-Ala-γ-D-Glu-mDAP tripeptide molecules used here contain a mixture of L,L-, D,D- and L,D-mDAP within their peptide structure. Non-native peptides (most likely containing D,D-mDAP) may not be recognized by YkfC$_{Ctr}$. Under the experimental conditions tested, the highest substrate turnover was observed after 2 hours of incubation (fig. 3.17.c). This incubation time was therefore used for all following assays.

Since PG recycling needs to be tightly controlled and product inhibition might act as a negative feedback mechanism in YkfC$_{Ctr}$, it was tested whether the addition of mDAP at concentrations equal to the applied substrate concentration has an inhibitory effect (fig. 3.17.e). Consistent with the results obtained with extended incubation times (fig. 3.17.d), the activity of the enzyme was not affected by additional added mDAP. Together, these observations make a negative feedback regulation of YkfC$_{Ctr}$ by its reaction products rather unlikely.

Overall, TLC-based analyses identified $YkfC_{Ctr}$ as a peptidase capable of hydrolyzing L-Ala-γ-D-Glu-mDAP tripeptide, resulting in the release of mDAP. The identity of the reaction products was further confirmed by MS-based analysis as shown in the following section (section 3.4.3). In addition, analysis of the active site mutant $YkfC_{Ctr}$C172A identified the cysteine of the catalytic triad as crucial for the enzymatic activity of $YkfC_{Ctr}$.

3.4.3. $YkfC_{Ctr}$ shows substrate specificity for PG-derived peptides

Sequence and structure similarities of $YkfC_{Ctr}$ with *Bacillus* YkfC (section 3.4.1) suggest that the chlamydial enzyme also plays a role in PG recycling. Since no signal peptide sequence for the transport across the cytoplasmic membrane can be detected $YkfC_{Ctr}$, the enzyme appears to be localized in the cytoplasm in *C. trachomatis*. There, the activity of a PG recycling enzyme has to be be tightly regulated to prevent disruption of the lipid II biosynthesis. To gain insight into how a possible control mechanism for chlamydial YkfC might work, different substrates, including PG, PG-derived peptides, and lipid II and its precursors, were tested in the optimized $YkfC_{Ctr}$ *in vitro* assay.

As described in section 3.4.2, TLC-based analysis confirmed the enzymatic activity of $YkfC_{Ctr}$ on PG-derived tripeptide. In addition, *in vitro* activity of $YkfC_{Ctr}$ on peptides derived from digestion of *E. coli* PG with the recombinant *B. subtilis* amidase $CwlC_{Bsu}$ could be demonstrated by mass spectrometric analysis (section 2.5.7). R. Kluj (Mayer lab, Department of Microbiology/Organismic Interactions, University of Tübingen) kindly provided the substrate and analyzed the reaction products by mass spectroscopy (MS) for this experiment. The method reconfirmed $YkfC_{Ctr}$ activity on PG-derived tripeptide (L-Ala-γ-D-Glu-mDAP) by detecting released mDAP and additionally allowed detection of its activity on PG-derived tetrapeptide (L-Ala-γ-D-Glu-mDAP-D-Ala), resulting in the release of the dipeptide mDAP-D-Ala (fig. 3.18.a & b). Furthermore, $YkfC_{Ctr}$ was shown to cleave not only single PG-derived peptides but also di-tetrapeptides interconnected via D-Ala−mDAP cross-links (L-Ala-γ-D-Glu-mDAP-D-Ala)-(L-Ala-D-γ-Glu-mDAP-D-Ala) (fig. 3.18.c). In line with the result of the TLC-based analysis, $YkfC_{Ctr}$ cleaved tri- and tetrapeptides between their γ-D-Glu and mDAP residue in both free and cross-linked peptides. The active site mutant $YkfC_{Ctr}$C172A showed no activity on all substrates tested.

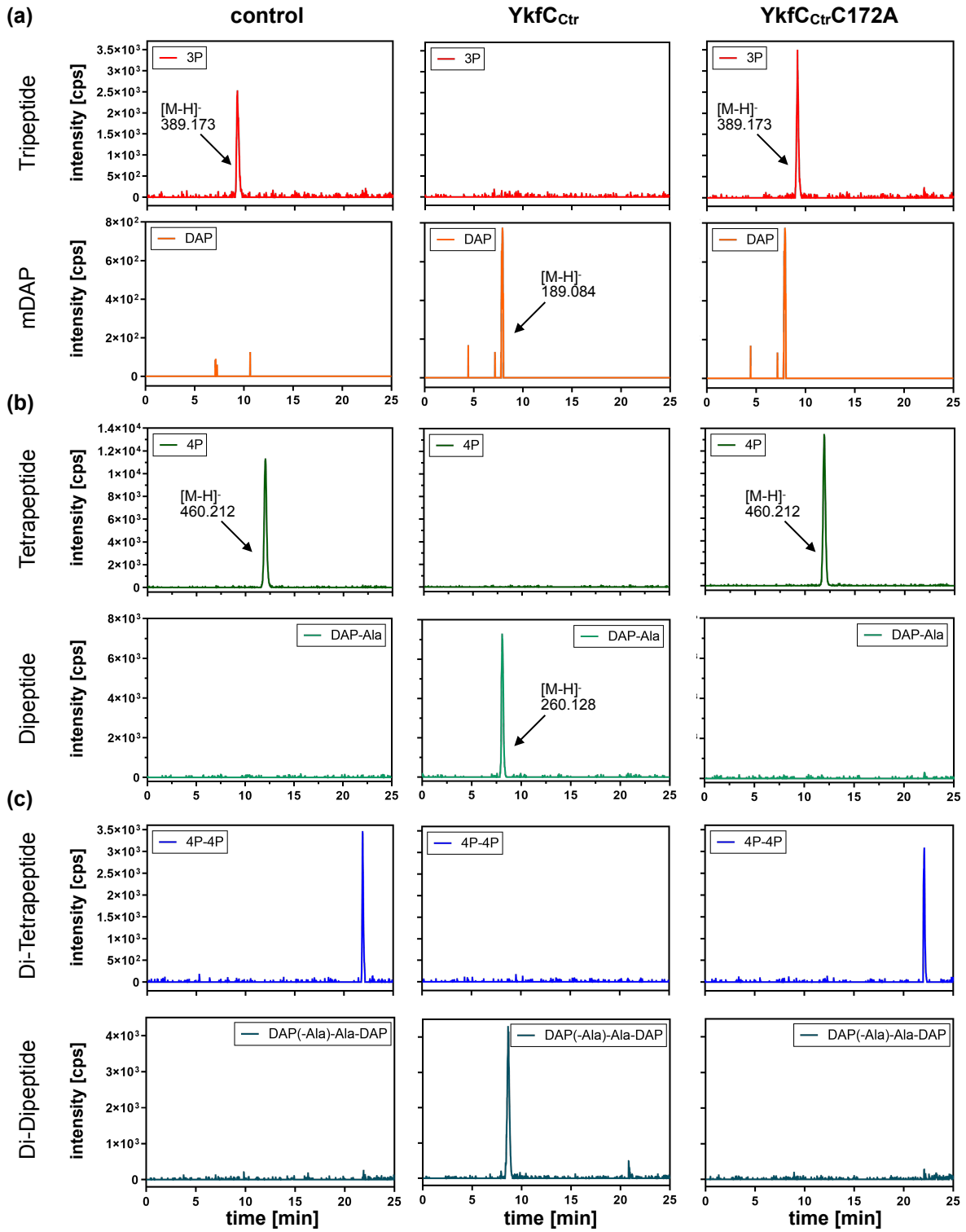

Figure 3.18. MS analysis of YkfC$_{Ctr}$ *in vitro* activity on peptides derived from *E. coli* PG by CwlC$_{Bsu}$ digestion. YkfC$_{Ctr}$, but not its active-site mutant YkfC$_{Ctr}$C172A, is active towards *E. coli* PG-derived **(a)** tripeptide (L-Ala-γ-D-Glu-mDAP; '3P') and **(b)** tetrapeptide (L-Ala-γ-D-Glu-mDAP-D-Ala; '4P') as shown by the release of mDAP and mDAP-D-Ala, respectively. PG-derived **(c)** di-tetrapeptide linked by a D-Ala−mDAP cross-link ((L-Ala-γ-D-Glu-mDAP-D-Ala)-(L-Ala-γ-D-Glu-mDAP-D-Ala); ‚4P-4P') is also hydrolyzed by YkfC$_{Ctr}$, but not by YkfC$_{Ctr}$C172A, as shown by the release of the di-dipeptide mDAP-(D-Ala)-D-Ala-mDAP. Dialysis buffer was added instead of recombinant protein for control reactions. R. Kluj (University of Tübingen) kindly provided *E. coli* PG-derived peptides and performed the MS-analysis.

In contrast to the TLC-based assay which tested a commercially available mixture of L,L-, D,D- and L,D-mDAP containing tripeptide as substrate (section 3.4.2), *E. coli* PG-derived peptides were used as substrate in the MS-based analysis. When using the bacterial PG-derived peptides, a complete turnover of the substrate could be observed (fig. 3.18), suggesting that the incomplete turnover observed in the TLC-based approach is due to the inability of $YkfC_{Ctr}$ to cleave non-native peptides.

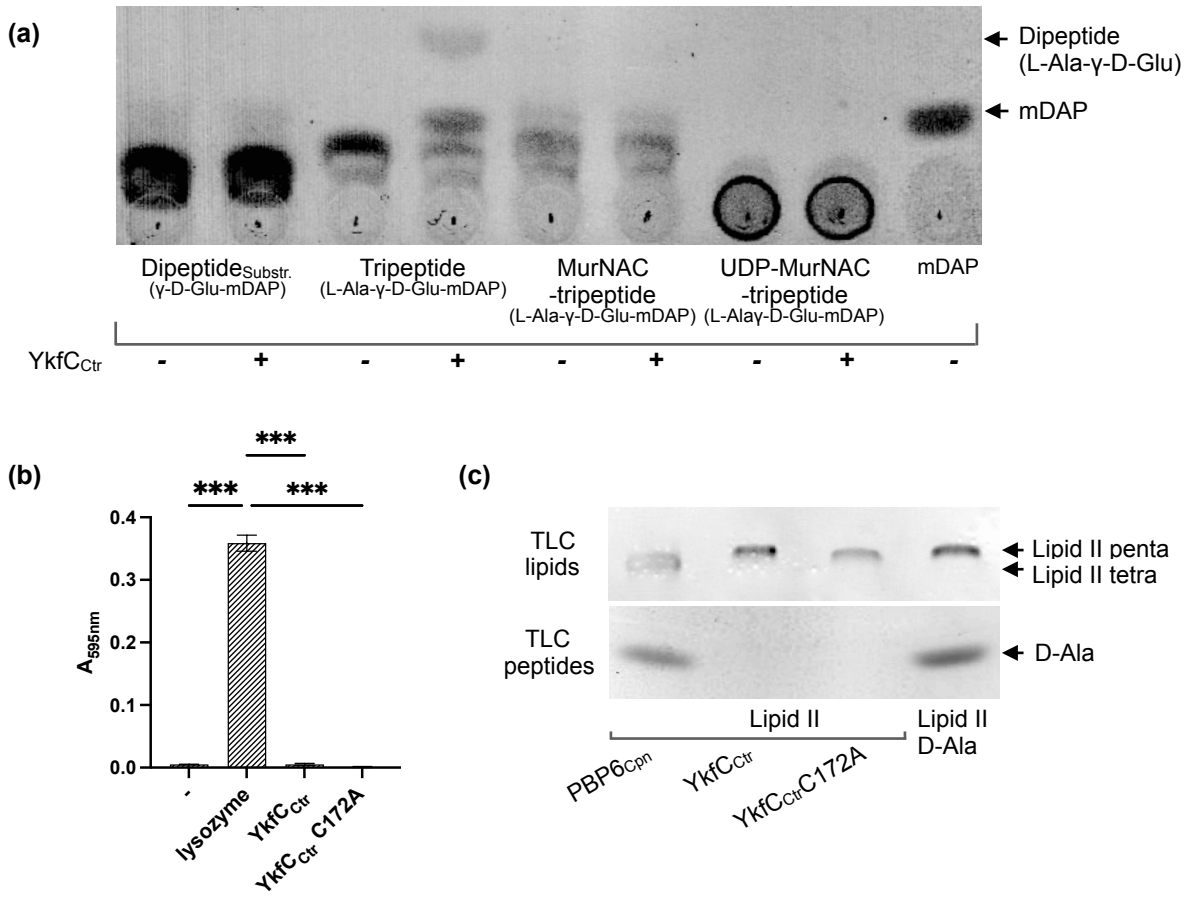

Figure 3.19. Substrate specificity of $YkfC_{Ctr}$. (a) *In vitro* activity of $YkfC_{Ctr}$ on soluble PG precursors and recycling products. TLC analysis showed that $YkfC_{Ctr}$ uses tripeptide derived from PG as a substrate but neither the lipid II precursor UDP-MurNAc-tripeptide nor the PG-recycling product MurNAc-tripeptide. The tripeptide appears to be the minimal substrate as the dipeptide γ-D-Glu-mDAP was not hydrolyzed under the conditions tested. **(b)** Dye-release assay and photometric analysis of the reaction product. $YkfC_{Ctr}$ and its active-site mutant $YkfC_{Ctr}C172A$ showed no hydrolytic activity when incubated with RBB labelled PG. Lysozyme served as a positive control, releasing labelled PG-derived peptides into the supernatant. Enzymatic activity was confirmed by measuring the absorbance of the supernatant at 595 nm. Samples were compared with the lysozyme control by one-way ANOVA analysis using GraphPad Prism (GraphPad Software). ***: P-value < 0.001. Error bars indicate ± s.d. (n=3). **(c)** *In vitro* activity of $YkfC_{Ctr}$ on the membrane bound PG precursor lipid II. TLC analysis showed that neither $YkfC_{Ctr}$ nor its active site mutant used lipid II as a substrate as shown for the chlamydial carboxypeptidase $PBP6_{Cpn}$. $PBP6_{Cpn}$ activity released the terminal D-Ala from lipid II thereby altering the migration behavior of lipid II on the lipid TLC and producing free D-Ala which is visible on the peptide TLCs**.** Recombinant $PBP6_{Cpn}$ was kindly provided by I. Löckener (Henrichfreise group).

While $YkfC_{Ctr}$ showed activity on free *E. coli* PG-derived peptides cleaved from the MurNAc sugar moiety by amidase digestion, it was unable to use MurNAc-L-Ala-γ-D-Glu-mDAP as a substrate (fig. 3.19.a). In addition, no activity of $YkfC_{Ctr}$ on isolated *E. coli* PG sacculi was detected in a remazol brilliant blue (RBB) dye release assay (fig. 3.19.b).

With regard to a possible interference of $YkfC_{Ctr}$ activity with PG biosynthesis, the PG building block lipid II (mDAP type) as well as its activated precursor UDP-MurNAc-tripeptide were tested as possible substrates. Due to its carrier molecule $C_{55}PP$, lipid II could not be visualized in the TLC system used to detect peptides. Therefore, an additional TLC method specialized in the detection of lipids was used ('TLC lipids', section 2.5.6.a). As a control, the activity of the recombinant *C. pneumoniae* DD-CPase PBP6 ($PBP6_{Cpn}$) (kindly provided by I. Löckener; Henrichfreise group) on lipid II was visualized using both methods. The D-Ala residue cleaved from lipid II by $PBP6_{Cpn}$ activity was visible in the peptide-specific TLC, and the lipid-specific TLC showed a change in migration between native lipid II and cleaved lipid II with a tetrapeptide stem (fig. 3.19.c). In the case of $YkfC_{Ctr}$, the lack of free detectable peptides and the unaltered migration behavior of lipid II indicated that lipid II was not used as a substrate (fig. 3.18.c). Likewise, $YkfC_{Ctr}$ did not cleave off any amino acid residues from the soluble lipid II precursor UDP-MurNAc-tripeptide (fig. 3.19.a).

Taken together, these results demonstrate that $YkfC_{Ctr}$ has high substrate specificity for PG-derived tripeptide (L-Ala-γ-D-Glu-mDAP) and tetrapeptide (L-Ala-γ-D-Glu-mDAP-D-Ala) and shows no activity on molecules involved in cytoplasmic PG biosynthesis, such as lipid II and UDP-MurNAc-tripeptide. While PG-derived peptides were used as a substrate, neither PG itself nor its recycling product MurNAc-tripeptide were cleaved by $YkfC_{Ctr}$. These observations are consistent with previous studies that showed that NlpC/P60 enzymes involved in PG recycling in free-living bacteria rely on the presence of a free L-Ala at the N-terminus for proper substrate recognition (Xu *et al.* 2015). Only the tri- and tetrapeptides have a freely accessible N-terminus, while in the case of all other substrates tested in this work the N-terminus is occupied by its binding to an N-acetyl-muramyl residue. Any observed activity of $YkfC_{Ctr}$ towards tested substrates depended on its catalytic Cys-His-His triad since the mutant $YkfC_{Ctr}C172A$ showed no activity in all assays. These results identify *C. trachomatis* YkfC as a PG recycling enzyme specific for free PG-derived peptides.

3.4.4. YkfC$_{Ctr}$ shows activity on *B. subtilis* PG-derived peptides

Since chlamydiae are Gram-negative organisms, peptides derived from *E. coli* PG were tested as substrates in the YkfC$_{Ctr}$ activity assays in this work (section 3.4.3). However, the chlamydial enzyme YkfC$_{Ctr}$ is an ortholog of the recycling enzyme YkfC of Gram-positive *Bacillus* species. In *B. subtilis,* the PG pentapeptide found in the vegetative cell form has an L−Ala−γ-D−Glu−mDAP−D−Ala−D−Ala sequence, with amidation of the carboxyl groups of mDAP occurring in most stem peptides (Atrih *et al*., 1999). This modification of the pentapeptide by amidation is only present in Gram−positive organisms and is not found in either *E. coli* or *Chlamydia* PG-derived peptides.

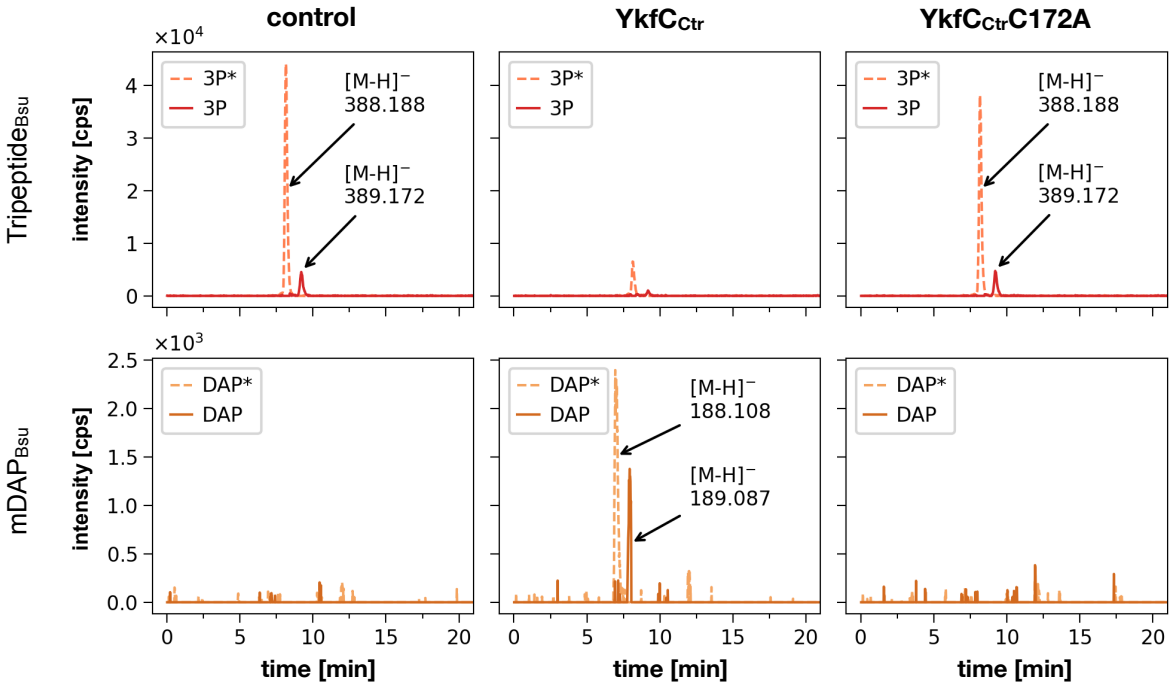

Figure 3.20. MS analysis of YkfC$_{Ctr}$ *in vitro* activity on peptides derived from *B. subtilis* PG by CwlC$_{Bsu}$ digestion. YkfC$_{Ctr}$, but not its active-site mutant YkfC$_{Ctr}$C172A, was active on both amidated (‚3P*') and not amidated ('3P') PG-derived L-Ala-γ-D-Glu-mDAP tripeptide, as shown by the release of amidated (‚DAP*') and not amidated ('DAP') mDAP, respectively. For control reactions, dialysis buffer was added instead of recombinant protein. R. Kluj (University of Tübingen) kindly provided the *B. subtilis* PG-derived peptide and performed the MS-analysis.

In this work, MS-based analysis was used to analyze the *in vitro* activity of YkfC$_{Ctr}$ on tripeptide derived by CwlC$_{Bsu}$ digestion of *B. subtilis* PG. For this purpose, R. Kluj (Mayer lab, Department of Microbiology/Organismic Interactions, University of Tübingen) kindly provided the substrate and carried out the MS analysis. Similar to

its activity towards *E. coli* PG-derived peptides (section 3.4.3), YkfC$_{Ctr}$ cleaved free *B. subtilis* PG-derived tripeptides (L-Ala-γ-D-Glu-mDAP), thereby releasing mDAP (fig. 3.20.). Again, its enzymatic activity depended on the catalytic triad since the active site mutant YkfC$_{Ctr}$C172A did not show activity in this assay. Although most of the *B. subtilis* PG-derived tripeptide is amidated at its mDAP residue, YkfC$_{Ctr}$ activity resulted in an almost complete turnover of the substrate. The *Chlamydia* enzyme is able to hydrolyze the γ-D-Glu-mDAP bond of peptides derived from both *B. subtilis* and *E. coli* PG. In contrast, the PG-degrading enzymes NlpD and SpoIID from the *Chlamydia*-like organism *Waddlia chondrophila* have been shown to interact only with PG from *E. coli* and not from *B. subtilis* (Frandi *et al*., 2014; Jacquier *et al*., 2019).

3.4.5. YkfC$_{Ctr}$ *in vitro* activity is inhibited by chloroacetone and E-64

A characteristic catalytic triad consisting of a cysteine, a histidine and a polar residue is conserved in all enzymes of the NlpC/P60 superfamily (Anantharaman & Aravind, 2003). *In silico* analysis found the residues to be present in the active site of YkfC$_{Ctr}$ (section 3.4.1) and the cysteine residue was shown to be essential for the enzyme's *in vitro* activity (sections 3.4.2 - 4). The presence of an essential cysteine in YkfC$_{Ctr}$ makes the enzyme a potential target for cysteine protease inhibitors which could be used to further characterize the enzyme's active site. To this end, four cysteine protease inhibitors were tested for their effect towards YkfC$_{Ctr}$ *in vitro* activity: chloroacetone, iodoacetamide, phenylmethylsulfonyl fluoride (PMSF) and E-64.

Chlamydia proteins typically contain a high number of cysteine residues which are otherwise relatively rare amino acids (Otten *et al*., 2015). In total, YkfC$_{Ctr}$ contains 8 cysteines of unknown redox state which might also be targeted by chloroacetone, iodoacetamide and PMSF, as these agents bind to all accessible sulfhydryl groups. For this reason, inhibitor concentrations for these compounds were tested in relation to the total number of all theoretically available cysteine residues. This adjustment was not required for the cysteine protease inhibitor E-64, as this compound binds selectively to the active site of cysteine proteases (Matsumoto *et al*., 1999).

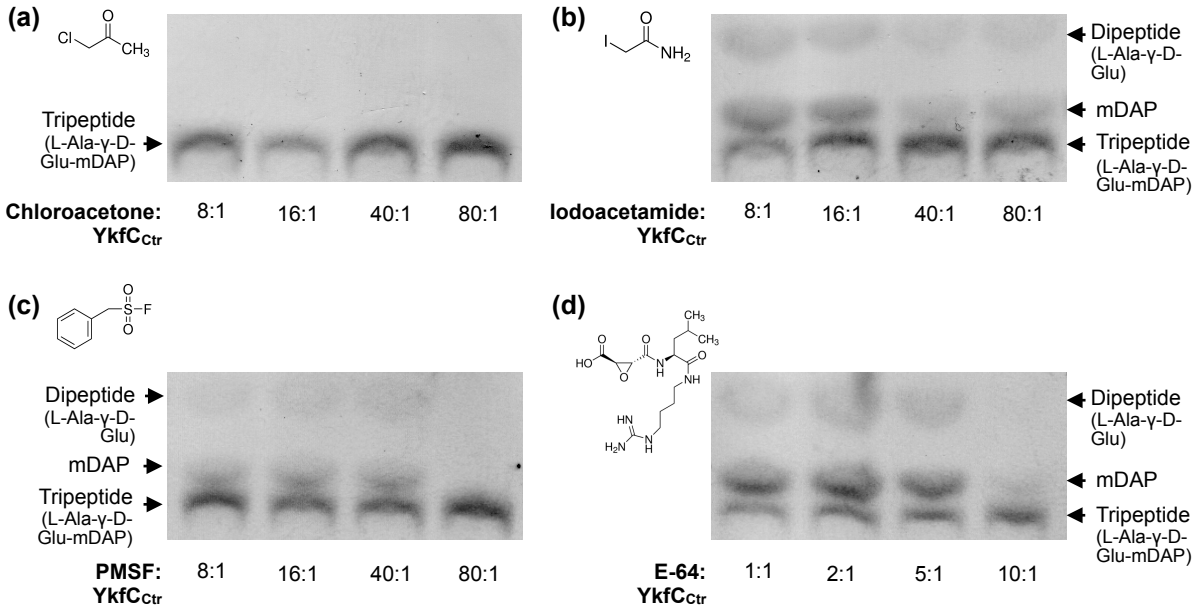

Figure 3.21. Effect of cysteine peptidase inhibitors on the enzymatic activity of YkfC$_{Ctr}$. TLC analysis of the inhibiting effects of chloroacteone, iodoacetamide, phenylmethylsulfonyl fluoride (PMSF) and E-64 on YkfC$_{Ctr}$ *in vitro* activity on L-Ala-γ-D-Glu-mDAP tripeptide. **(a)** The alkylating compound chloroacteone inhibited YkfC$_{Ctr}$ at an inhibitor:protein molar ratio of 8:1, as indicated by the absence of the reaction product mDAP. **(b)** The alkylating compound iodoacetamide did not inhibit YkfC$_{Ctr}$ at any of the inhibitor concentrations tested. **(c)** The non-selective, reversible serine- and cysteine protease inhibitor PMSF showed inhibition at an inhibitor:protein molar ratio of 80:1. **(d)** The cysteine protease inhibitor E-64, carrying a *trans*-epoxysuccinic acid group coupled to a dipeptide, inhibited YkfC$_{Ctr}$ at an inhibitor:protein molar ratio of 10:1.

Of the two alkylating compounds tested, only chloroacetone inhibited catalytic activity of YkfC$_{Ctr}$ on tripeptide at an inhibitor:protein molar ratio of 8:1 (corresponding to an inhibitor:active site cysteine molar ratio of 1:1) (fig. 3.21.a). Iodoacetamide showed no inhibitory effect under the conditions tested, even at an inhibitor:protein molar ratio of 80:1 (fig. 3.21.b). The same specific inhibition by chloroacetone but not by iodoacetamide has been reported for *Bacteroides ovatus* YkfC (Xu et al., 2015). The lack of inhibition by iodoacetamide could be attributed to the lower electronegativity of iodine compared to chlorine in chloroacetone. In presence of the reversible serine- and cysteine inhibitor phenyl-methylsulfonyl fluoride (PMSF), YkfC$_{Ctr}$ retained *in vitro* activity and total inhibition could only be observed at inhibitor:protein molar ratios of 80:1 (fig. 3.21.c). In contrast, the cysteine peptidase specific inhibitor E-64, which carries a *trans*-epoxysuccinic acid group coupled to a dipeptide, inhibited YkfC$_{Ctr}$ activity at a molar ratio of inhibitor:protein of 10:1 (fig. 3.21.d).

Together with the results of the *in silico* protein structure analyses of YkfC$_{Ctr}$ and the observed inactivity of the YkfC$_{Ctr}$C172A mutant in the *in vitro* assays, the result of the

cysteine peptidase inhibitors screening confirms an essential role of the active site cysteine for catalytic activity of $YkfC_{Ctr}$.

3.4.6. $YkfC_{Ctr}$ *in vitro* activity is not inhibited by α-X-chalcones

In addition to the cysteine-peptidase-inhibitors, a set of α,β-unsaturated carbonyl compounds, α-X-chalcones, were tested for their potential inhibitory effect on $YkfC_{Ctr}$ activity *in vitro.* The compounds were kindly provided by the group of S. Amslinger (Institute of Organic Chemistry, University of Regensburg). Consisting of an alkene conjugated to a ketone, the α-X-chalcones could interact with free sulhydryl-groups of cysteine residues due to their α,β-unsaturated carbonyl group (Amslinger, 2010). As mentioned above, the presence of a catalytic cysteine in $YkfC_{Ctr}$ makes the enzyme a potential target for inhibitors targeting this amino acid. Therefore, ten α-X-chalcone derivates were tested in the $YkfC_{Ctr}$ standard *in vitro* activity assay. The result showed that at the tested inhibitor:protein molar ratio of 10:1, none of the derivatives were able to significantly inhibit the detected $YkfC_{Ctr}$ *in vitro* activity (fig. 3.22).

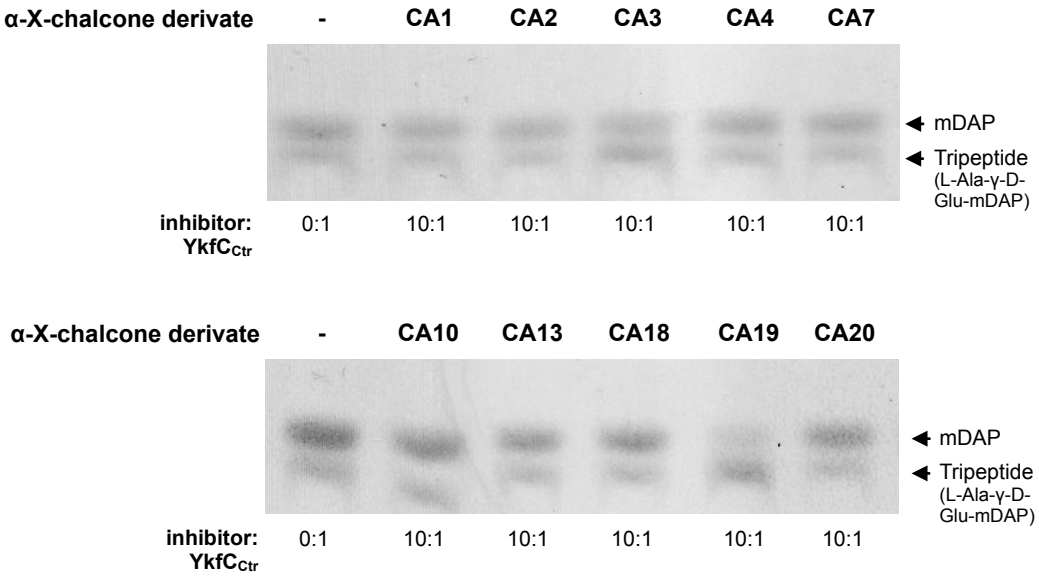

Figure 3.22. Effect of different α-X-chalcone derivates on the enzymatic activity of $YkfC_{Ctr}$. TLC analysis of the effect of the α-X-chalcone derivates CA1, CA2, CA3, CA4, CA7, CA10, CA13, CA18, CA19 and CA20 on $YkfC_{Ctr}$ *in vitro* activity on L-Ala-γ-D-Glu-mDAP tripeptide. None of the tested compounds did show an inhibitory effect on $YkfC_{Ctr}$ activity at an inhibitor:protein molar ratio of 10:1. Only in the presence of C19 did the activity of the enzyme decrease slightly.

3.4.7. *In silico* analysis of putative NlpC/P60 peptidases from *Chlamydia*-like organisms

$YkfC_{Bce}$, $YkfC_{Ctr}$ and $YkfC_{Cpn}$ were used as templates for BLAST alignments to identify putative YkfC homologs within *Chlamydia*-like organisms. Genes encoding for putative NlpC/P60 domain-containing proteins were found in members of the *Simkaniaceae*, *Parachlamydiaceae*, *Criblamydiaceae*, but not within the *Waddliaceae* family.

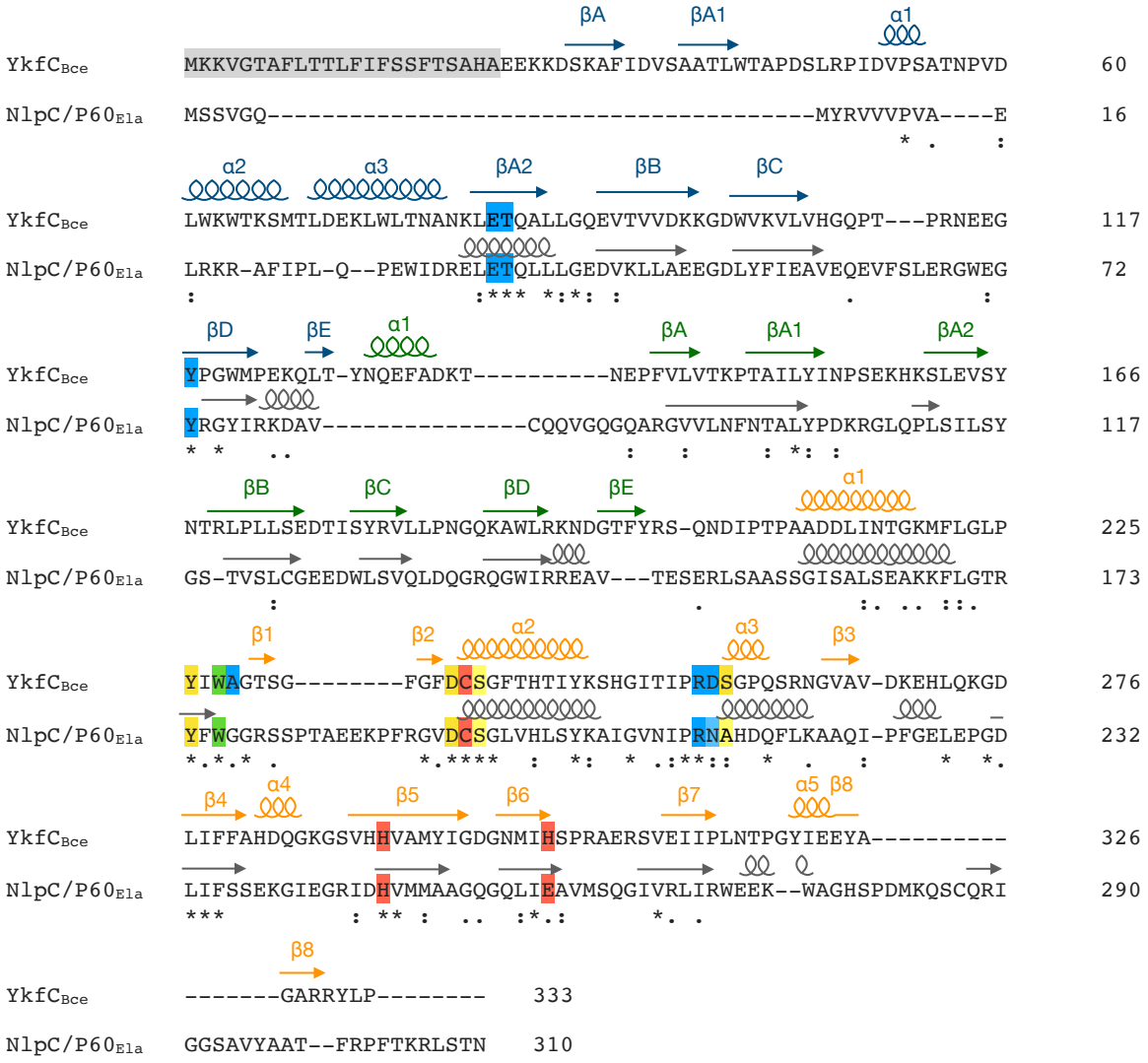

Figure 3.23. Primary sequence alignment of $YkfC_{Bce}$ and $NlpC/P60_{Ela}$. The secondary structure of $YkfC_{Bce}$ (Xu *et al.,* 2010) is shown above the sequence with the Sh3b1 domain in blue, the Sh3b2 domain in green and the NlpC/P60 domain in orange. The *in silico* predicted secondary structure of $NlpC/P60_{Ela}$ is shown in grey above the respective sequences. The catalytic triad comprising Cys, His and a polar residue is shown in red. Residues contributing to the S1 and S2 sites essential for substrate recognition in $YkfC_{Bce}$ are highlighted in yellow and blue, respectively, while residues contributing to both sites are highlighted in green. The signal peptide sequence of $YkfC_{Bce}$ is shown in grey.

To learn more about the role of these enzymes in *Chlamydia*-like organisms, two putative NlpC/P60 proteins from *Estrella lausannensis* (*Criblamydiaceae*) and *Simkania negevensis* (*Simkaniaceae*) were chosen for detailed *in silico* analyses. As described in section 3.4.1 for *Chlamydia* YkfC, the primary sequences and predicted structures of both, *E. lausannensis* NlpC/P60$_{Ela}$ and *S. negevensis* NlpC/P60$_{Sne}$, were compared to sequence and structure of *B. cereus* YkfC (YkfC$_{Bce}$).

NlpC/P60$_{Ela}$ and YkfC$_{Bce}$ share 28 % amino acid sequence identity. The catalytic residues as well as the majority of residues essential for substrates binding in YkfC$_{Bce}$ are conserved in NlpC/P60$_{Ela}$ (fig. 3.23). The amino acid changes of some conserved residues in the S1 and S2 binding sites in NlpC/P60$_{Ela}$ are the same as observed in YkfC$_{Ctr}$ and YkfC$_{Cpn}$ (see section 3.4.1). As discussed for *Chlamydia* YkfC, these changes should not significantly alter the proposed interaction between the enzyme and its substrate. The catalytic triad characteristic for NlpC/P60 family peptidases is conserved in NlpC/P60$_{Ela}$, but the third residue, which is a histidine in YkfC$_{Bce}$, is changed to glutamic acid. As observed for *Chlamydia* YkfC, no signal peptide sequence was predicted for NlpC/P60$_{Ela}$ neither with the SignalP-05 nor with the PrediSi tool (tab. 2.1). Sequence similarity of NlpC/P60$_{Ela}$ and YkfC$_{Bce}$ allowed for 3D *in silico* modeling using the Phyre2 tool (tab. 2.1). The resulting NlpC/P60$_{Ela}$ protein structure was visualized using Chimera (tab. 2.1) and compared to the crystal structure of YkfC$_{Bce}$ (Xu *et al.,* 2010) (fig. 3.24). The comparison revealed that both SH3b domains, the NlpC/P60 domain with its characteristic secondary structure (described in section 3.4.1) and the catalytic triad are conserved in the *E. lausannensis* protein.

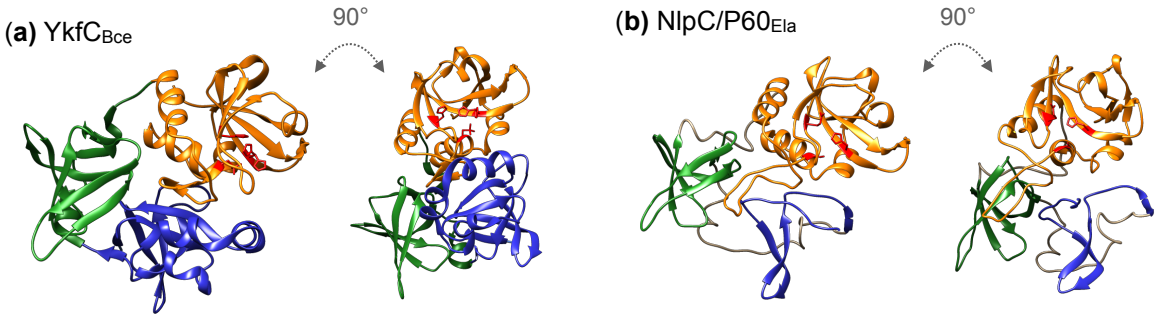

Figure 3.24. Comparison of 3D *in silico* models of YkfC$_{Bce}$ and NlpC/P60$_{Ela}$. Based on Phyre2 alignment against the structure of **(a)** YkfC$_{Bce}$ (Xu *et al.,* 2010), the 3 D structure of **(b)** NlpC/P60$_{Ela}$ was predicted and modeled using the Chimera tool. The Sh3b1 domain is highlighted in blue, the Sh3b2 domain in green and the NlpC/P60 domain in orange. The catalytic triad comprising Cys, His and a polar residue is shown in red.

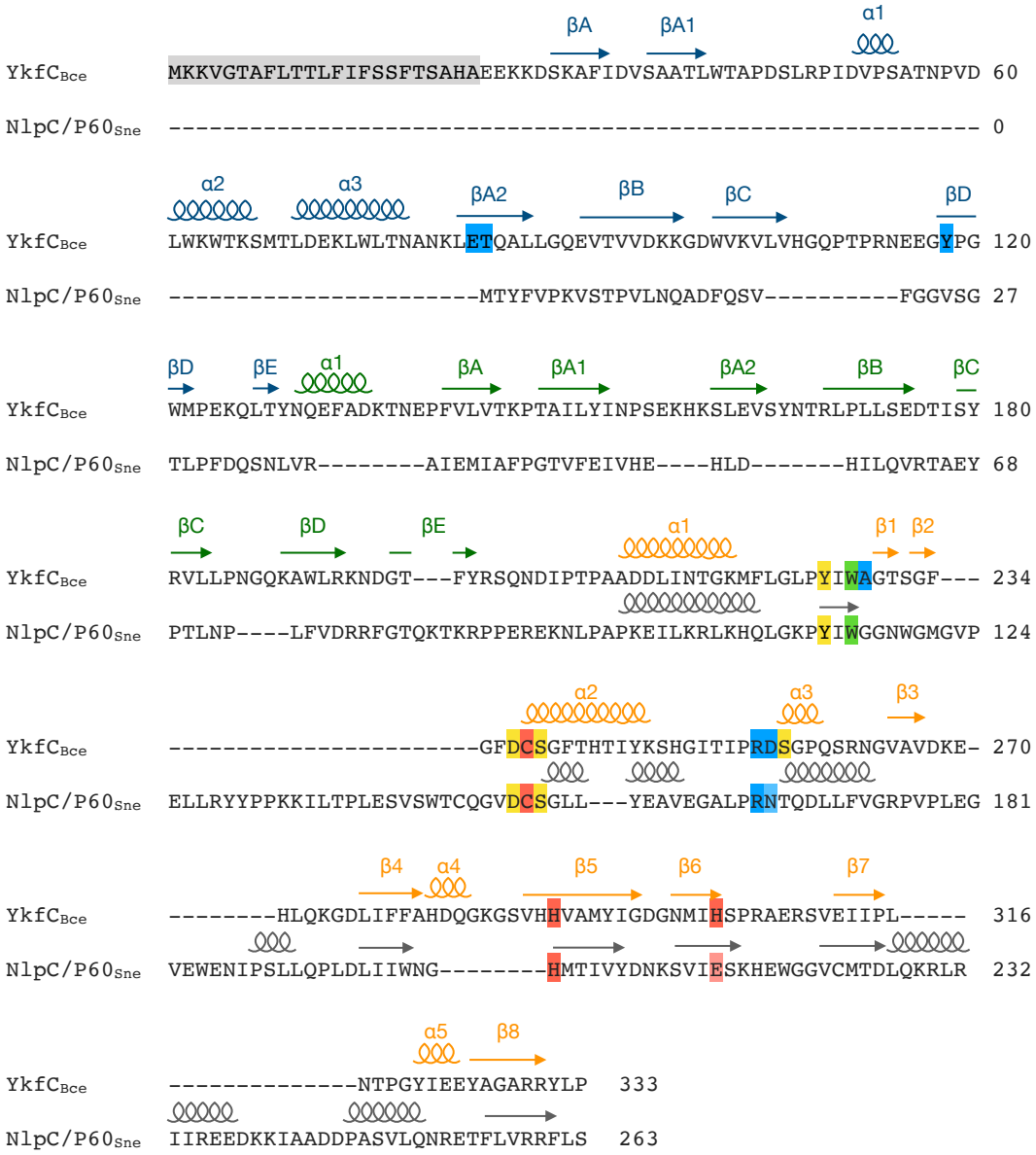

Figure 3.25. Primary sequence alignment of YkfC$_{Bce}$ and NlpC/P60$_{Sne}$. The secondary structure of YkfC$_{Bce}$ (Xu *et al.,* 2010) is shown above the sequence with the Sh3b1 domain in blue, the Sh3b2 domain in green and the NlpC/P60 domain in orange. The *in silico* predicted secondary structure of NlpC/P60$_{Sne}$ is shown in grey above the respective sequences. The catalytic triad comprising Cys, His and a polar residue is shown in red. Residues contributing to the S1 and S2 sites essential for substrate recognition in YkfC$_{Bce}$ are highlighted in yellow and blue, respectively, while residues contributing to both sites are highlighted in green. The signal peptide sequence of YkfC$_{Bce}$ is shown in grey.

While NlpC/P60$_{Ela}$ shows sequential and structural similarities to *Bacillus* and *Chlamydia* YkfC, the putative *S. negevensis* NlpC/P60 protein differs from these proteins. Alignment of the primary sequences of NlpC/P60$_{Sne}$ and YkfC$_{Bce}$ revealed that the two N-terminal Sh3b domains characteristic for YkfC peptidases are missing in NlpC/P60$_{Sne}$. Only the C-terminal part of the protein, which contains the NlpC/P60

domain, shows sequence similarities to YkfC$_{Bce}$ (fig. 3.25). Consequently, since NlpC/P60$_{Sne}$ lacks the SH3b1 domain, residues located in this domain that contribute to the S2-mDAP binding pocket in YkfC$_{Bce}$ are absent. The catalytic triad of the NlpC/P60 domain is conserved NlpC/P60$_{Sne}$, with the third residue being a glutamic acid as in NlpC/P60$_{Ela}$. As for NlpC/P60$_{Ela}$, no signal peptide sequence was predicted for NlpC/P60$_{Sne}$. The differences in the primary sequence of NlpC/P60$_{Sne}$ and the other YkfC proteins analyzed in this work are also reflected in the overall structure of NlpC/P60$_{Sne}$. Unlike the 3D *in silico* models of the other chlamydial YkfC proteins, which showed the closest similarities to the crystal structure of YkfC$_{Bce}$ (Xu *et al.,* 2010), the predicted structure of NlpC/P60$_{Sne}$ showed the closest similarity to the crystal structure of the *Trichomonas vaginalis* NlpC/P60 PG hydrolase NlpC_A2 (fig. 3.26).

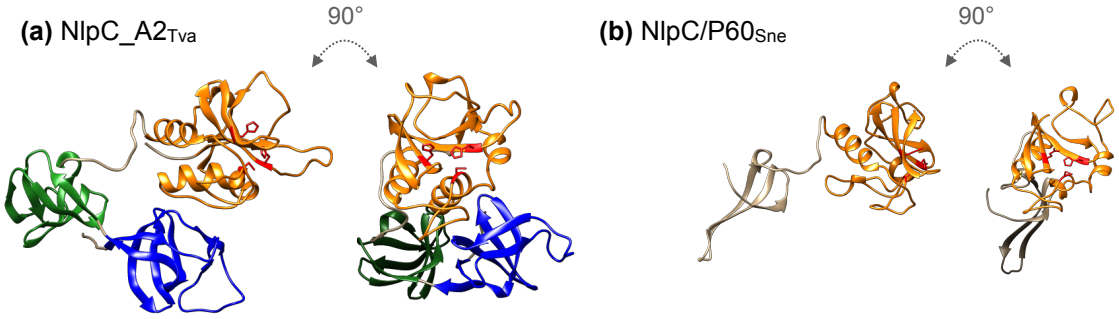

Figure 3.26. Comparison of 3D *in silico* models of NlpC_A2$_{Tva}$ and NlpC/P60$_{Sne}$. Based on Phyre2 alignment against the structure of **(a)** NlpC_A2$_{Tva}$ (Pinheiro *et al.,* 2018) the 3 D structure of **(b)** NlpC/P60$_{Sne}$ was predicted and modeled with the Chimera tool. The Sh3b1 and Sh3b2 domains of NlpC_A2$_{Tva}$ are highlighted in blue and green, respectively. The NlpC/P60 domain of both proteins is highlighted in orange with the catalytic triad comprising Cys, His and a polar residue is shown in red.

The prokaryotic parasite *T. vaginalis* is thought to have acquired bacterial genes encoding NlpC/P60 family PG hydrolases by lateral gene transfer (Pinheiro *et al.*, 2018). Similar to other NlpC/P60 peptidases such as YkfC$_{Bce}$, NlpC_A2 consists of a C-terminal NlpC/P60 domain which includes the catalytic triad and is preceded by two Sh3b domains (Pinheiro *et al.*, 2018) (fig. 3.26.a). As mentioned above, the two N-terminal Sh3b domains are absent in NlpC/P60$_{Sne}$, therefore the Phyre2 alignment against NlpC_A2 focused on the NlpC/P60 domain.

Taken together the *in silico* results indicate that NlpC/P60$_{Ela}$ is an ortholog of YkfC$_{Bce}$. NlpC/P60$_{Sne}$ carries the characteristic NlpC/P60 domain but differs significantly in its overall structure from YkfC$_{Bce}$ as well as from YkfC$_{Ctr}$, YkfC$_{Cpn}$ and NlpC/P60$_{Ela}$.

3.4.8. $YkfC_{Ctr}$, $NlpC/P60_{Ela}$ and $NlpC/P60_{Sne}$ act as tripeptide peptidases in *E. coli*

Many proteins of the NlpC/P60 peptidase superfamily function either as periplasmic PG endopeptidases or, like YkfC, as recycling enzymes that cleave peptides derived from PG degradation (Smith *et al*., 2001; Xu *et al*., 2010). To learn more about the putative role of NlpC/P60 enzymes in the PG turnover of *Chlamydia* and *Chlamydia*-like organisms, complementation assays with plasmids encoding either $YkfC_{Ctr}$, $YkfC_{Cpn}$, $NlpC/P60_{Ela}$ or $NlpC/P60_{Sne}$ were performed in two different *E. coli* surrogate systems.

Analysis of the *in vitro* activity of $YkfC_{Ctr}$ strongly suggests that this enzyme acts as a recycling enzyme on PG-derived peptides (section 3.4.3). Therefore, activity of chlamydial NlpC/P60 enzymes was tested in an *E. coli* mutant strain reporting on degradation of the PG-derived L-Ala-γ-D-Glu-mDAP tripeptide. The strain, referred to in this work as *E. coli dapD*$^-$ Δ*mpl* mutant (see sections 2.3.2.c and 2.6.1), was kindly provided by D. Mengin-Lecreulx (Université Paris-Sud). The *E. coli* mutant is auxotrophic for mDAP and deficient in the utilization of L-Ala-γ-D-Glu-mDAP tripeptide both through its incorporation into nascent PG precursors and through its degradation. Impairment of a critical enzyme of the L-Lys synthesis pathway encoded by *dapD* resulted in the mutant's autotrophy for mDAP. To prevent the direct incorporation of PG-derived tripeptide into newly synthesized PG precursors, the *mpl* gene, which encodes a ligase that links tripeptide to UDP-MurNAc, was deleted (Mengin-Lecreulx *et al.,*1996). In addition to the tripeptide ligase Mpl, *E. coli* also possesses a functional homolog of YkfC, the peptidase MpaA, which cleaves mDAP from the L-Ala-γ-D-Glu-mDAP tripeptide. Since MpaA expression in *E. coli* is reduced by the transcriptional regulator PgrR under nutrient-rich growth conditions (Uehara & Park, 2003; Shimada *et al.*, 2013), mDAP-release from tripetided by MpaA is hampered under these circumstances. Therefore, as described by Mengin-Lecreulx and colleagues, an *mpl*- deficient *E. coli* strain requires mDAP supplementation under nutrient-rich growth conditions (Mengin-Lecreulx *et al.,* 1996).

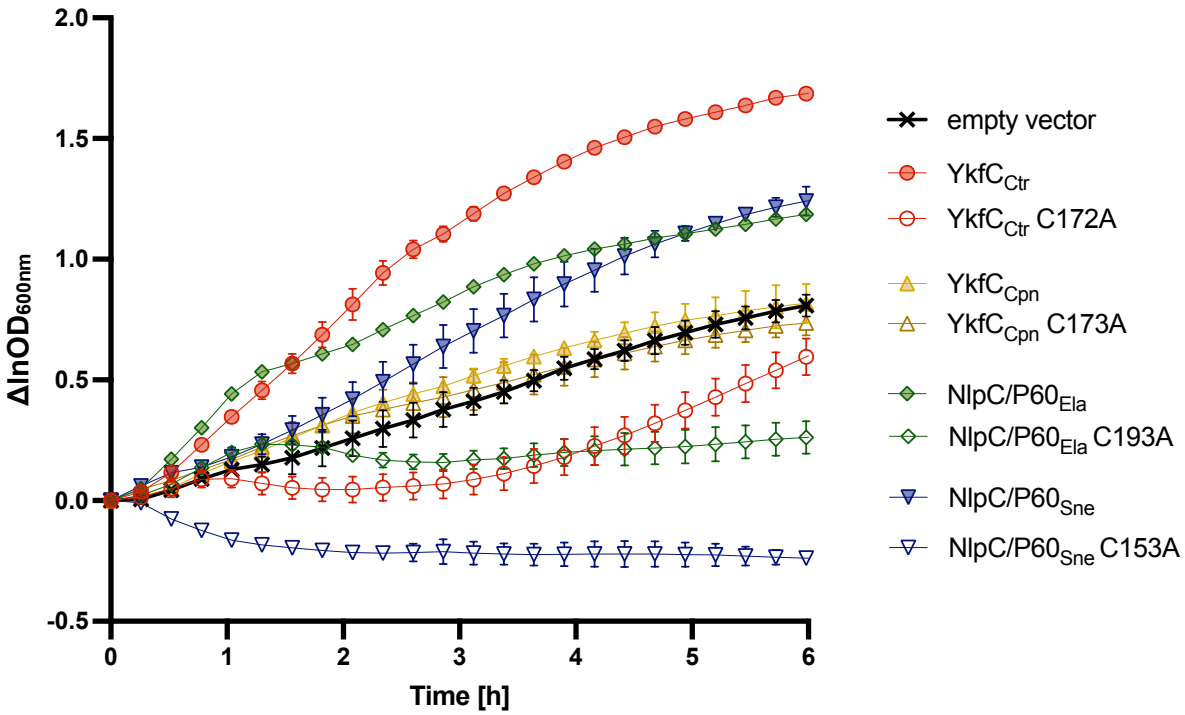

Figure 3.27. *In vivo* complementation of the *E. coli dapD*⁻ Δ*mpl* mutant using different chlamydial NlpC/P60 proteins. Growth kinetics of the *E. coli dapD*⁻ Δ*mpl* mutant in nutrient-rich media supplemented with 40 µM L-Ala-γ-D-Glu-mDAP tripeptide. The mutant was transformed with different pBAD24 constructs encoding $YkfC_{Ctr}$, $YkfC_{Cpn}$, $NlpC/P60_{Ela}$ and $NlpC/P60_{Sne}$ and active site mutants of these enzymes ($YkfC_{Ctr}$C172A, $YkfC_{Cpn}$C173A, $NlpC/P60_{Ela}$C193A and $NlpC/P60_{Sne}$C153A). Growth of the *E. coli dapD*⁻ Δ*mpl* mutant, which is auxotrophic for mDAP and cannot utilize PG-derived tripeptide under nutrient-rich conditions, was restored by cytoplasmic production of $YkfC_{Ctr}$, $NlpC/P60_{Sne}$ and $NlpC/P60_{Ela}$, but not by cytoplasmic production of $YkfC_{Cpn}$. Cytoplasmic production of the active site mutants of the NlpC/P60 enzymes did not enhance cell growth. Error bars indicate ±s.d. (n=3).

Incubating the *E. coli dapD*⁻ Δ*mpl* mutant in nutrient-rich medium during the complementation assay severely compromised its ability to utilize the L-Ala-γ-D-Glu-mDAP tripeptide as a source of mDAP, resulting in its defective growth (fig. 3.27, empty vector control). Expression of $YkfC_{Ctr}$, $NlpC/P60_{Sne}$ and $NlpC/P60_{Ela}$ restored growth, with expression of $YkfC_{Ctr}$ showing the strongest growth-promoting effect. The results suggest that all three proteins act as PG-derived tripeptide peptidases in *E. coli* and release sufficient amounts of mDAP promote growth (fig. 3.27). To investigate whether the observed growth rescue is conferred by the catalytic activity of the chlamydial NlpC/P60 enzymes, active site mutants of the enzymes were generated and tested in the complementation assay. In these mutants, $YkfC_{Ctr}$C172A, $NlpC/P60_{Ela}$C193A and $NlpC/P60_{Sne}$C153A, the conserved cysteine residue within the catalytic triad (Cys172 in $YkfC_{Ctr}$, Cys193 in $NlpC/P60_{Ela}$ and Cys153 in NlpC/

$P60_{Sne}$) was replaced by alanine. None of the mutants was able to restore the growth of the *E. coli dapD*$^-$ Δ*mpl* mutant strain beyond the level of empty vector control, suggesting that the complementation observed during expression of the chlamydial NlpC/P60 wild-type enzymes depends on their catalytic active site.

In contrast to the other three chlamydial enzymes tested, neither expression of wild-type $YkfC_{Cpn}$ nor expression of its active site mutant $YkfC_{Cpn}$C173A was able to restore the growth of the *E. coli dapD*$^-$ Δ*mpl* mutant strain (fig. 3.27). As described in section 3.4.2, unlike $YkfC_{Ctr}$, $YkfC_{Cpn}$ could not be overproduced as a soluble protein in *E. coli* Bl21 because it aggregated in inclusion bodies. Like the *E. coli* Bl21 producer strain, the *E. coli dapD*$^-$ Δ*mpl* mutant strain may not be able to produce $YkfC_{Cpn}$ in its active form under the conditions tested. Therefore, a possible function as a tripeptide peptidase for *C. pneumoniae* YkfC has yet to be investigated.

Like the *Bacillus* PG recycling peptidase $YkfC_{Bce}$, $YkfC_{Ctr}$ and $YkfC_{Cpn}$ carry a catalytic Cys-His-His triad in their active site (section 3.4.1). $NlpC/P60_{Ela}$ and $NlpC/P60_{Sne}$ differ from the *Chlamydia* YkfCs in that in them the third catalytic residue of the triad is glutamic acid instead of histidine (section 3.4.7). Since some NlpC/P60 proteins with a Cys-His-Glu catalytic triad tend to be PG hydrolytic enzymes rather than PG recycling peptidases (Anantharaman & Aravind 2003), the difference in their catalytic triad could indicate a different physiological role of the chlamydial enzymes. To investigate this possibility, a second *E. coli* surrogate system was introduced to test whether the chlamydial NlpC/P60 proteins function as periplasmic endopeptidases that cleave the cross-bridges between PG glycan chains.

The *E. coli* NlpC/P60 protein MepS (formerly named Spr) is a DD-endopeptidase that specifically cleaves D-Ala-mDAP cross-links within PG to allow incorporation of new glycan strands (Singh *et al*., 2012). It is known that *E. coli* mutants deficient in MepS exhibit a thermosensitive growth defect at low osmolarity (Hara *et al*., 1996). This phenotype was also observed in the *E. coli* ΔmepS mutant used in this work (see sections 2.3.2.c and 2.6.2). When *E. coli* ΔmepS expressed only the empty vector, its viability on low osmolarity nutrient broth agar plates decreased with increasing temperature (fig. 3.28.a-c). At an incubation temperature of 42 °C, cells became unable to grow (fig. 3.28.c).

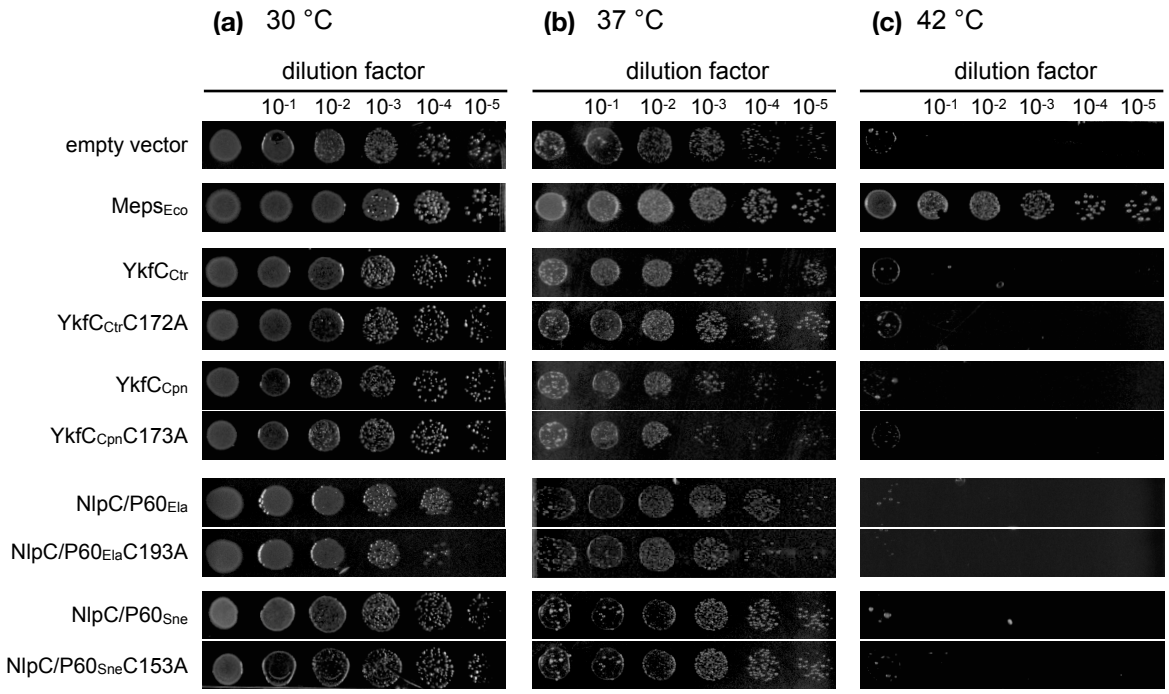

Figure 3.28. *In vivo* complementation of the *E. coli* Δ*mepS* mutants using different chlamydial NlpC/P60 proteins. Spot plate assay of an *E. strain coli* carrying a deletion for the gene encoding the periplasmic NlpC/P60 domain-containing PG endopeptidase MepS. *E. coli ΔmepS* was transformed with different pBAD24+ constructs encoding for *E. coli* $MepS_{Eco}$ and for the cytoplasmic chlamydial NlpC/P60 proteins $YkfC_{Ctr}$, $YkfC_{Cpn}$, $NlpC/P60_{Ela}$ and $NlpC/P60_{Sne}$ and active-site mutants of the enzymes ($YkfC_{Ctr}$C172A, $YkfC_{Cpn}$C173A, $NlpC/P60_{Ela}$C193A and $NlpC/P60_{Sne}$C153A). The *E. coli* Δ*mepS* mutant was incubated under low osmolarity conditions at **(a)** 30 °C, **(b)** 37 °C and **(c)** 42 °C. As a negative control, *E. coli ΔmepS* was transformed with the empty pBAD24+ vector. While expression of $MepS_{Eco}$ restored growth of the osmo- and temperature-sensitive mutant, expression of the chlamydial NlpC/P60 proteins did not result in complementation.

Since expression of the *E. coli* MepS protein compensated for the growth defect, the complementation assay allowed to examine possible periplasmic endopeptidase activity of $YkfC_{Ctr}$, $YkfC_{Cpn}$, $NlpC/P60_{Ela}$, and $NlpC/P60_{Sne}$. For all four enzymes tested, neither expression of the full-length wild-type protein nor expression of the respective active site mutant restored the growth of the *E. coli* ΔmepS mutant at 42 °C (fig. 3.28.c). This result is consistent with the predicted lack of a signal peptide in the chlamydial enzymes (sections 3.4.1, 3.4.7), making periplasmic localization and hence PG endopeptidase activity unlikely. In case of $YkfC_{Cpn}$, its inability to restore growth could also be caused by the production of insoluble protein in *E. coli,* as discussed for its expression in the *E. coli dapD*$^-$ Δ*mpl* mutant strain.

The results of the complementation assays support the hypothesis that $YkfC_{Ctr}$ plays a role in peptide recycling rather than in PG degradation. Consistent with its *in vitro* activity on PG-derived peptides (section 3.4.3), $YkfC_{Ctr}$ could restore cell growth when expressed in the *E. coli dapD*$^-$ Δ*mpl* mutant strain. The data indicate that $YkfC_{Ctr}$ is a functional γ-D-Glu-mDAP peptidase operating in cytoplasmic recycling of PG-derived peptides. Its predicted cytoplasmic localization makes a function as a periplasmic PG endopeptidase unlikely and indeed expression of $YkfC_{Ctr}$ could not compensate for an *E. coli* ΔmepS mutant's growth defect. This result is also consistent with the observed inability of purified $YkfC_{Ctr}$ to use PG as a substrate (section 3.4.3).

Not only $YkfC_{Ctr}$, but also the two tested NlpC/P60 enzymes from *Chlamydia*-like organisms were able to enhance the growth of the *E. coli dapD*$^-$ Δ*mpl* mutant. Thus, $NlpC/P60_{Ela}$ and $NlpC/P60_{Sne}$, can be identified as functional γ-D-Glu-mDAP peptidases in *E. coli*. In contrast, neither enzyme restored the growth of the *E. coli* ΔmepS mutant. Combined with the lack of a predictable signal peptide, these results suggest a cytoplasmic localization of $NlpC/P60_{Ela}$ and $NlpC/P60_{Sne}$. The suggestion that $NlpC/P60_{Ela}$ is a recycling rather than a degrading enzyme of PG is consistent with the predicted structural similarities with $YkfC_{Bce}$ (section 3.4.7), despite the fact that the enzymes differ in the last residue of the catalytic triad. Interestingly, the results of the complementation assays indicate that $NlpC/P60_{Sne}$, despite its structural differences from $YkfC_{Bce}$ and the other chlamydial NlpC/P60 proteins, is also involved in peptide recycling rather than PG degradation.

3.4.9. Recombinant *B. subtilis* YkfC does not show *in vitro* activity on lipid II

Previous studies showed that YkfC orthologs from many free-living bacteria are γ-D-Glu-mDAP peptidases that depend on a free N-terminal L-Ala terminus of the peptide for proper substrate recognition. This substrate specificity is thought to be essential to prevent interference with bacterial PG synthesis (Xu *et al.* 2010; 2015). In a previous study, *B. cereus* YkfC showed no activity on UDP-MurNAC-tripeptide which is the activated precursor of lipid II in PG biosynthesis (Xu *et al.* 2015). Here, the activity of recombinant *B. subtilis* YkfC ($YkfC_{Bsu}$) on the ultimate PG precursor lipid II (mDAP type) was tested. $YkfC_{Bsu}$ was kindly provided by R. Kluj (Mayer group, Department of Microbiology/Organismic Interactions, University of Tübingen) and the *in vitro* activity assay was performed as described for $YkfC_{Ctr}$ with the exception of adjustments in regard to the pH optimum of $YkfC_{Bsu}$. As observed for the *Chlamydia* enzyme, $YkfC_{Bsu}$ did not use the PG precursor lipid II as a substrate. Reaction products of lipid II could not be detected, neither on the TLC specific for peptides nor due to changes in the running behavior of lipid II on the TLC specific for lipids (fig. 3.29). This result is consistent with the previous findings by Xu and colleagues (Xu *et al.,* 2015) and further confirms the substrate specificity of the YkfC recycling peptidase for PG-derived peptides with a free N-terminal L-Ala residue.

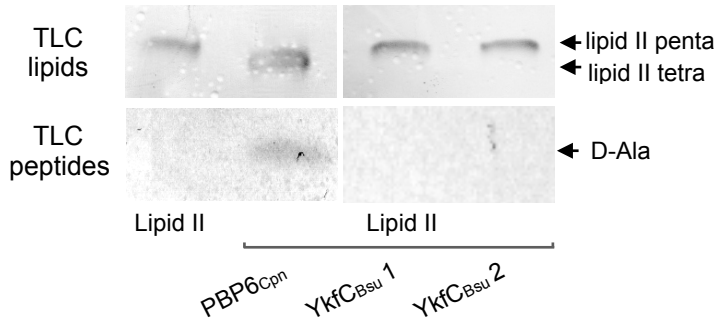

Figure 3.29. *In vitro* activity of $YkfC_{Bsu}$ on PG precursor lipid II (mDAP type). TLC analysis showed that recombinant $YkfC_{Bsu}$ from two different purifications ($YkfC_{Bsu}$ 1 and 2; kindly provided by R. Kluj, University of Tübingen) did not use lipid II as a substrate as shown for the chlamydial carboxypeptidase $PBP6_{Cpn}$ (kindly provided by I. Löckener, Henrichfreise lab). DD-CPase activity of $PBP6_{Cpn}$ releases the C-terminal D-Ala residue from the pentapeptide stem of lipid II ('lipid II penta'), generating lipid II with a tetrapeptide stem ('lipid II tetra') that showed altered migratory behavior on the lipid TLC. Free D-Ala released during this process becomes visible on the peptide TLC.

4. Discussion

During the course of evolution, chlamydiae became more and more adapted to their intracellular lifestyle and developed into experts in surviving inside their host cells. Due to their special characteristics, some difficulties hampered research on chlamydiae. After the first description of *C. trachomatis* as causing agent of the infectious eye disease trachoma in 1907 (von Prowazek & Halberstadter, 1907), it took over fifty years until chlamydiae were identified as bacteria (Moulder, 1966). Their obligate intracellular lifestyle and the resulting impossibility to cultivate these organisms in classical nutrient media had lead to their previous classification as viruses. To make the matter even more difficult, these organisms appeared to be deprived of peptidoglycan (PG), while being susceptible towards cell wall targeting β-lactam antibiotics (Matsumoto & Manire, 1970; Moulder 1993). This phenomenon, called ‘chlamydial anomaly’ (Moulder 1993), was explained by the finding that PG biosynthesis in *Chlamydiaceae* is tightly regulated in terms of both time and space and was therefore difficult to detect (Liechti *et al*., 2014).

As human pathogens, chlamydiae are versatile in terms of host species and tissue. While *C. trachomatis* serovars A-C infect the eye, serovars D-K cause chlamydial urogenital tract infection and are considered to be one of the most prevalent sexually transmitted diseases. However, it was estimated that only about 10 % of men and 5-30 % of women with laboratory-confirmed chlamydial urogenital tract infection develop symptoms (Farley *et al*., 2003; Korenromp *et al*., 2002), which means that the infection is often ‘silent‘ and may be overlooked. If the infection is left untreated, *C. trachomatis* could ascend to the upper genital tract where it causes pelvic inflammatory disease which may lead to ectopic pregnancy and infertility in women (Price *et al.*, 2013; Brunham *et al*., 2015).

The prevalence of chlamydial infection and the resulting burden of disease in Germany however relies on estimations since epidemiological data is scarce. While female infertility as a long term consequence of *C. trachomatis* infection has been extensively studied, male infertility due to chlamydial infection has only recently come to researchers' attention. Recent studies indicate that asymptomatic urogenital infections caused by *C. trachomatis* are correlated with male infertility (Ahmadi *et al*., 2018; Bryan *et al*., 2019). A gap in knowledge regarding the causing mechanisms of infertility between female and male patients is not limited to chlamydial infections but

is also the outcome of gender-biased neglect, a systemic problem in all scientific fields but with dire consequences in medicine. Although men and woman are just as likely to contribute to a couple's infertility, historically female factors are more often assumed to be its cause (Schilit, 2019; Turner *et al*., 2020). Therefor male factors of infertility are often overlooked creating situations in which 'women are the patients when male infertility is the disease' (Turner *et al*., 2020).

How is it that chlamydia among all pathogens are so adept at escaping not only researcher's notice but also the immune response of their hosts? As far as pathogens go, chlamydiae come up as almost pathetically small and non-virulent. The insidiousness of chlamydial infection lies not in toxins or other factors of pathogenicity, but rather in their ability to persist long term by halting their cell division and evade immune response. In the persisting state, chlamydiae can endure cellular stress induced by pro-inflammatory cytokines, antibodies, and antimicrobial substances (Hogan *et al*., 2004). When more favorable environmental conditions are reestablished, they return to their regular life cycle. Over an extended period of time tissue damage and scarification adds up. In addition to long term infection, unnoticed infections and treatment failures may also lead to reinfection. The gastrointestinal tract can become a chlamydiae reservoir from which reinfection of the urogenital tract by a fecal-oral-route can occur (Yeruva *et al*., 2013). Additionally, renewed sexual contact with a insufficiently treated partner may also result in a reoccurring of the infection. The epidemiological extent of a long term chlamydial infection, wether it is caused by persistence or reinfection, is unknown. Although a follow up screen approximately 3 months after treatment of a chlamydial infection is recommended in the treatment guideline for STIs by the US Centers for Disease Control and Prevention (Workowski *et al*., 2021), surveillance data is lacking - especially in males.

However, key to this insidious but effective lifestyle and strategy lies within chlamydial cell division and its regulation. The bacterial cell division machinery is inextricably linked to the PG biosynthesis process during septum formation, even in cell wall-less *Chlamydia*. At the same time elaborate and minimalist, chlamydial PG turnover seems to be a precisely set process which preserves the steps necessary for cell division but which is also adapted to the intracellular lifestyle. The following sections will discuss this work's results and their role in understanding the interplay between

chlamydial (i) peptidoglycan biosynthesis and cell division (ii) peptidoglycan degradation, and (iii) recycling of peptidoglycan.

Chlamydial peptidoglycan biosynthesis and cell division

The bacterial phylum *Chlamydiae* is part of the PVC superphylum which is named after its three first known members, *Planctomycetes*, *Verrucomicrobia* and *Chlamydiae,* but also includes *Lentisphaerae*, *Kirimatiellaeota* and some uncultured candidate phyla (Wagner & Horn, 2006; Rivas-Marín & Devos, 2018). Bacteria inside this superphylum exhibit very different lifestyles and phenotypes. While all known members of *Chlamydiae* depend on distinct host cells due to their obligate intracellular lifestyle, many species of the other phyla are mainly free-living bacteria. Most PVC superphylum members especially inside *Verrucomicrobia* possess a cell envelope with a PG sacculus and typical characteristics of Gram-negative bacteria (Rivas-Marín & Devos, 2018).

Of note, in free-living members of *Planctomycetes,* PG structures were difficult to detect and their exact composition remained unsolved for a long time. Unlike *Chlamydia*, these bacteria are not susceptible to β-lactam antibiotics (Cayrou *et al*., 2010) with exception of anaerobic ammonium-oxidizing (anammox) planctomycetes whose growth is inhibited in presence of penicillin (Hu *et al*., 2013). However, in 2015, two studies proved the existence of a mDAP-containing PG layer in members of *Planctomycetes* and anammox *Planctomycetes* (Jeske *et al*., 2015; van Teeseling *et al*., 2015). Thickness of these PG layers were relatively thin but still within the range reported for PG in other Gram-negative bacteria. Based on light and electron microscopic experiments, the authors assumed that PG sacculi completely cover the cells (Jeske *et al*., 2015; van Teeseling *et al*., 2015).

Inside *Chlamydiae*, an intact PG sacculus enclosing the cell was so far only detected in *Protochlamydia amoebophila* of the *Parachlamydiaeceae* (Pilhofer *et al*., 2013). Members of pathogenic *Chlamydiaceae* are lacking a PG envelope. In these organisms, metabolism and turnover of PG is tightly controlled and it is only found in a narrow ring that is transiently formed at cell division septum (Liechti *et al*. 2014; 2016; Packiam *et al*., 2015). Assembly of a septal PG ring combined with an otherwise reduced PG content is a phenomena which members of *Chlamydiaceae* share with anammox *Planctomycetes K. stuttgartiensis.* In this organism, PG was not

only found to be located in the cell wall but also in the exact same cell compartment in which the cell division ring was observed (van Teeseling *et al*., 2015; van Niftrik, 2009).

Although PG is present at the cell division septum in both phyla, neither genomes of *Chlamydiae* nor *Planctomycetes* encode the tubulin-like homolog GTPase FtsZ. In almost all other bacteria, FtsZ is essential for bacterial cell division due to its role in divisome recruitment as well as septal constriction (Weiss, 2004). Other members of PVC superphylum like *Verrucomicrobia* and *Candidatus* Omnitrophica retained FtsZ (Rivas-Marín & Devos, 2018). FtsZ becomes non-essential in the L-form of Gram-positive *Bacillus* which temporarily lacks a PG sacculus and seems to propagate by a bleeping-like process of poorly regulated membrane distortions by which vesicles are formed and released (Leaver *et al*., 2009). It was speculated that this mechanism, which is highly susceptible to changes in osmolarity and desiccation, might be a primordial form of bacterial propagation before a cell wall and binary fission were developed (Errington *et al.* 2016). However, there are bacteria which seemingly lack a PG sacculus but retain FtsZ, such as intracellular endosymbiontic *Wolbachia* (Lefoulon *et al*., 2016). Furthermore, in contrast to the presumably evolutionary old form of cell propagation described by Errington and colleagues, FtsZ-lacking cell division in *Chlamydiaceae* does not correlate with the complete absence of PG and in cases of *Planctomycetes* and *Protochlamydiaeceae* not even with the absence of a PG cell wall. In these organisms, division is a highly regulated process which is characterized by polarized budding rather than by binary fission (Tekniepe *et al*, 1981; Abdelrahman *et al*., 2016).

In *C. trachomatis*, cell division starts with enlargement of a polarized RB, followed by asymmetric expansion of its MOMP-enriched pole which results in the formation of a budding nascent daughter cell (Abdelrahman *et al*., 2016). In the further progress, asymmetric cell poles mature into two equally sized daughter cells separated by a septum containing a transient PG ring which is remodeled during constriction and degraded afterwards (Liechti *et al*., 2016). In FtsZ lacking chlamydiae, actin-like homolog MreB which is associated with PG sidewall synthesis during cell growth in free-living bacteria such as *E. coli* and *B. subtilis* (Doi *et al*., 1988; Jones *et al*., 2011), appears to act as the constrictive filament in combination with RodZ by controlling assembly and degradation of the PG ring (Pilhofer *et al*., 2008; Ouellette *et al*., 2012;

Liechti *et al*., 2016). In line with a function of MreB in chlamydial cell division, a recent study detected MreB rings at the division site of *C. trachomatis* (Lee *et al*., 2020).

In free-living bacteria, a tight interplay of PG turn-over and cell cycle is essential to allow necessary changes of the cell wall during division, while simultaneously ensuring maintenance of a osmoprotective and thereby vital PG sacculus. Existence of a rudimentary PG biosynthesis machinery in obligatory intracellular chlamydiae indicates that even in a habitat in which osmoprotective qualities become obsolete, PG turnover and division are tightly coupled processes which can not be separated.
In the course of evolutionary adaption to an intracellular lifestyle, chlamydial genome size was highly reduced (Collingro *et al*, 2011), but a nearly complete set of genes required for synthesis of PG precursor lipid II is still present (Stephens *et al*., 1998). A recent study found a pattern of loss and retention of genes associated with PG biosynthesis which is common in a group of unrelated obligate intracellular bacteria. This group includes the *Chlamydia*-like organism *P. amoebophila* as well as *C. trachomatis* and is characterized by the presence of genes encoding orthologs of MurA-MurG, MraY, the SEDS proteins RodA/FtsW and the class B (monofunctional transpeptidases) PBPs PBP2/PBP3 (FtsI), but the absence of any class A (bifunctional transpeptidases and transglycosylases) PBPs (Otten *et al*., 2018). In *C. trachomatis*, transcriptional activity of genes associated with lipid II biosynthesis peaks when RB replication is in full swing at 16-18 hours post infection (hpI) (Nicholson *et al*., 2003; Belland *et al*., 2003).
While the soluble PG precursor UDP-MurNAc-pentapeptide is assembled in the cytoplasm, final assembly the of ultimate cell wall building block, lipid II, takes place at the inner membrane. UDP-MurNAc-pentapeptide is linked to membrane carrier undecaprenyl phosphate (C_{55}-P), yielding the precursor lipid I. This reaction is catalyzed in a Mg^{2+}-dependent manner by the integral membrane protein MraY. Next, the sugar unit GlucNAc is added by membrane-associated transferase MurG, producing lipid II (Bouhss *et al*., 2008). Functional conservation of MraY and MurG has been shown for *C. pneumoniae* (Henrichfreise *et al*., 2009). Subsequent transport of lipid II across the cytoplasmic membrane to incorporate the precursor into the PG network could be facilitated by MurJ which is conserved in the chlamydial

genome and was shown to act as a lipid II flippase in free-living Gram-negative bacteria (Sham *et al*., 2014).

In this work, muraymycin D2 and its derivates M22, M38, M76 and M92 were tested for their effect on the activity of the recombinant *Chlamydia* translocase MraY. Muraymycins are uridine-derived nucleoside-peptide antibiotics and known inhibitors of MraY in free-living bacteria (McDonald *et al*., 2002; Yamashita *et al*., 2003). Previous studies in the Henrichfreise group revealed a persistence-like phenotype in cell culture experiments with *C. trachomatis* that was interpreted as a chlamydial stress response to treatment with muraymycins (Klöckner, 2016). However, it was not established whether the effect might also be influenced by host cell stress, since cytotoxicity and interaction of these compounds with chlamydial MraY have not been analyzed yet.
Due to its ten transmembrane domaines, heterologous overproduction of chlamydial MraY for biochemical characterization is a tedious and elaborate process. A protocol by Henrichfreise an colleagues allows for the purification of active *C. pneumoniae* MraY ($MraY_{Cpn}$) but does not preclude contamination with co-purified MraY of the *E. coli* producer strain ($MraY_{Eco}$) (Henrichfreise *et al*., 2009). Different approaches in this work to optimize the purification of $MraY_{Cpn}$ and to avoid contamination with $MraY_{Eco}$ remained unsuccessful. However, the production of lipid I detected in this work's *in vitro* assay can also be attributed to the activity of $MraY_{Cpn}$. Its complete inhibition in the presence of a muraymycin D2 and its derivates M22, M38, M76 and M92 suggests an inhibitory effect of these compounds on the chlamydial enzyme. The antichlamydial effect of muraymycin and its derivates against *C. trachomatis* in cell culture experiments could therefore not only be due to host cell stress alone, but also be the result of MraY inhibition.

To determine how blocking of lipid I biosynthesis affects the infectious cycle of pathogenic Chlamydia, muraymycins and caprazamycins were tested in an infection model. While an actual in situ chlamydial infection of the human urogenital tract can not be simulated within the cell culture model used here, it enables valuable insights into an agent's effects on chlamydial cell cycle and on the interplay between C. trachomatis D/UW-3/CX and their Hep2 hosts cells. Core element of this model,

established for the Henrichfreise group by A. Klöckner and further optimized by M. Brunke, is the fluorescence microscopy-based analysis of chlamydial infection as described by Kintner and colleagues (Klöckner, 2016; Brunke, 2018; Kintner et al., 2014). Klöckner additionally introduced the parallel performances of Alamar Blue cytotoxicity assays that allow monitoring of the host cell's viability (Klöckner, 2016). It should be noted, that not all impairments of the host cells are necessarily reflected in this kind of cytotoxicity assay. In this work, viability of Hep2 cells appeared to be only slightly affected in the presence of a set of tested antimicrobial candidate compounds (CC3, CC4, CC6 and CC7) when the effects were monitored by the cytotoxicity assay alone. However, additional microscopy-based analysis revealed severe disruptions of the host cell cytoplasm structure under treatment with those test compounds. Thus, to reliable monitor host cell viability, it is necessary to combine conventional cytotoxicity assays and microscopy-based analysis. Using this method, it was shown that muraymycin D2 and its derivates M22, M23, M38 and M100 are likely to directly affect the chlamydial development since anti-chlamydia activity was observed at concentrations at which the compounds had no detectable cytotoxic effect on Hep2 cells, neither in the Alamar Blue assay nor in the microscopic analysis.

As described above, in previous studies at the Henrichfreise group, treatment of a productive *C. trachomatis* infection with muraymycin D2 and derivates of this agent induced a chlamydial phenotype similar to that observed for β-lactam-induced persistence. The only exception was derivate M98 that exhibited a bactericidal effect (Klöckner, 2016). In this work, testing these compounds in a *C. trachomatis* infection model for MIC determination at an early stage of infection confirmed the previous results. Muraymycin D2 and the tested derivates induced a persistent state with enlarged AB morphology, while M98 cleared the infection. Since, in this work, an inhibiting effect of muraymycin on chlamydial MraY was observed *in vitro*, these results indicate that MraY plays an essential role in the chlamydial cell division process and blocking of the translocase impairs chlamydial fitness.
To understand a drug's effect towards chlamydiae, its specific target structures within the chlamydial cell needs to be assessed. It was shown that PG-targeting antibiotics affect the chlamydial division differently depending on wether they block septal PG

ring assembly or the biochemically upstream process of PG precursor biosynthesis (Jacquier et al., 2014; Cox et al., 2020; Brockett & Liechti, 2021).

When subjected to β-lactams such as ampicillin, penicillin G and piperacillin, which target the final, periplasmic steps of PG assembly, *C. trachomatis* is still capable of synthesizing PG material to a detectable amount (Liechti *et al*., 2016; Cox *et al*., 2020; Brockett & Liechti, 2021). During ampicillin-induced persistent state, PG glycan strands are still produced in *Chlamydia*, but their localization is no longer restricted to a single division septum (Brockett & Liechti, 2021). Under penicillin G and piperacillin treatment, *C. trachomatis* can initiate division by asymmetric membrane expansion but it arrests at a very early stage of nascent daughter cell formation with only a partial PG ring being detectable at the division site (Cox *et al*., 2020). In comparison, chlamydial division halts at an earlier stage when cells are treated with antibiotics blocking PG precursor lipid II biosynthesis rather than septal PG assembly. D-cycloserine is a structural analog of amino acid D-Ala found in the PG stem peptide and a compound with antichlamydial activity (Moulder *et al.,* 1963). Studies found two targets of this agent inside the chlamydial lipid II biosynthesis pathway: D-Ala ligase activity of the *C. trachomatis* MurC-Ddl fusion protein as well as activity of the *C. pneumoniae* alternative alanine racemase GlyA (McCoy & Maurelli, 2005; De Benedetti *et al*., 2014). Interestingly, D-cycloserine treatment affects *C. trachomatis* development similar to treatment with inhibitors of MreB, the major organizer of chlamydial division complex (Ouellette *et al*., 2012; Cox *et al*., 2020). When MreB activity is inhibited in *C. trachomatis*, PG is no longer detectable (Liechti *et al*., 2016; Brockett & Liechti, 2021). Under treatment with D-cycloserine as under treatment with MreB inhibitor A22, chlamydial cells become unable to innate polarized division by asymmetric membrane expansion and thus to enter a stage of septal PG assembly (Cox *et al*., 2020).

Looking at *Chlamydia*-like organisms, in which PG metabolism encoding genes are conserved to varying degrees, helps putting these observations into context. In *Waddlia chondrophila,* inhibition of cytoplasmic lipid II synthesis blocks not only cell division but also diminishes septal localization of RodZ, which is thought to be the early division regulator of MreB in *Waddlia* (Jacquier *et al*. 2014; Liechti *et al*. 2016). Consistently, septal localization of the PG degrading enzyme SpoIID in *W. chondrophila* also depends on PG precursor synthesis (Jacquier *et al*., 2019). In

Chlamydiaceae, the cell division process cannot start when the cytoplasmic lipid II biosynthesis is blocked (Cox *et al*., 2020). Furthermore, chlamydial division organizer MreB was shown to interact with cytoplasmic lipid II biosynthesis enzymes MurF and MurG and with MraY which catalyzes the first membrane-bound step of this synthesis pathway (Gaballah *et al.*, 2011; Ouellette *et al*., 2014). These findings suggest that the chlamydial division machinery is stabilized at the division site during the act of PG synthesis. According to this model, muraymycins which block generation of PG precursor lipid I by inhibiting chlamydial MraY would diminish assembly of the division machinery and thus the division process in *Chlamydia*. Consistent with this hypothesis, it was shown in this work that susceptibility of *C. trachomatis* to muraymycin D2 was increased if the compound was added to the infection when division of RBs is nearing its peak as compared to an earlier treatment.

While formation of ABs under treatment with muraymycin is consistent with effects observed for other antibiotics targeting chlamydial lipid II biosynthesis, a bactericidal effect of any of these derivates is unexpected. Due to residence within an osmotically-stable environment, *Chlamydia* appears to be protected from bactericidal effects of PG biosynthesis-targeting antibiotics that occur in free-living bacteria. Neither treatment with D-cycloserine nor with fosmidomycin, an inhibitor of isoprenoid biosynthesis that induces shortage of membrane carrier undecaprenyl phosphate and thereby affects lipid II biosynthesis in *Chlamydia,* resulted in clearance of chlamydial infection but induced persistence instead (Cox *et al*., 2020; Slade *et al*., 2019). However, the productive *C. trachomatis* infection was cleared when subjected to muraymycin derivate M98 in MIC determination assays. Additionally it was observed that muraymycin D2 did not change the RB phenotype but significantly reduced the number of infected host cell, when added to late active infection.

If the observed bactericidal effect of muraymycin derivat M98 is not entirely due to an interfering effect of this compound on host cells, a reasoning supported by the fact that Hep2 morphology appears unaffected by the compound, it could be explained by additional targets beside MraY as postulated by Klöckner in 2016 (Klöckner, 2016). It stands to reasons that either inhibition of a putative additional target or the combined effect of the muraymycin derivate on this target and MraY reduces the chlamydial infection rate. However, it is not yet known whether further targets exist within chlamydiae. The nucleoside antibiotic tunicamycin inhibits different enzymes that link

UDP-activated hexose sugar moieties to membrane-embedded lipid carriers (Price *et al*., 2007). Thus, tunicamycin does not only inhibit MraY (Ikeda *et al*., 1991), but also TarO which catalyzes the transfer of the UDP-activated GlucNAc to C55-P during wall teichonic acid (WTA) synthesis in Gram-positive *Staphylococcus aureus* (Campbell *et al*., 2011). Within this pathway, another additional target of tunicamyin can be found, the epimerase MnaA that catalyzes the conversion of UDP-Glc-NAc to UDP-ManNAc (Mann et al., 2016). It remains to be elucidated whether muraymycins could also be able to affect other enzymes besides MraY that use UDP-activated hexose sugar moieties as substrates. However, since the chlamydial cell envelope does not contain WTA, none of the enzymes involved in its biosynthesis are present or plausible in *C. trachomatis*. Apart from the septal PG ring, only one other sugar-containing polymer of the cell envelope is known for chlamydiae which is the outer membrane's LPS. In contrast to free-living Gram-negative bacteria, but consistent with the specific structure of chlamydial LPS, *Chlamydia* lacks a homolog of sugar transferase WecA, which would otherwise be a potential target of muraymycins. However, in the first step of chlamydial LPS biosynthesis, UDP-activated GlucNAc is linked to myristic acid by the transferase LpxA and further upstream in the process, hydroxylated arachidic acid is transferred to the sugar unit by LpxD (Kosma, 1999; Sweet *et al*., 2001). In order to analyze the bactericidal effect of muraymycin D and M98, it might be interesting to investigate whether they are able to affect activity of these enzymes.

The ability to change into a persistent state protects chlamydiae against antibiotic treatment resulting in long-term unnoticed, possibly subclinical infection. Thus, although acquisition of canonical antibiotic resistance mechanisms rarely occurs in *Chlamydia* (Suchland *et al*., 2017), treatment failure and long term subclinical chlamydial infection are common problems (Geisler *et al*., 2013). Antichlamydial compounds that eliminate a persistent *C. trachomatis* infection could therefore be promising to find novel treatment options.

The cell culture model for Chlamydia infection was expanded by A. Klöckner and M. Brunke to allow systematical analysis of a persisting infections's susceptibility to antimicrobial agents (Klöckner, 2016; Brunke, 2018). In this approach, persistence is induced by treatment with β-lactam penicillin G prior to adding the compound of interest to the chlamydial infection. In C. trachomatis under penicillin treatment, AB

formation is induced and division is rested at an early stage of daughter cell formation (Matsumoto & Manire 1970; Cox *et al*., 2020). In this work, muraymycin D2 had an antichlamydial effect when added at high concentrations to the persistent infection model. The number of infected host cells decreased and the size of remaining inclusions was reduced compared to the phenotype observed for treatment with penicillin G. However, it is still unknown which number of remaining chlamydial cells is needed to endure in a host and cause long-term (re)infection. Therefore further studies are needed to assess whether muraymycin D2 could eradicate persistent *C. trachomatis* to an extent sufficient to prevent the infection from recurring after the end of treatment.

Even though a clinical application remains unlikely, muraymycin D2 and it derivates remain enthralling tools in the further understanding of chlamydial physiology. Due to their non-toxic effect towards Hep2 host cells, these compounds as well as the MurJ-inhibitor 3 could be of use to learn more about the role of the membrane-bound steps of lipid II synthesis during chlamydial division.

Chlamydial peptidoglycan degradation

In order to successfully complete the division process by daughter cell separation in chlamydiae, the chlamydial PG ring has to be degraded by enzymes located inside the periplasm. While a large and diverse group of PG hydrolyzing enzymes can be found in free-living bacteria, the set of chlamydial PG degrading enzymes appears to be limited (Klöckner *et al*., 2018).

Genomes of *Chlamydia* as well as of *Chlamydia*-like organisms code for a cell division amidase as well as for a protein named ‘SpoIID’ which is thought to act as a lytic transglycosylase on PG (Klöckner *et al*., 2014; Frandi *et al*., 2014; Jacquier *et al*., 2019). Whereas it is thought that in *Chlamydia*-like organism *W. chondrophila* a septal enzyme might act as an endopeptidase (Frandi *et al*., 2014), members of *Chlamydia* seem to lack genes encoding common endopeptidases which cut cross-linked peptide side chains of PG. Chlamydial genomes encode a protein containing an NlpC/P60 domain which might identify this enzyme as a PG hydrolase. However, this domain is also found in a range of other enzymes that play a role in PG-derived peptide recycling (Anantharaman & Aravind, 2003). PG hydrolytic activity was observed for the NlpC/P60 enzyme of *C. pneumoniae* (Cpn0245) in a dye-release

assay (Bühl, 2019). Here it was shown that the ortholog of *C. trachomatis* (Ct127) shows no *in vitro* activity towards PG but is rather a recycling peptidase of PG-derived peptides (see ‘Chlamydial peptidoglycan recycling’).

While existence of chlamydial endopeptidase activity remains controversial, it is known that *Chlamydia* as well as *Chlamydia*-like organisms encode a PG hydrolyzing N-acetylmuramyl-L-alanine amidase (AmiA) (Klöckner *et al*., 2014; Frandi *et al*., 2014). In contrast to *E. coli* harboring three major amidases (AmiA, AmiB, AmiC) with overlapping, but not necessarily redundant, activities that are needed for proper cell separation (Uehara & Bernhardt, 2011), *C. trachomatis* only has one. By cutting between L-Ala at the first position of the peptide stem and MurNAc, these amidases remove the entire peptide side chain from the PG sugar backbone (Vollmer *et al*., 2008b). Their activity needs to be tightly controlled to ensure that these enzymes hydrolyzes PG at the appropriate time and place. On a structural level, amidase activity is regulated by a conserved α-helix which occupies the active site and whose autoinhibitory effect can only be reversed in presence of regulatory proteins (Yang *et al*., 2012). Activator protein EnvC specifically stimulates AmiA and AmiB, whereas NlpD is responsible for AmiC activation (Uehara *et al*., 2009; 2010). A similar mechanism with an autohinibitory domain occupying the active site can be found in other enzymes associated with PG degradation, such as Auto, an aminidase of *Listeria monocytogenes,* RipA an endopeptidase of *Mycobacterium tuberculosis* and possibly also in *E. coli* EnvC (Bublitz *et al*., 2009; Ruggiero *et al*., 2010; Cook *et al.*, 2020).

By the start of cell division in *E. coli*, Z-ring formation recruits the FtsEX protein complex midcell by which EnvC is also recruited, whereas NlpD localization occurs latter in the process (Schmidt *et al*., 2004; Peters *et al*., 2011). In contrast to AmiB and AmiC which are specifically recruited to the divisome where they find their corresponding activators, AmiA localizes peripherally (Bernhardt & de Boer, 2003). However, cell separation is not strongly affected in *E. coil* mutants lacking AmiB and AmiC, indicating that AmiA alone can promote relatively efficient septal PG splitting (Chung *et al*., 2009). Furthermore, while AmiB and AmiC alone cannot support normal cell separation or cell wall integrity in neutral medium, AmiA appears to be active during both neutral and acidic conditions (Mueller *et al*., 2021). The observations that AmiA is neither specifically located at the division site nor sensitive

in its activity towards changes in the pH value, emphasize the importance of the enzyme's autoinhibitory mechanism to prevent uncontrolled PG hydrolyzing activity. Structural analysis revealed that the domain, which changes its conformation to either allow access to or block the amidase active site, includes the autoinhibitory α-helix, an unstructured loop region and the first part of a following α-helix (Yang *et al*., 2012). Interestingly, it was shown that the amino acid sequence of chlamydial AmiA lacks an autoinhibitory α-helix and consistently proven that *C. pneumoniae* AmiA is active by default (Klöckner *et al*., 2014). Here, comparison of 3D structures models of AmiA from *E. coli* ($AmiA_{Eco}$), *C. pneumoniae* ($AmiA_{Cpn}$) and *C. trachomatis* ($AmiA_{Ctr}$) further revealed that the complete structure associated with autoinhibition in $AmiA_{Eco}$ is missing in both chlamydial orthologs (fig. 4.1). Based on this result, $AmiA_{Eco}$ mutant $AmiA_{Eco}$_ΔA148-S191 lacking this domain was generated by M. Brunke for this work. Here, similar to $AmiA_{Cpn}$, the $AmiA_{Eco}$_ΔA148-S191 mutant showed basal activity when being produced in *E. coli* that results in lysis of the expression strain.

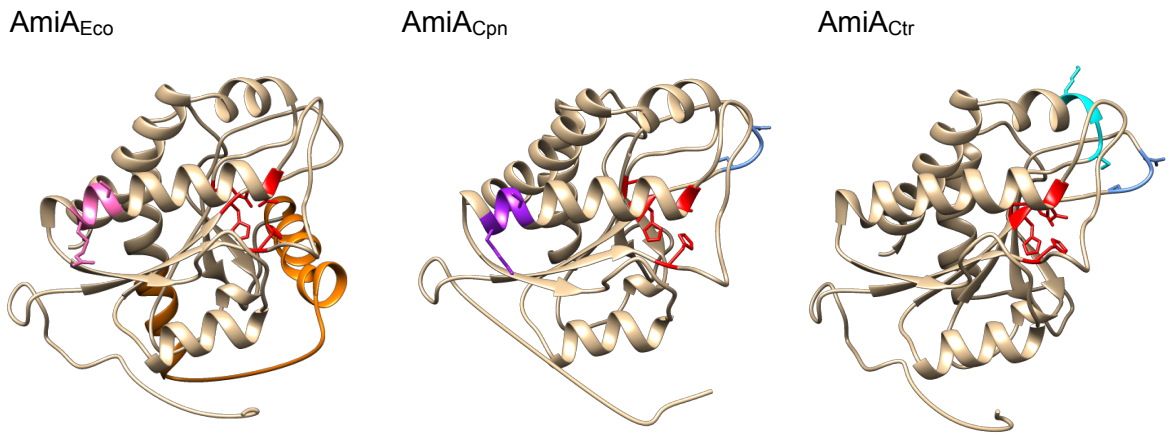

Figure 4.1. Comparison of 3D *in silico* models of $AmiA_{Eco}$, $AmiA_{Cpn}$ and $AmiA_{Ctr}$. Conserved residues of the amidase active site are highlighted in red. The autoinhibitory structure of $AmiA_{Eco}$ (highlighted in orange) is missing in both chlamydial homologs. In $AmiA_{Cpn}$, a SxxK and a SxN motif are conserved which are typically found in PBP DD-CPases. SxxK (highlighted in purple) is located at the first a-helix distal to the SxN motif (highlighted in light blue). The serine residue of the SxxK motif is essential for the additional DD-CPases activity of bifunctional $AmiA_{Cpn}$ (Klöckner *et al*., 2014). In $AmiA_{Eco}$, the SxxK motif's serine is conserved, while lysine at the motif's fourth position is replaced by arginine (highlighted in pink) and the complete SxN motif is missing. In $AmiA_{Ctr}$ the SxN motif is preserved, but the SxxK motif found in $AmiA_{Cpn}$ is absent. Instead, another SxxK motif (highlighted in cyan) is located next to SxN (highlighted in light blue). All 3D models are based on Phyre2 alignment against the structure of *E. coli* AmiC (Rocaboy *et al*., 2013).

It was shown by Yang and colleagues that basal hydrolytic activity of *E. coli* amidases on RBB-stained PG in a dye-please assay is inversely correlated with the stability of

interaction between autoinhibotory α-helix and active site. $AmiA_{Eco}$ has almost no activity without regulatory protein $EnvC_{Eco}$, while its mutant $AmiA_{Eco}$E167L in which a residue important for inserting the α-helix into the active site was changed to lysine showed approximately 29 % of activated $AmiA_{Eco}$ activity (Yang *et al.*, 2012). Here, it was shown that the basal activity of $AmiA_{Eco}$ in a dye-release assays is even further enhanced when the whole autoinhibitory domain is deleted. $AmiA_{Eco}$_ΔA148-S191 showed approximately 66 % of the PG hydrolyzing activity of $EnvC_{Eco}$-activated $AmiA_{Eco}$. Since interaction between regulatory α-helix and active site is destabilized, but the autoinhibitory domain is still present in $AmiA_{Eco}$E167L, it is no surprise that its basal activity is lower compared to a mutant completely lacking this domain. Interestingly, this changed when an activator was present. Under these conditions, activity of $AmiA_{Eco}$E167L was even higher than that of wild type $AmiA_{Eco}$ (Yang *et al.*, 2012), while activity of $AmiA_{Eco}$_ΔA148-S191 decreased to 22 % in presence of $EnvC_{Eco}$. Yang and colleagues did not use full length $EnvC_{Eco}$ but rather a C-terminal fragment which carries a LytM domain which directly interacts with *E. coli* amidases (Peters *et al.*, 2013) and has been shown to be sufficient for their activation (Uehara *et al.*, 2010). Here, full length $EnvC_{Eco}$ was used to induced PG hydrolytic activity of $AmiA_{Eco}$ *in vitro*, consistent with its proven activating activity on $AmiA_{Eco}$ using lipid II as a substrate (Klöckner, 2016). Prove of full length EnvC's ability to activate $AmiA_{Eco}$ *in vitro* questions the current hypothesis that $EnvC_{Eco}$ is itself also autoinhibited by a restraining domain and can thereby not interact with amidases until it itself is activated by the FtsEX complex (Cook *et al.*, 2020). However, PG hydrolyzing activity of the $AmiA_{Eco}$ autoinhibitory domain deletion mutant is not only basal without necessity to be activated by $EnvC_{Eco}$, but is even reduced in its presence. This observation might indicate a possibility of further interactions between both proteins. If the autoinhibitory domain is missing, the ‘correct’ activating interaction could no longer occur, so there might be another, misdirected interaction by which amidase activity is hindered.

The complete autoinhibitory domain structure, whose importance for suppressing uncontrolled PG hydrolyzing activity of $AmiA_{Eco}$ was confirmed by this study, is missing in AmiA orthologes of *Chlamydia*. It has been shown that $AmiA_{Cpn}$ is by default an active enzyme (Klöckner *et al.*, 2014; Klöckner, 2016) and the same was shown to be true for $AmiA_{Ctr}$ in this work. Consistently, *Chlamydia* genomes neither

code for regulatory factors EnvC and NlpD nor for the FtsEX complex. Obviously, in absence of an inhibitory domain, there must be an alternative mechanism by which chlamydial AmiA is regulated, but so far it can only be speculated how this regulation works. Paucity of an autoinhibitory domain has been described for amidases involved in mother cell lysis following sporulation in *Bacillus* (Smith & Foster, 1995; Korndörfer *et al*., 2006; Yang *et al*., 2012). Expression of these amidases in *Bacillus* species is thought to depend on sigma factor K (Chen *et al*., 2018) which belongs to a group of transcription factors which primarily control sporulation in this organism (Losick & Stragier, 1992). Transcriptional regulation of chlamydial amidase activity is also conceivable, since expression of chlamydial AmiA appears to be upregulated during cell division (Belland *et al*., 2003; Albrecht *et al*., 2011). The hypothesis of regulation at a transcriptional level is further supported by the presence of a two-component stress response system in *C. trachomatis* (CtcB-CtcC) which is activated during treatment with compounds targeting the chlamydial cell envelope (Koo & Stephens, 2003; Bobrovsky *et al*., 2016). Similar two-component systems play a role in regulating amidase activity in free-living bacteria, in addition to regulation by an autoinhibitory domain which is present in these orthologes. Activation of this stress response system was shown to enhance expression of AmiA and AmiC in *Salmonella* and also to suppress cell division defects displayed by a *Pseudomonas aeruginosa amiB* mutant (Weatherspoon-Griffin *et al*., 2011; Yakhnina *et al*., 2015).

Interestingly, proteinbiochemical analysis in this work revealed that AmiA orthologs in the closely related species *C. pneumoniae* and *C. trachomatis,* that share 59 % overall amino acid sequence identity, differ in their activity. AmiA, the only amidase conserved in *Chlamydia*, was found to exhibit a dual activity in *C. pneumoniae.* Besides cleaving the peptide side chain from sugar units of PG and lipid II, it also possesses DD-carboxypeptidase (DD-CPase) activity, releasing terminal D-Ala from the stem peptide (Klöckner *et al*., 2014). Amidase activity on lipid II was also shown for amidases of free-living *E. coli* as well as obligate intracellular *Wolbachia* (Klöckner, 2016; Wilmes *et al*., 2017) and AmiC from *Neisseria gonorrhoeae* exhibits amidase activity towards PG fragments, that consists of two disaccharide units with a pentapeptide stem each (Lenz *et al*., 2016). Bifunctionality also occurs in other amidases, such as SpoIIP from *B. subtilis* that shows amidase and endopeptidase

activity and Atl-like autolysin of staphylococci that exhibits amidase and N-acetylglucosaminidase function (Oshida *et al*., 1995; Bourgeois *et al*., 2009; Morlot *et al*., 2010). But $AmiA_{Cpn}$ is the first amidase for which additional DD-CPase function was proven by the Henrichfreise group (Klöckner *et al*., 2014). Following *in vitro* assays showed that *E. coli* $AmiA_{Eco}$ is also capable of cleaving terminal D-Ala from lipid II in addition to its amidase activity towards this substrate. It was indicated that this function is inhibited in presence of $EnvC_{Eco}$, which could suggest that, in free-living bacteria, AmiA acts as an amidase at the constriction site, where NlpD is present, and as DD-CPase during cell elongation (Klöckner, 2016).

However, despite high sequence similarity between both chlamydial AmiA orthologes, $AimA_{Ctr}$ differs from $AmiA_{Cpn}$ in its *in vitro* activity and shows amidase but no additional carboxypeptidase activity on lipid II. Consistent with this observation, the motif which was shown to be essential for DD-CPase function in $AmiA_{Cpn}$ by Klöckner and colleagues is missing in $AmiA_{Ctr}$, while the amidase active site is conserved between both proteins. DD-CPase function of $AmiA_{Cpn}$ was shown to be penicillin sensitive and was assigned to a penicillin-binding protein motif (Klöckner *et al.*, 2014). Conventional bacterial PBP DD-CPases contain three motifs, SxxK, SxN and KTG and depend on all three of them for substrate recognition and catalysis (Goffin & Ghuysen, 2002; Ghosh *et al,* 2008). $AmiA_{Cpn}$ carries an SxxK and an SxN motif, while the KTG motif is missing (Klöckner *et al*., 2014). Although an SxN motif is conserved, it does not contribute to the DD-CPase function of $AmiA_{Cpn.}$ It appears to depend solely on SxxK and especially on the catalytic serine residue which is also conserved in bifunctional $AmiA_{Eco}$ (Klöckner *et al.*, 2014; Klöckner, 2016). Here, it was further confirmed that SxN does not contribute to DD-CPase activity of *Chlamydia* AmiA. Firstly, 3D *in silico* modeling revealed that this motif is located distant to the SxxK motif in the protein's periphery and that its residues are orientated in opposite direction from the active site in both chlamydial AmiA orthologs (fig. 4.1). And secondly, an SxN motif is not conserved in $AmiA_{Eco}$ which appears to be a bifunctional enzyme (Klöckner, 2016), while being present in $AmiA_{Ctr}$ which was shown to exhibit no DD-CPase activity. Furthermore, comparison of the 3D structures of $AmiA_{Cpn}$ and $AmiA_{Eco}$ (fig. 4.1) questions the importance of the full SxxK motif for carboxypeptidase function of these enzymes, while underlining the importance of the serine residue. Only the serine residue, which was shown to be essential for DD-

CPase activity of $AmiA_{Cpn}$ (Klöckner *et al.*, 2014), is conserved in $AmiA_{Eco}$, while the lysine residues of the motif is replaced by arginine. Consistent with its lack of DD-CPase function, $AmiA_{Ctr}$ completely lacks the SxxK domain found in $AmiA_{Cpn}$ and thus the catalytic serine residue. Interestingly, another SxxK motif located more C-terminal compared to $AmiA_{Cpn}$ can be found in $AmiA_{Ctr}$. However, its presence and location in vicinity of the SxN motif does not seem to match structural requirements for a catalytic site, since location of both motives appears too peripheral to play a role in the enzyme's activity.

While comparative protein structure analysis can explain different functions of $AmiA_{Cpn}$ and $AmiA_{Ctr}$, the reason for their different activity remains unclear. So far, two other enzymes with DD-CPase function on lipid II are known in *Chlamydia*, a homolog of PBP6 and a protein which is misannotated as 'NlpD' despite lacking a LytM domain (Otten *et al*., 2015; Klöckner *et al*., 2014). The latter appears to be an protein unique in *Chlamydia*, since homologous proteins cannot be found in other bacteria (Klöckner *et al*., 2014). The lack of an additional DD-CPase function of $AmiA_{Ctr}$ might indicate that, in *C. trachomatis*, carboxypeptidase activity of PBP6 and 'NlpD' might be sufficient.

For spatiotemporal regulation of PG metabolism during division, FtsZ-lacking chlamydiae appear to rely on actin homologue MreB and its associated membrane anchoring protein, RodZ (Gaballah *et al.*, 2011; Ouellette *et al*., 2012; Jacquier *et al.*, 2014). However, the precise mechanism and the regulation of PG remodeling and degradation at the chlamydial division septum are not fully understood. AmiA is found in *Chlamydia* as well as *Chlamydia*-like organisms of the *Waddlia* family and while it is so far unknown how its activity is regulated, AmiA has been demonstrated to cleave peptide stems at the amide bond of the glycan strands *in vitro* in both (Klöckner *et al*., 2014; Frandi *et al*., 2014). Chlamydial genomes lack homologs of classical lytic transglycosylases, but recent finding of a gene conserved among members of *Chlamydiales* which codes for a SpoIID protein (Jacquier *et al*., 2019), helps to shed further light on the process of PG degradation in these intracellular organisms. An SpoIID domain containing protein was first described in *B. subtilis* in which it acts as a lytic transglycosylase involved in sporulation (Morlot *et al*., 2010, Gutierrez *et al*., 2010). The recently described SpoIID ortholog of *W. chondrophila* is not only able to act as a lytic transglycosylase on PG, but shows additional

muramidase activity on PG-derived glycan strands *in vitro* (Jacquier *et al*., 2019). Activity of chlamydial AmiA on PG should produce such denuded glycan strands (Klöckner *et al*., 2014; Frandi *et al*., 2014), and thus combined activity of both, AmiA and the SpoIID protein, might lead to separation of peptide and sugar moieties of PG as well as to degradation of the glycan chain itself. Consistently with this hypothesis, it was demonstrated by Jacquier and colleagues that SpoIID and AmiA of *W. chondrophila* can act together *in vitro* to digest PG. Furthermore, SpoIID domain containing proteins are not only conserved in *Chlamydia*-like organisms, but are also encoded in the genomes of *C. trachomatis* and *C. pneumoniae.* For both organisms, amidase activity of AmiA towards PG was shown, for $AmiA_{Cpn}$ by Klöckner and colleagues in 2014 and in this work for $AmiA_{Ctr}$.

While combined activity of an amidase and an uncommon bifunctional enzyme with lytic transglycosylase and muramidase activity might be sufficient to explain the basic mechanism of PG degradation in minimal bacteria like *Chlamydiales*, the fate of peptide components of PG remains unclear. Common endopeptidases, which play a major role in PG remodeling in free-living bacteria, appear to be absent in *Chlamydia*, whereas in *W. chondrophila* evidence for endopeptidase activity of 'NlpD' was provided (Frandi *et al.*, 2014). Interestingly, as mentioned above, three functional carboxypeptidases are known for *C. pneumoniae***:** PBP6, bifunctional AmiA and 'NlpD' (Otten *et al*., 2015; Klöckner *et al*., 2014). And while it was shown here that $AmiA_{Ctr}$ seems to lack additional DD-CPase function described for $AmiA_{Cpn}$, the other two enzymes are likely to act as carboxypeptidases in *C. trachomatis*. Presence of multiple carboxypeptidases in *Chlamydia*, which otherwise has a rather limited arsenal of PG remodeling enzymes, raises questions about their functions in chlamydial cell biology. These enzymes might play a role in chlamydial cell division in that they control the spatiotemporal dynamics of the formation of a robust PG structure in the septal ring by controlling the level of cross-linking.

As adaption to a pathogenic lifestyle within a vertebrate host and in order to minimize recognition by the innate immune system, the PG level of obligate intracellular *Chlamydia* is drastically reduced compared to free-living bacteria. In these organisms, PG is only present as a narrow ring in replicating RBs, while it is missing in the infectious EB form (Liechti *et al*., 2016). However, during replication soluble PG turnover products are inevitably released into the environment. This harbors a risk for

pathogenic bacteria, since PG and its derived muropeptides are important pathogen associated molecular patterns (PAMPs) which are recognized by host immune surveillance mechanisms as non-self structures (Sukhithasri *et al*., 2013; Neyen & Lemaitre, 2016). For *Chlamydia*, as for other obligate intracellular bacteria which replicate inside of vesicles or directly inside the host cell's cytoplasm, this means releasing immunostimulatory agents inside the host cell. Thereby PG turnover products are hidden from extracellular innate immune response but are in proximity to cytosolic nucleotide organization domain (NOD1 and NOD2) receptors specific for PG recognition (Chaput & Boneca, 2007; Wolf & Underhill, 2018). Both receptors, NOD1 and NOD2, recognize *C. pneumoniae* and play an essential role in bacterial clearance *in vivo* (Shimada *et al*., 2009). It was further shown that PG signaling through NOD1 contributes to an overall inflammatory cytokine interleukin-8 (IL-8) response to *C. trachomatis* infection (Buchholz & Stephens, 2008). Using NOD receptors to recognize PG fragments, highly sensitive immunodetection approaches are able to detect even small amounts of chlamydial PG in lysates of infected cells (Packiam *et al*., 2015; Liechti *et al*., 2016). A recent study, in which muropeptide release from a *C. trachomatis* infection was monitored with this method, showed that the peak of NOD1 signaling roughly correlates with the time point at which IL-8 transcription is up-regulated in the host cells (Brockett & Liechti, 2021; Buchholz & Stephens, 2008).

Since release of PG fragments during replication seems inevitable, *Chlamydia* might use activity of PG modifying enzymes to minimize their immunostimulatory potential. To understand which modifications could be useful, it is helpful to have a look on the minimal ligands of NOD1 and NOD2 which have to be present for signaling to occur. Minimal ligand of NOD1 is the γ-D-Glu–mDAP dipeptide of the peptide stem of mDAP-type PG specific to Gram-negative bacteria (Chamaillard *et al*., 2003; Girardin *et al*., 2003a), so this receptor senses PG-derived peptides disconnected from MurNAc, as long as they harbor this dipeptide. In case of NOD2, the minimal PG fragment which is a ligand of this receptor consists of MurNAc covalently linked to the first two amino acids of the peptide stem (Girardin *et al*., 2003b; Inohara *et al*., 2003). Thus activity of chlamydial AmiA, by which the peptide stem of PG is cut off from the MurNAc unit, might play a role in reducing pathogen recognition by NOD2, as has already been shown for amidases of other bacterial pathogens. *Helicobacter pylori*

infects human gastric mucosa and, in the course of infection, changes its cell morphology (Viala *et al*., 2004). Change from spiral to coccoid form appears to minimize the inflammatory immune response and *H. pylori* AmiA was shown to be essential for this conversion (Chaput *et al*., 2006). Immune escape is further supported by the fact that muropeptides released from PG by activity of *H. pylori* AmiA are not recognized by NOD2 (Girardin *et al*., 2003b; Humann & Lenz, 2009). Also in *N. gonorrhoeae,* a pathogen which causes human genitourinary infections, activity of amidase AmiC is associated with a lowered release of specific immune-stimulatory muropeptides (Garcia & Dillard, 2006; Humann & Lenz, 2009). Modifying PG-derived fragments as a tactic to circumvent innate immune response is not limited to bacteria. Amidase function can be found for the eukaryotic PG recognition protein-L that contributes to a lowering of host pro-inflammatory response to the bacterial cell wall (Wang *et al*., 2003).

While amidase activity could help to hide PG fragments from NOD2 detection, it is not a suitable tool to bypass recognition by NOD1. On the contrary, amidase activity is more likely to increase the risk of this kind of detection, because it produces peptides which are disconnected from the MurNAc sugar unit. If these free PG-derived peptides contain D-Glu–mDAP dipeptide, they can be recognized by NOD1 (Chamaillard *et al*., 2003; Girardin *et al*., 2003a). Therefore it would be advantageous for pathogen *Chlamydiaceae* to keep the proportion of these immunostimulatory fragments low. Besides, even without the risk of detection, loss of PG components, whose production is energy cost-intensive, might be unfavorable for these highly specialized organisms. However, up to now, little is known about the fate of PG ring turnover products during chlamydial cell division. Here, an NlpC/P60 protein was found in *C. trachomatis* which specifically hydrolyses PG-derived peptides between their D-Glu and mDAP residues and could therefore help to reduce NOD1 sensing. In addition to its possible role in minimizing an immune response, this enzyme is thought to catalyze the recycling of peptides released during PG ring degradation. Our finding of a chlamydial NlpC/P60 protein together with the current description of a transmembrane transport system for PG-derived peptides (Singh *et al.,* 2020) might give first insights into the rudimentary recycling process of PG ring degradation products in *Chlamydiaceae*.

Chlamydial peptidoglycan recycling

To complete the cycle of PG ring synthesis, remodeling and disassembly in chlamydiae, maintaining a mechanism of PG recycling might be essential. Especially for pathogenic *Chlamydia,* recycling of PG-derived fragments appears to be important to reduce the amount of immunostimulatory agents and thus minimize interaction with the host's immune system. Additionally, recycling of PG is a common strategy in bacteria to conserve the energy required for *de novo* synthesis of its precursors, as it was shown that free-living bacteria reuse 40 to 50 % of their PG (Doyle *et al*., 1988; Park, 1995). However, there is little insight into how this process works in chlamydiae. Here, a *C. trachomatis* protein was found and characterized, to our knowledge, as the first known chlamydial PG recycling enzyme which takes over the essential step of decomposing PG ring-derived peptides. Due to its similarities to the *Bacillus* recycling enzyme YkfC regarding amino acid sequence, predicted protein structure and peptidase function, it was named $YkfC_{Ctr}$. $YkfC_{Ctr}$ acts as γ-D-Glu-mDAP peptidase that specifically recycles PG-derived peptides in the human pathogen *C. trachomatis.*

The PG recycling peptidase found in *Chlamydiaceae* belongs to the NlpC/P60 protein family. NlpC/P60 proteins are a widely distributed class of enzymes which hydrolyze PG and/or PG-derived peptides and are found not only in bacteria but also in viruses, archaea and eukaryotes (Anantharaman & Aravind, 2003; Bateman & Rawlings, 2003; Rigden *et al*., 2003). Typical characteristics of the NlpC/P60 domain are a prototypical papain-like fold and an active site consisting of a Cys-His dyad and a third polar residue (Anantharaman & Aravind, 2003; Aramini *et al*., 2008; Xu *et al*., 2009; 2010). Putative proteins harboring a NlpC/P60 domain carrying these features are encoded in the genomes of *Chlamydia* as well as *Chlamydia*-like organisms.

Members of the NlpC/P60 protein family play different physiological roles in free-living bacteria. They include PG degrading enzymes that cleave peptide cross-links of the PG sacculus as well as PG recycling enzymes that specifically cut peptides derived from the PG stem peptide (Smith *et al*., 2000; Anantharaman & Aravind, 2003; Xu *et al*., 2010; 2015). PG degrading NlpC/P60 proteins can be found among autolysins of Gram-positive bacteria, such as P60 of *L. monocytogenes* (Kuhn & Goebel, 1989), LytF and LytE of *B. subtilis* (Margot *et al.,* 1998; Ohnishi *et al*., 1999), and the bifunctional cell wall hydrolase CtlW (Fukushima *et al*., 2008; Xu *et al*.,

2014). In *E. coli*, NlpC/P60 domain containing proteins MepS and MepH are periplasmic DD-endopeptidases which are involved in cleavage of peptide cross-links of PG during cell growth and MepS activity depends on the domain's catalytic Cys-His-His triad (Singh *et al*., 2012; 2015). In *Bacillus* as well as in *Bacteroides* species, which are Gram-negative members of the human gut microbiome, the NlpC/P60 peptidase YkfC is essential for PG-derived peptide recycling (Schmidt *et al*., 2001; Xu *et al*., 2010; 2015). Although most characterized orthologs, such as YkfCs of *Bacillus cereus* ($YkfC_{Bce}$), *Bacteroides thetaiotaomicron* and *Bacteroides ovatus* appear to be extracellular or periplasmic proteins due to predicted signal peptides, *B. subtilis* YkfC lacks a signal peptide and thus might be located inside the cytoplasm (Xu *et al*., 2010; 2015). As the recycling peptidase YkfC targets the γ-D-Glu-mDAP linkage that is also present in the stem peptide of PG, as well as in intermediates of cytoplasmic lipid II synthesis, its activity has to be highly specific toward PG-derived peptides, so as not to compromise PG integrity or biosynthesis. It was shown that YkfC is only active toward free stem peptides with a free N-terminal L-Ala residue. Substrate specificity is maintained by its binding site's architecture that is determined by the interplay of the first (of the enzyme's two) SH3b domains and the active site of the catalytic NlpC/P60 domain (Xu *et al*., 2010; 2015).

C. trachomatis YkfC *in vitro* substrate specificity determined in this work indicates that this NlpC/P60 protein is a peptide-recycling rather than a PG ring-hydrolyzing enzyme. $YkfC_{Ctr}$ is a cytoplasmic γ-D-Glu-mDAP peptidases, highly specific for PG-derived peptides which are no longer connected to the MurNAc unit of PG and have a free N-terminal L-Ala residue. The enzyme neither cleaved PG and its recycling product MurNAc-tripeptide nor PG precursors lipid II and UDP-MurNAc-tripeptide. Consistently, the predicted overall protein structure of $YkfC_{Ctr}$ shares similarities with that of $YkfC_{Bce}$, not only regarding the NlpC/P60 domain but also in the N-terminal SH3b domain important for substrate binding. Moreover, by cleaving externally added L-Ala-γ-D-Glu-mDAP tripeptide and thus providing free mDAP, expression of $YkfC_{Ctr}$ was able to enhance growth of an *E. coli* $dapD^-$ Δ*mpl* mutant strain which is unable to generate mDap *de novo* as well as to utilize PG-derived L-Ala-γ-D-Glu-mDAP tripeptide. In contrast, expression of $YkfC_{Ctr}$ could not restore growth of a

temperature-sensitive DD-endopeptidase MepS-deficient *E. coli* mutant strain, further supporting a role as a recycling peptidase rather than a PG degrading enzyme.
While the NlpC/P60 protein could be identified as a novel chlamydial PG-derived peptide-recycling enzyme in *C. trachomatis*, its functionality could not be confirmed in *C. pneumoniae*. Resemblance in the predicted structure of the *C. pneumoniae* enzyme to $YkfC_{Bce}$, and particularly similarities in the active and substrate binding sites, allow high confidence identification as YkfC ortholog, hence the enzyme is referred to as $YkfC_{Cpn}$ in this work. In a previous study in the Henrichfreise group, however, PG hydrolytic activity was shown for the same NlpC/P60 enzyme *in vitro* (Bühl, 2019). Based on this observation, it was speculated that this protein might function as the elusive chlamydial DD-endopeptidase similar to MepS of *E. coli* (Bühl, 2019; Singh *et al*., 2012). Since $YkfC_{Cpn}$ lacks a signal peptide, it appears to be located inside the cytoplasm, questioning its involvement in the chlamydial PG breakdown process. Unfortunately, different attempts of heterologous expression of $YkfC_{Cpn}$ in *E. coli* failed in this work, so it was neither possible to determine the *in vitro* substrate range of recombinant $YkfC_{Cpn}$, nor to analyze its *in vivo* activity in complementation assays. Hence, future research is needed to determine whether $YkfC_{Cpn}$ is a recycling enzyme with a broader substrate specificity than common YkfC orthologs, or whether the physiological role of the NlpC/P60 domain-containing protein differs between *C. trachomatis* and *C. pneumoniae*.

Proteins containing an NlpC/P60 domain are not exclusive to pathogenic *Chlamydia*, but are also present in *Chlamydia*-like organisms. Since it is known that *Protochlamydia amoebophila* of the *Parachlamydiaceae* family is surrounded by a PG sacculus (Pilhofer *et al*. 2013), it is likely that the organism maintained a PG recycling machinery. Consistently, a putative NlpC/P60 protein was found to be encoded in the genome of *P. amoebophila* and sequence alignment shows that the catalytic Cys-His-His trial and residues important for substrate binding of YkfC are conserved in it (fig. 4.2). PG was also shown to be present in members of the *Waddliaceae* family and, as in *Chlamydiaceae*, the process of PG synthesis might stabilize the divisome at the septum in *Waddlia* (Jacquier *et al*., 2015a; 2019). However, the genome of *W. chondrophila* does not encode an ortholog of the chlamydial NlpC/P60 domain-containing protein characterized in this work.

Interestingly, proteins containing the NlpC/P60 domain were found to be conserved in the genomes of two *Chlamydia*-related species whose degree of PG sacculus conservation is currently unknown: NlpC/P60$_{Ela}$ in *Estrella lausannensis* and NlpC/P60$_{Sne}$ in *Simkania negevensis* (fig. 4.2). *E. lausannensis* belongs to the *Criblamydiaceae* family whose peculiar star-shaped EBs indicate cell envelope structures distinct from other members of the *Chlamydiales* (Lienard *et al*., 2011; Thomas *et al*., 2006). In *S. negevensis,* the study which confirmed the existence of a PG sacculus in *P. amoebophila* was unable to detect PG material (Pilhofer *et al*. 2013).

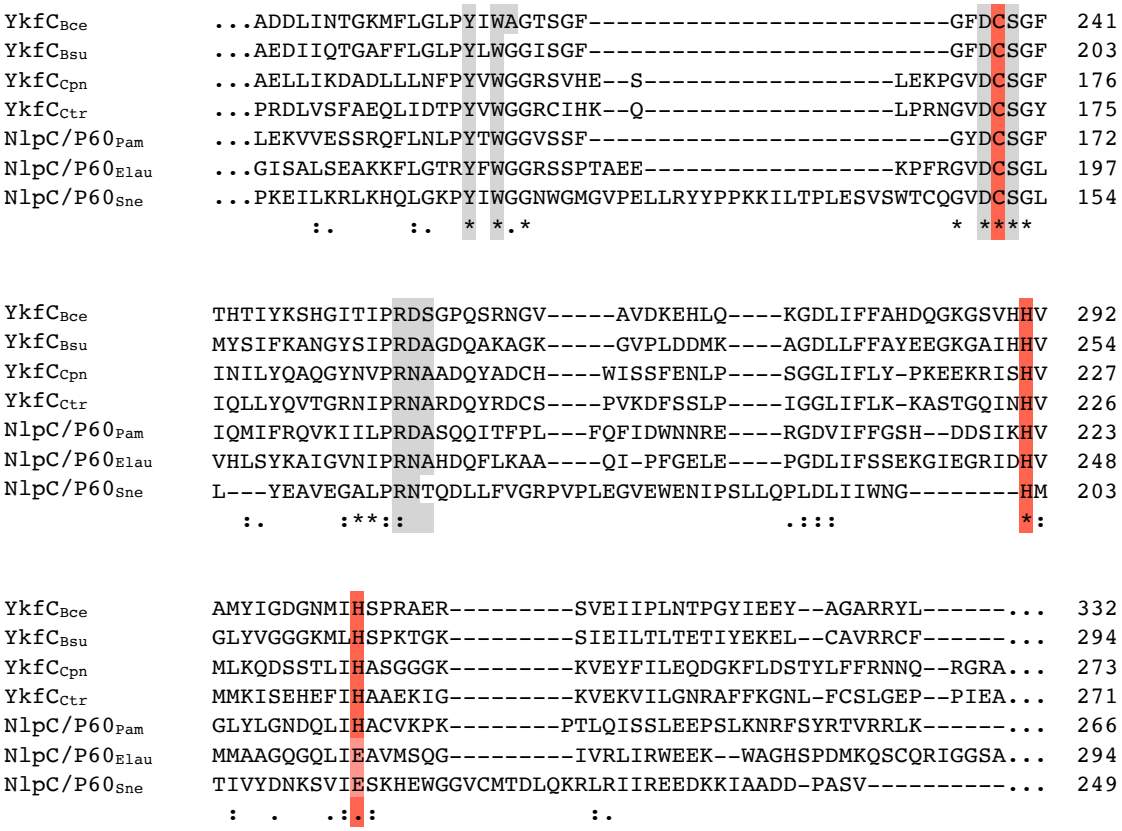

Figure 4.2. Primary sequence alignment of the NlpC/P60 domain found in proteins of *Bacillus*, *Chlamydia* and *Chlamydia*-like organisms. The catalytic triad comprising Cys, His and a polar residue is shown in red. Conserved residues essential for substrate recognition in YkfC$_{Bce}$ (Xu *et al*., 2010) are highlighted in grey. Shown are the domains of proteins from *B. cereus* (Bce), *B. subtilis* (Bsu), *C. pneumoniae* (Cpn), *C. trachomatis* (Ctr), *P. amoebophila* (Pam), *E. lausannensis* (Ela) and *S. negevensis* (Sne).

The predicted protein structures of NlpC/P60$_{Ela}$ and NlpC/P60$_{Sne}$ differ both from *Chlamydia* YkfC orthologs and from each other. Noticeably, the third residue of the catalytic triad of the putative peptidase domain is changed from histidine to glutamic

acid in both (fig. 4.2). While members of the NlpC/P60 protein family are characterized by a high degree of conservation of the cysteine and histidine residues at the first and second position of the catalytic triad, the third position is less conserved and requires only a polar residue (Anantharaman & Aravind, 2003). However, in functional YkfC recycling peptidases (Xu *et al*., 2010; 2015) as well as in $YkfC_{Ctr}$ and $YkfC_{Cpn}$, a histidine residue is conserved at this position (fig. 4.2). Moreover, unlike the *E. lausannensis* protein, $NlpC/P60_{Sne}$ lacks both N-terminal Sh3b domains involved in determining YkfC's substrate specificity and differs significantly in its overall structure from $YkfC_{Bce}$ (Xu *et al*., 2015). Surprisingly, its predicted structure shows high similarities with that of an NlpC/P60 PG hydrolase found in the eukaryotic parasite *Trichomonas vaginalis* (Pinheiro *et al*., 2018). *T. vaginalis* is intimately associated with the human vaginal mucosa and microbiota (Kalia *et al*., 2020). It was suggested that the genes coding for the *T. vaginalis* NlpC/P60 proteins were received through lateral gene transfer from bacteria (Pinheiro *et al*., 2018). While *S. negevensis* is traditionally described as an amoebal symbiont (Kahane *et al*. 2001), it was speculated wether it could colonize the human genital tract due to its ability to growth and replicate in human endometrial cells (Vouga *et al*., 2017a). Susceptibility to horizontal gene transfer was shown for members of the *Chlamydiaceae,* but this phenomena appears to be restricted to interspecies or intergenus transfers (Kim *et al*., 2018; Suchland *et al*., 2019). Direct contact between an obligate intracellular *Chlamydia*-related organism and an extracellular eukaryotic parasite is also rather improbable. Thus, a common bacterial donor lineage of the NlpC/P60 proteins found in *S. negevensis* and *T. vaginalis* remains speculative.

Although it is unknown whether PG exists in *E. lausannensis* and *S. negevensis*, the presence of an NlpC/P60 domain-containing protein indicates that both species maintain the ability to break down PG or PG-derived peptides. Immunofluorescence microscopy analysis using antibodies targeting the NlpC/P60 proteins in both organisms was performed by Dr. Nicolas Jacquier of the University of Lausanne's Institute of Microbiology as part of a collaboration and suggests peripheral localization of $NlpC/P60^{Ela}$ and $NlpC/P60_{Sne}$ *in vivo* (personal communication). Additionally, evidence for a possible γ-D-Glu-mDAP peptidase activity of both enzymes was found in this work based on their ability to enhance growth when heterologously expressed in the *E. coli dapD*- Δ*mpl* mutant strain. Together, these

findings might indicate an involvement of NlpC/P60$_{Ela}$ and NlpC/P60$_{Sne}$ in a putative peptide recycling process. Nevertheless, especially with regard to the protein structure of NlpC/P60Sne, which differs significantly from YkfC, further studies are required to assess their physiological functions.

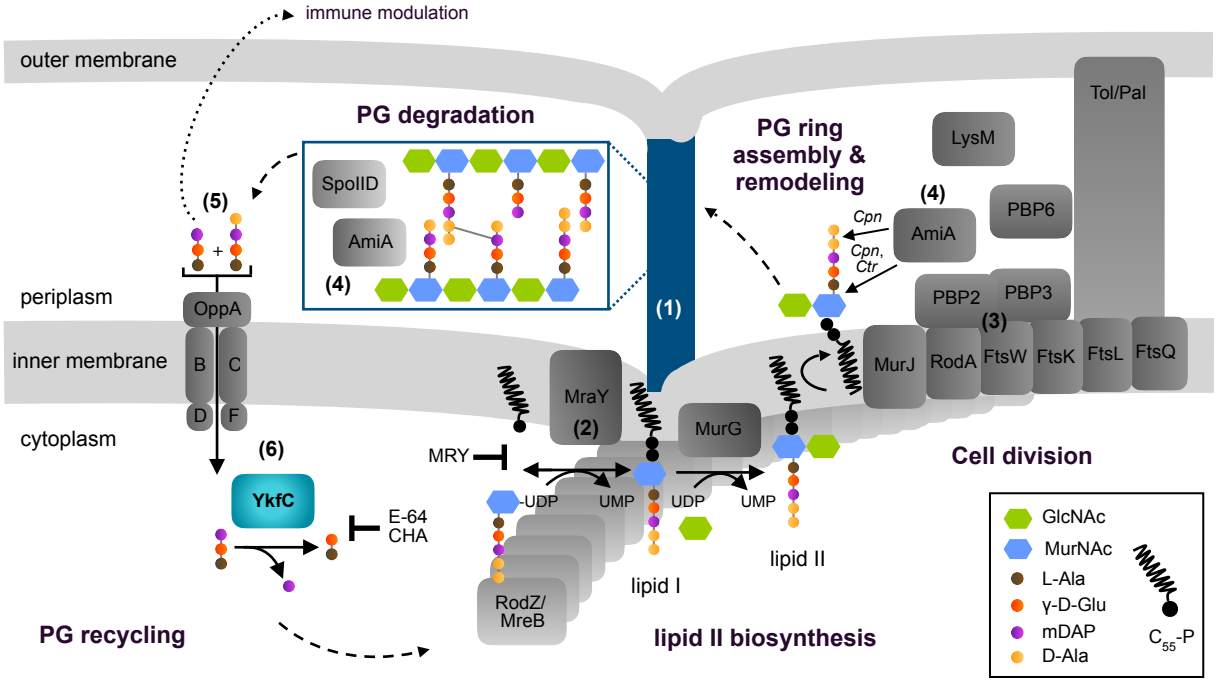

Figure 4.3. Proposed model of the PG turnover process at the division site in *Chlamydia*.
(1) The PG polymer (indicated in blue) is shaped like to a ring located at the septum of dividing cells (Liechti *et al*., 2014). The PG precursor lipid II biosynthesis is completed at the inner leaflet of the cytoplasmic membrane. The actin homolog MreB, together with RodZ, functionally replace the bacterial division organizer FtsZ, which is absent in *Chlamydia* (reviewed in Ouellette *et al*., 2020).
(2) MraY catalyzes the first membrane-bound step of the lipid II biosynthesis, the linking of UDP-MurNAc pentapeptide to the membrane carrier C_{55}-P (Henrichfreise *et al*., 2009). This work provides proof that this reaction is inhibited by muraymycins (MRY) resulting in stunted chlamydial replication.
(3) The periplasmic assembly of PG is likely mediated by the enzyme pairs RodA-PBP2 and FtsW-PBP3 acting as transpeptidase-glycosyltransferase complexes (Liechti, 2021). In addition to FtsW and PBP3, *Chlamydia* retain the cell division proteins FtsK, FtsL, FtsQ, and AmiA and the Tol-Pal system (reviewed in Ouellette *et al*., 2020).
(4) Chlamydial AmiA incessantly degrades PG and additionally processes lipid II. This work confirmed amidase activity in AmiA from *C. trachomatis.* Additional DD-CPase activity described in AmiA from *C. pneumoniae* (Klöckner *et al*., 2014) was not observed in *C. trachomatis*.
(5) PG degradation products can initiate the host immune response. PG-derived peptides are transported back into the bacterial cytoplasm by the olipeptide permease complex (Opp) (Singh *et al*., 2020).
(6) This work describes a first mode of recycling of PG-derived degradation products in *Chlamydia*. The cytoplasmic peptidase YkfC further degrades PG-derived peptides, providing free mDAP for lipid II assembly. Enzymatic *in vitro* activity of YkfC has been shown to be inhibited by the inhibitors E-64 and chloroactone (CHA).

Screening for orthologs of enzymes which catalyze the recycling of PG-derived peptides in free living bacteria indicates that *Chlamydiaceae* maintain a reduced, essential PG turnover process. Their genomes neither contain gene orthologs coding for proteins involved in *E. coli* PG recycling, nor an ortholog of key recycling permease AmpG which catalyzes the transport of anhydro-muropeptides into the cytoplasm in *E. coli* (Cheng & Park, 2002; Park & Uehara, 2008). While AmpG is lacking, a functional oligopeptide permease complex composed of a substrate binding protein (OppA), two transmembrane proteins (OppB, OppC), and two ATPase subunits (OppD, OppF) was shown to exist in *C. trachomatis* (Singh *et al.,* 2020). The OppABCDF complex of *E. coli* allows uptake of oligopeptides across the cytoplasmic membrane, but plays no detectable role in the PG recycling process (Park *et al*., 1993). In order to transport PG-derived peptides into the cytoplasm, the core of the Opp transporter (OppBCDF) is required to form a complex with the periplasmic murein subunit binding protein MppA (Park *et al*., 1998; Maqbool *et al*., 2011). While the genome of *C. trachomatis* lacks an *mppA* gene, three genes encoding putative substrate binding proteins (OppA1-3) are present. It was shown that an Opp transporter complex including OppA3 is able to facilitate the transport of free PG-derived peptides into the chlamydial cytoplasm (Singh *et al.,* 2020). Together with the proof of the existence of a functional peptide transporter by Singh and colleagues, this work's results on $YkfC_{Ctr}$ help to expand the current model of the PG turnover process in *Chlamydia* (fig. 4.3). While the fate of anhydro-muropeptides and sugar moieties released from PG by activity of $AmiA_{Ctr}$ and the putative SpoIID protein remains unclear, peptides derived from amidase activity on PG can enter the chlamydial cytoplasm through the OppA3BCDF complex. There they might be further processed by $YkfC_{Ctr}$ to provide amino acids for biosynthetic pathways. Since ability to cleave L-Ala-γ-D-Glu-mDAP tripeptides has been demonstrated for $YkfC_{Ctr}$, both *in vitro* and in an *E. coli* surrogate system, the enzyme should be able to generate free mDAP. This amino acid is essential for PG biosynthesis, but cannot be provided by the eukaryotic host cells of chlamydiae. *De novo* synthesis of mDAP to construct PG stem peptides requires six independent, energy-intensive biochemical reactions in *C. trachomatis* (McCoy *et al*., 2006). Thus recycling of PG-derived peptides by $YkfC_{Ctr}$ might not only be a result of chlamydial pathoadaption, but additionally helps the bacterium to save a significant amount of energy.

This work's findings suggest that YkfC is a key enzyme of the chlamydial peptide recycling process. However, it remains to be seen whether other amino acids of the PG stem peptide besides mDAP are also recycled. *B. subtilis* relies on the combined activity of three enzymes, L,D-CPase YkfA, γ-D-Glu-mDAP peptidase YkfC and L-Ala-γ-D-Glu epimerase YkfB, to completely restore amino acids from PG-derived peptides (Schmidt *et al*., 2001). *Chlamydiaceae* genomes are not only lacking the *ykfABCD* peptide recycling gene cluster found in *B. subtilis* (Schmidt *et al*., 2001; Molle *et al*., 2003), but are completely lacking homologs of genes coding for YkfA and YkfB. Instead, $YkfC_{Ctr}$ is encoded in close vicinity of genes coding for enzymes involved in glutamine uptake, a process which was recently identified to be crucial for the initiation of chlamydial PG synthesis and replication (Rajeeve *et al*., 2020). Consistent with its possible role in the PG turnover process, $ykfC_{Ctr}$ (*ct127*) is expressed during the mid-phase of *C. trachomatis*' lifecycle when replication of RBs takes place (Belland *et al*., 2003). Expression is also detectable during the late phase of the developmental cycle (Belland *et al*., 2003), at which $YkfC_{Ctr}$ may support energy recovery during re-differentiation from RB to EB through recycling peptides that are not further needed for maintaining cell division.

In pathogenic bacteria such as chlamydiae, whose survival strategy is to avoid an inflammatory immune response, the process of PG recycling plays an important role. It reduces the risk of immunostimulatory fragments being released from the cell, since PG degradation products are transported into the cytoplasm. But not only the uptake of these fragments, also the subsequent recycling steps are important for pathogenesis. In *Salmonella* Typhimurium, accumulation of PG-derived peptides, as a result of impaired activity of the cytosolic amidase AmpD, decreases the pathogen's ability to invade and grow within cultured macrophages (Folkesson *et al*., 2005). Enzymes such as YkfC, that are involved in the cytoplasmic steps of the PG recycling process, might be interesting target structures for anti-bacterial drug design. With the exception of PBP transpeptidases, which are targeted by β-lactams, there are no antibiotic protease inhibitors in the clinic, thus bacterial peptide degrading enzymes could be interesting, so far untapped drug targets (Culp & Wright, 2017). It was shown here that cysteine inhibitor E-64 which is a natural product of *Aspergillus japonicus* (Hanada *et al*., 1978) inhibits $YkfC_{Ctr}$ peptidase activity *in vitro*. Hence,

E-64 might be a promising candidate for further research on NlpC/P60 peptidases as bacterial target structures.
However, it is questionable whether inhibitors targeting YkfC are suitable agents for combating chlamydial infections. If YkfC, as suggested here, plays an important role in the provision of mDAP in *Chlamydia*, inhibition of its activity would, above all, restrict synthesis of lipid II. As discussed earlier, disruption of this pathway affects the chlamydial division process and would likely induce persistence, thereby enabling chlamydiae to evade this treatment.

Chlamydiae are highly adapted to their obligate intracellular lifestyle and their success as pathogens relies on their ability to take advantage from this habitat, as well as their ability to evade an immune response. This work's results help to gain some new insights into how the chlamydial cell division and PG turnover process evolved to contribute to this strategy. Within the osmotically-stable niche which is the chlamydial inclusion, a stabilizing cell wall becomes superfluous. Moreover, presence of classical bacterial cell envelope structures increases the risk of detection by the host immune system. Since cells naturally cannot exist without a surrounding layer, chlamydiae maintained the bacterial outer membrane. However, structure of chlamydial LPS differs from other types of bacterial LPS and is at least 100-fold less potent at eliciting the pro-inflammatory cytokine response (Ingalls *et al*., 1995; Brunham & Rey-Ladino, 2005). As a further adaption, *Chlamydia* lacks a stabilizing PG sacculus, but maintain a discrete and transient PG ring which constricts together with the septum of dividing cells (Liechti *et al*., 2016; Packiam *et al*., 2015). It was suggested that the chlamydial division process is interlinked with and relies on the biosynthesis of PG precursors (Henrichfreise *et al*., 2009; Jacquier *et al*., 2014; 2015b). Consistently, it was observed in this work that inhibition of MraY, which catalyzes the first membrane bound step of lipid II biosynthesis, impairs chlamydial development.
Although the loss of a PG sacculus reduces the proportion of PG-derived immunostimulatory fragments, *Chlamydia* cannot prevent their release into the periplasm during PG ring degradation. The results of this work suggest that AmiA and YkfC from *C. trachomatis*, enzymes thought to be involved in the PG degradation and recycling process, are able to process PG fragments and free PG-derived peptides in

such a way that they are no longer recognized by their corresponding NOD immunity receptors. Thus, both enzymes could help minimize recognition of *C. trachomatis* by the host's intracellular immune response. While *C. trachomatis* AmiA is a periplasmic enzyme, *C. trachomatis* YkfC is located in the cytoplasm. In order to be processed by YkfC, peptides derived from the PG stem peptide have to be transported across the inner membrane. Their transport could be facilitated by a recently described chlamydial Opp transporter complex (Singh *et al*., 2020). In the absence of other genes encoding classical bacterial PG recycling enzymes in the *C. trachomatis* genome, the Opp complex and YkfC together might form a rudimentary recycling machinery for PG-derived peptides (fig 4.3). This reduced recycling machinery might be sufficient for obligate intracellular *C. trachomatis* since the majority of amino acids are not produced *de novo* in this organism but are imported from the host cell and used directly for chlamydial biosynthetic processes (Mehlitz *et al*., 2017). However, *de novo* synthesis of mDAP remains essential for *Chlamydia* since this amino acid cannot be provided by their mammalian host cells. Therefore, recycling of PG-derived peptides by YkfC activity could be beneficial for the chlamydial fitness. Taken together, the existence of a reduced chlamydial PG recycling machinery suggests that *C. trachomatis* utilizes its host cell's resources whenever possible while maintaining a pathway for the reuse of PG-derived mDAP through the interplay of the Opp transporter complex and the recycling peptidase YkfC. In addition to providing mDAP for the PG precursor biosynthesis, the recycling machinery of *C. trachomatis* could be another tool used by this well-adapted pathogen to evade the host immune system by reducing the release of immunostimulatory agents.

5. Summary

The obligate intracellular chlamydiae evolved mechanisms to persist inside their host and to evade the host immune system, making them intriguing and highly successful pathogens. This work aimed to asses how these strategies are interlinked with the chlamydial peptidoglycan (PG) turnover process.

First, antimicrobial compounds were used as tools to study the interplay between PG biosynthesis and the chlamydial lifecycle. These experiments included analysis of the host cell, since an antichlamydial effect can be caused by both host cell stress and by inhibition of a bacterial target. In a cell culture based approach combining cytotoxicity analysis and fluorescence microscopy, muraymycin D2 and derivates were verified to induce a persistent state in productive *Chlamydia* infection. The antichlamydial effect could be attributed to the inhibition of PG precursor synthesis, since no damaging effect on the host cells was observed and biochemical analysis identified *Chlamydia* MraY as a target. In addition, muraymycin D2 was found to break penicillin-induced persistence in *C. trachomatis,* suggesting the presence of additional targets.

Degradation of the PG ring during the unique chlamydial cell division poses risks to the organism, as products of this process initiate host immune response. In this work, comparative analyses on cell division amidases from *Chlamydia* and *E. coli* corroborated the importance of an autoinhibitory domain in the *E. coli* enzyme that is absent in the *Chlamydia* homologs. In line, *C. trachomatis* AmiA was found to be active by default and to degraded the recognition substrate of immunity receptor NOD2 *in vitro*. Unlike the dual functioning *C. pneumoniae* AmiA, *C. trachomatis* AmiA did not show additional carboxypeptidase activity on PG precursor lipid II, suggesting that different PG degradation machineries exist in *Chlamydia*. PG-derived peptides generated by amidase activity trigger NOD1 mediated immune response. Here, an ortholog of a *Bacillus* NlpC/P60 protein was found to be widely conserved among *Chlamydia* and *Chlamydia*-related organisms and to cleave the minimal recognition site of NOD1. *In silico*, biochemical and surrogate host experiments indicate that *C. trachomatis* YkfC is tailored to recycle PG-derived peptides in the cytoplasm and shows high substrate specificity that prevents interference with PG precursor synthesis. The identification of *C. trachomatis* YkfC targeting cysteine protease inhibitors provides a basis for future studies on the intersection of energy recovery, cell division and immune evasion in *Chlamydia* and on the host-pathogen interplay.

6. References

Abdelrahman, Y. M., & **Belland**, R. J. (**2005**). The chlamydial developmental cycle. FEMS Microbiology Reviews, 29(5), 949–959. https://doi.org/10.1016/j.femsre.2005.03.002

Abdelrahman, Y., Ouellette, S. P., Belland, R. J., & Cox, J. V. (**2016**). Polarized Cell Division of *Chlamydia trachomatis*. PLOS Pathogens, 12(8), e1005822. https://doi.org/10.1371/journal.ppat.1005822

Abraham, S., Juel, H. B., Bang, P., Cheeseman, H. M., Dohn, R. B., Cole, T., … Follmann, F. (**2019**). Safety and immunogenicity of the chlamydia vaccine candidate CTH522 adjuvanted with CAF01 liposomes or aluminium hydroxide: a first-in-human, randomised, double-blind, placebo-controlled, phase 1 trial. The Lancet. Infectious Diseases, 19(10), 1091–1100. https://doi.org/10.1016/S1473-3099(19)30279-8

Ahmadi, M. H., Mirsalehian, A., Sadighi Gilani, M. A., Bahador, A., & Afraz, K. (**2018**). Association of asymptomatic *Chlamydia trachomatis* infection with male infertility and the effect of antibiotic therapy in improvement of semen quality in infected infertile men. Andrologia. https://doi.org/10.1111/and.12944

Aistleitner, K., Anrather, D., Schott, T., Klose, J., Bright, M., Ammerer, G., & Horn, M. (**2015**). Conserved features and major differences in the outer membrane protein composition of chlamydiae. Environmental Microbiology, 17(4), 1397–1413. https://doi.org/10.1111/1462-2920.12621

Akande, V., Turner, C., Horner, P., Horne, A., & Pacey, A. (**2010**). Impact of *Chlamydia trachomatis* in the reproductive setting: British Fertility Society Guidelines for practice. Human Fertility (Cambridge, England), 13(3), 115–125. https://doi.org/10.3109/14647273.2010.513893

Albrecht, M., Sharma, C. M., Dittrich, M. T., Müller, T., Reinhardt, R., Vogel, J., & Rudel, T. (**2011**). The transcriptional landscape of *Chlamydia pneumoniae*. Genome Biology, 12(10), R98. https://doi.org/10.1186/gb-2011-12-10-r98

Altschul, S. F., Gish, W., Miller, W., Myers, E. W., & Lipman, D. J. (**1990**). Basic local alignment search tool. Journal of Molecular Biology, 215(3), 403–410. https://doi.org/10.1016/S0022-2836(05)80360-2

Amslinger, S. (**2010**). The tunable functionality of alpha,beta-unsaturated carbonyl compounds enables their differential application in biological systems. ChemMedChem, 5(3), 351–356. https://doi.org/10.1002/cmdc.200900499

Anantharaman, V., & **Aravind**, L. (**2003**). Evolutionary history, structural features and biochemical diversity of the NlpC/P60 superfamily of enzymes. Genome Biology, 4(2), R11. https://doi.org/10.1186/gb-2003-4-2-r11

Andrews, J. M. (**2001**). Determination of minimum inhibitory concentrations. The Journal of Antimicrobial Chemotherapy, 48 Suppl 1, 5–16. https://doi.org/10.1093/jac/48.suppl_1.5

Aramini, J. M., Rossi, P., Huang, Y. J., Zhao, L., Jiang, M., Maglaqui, M., … Montelione, G. T. (**2008**). Solution NMR structure of the NlpC/P60 domain of

lipoprotein Spr from *Escherichia coli*: structural evidence for a novel cysteine peptidase catalytic triad. Biochemistry, 47(37), 9715–9717. https://doi.org/10.1021/bi8010779

Atrih, A., Bacher, G., Allmaier, G., Williamson, M. P., & Foster, S. J. (**1999**). Analysis of peptidoglycan structure from vegetative cells of *Bacillus subtilis* 168 and role of PBP 5 in peptidoglycan maturation. Journal of Bacteriology, 181(13), 3956–3966. https://doi.org/10.1128/JB.181.13.3956-3966.1999

Baba, T., Ara, T., Hasegawa, M., Takai, Y., Okumura, Y., Baba, M., … Mori, H. (**2006**). Construction of *Escherichia coli* K-12 in-frame, single-gene knockout mutants: the Keio collection. Molecular Systems Biology, 2, 2006.0008. https://doi.org/10.1038/msb4100050

Bachmann, N. L., Polkinghorne, A., & Timms, P. (**2014**). Chlamydia genomics: providing novel insights into chlamydial biology. Trends in Microbiology, 22(8), 464–472. https://doi.org/10.1016/j.tim.2014.04.013

Barbour, A. G., Amano, K., Hackstadt, T., Perry, L., & Caldwell, H. D. (**1982**). *Chlamydia trachomatis* has penicillin-binding proteins but not detectable muramic acid. Journal of Bacteriology, 151(1), 420–428. https://doi.org/10.1128/jb.151.1.420-428.1982

Bastidas, R. J., Elwell, C. A., Engel, J. N., & Valdivia, R. H. (**2013**). Chlamydial intracellular survival strategies. Cold Spring Harbor Perspectives in Medicine, 3(5), a010256–a010256. https://doi.org/10.1101/cshperspect.a010256

Bateman, A., **& Rawlings**, N. D. (**2003**). The CHAP domain: a large family of amidases including GSP amidase and peptidoglycan hydrolases. Trends in Biochemical Sciences, 28(5), 234–237. https://doi.org/10.1016/S0968-0004(03)00061-6

Bateman, A., Martin, M.-J., Orchard, S., Magrane, M., Agivetova, R., Ahmad, S., … Teodoro, D. (**2021**). UniProt: the universal protein knowledgebase in 2021. Nucleic Acids Research, 49(D1), D480–D489. https://doi.org/10.1093/nar/gkaa1100

Baud, D., Thomas, V., Arafa, A., Regan, L., & Greub, G. (**2007**). *Waddlia chondrophila*, a potential agent of human fetal death. Emerging Infectious Diseases, 13(8), 1239–1243. https://doi.org/10.3201/eid1308.070315

Baud, D., Goy, G., Osterheld, M.-C., Croxatto, A., Borel, N., Vial, Y., … Greub, G. (**2014**). Role of *Waddlia chondrophila* placental infection in miscarriage. Emerging Infectious Diseases, 20(3), 460–464. https://doi.org/10.3201/eid2003.131019

Belland, R. J., Zhong, G., Crane, D. D., Hogan, D., Sturdevant, D., Sharma, J., … Caldwell, H. D. (**2003**). Genomic transcriptional profiling of the developmental cycle of *Chlamydia trachomatis*. Proceedings of the National Academy of Sciences of the United States of America, 100(14), 8478–8483. https://doi.org/10.1073/pnas.1331135100

Bernhardt, T. G., & de Boer, P. A. J. (**2003**). The *Escherichia coli* amidase AmiC is a periplasmic septal ring component exported via the twin-arginine transport pathway.

Molecular Microbiology, 48(5), 1171–1182. https://doi.org/10.1046/j.1365-2958.2003.03511.x

Bertani, G. (**1951**). Studies on lysogenesis. I. The mode of phage liberation by lysogenic *Escherichia coli*. Journal of Bacteriology, 62(3), 293–300. https://doi.org/10.1128/jb.62.3.293-300.1951

Bertelli, C., Collyn, F., Croxatto, A., Rückert, C., Polkinghorne, A., Kebbi-Beghdadi, C., … Greub, G. (**2010**). The *Waddlia* genome: a window into chlamydial biology. PloS One, 5(5), e10890–e10890. https://doi.org/10.1371/journal.pone.0010890

Bi, E. F., & **Lutkenhaus**, J. (**1991**). FtsZ ring structure associated with division in *Escherichia coli.* Nature, 354(6349), 161–164. https://doi.org/10.1038/354161a0

Blum, M., Chang, H.-Y., Chuguransky, S., Grego, T., Kandasaamy, S., Mitchell, A., … Finn, R. D. (**2021**). The InterPro protein families and domains database: 20 years on. Nucleic Acids Research, 49(D1), D344–D354. https://doi.org/10.1093/nar/gkaa977

Bobrovsky, P., Manuvera, V., Polina, N., Podgorny, O., Prusakov, K., Govorun, V., & Lazarev, V. (**2016**). Recombinant human peptidoglycan recognition proteins reveal antichlamydial activity. Infection and Immunity, 84(7), 2124–2130. https://doi.org/10.1128/IAI.01495-15

Bodetti, T. J., Jacobson, E., Wan, C., Hafner, L., Pospischil, A., Rose, K., & Timms, P. (**2002**). Molecular evidence to support the expansion of the host range of *Chlamydophila pneumoniae* to include reptiles as well as humans, horses, koalas and amphibians. Systematic and Applied Microbiology, 25(1), 146–152. https://doi.org/10.1078/0723-2020-00086

Borel, N., Summersgill, J. T., Mukhopadhyay, S., Miller, R. D., Ramirez, J. A., & Pospischil, A. (**2008**). Evidence for persistent *Chlamydia pneumoniae* infection of human coronary atheromas. Atherosclerosis, 199(1), 154–161. https://doi.org/10.1016/j.atherosclerosis.2007.09.026

Bouhss, A., Trunkfield, A. E., Bugg, T. D. H., & Mengin-Lecreulx, D. (**2008**). The biosynthesis of peptidoglycan lipid-linked intermediates. FEMS Microbiology Reviews, 32(2), 208–233. https://doi.org/10.1111/j.1574-6976.2007.00089.x

Bourgeois, I., Camiade, E., Biswas, R., Courtin, P., Gibert, L., Götz, F., … Pestel-Caron, M. (**2009**). Characterization of AtlL, a bifunctional autolysin of *Staphylococcus lugdunensis* with N-acetylglucosaminidase and N-acetylmuramoyl-l-alanine amidase activities. FEMS Microbiology Letters, 290(1), 105–113. https://doi.org/10.1111/j.1574-6968.2008.01414.x

Bradford, M. M. (**1976**). A rapid and sensitive method for the quantitation of microgram quantities of protein utilizing the principle of protein-dye binding. Analytical Biochemistry, 72, 248–254. https://doi.org/10.1006/abio.1976.9999

Brockett, M. R., & **Liechti**, G. W. (**2021**). Persistence alters the interaction between *Chlamydia trachomatis* and its host cell. Infection and Immunity, 89(8), e0068520. https://doi.org/10.1128/IAI.00685-20

Brunham, R. C., & Rey-Ladino, J. (**2005**). Immunology of *Chlamydia* infection: implications for a *Chlamydia trachomatis* vaccine. Nature Reviews. Immunology, 5(2), 149–161. https://doi.org/10.1038/nri1551

Brunham, R. C., Gottlieb, S. L., & Paavonen, J. (**2015**). Pelvic inflammatory disease. The New England Journal of Medicine, 372(21), 2039–2048. https://doi.org/10.1056/NEJMra1411426

Brunke, M. (**2018**) Novel aspects of peptidoglycan metabolism, persistent infection and pathogenicity in *Chlamydiae*. PhD Thesis. University Bonn.

Bryan, E. R., McLachlan, R. I., Rombauts, L., Katz, D. J., Yazdani, A., Bogoevski, K., … Beagley, K. W. (**2019**). Detection of chlamydia infection within human testicular biopsies. Human Reproduction (Oxford, England), 34(10), 1891–1898. https://doi.org/10.1093/humrep/dez169

Bublitz, M., Polle, L., Holland, C., Heinz, D. W., Nimtz, M., & Schubert, W.-D. (**2009**). Structural basis for autoinhibition and activation of Auto, a virulence-associated peptidoglycan hydrolase of *Listeria monocytogenes*. Molecular Microbiology, 71(6), 1509–1522. https://doi.org/10.1111/j.1365-2958.2009.06619.x

Buchholz, K. R., **& Stephens**, R. S. (**2008**). The cytosolic pattern recognition receptor NOD1 induces inflammatory interleukin-8 during *Chlamydia trachomatis* infection. Infection and Immunity, 76(7), 3150–3155. https://doi.org/10.1128/IAI.00104-08

Bugg, T. D. H., Lloyd, A. J., & Roper, D. I. (**2006**). Phospho-MurNAc-pentapeptide translocase (MraY) as a target for antibacterial agents and antibacterial proteins. Infectious Disorders Drug Targets, 6(2), 85–106. https://doi.org/10.2174/187152606784112128

Bukhari, A. I., **& Taylor**, A. L. (**1971**). Genetic analysis of diaminopimelic acid- and lysine-requiring mutants of *Escherichia coli*. Journal of Bacteriology, 105(3), 844–854. https://doi.org/10.1128/jb.105.3.844-854.1971

Burillo, A., & **Bouza**, E. (**2010**). *Chlamydophila pneumoniae*. Infectious Disease Clinics of North America, 24(1), 61–71. https://doi.org/10.1016/j.idc.2009.10.002

Burton, M. J., & Mabey, D. C. W. (**2009**). The global burden of trachoma: a review. PLoS Neglected Tropical Diseases, 3(10), e460. https://doi.org/10.1371/journal.pntd.0000460

Bühl, H. (**2019**). The *Chlamydiales*: new insights into the role as pathogens, serine/threonine signaling, and peptidoglycan remodeling. PhD Thesis. University Bonn.

Caldwell, H. D., Kromhout, J., & Schachter, J. (**1981**). Purification and partial characterization of the major outer membrane protein of *Chlamydia trachomatis*. Infection and Immunity, 31(3), 1161–1176. https://doi.org/10.1128/iai.31.3.1161-1176.1981

Campbell, J., Singh, A. K., Santa Maria, J. P. J., Kim, Y., Brown, S., Swoboda, J. G., … Walker, S. (**2011**). Synthetic lethal compound combinations reveal a fundamental connection between wall teichoic acid and peptidoglycan biosyntheses in

Staphylococcus aureus. ACS Chemical Biology, 6(1), 106–116. https://doi.org/10.1021/cb100269f

Capmany, A., **& Damiani**, M. T. (**2010**). *Chlamydia trachomatis* intercepts Golgi-derived sphingolipids through a Rab14-mediated transport required for bacterial development and replication. PloS One, 5(11), e14084. https://doi.org/10.1371/journal.pone.0014084

Casson, N., Medico, N., Bille, J., & Greub, G. (**2006**). *Parachlamydia acanthamoebae* enters and multiplies within pneumocytes and lung fibroblasts. Microbes and Infection, 8(5), 1294—1300. https://doi.org/10.1016/j.micinf.2005.12.011

Cayrou, C., Raoult, D., & Drancourt, M. (**2010**). Broad-spectrum antibiotic resistance of *Planctomycetes* organisms determined by Etest. The Journal of Antimicrobial Chemotherapy, 65(10), 2119–2122. https://doi.org/10.1093/jac/dkq290

Chamaillard, M., Hashimoto, M., Horie, Y., Masumoto, J., Qiu, S., Saab, L., … Inohara, N. (**2003**). An essential role for NOD1 in host recognition of bacterial peptidoglycan containing diaminopimelic acid. Nature Immunology, 4(7), 702–707. https://doi.org/10.1038/ni945

Chaput, C., & **Boneca**, I. G. (**2007**). Peptidoglycan detection by mammals and flies. Microbes and Infection, 9(5), 637–647. https://doi.org/10.1016/j.micinf.2007.01.022

Chaput, C., Ecobichon, C., Cayet, N., Girardin, S. E., Werts, C., Guadagnini, S., … Boneca, I. G. (**2006**). Role of AmiA in the morphological transition of *Helicobacter pylori* and in immune escape. PLoS Pathogens, 2(9), e97–e97. https://doi.org/10.1371/journal.ppat.0020097

Cheggour, A., Fanuel, L., Duez, C., Joris, B., Bouillenne, F., Devreese, B., … Goffin, C. (**2000**). The dppA gene of *Bacillus subtilis* encodes a new D-aminopeptidase. Molecular Microbiology, 38(3), 504–513. https://doi.org/10.1046/j.1365-2958.2000.02117.x

Chen, X., Gao, T., Peng, Q., Zhang, J., Chai, Y., & Song, F. (**2018**). Novel cell wall hydrolase CwlC from *Bacillus thuringiensis* is essential for mother cell lysis. Applied and Environmental Microbiology, 84(7), e02640-17. https://doi.org/10.1128/AEM.02640-17

Cheng, Q., & **Park**, J. T. (**2002**). Substrate specificity of the AmpG permease required for recycling of cell wall anhydro-muropeptides. Journal of Bacteriology, 184(23), 6434–6436. https://doi.org/10.1128/JB.184.23.6434-6436.2002

Cheong, H. C., Lee, C. Y., Cheok, Y. Y., Tan, G. M., Looi, C. Y., & Wong, W. F. (**2019**). *Chlamydiaceae*: Diseases in Primary Hosts and Zoonosis. Microorganisms. https://doi.org/10.3390/microorganisms7050146

Chung, H. S., Yao, Z., Goehring, N. W., Kishony, R., Beckwith, J., & Kahne, D. (**2009**). Rapid beta-lactam-induced lysis requires successful assembly of the cell division machinery. Proceedings of the National Academy of Sciences of the United States of America, 106(51), 21872–21877. https://doi.org/10.1073/pnas.0911674106

Chung, B. C., Zhao, J., Gillespie, R. A., Kwon, D.-Y., Guan, Z., Hong, J., … Lee, S.-Y. (**2013**). Crystal structure of MraY, an essential membrane enzyme for bacterial cell wall synthesis. Science (New York, N.Y.), 341(6149), 1012–1016. https://doi.org/10.1126/science.1236501

Cochrane, M., Walker, P., Gibbs, H., & Timms, P. (**2005**). Multiple genotypes of *Chlamydia pneumoniae* identified in human carotid plaque. Microbiology, 151(7), 2285–2290. https://doi.org/10.1099/mic.0.27781-0

Collingro, A., Tischler, P., Weinmaier, T., Penz, T., Heinz, E., Brunham, R. C., … Horn, M. (**2011**). Unity in variety--the pan-genome of the *Chlamydiae*. Molecular Biology and Evolution, 28(12), 3253–3270. https://doi.org/10.1093/molbev/msr161

Collingro, A., Köstlbacher, S., & Horn, M. (**2020**). *Chlamydiae* in the Environment. Trends in Microbiology, 28(11), 877–888. https://doi.org/10.1016/j.tim.2020.05.020

Cook, J. A. (**2008**). Eliminating Blinding Trachoma. New England Journal of Medicine, 358(17), 1777–1779. https://doi.org/10.1056/NEJMp0708546

Cook, J., Baverstock, T. C., McAndrew, M. B. L., Stansfeld, P. J., Roper, D. I., & Crow, A. (**2020**). Insights into bacterial cell division from a structure of EnvC bound to the FtsX periplasmic domain. Proceedings of the National Academy of Sciences of the United States of America, 117(45), 28355–28365. https://doi.org/10.1073/pnas.2017134117

Cox, R. J., Sutherland, A., & Vederas, J. C. (**2000**). Bacterial diaminopimelate metabolism as a target for antibiotic design. Bioorganic & Medicinal Chemistry, 8(5), 843–871. https://doi.org/10.1016/s0968-0896(00)00044-4

Cox, J. V, Abdelrahman, Y. M., & Ouellette, S. P. (**2020**). Penicillin-binding proteins regulate multiple steps in the polarized cell division process of *Chlamydia*. Scientific Reports, 10(1), 12588. https://doi.org/10.1038/s41598-020-69397-x

Culp, E., & **Wright**, G. D. (**2017**). Bacterial proteases, untapped antimicrobial drug targets. The Journal of Antibiotics, 70(4), 366–377. https://doi.org/10.1038/ja.2016.138

Dai, W., & **Li**, Z. (**2014**). Conserved type III secretion system exerts important roles in *Chlamydia trachomatis*. International Journal of Clinical and Experimental Pathology, 7(9), 5404–5414.

Darville, T. (**2005**). *Chlamydia trachomatis* infections in neonates and young children. Seminars in Pediatric Infectious Diseases, 16(4), 235–244. https://doi.org/10.1053/j.spid.2005.06.004

de Barsy, M., Bottinelli, L., & Greub, G. (**2014**). Antibiotic susceptibility of *Estrella lausannensis*, a potential emerging pathogen. Microbes and Infection, 16(9), 746–754. https://doi.org/10.1016/j.micinf.2014.08.003

De Benedetti, S., Bühl, H., Gaballah, A., Klöckner, A., Otten, C., Schneider, T., … Henrichfreise, B. (**2014**). Characterization of serine hydroxymethyltransferase GlyA as a potential source of D-alanine in *Chlamydia pneumoniae*. Frontiers in Cellular and Infection Microbiology, 4, 19. https://doi.org/10.3389/fcimb.2014.00019

de la Maza, L. M., Darville, T. L., & Pal, S. (**2021**). *Chlamydia trachomatis* vaccines for genital infections: where are we and how far is there to go? Expert Review of Vaccines, 20(4), 421–435. https://doi.org/10.1080/14760584.2021.1899817

Dharamshi, J. E., Tamarit, D., Eme, L., Stairs, C. W., Martijn, J., Homa, F., … Ettema, T. J. G. (**2020**). Marine Sediments Illuminate *Chlamydiae* Diversity and Evolution. Current Biology : CB, 30(6), 1032-1048.e7. https://doi.org/10.1016/j.cub.2020.02.016

Di Pietro, M., Filardo, S., De Santis, F., & Sessa, R. (**2013**). *Chlamydia pneumoniae* infection in atherosclerotic lesion development through oxidative stress: a brief overview. International Journal of Molecular Sciences, 14(7), 15105–15120. https://doi.org/10.3390/ijms140715105

Di Pietro, M., Filardo, S., Romano, S., & Sessa, R. (**2019**). *Chlamydia trachomatis* and *Chlamydia pneumoniae* interaction with the host: Latest advances and future prospective. Microorganisms, 7(5). https://doi.org/10.3390/microorganisms7050140

Doi, M., Wachi, M., Ishino, F., Tomioka, S., Ito, M., Sakagami, Y., … Matsuhashi, M. (**1988**). Determinations of the DNA sequence of the mreB gene and of the gene products of the mre region that function in formation of the rod shape of *Escherichia coli* cells. Journal of Bacteriology, 170(10), 4619–4624. https://doi.org/10.1128/jb.170.10.4619-4624.1988

Donati, M., Di Francesco, A., D'Antuono, A., Delucca, F., Shurdhi, A., Moroni, A., … Cevenini, R. (**2010**). *In vitro* activities of several antimicrobial agents against recently isolated and genotyped *Chlamydia trachomatis* urogenital serovars D through K. Antimicrobial Agents and Chemotherapy, 54(12), 5379–5380. https://doi.org/10.1128/AAC.00553-10

Doyle, R. J., Chaloupka, J., & Vinter, V. (**1988**). Turnover of cell walls in microorganisms. Microbiological Reviews, 52(4), 554–567. https://doi.org/10.1128/mr.52.4.554-567.1988

Dreses-Werringloer, U., Gérard, H. C., Whittum-Hudson, J. A., & Hudson, A. P. (**2006**). *Chlamydophila* (*Chlamydia*) *pneumoniae* infection of human astrocytes and microglia in culture displays an active, rather than a persistent, phenotype. The American Journal of the Medical Sciences, 332(4), 168–174. https://doi.org/10.1097/00000441-200610000-00003

Egan, A. J. F., Biboy, J., van't Veer, I., Breukink, E., & Vollmer, W. (**2015**). Activities and regulation of peptidoglycan synthases. Philosophical Transactions of the Royal Society of London. Series B, Biological Sciences, 370(1679). https://doi.org/10.1098/rstb.2015.0031

Elwell, C., Mirrashidi, K., & Engel, J. (**2016**). Chlamydia cell biology and pathogenesis. Nature Reviews. Microbiology, 14(6), 385–400. https://doi.org/10.1038/nrmicro.2016.30

Ende, R. J., **& Derré**, I. (**2020**). Host and bacterial glycolysis during *Chlamydia trachomatis* infection. Infection and Immunity, 88(12). https://doi.org/10.1128/IAI.00545-20

Errington, J., Mickiewicz, K., Kawai, Y., & Wu, L. J. (**2016**). L-form bacteria, chronic diseases and the origins of life. Philosophical Transactions of the Royal Society of London. Series B, Biological Sciences, 371(1707), 20150494. https://doi.org/10.1098/rstb.2015.0494

European Centre for Disease Prevention and Control. (**2021**). Technical Report: Technologies, strategies and approaches for testing populations at risk of sexually transmitted infections in the EU/EEA. Retrieved from www.ecdc.europa.eu

Farley, T. A., Cohen, D. A., & Elkins, W. (**2003**). Asymptomatic sexually transmitted diseases: the case for screening. Preventive Medicine, 36(4), 502–509. https://doi.org/10.1016/s0091-7435(02)00058-0

Folkesson, A., Eriksson, S., Andersson, M., Park, J. T., & Normark, S. (**2005**). Components of the peptidoglycan-recycling pathway modulate invasion and intracellular survival of *Salmonella enterica* serovar Typhimurium. Cellular Microbiology, 7(1), 147–155. https://doi.org/10.1111/j.1462-5822.2004.00443.x

Frandi, A., Jacquier, N., Théraulaz, L., Greub, G., & Viollier, P. H. (**2014**). FtsZ-independent septal recruitment and function of cell wall remodelling enzymes in chlamydial pathogens. Nature Communications, 5, 4200. https://doi.org/10.1038/ncomms5200

Friedman, M. G., Kahane, S., Dvoskin, B., & Hartley, J. W. (**2006**). Detection of *Simkania negevensis* by culture, PCR, and serology in respiratory tract infection in Cornwall, UK. Journal of Clinical Pathology, 59(3), 331–333. https://doi.org/10.1136/jcp.2004.025601

Fukushima, T., Kitajima, T., Yamaguchi, H., Ouyang, Q., Furuhata, K., Yamamoto, H., … Sekiguchi, J. (**2008**). Identification and characterization of novel cell wall hydrolase CwlT: a two-domain autolysin exhibiting n-acetylmuramidase and DL-endopeptidase activities. The Journal of Biological Chemistry, 283(17), 11117–11125. https://doi.org/10.1074/jbc.M706626200

Fukushima, T., Uchida, N., Ide, M., Kodama, T., & Sekiguchi, J. (**2018**). DL-endopeptidases function as both cell wall hydrolases and poly-γ-glutamic acid hydrolases. Microbiology (Reading, England), 164(3), 277–286. https://doi.org/10.1099/mic.0.000609

Gaballah, A., Kloeckner, A., Otten, C., Sahl, H.-G., & Henrichfreise, B. (**2011**). Functional analysis of the cytoskeleton protein MreB from *Chlamydophila pneumoniae*. PloS One, 6(10), e25129. https://doi.org/10.1371/journal.pone.0025129

Garcia, D. L., & **Dillard**, J. P. (**2006**). AmiC functions as an N-acetylmuramyl-l-alanine amidase necessary for cell separation and can promote autolysis in Neisseria gonorrhoeae. Journal of Bacteriology, 188(20), 7211–7221. https://doi.org/10.1128/JB.00724-06

Geisler, W. M. (**2010**). Duration of untreated, uncomplicated *Chlamydia trachomatis* genital infection and factors associated with chlamydia resolution: a review of human studies. The Journal of Infectious Diseases, 201 Suppl, S104-13. https://doi.org/10.1086/652402

Geisler, W. M., Lensing, S. Y., Press, C. G., & Hook, E. W. 3rd. (**2013**). Spontaneous resolution of genital *Chlamydia trachomatis* infection in women and protection from reinfection. The Journal of Infectious Diseases, 207(12), 1850–1856. https://doi.org/10.1093/infdis/jit094

Ghosh, A. S., Chowdhury, C., & Nelson, D. E. (**2008**). Physiological functions of D-alanine carboxypeptidases in *Escherichia coli.* Trends in Microbiology, 16(7), 309–317. https://doi.org/10.1016/j.tim.2008.04.006

Girardin, S. E., Boneca, I. G., Carneiro, L. A. M., Antignac, A., Jéhanno, M., Viala, J., … Philpott, D. J. (**2003a**). Nod1 detects a unique muropeptide from gram-negative bacterial peptidoglycan. Science (New York, N.Y.), 300(5625), 1584–1587. https://doi.org/10.1126/science.1084677

Girardin, S. E., Boneca, I. G., Viala, J., Chamaillard, M., Labigne, A., Thomas, G., … Sansonetti, P. J. (**2003b**). Nod2 is a general sensor of peptidoglycan through muramyl dipeptide (MDP) detection. The Journal of Biological Chemistry, 278(11), 8869–8872. https://doi.org/10.1074/jbc.C200651200

Goffin, C., **& Ghuysen**, J.-M. (**2002**). Biochemistry and comparative genomics of SxxK superfamily acyltransferases offer a clue to the mycobacterial paradox: presence of penicillin-susceptible target proteins versus lack of efficiency of penicillin as therapeutic agent. Microbiology and Molecular Biology Reviews : MMBR, 66(4), 702–738, table of contents. https://doi.org/10.1128/MMBR.66.4.702-738.2002

Grayston, J. T., Aldous, M. B., Easton, A., Wang, S. P., Kuo, C. C., Campbell, L. A., & Altman, J. (**1993**). Evidence that *Chlamydia pneumoniae* causes pneumonia and bronchitis. The Journal of Infectious Diseases, 168(5), 1231–1235. https://doi.org/10.1093/infdis/168.5.1231

Grieshaber, S. S., Grieshaber, N. A., Miller, N., & Hackstadt, T. (**2006**). *Chlamydia trachomatis* causes centrosomal defects resulting in chromosomal segregation abnormalities. Traffic (Copenhagen, Denmark), 7(8), 940–949. https://doi.org/10.1111/j.1600-0854.2006.00439.x

Grieshaber, S. S., Swanson, J. A., & Hackstadt, T. (**2002**). Determination of the physical environment within the *Chlamydia trachomatis* inclusion using ion-selective ratiometric probes. Cellular Microbiology, 4(5), 273–283. https://doi.org/10.1046/j.1462-5822.2002.00191.x

Griesinger, G., Gille, G., Klapp, C., von Otte, S., & Diedrich, K. (**2007**). Sexual behaviour and *Chlamydia trachomatis* infections in German female urban adolescents, 2004. Clinical Microbiology and Infection : The Official Publication of the European Society of Clinical Microbiology and Infectious Diseases, 13(4), 436–439. https://doi.org/10.1111/j.1469-0691.2006.01680.x

Gupta, R. S. (**2011**). Origin of diderm (Gram-negative) bacteria: antibiotic selection pressure rather than endosymbiosis likely led to the evolution of bacterial cells with two membranes. Antonie van Leeuwenhoek, 100(2), 171–182. https://doi.org/10.1007/s10482-011-9616-8

Gutierrez, J., Smith, R., & Pogliano, K. (**2010**). SpoIID-mediated peptidoglycan degradation is required throughout engulfment during *Bacillus subtilis* sporulation. Journal of Bacteriology, 192(12), 3174–3186. https://doi.org/10.1128/JB.00127-10

Haggerty, C. L., & Ness, R. B. (**2006**). Epidemiology, pathogenesis and treatment of pelvic inflammatory disease. Expert Review of Anti-Infective Therapy, 4(2), 235–247. https://doi.org/10.1586/14787210.4.2.235

Hanada, K., Tamai, M., Yamagishi, M., Ohmura, S., Sawada, L., & Tanaka, I. (**1978**). Isolation and characterization of e-64, a new thiol protease inhibitor. Agricultural and Biological Chemistry, 42(3), 523–528. https://doi.org/10.1080/00021369.1978.10863014

Hara, H., Abe, N., Nakakouji, M., Nishimura, Y., & Horiuchi, K. (**1996**). Overproduction of penicillin-binding protein 7 suppresses thermosensitive growth defect at low osmolarity due to an spr mutation of *Escherichia coli*. Microbial Drug Resistance (Larchmont, N.Y.), 2(1), 63–72. https://doi.org/10.1089/mdr.1996.2.63

Hatch, T. P. (**1996**). Disulfide cross-linked envelope proteins: the functional equivalent of peptidoglycan in chlamydiae? Journal of Bacteriology, 178(1), 1–5. https://doi.org/10.1128/jb.178.1.1-5.1996

Heine, H., Gronow, S., Zamyatina, A., Kosma, P., & Brade, H. (**2007**). Investigation on the agonistic and antagonistic biological activities of synthetic *Chlamydia* lipid A and its use in in vitro enzymatic assays. Journal of Endotoxin Research, 13(2), 126–132. https://doi.org/10.1177/0968051907079122

Henrichfreise, B., Schiefer, A., Schneider, T., Nzukou, E., Poellinger, C., Hoffmann, T.-J., … Sahl, H. G. (**2009**). Functional conservation of the lipid II biosynthesis pathway in the cell wall-less bacteria *Chlamydia* and *Wolbachia*: why is lipid II needed? Molecular Microbiology, 73(5), 913–923. https://doi.org/10.1111/j.1365-2958.2009.06815.x

Henrichfreise, B., Brunke, M., & Viollier, P. H. (**2016**). Bacterial Surfaces: The Wall that SEDS Built. Current Biology : CB, 26(21), R1158–R1160. https://doi.org/10.1016/j.cub.2016.09.028

Hervé, M., Boniface, A., Gobec, S., Blanot, D., & Mengin-Lecreulx, D. (**2007**). Biochemical characterization and physiological properties of *Escherichia coli* UDP-N-acetylmuramate:L-alanyl-gamma-D-glutamyl-meso-diaminopimelate ligase. Journal of Bacteriology, 189(11), 3987–3995. https://doi.org/10.1128/JB.00087-07

Herweg, J.-A., **& Rudel**, T. (**2016**). Interaction of *Chlamydiae* with human macrophages. The FEBS Journal, 283(4), 608–618. https://doi.org/10.1111/febs.13609

Hesse, L., Bostock, J., Dementin, S., Blanot, D., Mengin-Lecreulx, D., & Chopra, I. (**2003**). Functional and biochemical analysis of *Chlamydia trachomatis* MurC, an enzyme displaying UDP-N-acetylmuramate:amino acid ligase activity. Journal of Bacteriology, 185(22), 6507–6512. https://doi.org/10.1128/JB.185.22.6507-6512.2003

Hogan, R. J., Mathews, S. A., Mukhopadhyay, S., Summersgill, J. T., & Timms, P. (**2004**). Chlamydial persistence: beyond the biphasic paradigm. Infection and Immunity, 72(4), 1843–1855. https://doi.org/10.1128/IAI.72.4.1843-1855.2004

Höltje, J. V. (**1998**). Growth of the stress-bearing and shape-maintaining murein sacculus of *Escherichia coli*. Microbiology and Molecular Biology Reviews : MMBR, 62(1), 181–203. https://doi.org/10.1128/MMBR.62.1.181-203.1998

Horn, M. (**2008**). Chlamydiae as symbionts in eukaryotes. Annual Review of Microbiology, 62, 113–131. https://doi.org/10.1146/annurev.micro.62.081307.162818

Hotzel, H., Grossmann, E., Mutschmann, F., & Sachse, K. (**2001**). Genetic characterization of a *Chlamydophila pneumoniae* isolate from an African frog and comparison to currently accepted biovars. Systematic and Applied Microbiology, 24(1), 63–66. https://doi.org/10.1078/0723-2020-00016

Hu, Z., van Alen, T., Jetten, M. S. M., & Kartal, B. (**2013**). Lysozyme and penicillin inhibit the growth of anaerobic ammonium-oxidizing planctomycetes. Applied and Environmental Microbiology, 79(24), 7763–7769. https://doi.org/10.1128/AEM.02467-13

Huang, Y. J., **& Boushey**, H. A. (**2015**). The microbiome in asthma. The Journal of Allergy and Clinical Immunology, 135(1), 25–30. https://doi.org/10.1016/j.jaci.2014.11.011

Humann, J., & **Lenz**, L. L. (**2009**). Bacterial peptidoglycan degrading enzymes and their impact on host muropeptide detection. Journal of Innate Immunity, 1(2), 88–97. https://doi.org/10.1159/000181181

Hybiske, K., **& Stephens**, R. S. (**2007**). Mechanisms of host cell exit by the intracellular bacterium *Chlamydia*. Proceedings of the National Academy of Sciences of the United States of America, 104(27), 11430–11435. https://doi.org/10.1073/pnas.0703218104

Ikeda, M., Wachi, M., Jung, H. K., Ishino, F., & Matsuhashi, M. (**1991**). The *Escherichia coli mraY* gene encoding UDP-N-acetylmuramoyl-pentapeptide: undecaprenyl-phosphate phospho-N-acetylmuramoyl-pentapeptide transferase. Journal of Bacteriology, 173(3), 1021–1026. https://doi.org/10.1128/jb.173.3.1021-1026.1991

Ingalls, R. R., Rice, P. A., Qureshi, N., Takayama, K., Lin, J. S., & Golenbock, D. T. (**1995**). The inflammatory cytokine response to *Chlamydia trachomatis* infection is endotoxin mediated. Infection and Immunity, 63(8), 3125–3130. https://doi.org/10.1128/iai.63.8.3125-3130.1995

Inohara, N., Ogura, Y., Fontalba, A., Gutierrez, O., Pons, F., Crespo, J., … Nuñez, G. (**2003**). Host recognition of bacterial muramyl dipeptide mediated through NOD2. Implications for Crohn's disease. The Journal of Biological Chemistry, 278(8), 5509–5512. https://doi.org/10.1074/jbc.C200673200

Jacquier, N., Frandi, A., Pillonel, T., Viollier, P. H., & Greub, G. (**2014**). Cell wall precursors are required to organize the chlamydial division septum. Nature Communications, 5, 3578. https://doi.org/10.1038/ncomms4578

Jacquier, N., Frandi, A., Viollier, P. H., & Greub, G. (**2015a**). Disassembly of a medial transenvelope structure by antibiotics during intracellular division. Chemistry & Biology, 22(9), 1217–1227. https://doi.org/https://doi.org/10.1016/j.chembiol.2015.08.009

Jacquier, N., Viollier, P. H., & Greub, G. (**2015b**). The role of peptidoglycan in chlamydial cell division: towards resolving the chlamydial anomaly. FEMS Microbiology Reviews, 39(2), 262–275. https://doi.org/10.1093/femsre/fuv001

Jacquier, N., Yadav, A. K., Pillonel, T., Viollier, P. H., Cava, F., & Greub, G. (**2019**). A SpoIID homolog cleaves glycan strands at the chlamydial division septum. MBio, 10(4), e01128-19. https://doi.org/10.1128/mBio.01128-19

Jeske, O., Schüler, M., Schumann, P., Schneider, A., Boedeker, C., Jogler, M., … Jogler, C. (**2015**). *Planctomycetes* do possess a peptidoglycan cell wall. Nature Communications, 6, 7116. https://doi.org/10.1038/ncomms8116

Jones, L. J., Carballido-López, R., & Errington, J. (**2001**). Control of cell shape in bacteria: helical, actin-like filaments in *Bacillus subtilis*. Cell, 104(6), 913–922. https://doi.org/10.1016/s0092-8674(01)00287-2

Kahane, S., Dvoskin, B., Mathias, M., & Friedman, M. G. (**2001**). Infection of *Acanthamoeba polyphaga* with *Simkania negevensis* and *S. negevensis* survival within amoebal cysts. Applied and Environmental Microbiology, 67(10), 4789–4795. https://doi.org/10.1128/AEM.67.10.4789-4795.2001

Kalia, N., Singh, J., & Kaur, M. (**2020**). Microbiota in vaginal health and pathogenesis of recurrent vulvovaginal infections: a critical review. Annals of Clinical Microbiology and Antimicrobials, 19(1), 5. https://doi.org/10.1186/s12941-020-0347-4

Kalman, S., Mitchell, W., Marathe, R., Lammel, C., Fan, J., Hyman, R. W., … Stephens, R. S. (**1999**). Comparative genomes of *Chlamydia pneumonia*e and *C. trachomatis*. Nature Genetics, 21(4), 385–389. https://doi.org/10.1038/7716

Kamneva, O. K., Knight, S. J., Liberles, D. A., & Ward, N. L. (**2012**). Analysis of genome content evolution in PVC bacterial super-phylum: assessment of candidate genes associated with cellular organization and lifestyle. Genome Biology and Evolution, 4(12), 1375–1390. https://doi.org/10.1093/gbe/evs113

Kanehisa, M., **& Goto**, S. (**2000**). KEGG: kyoto encyclopedia of genes and genomes. Nucleic Acids Research, 28(1), 27–30. https://doi.org/10.1093/nar/28.1.27

Kelley, L. A., Mezulis, S., Yates, C. M., Wass, M. N., & Sternberg, M. J. E. (**2015**). The Phyre2 web portal for protein modeling, prediction and analysis. Nature Protocols, 10(6), 845–858. https://doi.org/10.1038/nprot.2015.053

Kemege, K. E., Hickey, J. M., Barta, M. L., Wickstrum, J., Balwalli, N., Lovell, S., … Hefty, P. S. (**2015**). *Chlamydia trachomatis* protein CT009 is a structural and functional homolog to the key morphogenesis component RodZ and interacts with division septal plane localized MreB. Molecular Microbiology, 95(3), 365–382. https://doi.org/10.1111/mmi.12855

Kim, H., Kwak, W., Yoon, S. H., Kang, D.-K., & Kim, H. (**2018**). Horizontal gene transfer of *Chlamydia*: Novel insights from tree reconciliation. PloS One, 13(4), e0195139–e0195139. https://doi.org/10.1371/journal.pone.0195139

Kintner, J., Lajoie, D., Hall, J., Whittimore, J., & Schoborg, R. V. (**2014**). Commonly prescribed β-lactam antibiotics induce *C. trachomatis* persistence/stress in culture at physiologically relevant concentrations. Frontiers in Cellular and Infection Microbiology, 4, 44. https://doi.org/10.3389/fcimb.2014.00044

Klöckner, A., Otten, C., Derouaux, A., Vollmer, W., Bühl, H., De Benedetti, S., … Henrichfreise, B. (**2014**). AmiA is a penicillin target enzyme with dual activity in the intracellular pathogen *Chlamydia pneumoniae*. Nature Communications, 5, 4201. https://doi.org/10.1038/ncomms5201

Klöckner, A. (**2016**). Chlamydiae as non-model organisms to study antibiotic activity-evolutionary, cellular and molecular aspects. PhD Thesis. University Bonn.

Klöckner, A., Bühl, H., Viollier, P., & Henrichfreise, B. (**2018**). Deconstructing the Chlamydial Cell Wall. Current Topics in Microbiology and Immunology, 412, 1–33. https://doi.org/10.1007/82_2016_34

Knittler, M. R., **& Sachse**, K. (**2015**). *Chlamydia psittaci*: update on an underestimated zoonotic agent. Pathogens and Disease, 73(1), 1–15. https://doi.org/10.1093/femspd/ftu007

Koo, I. C., **& Stephens**, R. S. (**2003**). A developmentally regulated two-component signal transduction system in *Chlamydia*. The Journal of Biological Chemistry, 278(19), 17314–17319. https://doi.org/10.1074/jbc.M212170200

Korenromp, E. L., Sudaryo, M. K., de Vlas, S. J., Gray, R. H., Sewankambo, N. K., Serwadda, D., … Habbema, J. D. F. (**2002**). What proportion of episodes of gonorrhoea and chlamydia becomes symptomatic? International Journal of STD & AIDS, 13(2), 91–101. https://doi.org/10.1258/0956462021924712

Korndörfer, I. P., Danzer, J., Schmelcher, M., Zimmer, M., Skerra, A., & Loessner, M. J. (**2006**). The crystal structure of the bacteriophage PSA endolysin reveals a unique fold responsible for specific recognition of Listeria cell walls. Journal of Molecular Biology, 364(4), 678–689. https://doi.org/10.1016/j.jmb.2006.08.069

Kosma, P. (**1999**). Chlamydial lipopolysaccharide. Biochimica et Biophysica Acta, 1455(2–3), 387–402. https://doi.org/10.1016/s0925-4439(99)00061-7

Köstlbacher, S., Collingro, A., Halter, T., Schulz, F., Jungbluth, S. P., & Horn, M. (**2021**). Pangenomics reveals alternative environmental lifestyles among chlamydiae. Nature Communications, 12(1), 4021. https://doi.org/10.1038/s41467-021-24294-3

Krogh, A., Larsson, B., von Heijne, G., & Sonnhammer, E. L. (**2001**). Predicting transmembrane protein topology with a hidden Markov model: application to complete genomes. Journal of Molecular Biology, 305(3), 567–580. https://doi.org/10.1006/jmbi.2000.4315

Kuhn, M., **& Goebel**, W. (**1989**). Identification of an extracellular protein of *Listeria monocytogenes* possibly involved in intracellular uptake by mammalian cells. Infection and Immunity, 57(1), 55–61. https://doi.org/10.1128/iai.57.1.55-61.1989

Laemmli, U. K. (**1970**). Cleavage of structural proteins during the assembly of the head of bacteriophage T4. Nature, 227(5259), 680–685. https://doi.org/10.1038/227680a0

Lagkouvardos, I., Weinmaier, T., Lauro, F. M., Cavicchioli, R., Rattei, T., & Horn, M. (**2014**). Integrating metagenomic and amplicon databases to resolve the phylogenetic and ecological diversity of the *Chlamydiae*. The ISME Journal, 8(1), 115–125. https://doi.org/10.1038/ismej.2013.142

Lambden, P. R., Pickett, M. A., & Clarke, I. N. (**2006**). The effect of penicillin on *Chlamydia trachomatis* DNA replication. Microbiology (Reading, England), 152(Pt 9), 2573–2578. https://doi.org/10.1099/mic.0.29032-0

Lamoth, F., Jaton, K., Vaudaux, B., & Greub, G. (**2011**). *Parachlamydia* and *Rhabdochlamydia*: emerging agents of community-acquired respiratory infections in children. Clinical Infectious Diseases : An Official Publication of the Infectious Diseases Society of America. United States. https://doi.org/10.1093/cid/cir420

Last, A., Versteeg, B., Shafi Abdurahman, O., Robinson, A., Dumessa, G., Abraham Aga, M., … Burton, M. J. (**2020**). Detecting extra-ocular *Chlamydia trachomatis* in a trachoma-endemic community in Ethiopia: Identifying potential routes of transmission. PLOS Neglected Tropical Diseases, 14(3), 1–16. https://doi.org/10.1371/journal.pntd.0008120

Leaver, M., Domínguez-Cuevas, P., Coxhead, J. M., Daniel, R. A., & Errington, J. (**2009**). Life without a wall or division machine in *Bacillus subtilis*. Nature, 457(7231), 849–853. https://doi.org/10.1038/nature07742

Lee, J., Cox, J. V, & Ouellette, S. P. (**2020**). Critical Role for the Extended N Terminus of Chlamydial MreB in Directing Its Membrane Association and Potential Interaction with Divisome Proteins. Journal of Bacteriology, 202(9). https://doi.org/10.1128/JB.00034-20

Lefoulon, E., Bain, O., Makepeace, B. L., d'Haese, C., Uni, S., Martin, C., & Gavotte, L. (**2016**). Breakdown of coevolution between symbiotic bacteria *Wolbachia* and their filarial hosts. PeerJ, 4, e1840–e1840. https://doi.org/10.7717/peerj.1840

Lenz, J. D., Stohl, E. A., Robertson, R. M., Hackett, K. T., Fisher, K., Xiong, K., … Dillard, J. P. (**2016**). Amidase activity of AmiC controls cell separation and stem peptide release and is enhanced by NlpD in *Neisseria gonorrhoeae*. The Journal of Biological Chemistry, 291(20), 10916–10933. https://doi.org/10.1074/jbc.M116.715573

Liechti, G. W., Kuru, E., Hall, E., Kalinda, A., Brun, Y. V, VanNieuwenhze, M., & Maurelli, A. T. (**2014**). A new metabolic cell-wall labelling method reveals peptidoglycan in *Chlamydia trachomatis*. Nature, 506(7489), 507–510. https://doi.org/10.1038/nature12892

Liechti, G., Kuru, E., Packiam, M., Hsu, Y.-P., Tekkam, S., Hall, E., … Maurelli, A. T. (**2016**). Pathogenic *Chlamydia* lack a classical sacculus but synthesize a narrow, mid-cell peptidoglycan ring, regulated by MreB, for cell division. PLoS Pathogens, 12(5), e1005590. https://doi.org/10.1371/journal.ppat.1005590

Liechti, G., Singh, R., Rossi, P. L., Gray, M. D., Adams, N. E., & Maurelli, A. T. (**2018**). *Chlamydia trachomatis dapF* encodes a bifunctional enzyme capable of both D-glutamate racemase and diaminopimelate epimerase activities. MBio, 9(2), e00204-18. https://doi.org/10.1128/mBio.00204-18

Liechti, G. W. (**2021**). Localized peptidoglycan biosynthesis in *Chlamydia trachomatis* conforms to the polarized division and cell size reduction developmental models. Frontiers in Microbiology, 12, 733850. https://doi.org/10.3389/fmicb.2021.733850

Lienard, J., Croxatto, A., Prod'hom, G., & Greub, G. (**2011**). *Estrella lausannensis*, a new star in the *Chlamydiales* order. Microbes and Infection, 13(14–15), 1232–1241. https://doi.org/10.1016/j.micinf.2011.07.003

Losick, R., **& Stragier**, P. (**1992**). Crisscross regulation of cell-type-specific gene expression during development in *B. subtilis*. Nature, 355(6361), 601–604. https://doi.org/10.1038/355601a0

Lupoli, T. J., Taniguchi, T., Wang, T.-S., Perlstein, D. L., Walker, S., & Kahne, D. E. (**2009**). Studying a cell division amidase using defined peptidoglycan substrates. Journal of the American Chemical Society, 131(51), 18230–18231. https://doi.org/10.1021/ja908916z

Madeira, F., Pearce, M., Tivey, A. R. N., Basutkar, P., Lee, J., Edbali, O., … Lopez, R. (**2022**). Search and sequence analysis tools services from EMBL-EBI in 2022. Nucleic Acids Research, gkac240. https://doi.org/10.1093/nar/gkac240

Malhotra, M., Sood, S., Mukherjee, A., Muralidhar, S., & Bala, M. (**2013**). Genital *Chlamydia trachomatis*: an update. The Indian Journal of Medical Research, 138(3), 303–316. Retrieved from https://pubmed.ncbi.nlm.nih.gov/24135174

Mann, P. A., Müller, A., Wolff, K. A., Fischmann, T., Wang, H., Reed, P., … Roemer, T. (**2016**). Chemical genetic analysis and functional characterization of Staphylococcal wall teichoic acid 2-Epimerases reveals unconventional antibiotic drug targets. PLoS Pathogens, 12(5), e1005585. https://doi.org/10.1371/journal.ppat.1005585

Maqbool, A., Levdikov, V. M., Blagova, E. V, Hervé, M., Horler, R. S. P., Wilkinson, A. J., & Thomas, G. H. (**2011**). Compensating stereochemical changes allow murein tripeptide to be accommodated in a conventional peptide-binding protein*. Journal of Biological Chemistry, 286(36), 31512–31521. https://doi.org/https://doi.org/10.1074/jbc.M111.267179

Margot, P., Wahlen, M., Gholamhoseinian, A., Piggot, P., & Karamata, D. (**1998**). The *lytE* gene of *Bacillus subtilis* 168 encodes a cell wall hydrolase. Journal of Bacteriology, 180(3), 749–752. https://doi.org/10.1128/JB.180.3.749-752.1998

Mathiopoulos, C., Mueller, J. P., Slack, F. J., Murphy, C. G., Patankar, S., Bukusoglu, G., & Sonenshein, A. L. (**1991**). A *Bacillus subtilis* dipeptide transport

system expressed early during sporulation. Molecular Microbiology, 5(8), 1903–1913. https://doi.org/10.1111/j.1365-2958.1991.tb00814.x

Matsumoto, A., **& Manire**, G. P. (**1970**). Electron microscopic observations on the effects of penicillin on the morphology of *Chlamydia psittaci*. Journal of Bacteriology, 101(1), 278–285. https://doi.org/10.1128/jb.101.1.278-285.1970

Matsumoto, K., Mizoue, K., Kitamura, K., Tse, W. C., Huber, C. P., & Ishida, T. (**1999**). Structural basis of inhibition of cysteine proteases by E-64 and its derivatives. Biopolymers, 51(1), 99–107. https://doi.org/10.1002/(SICI)1097-0282(1999)51:1<99::AID-BIP11>3.0.CO;2-R

Matthiesen, S., von Rüden, U., Dekker, A., Briken, P., Cerwenka, S., Fedorowicz, C., & Wiessner, C. (**2021**). How good is the knowledge about sexually transmitted infections in Germany?: Results of the first nationwide representative German health and sexuality survey (GeSiD). Bundesgesundheitsblatt - Gesundheitsforschung - Gesundheitsschutz, 64(11), 1355–1363. https://doi.org/10.1007/s00103-021-03319-8

McCoy, A. J., Adams, N. E., Hudson, A. O., Gilvarg, C., Leustek, T., & Maurelli, A. T. (**2006**). L,L-diaminopimelate aminotransferase, a trans-kingdom enzyme shared by *Chlamydia* and plants for synthesis of diaminopimelate/lysine. Proceedings of the National Academy of Sciences of the United States of America, 103(47), 17909–17914. https://doi.org/10.1073/pnas.0608643103

McCoy, A. J., & Maurelli, A. T. (**2005**). Characterization of *Chlamydia* MurC-Ddl, a fusion protein exhibiting D-alanyl-D-alanine ligase activity involved in peptidoglycan synthesis and D-cycloserine sensitivity. Molecular Microbiology, 57(1), 41–52. https://doi.org/10.1111/j.1365-2958.2005.04661.x

McCoy, A. J., Sandlin, R. C., & Maurelli, A. T. (**2003**). *In vitro* and *in vivo* functional activity of *Chlamydia* MurA, a UDP-N-acetylglucosamine enolpyruvyl transferase involved in peptidoglycan synthesis and fosfomycin resistance. Journal of Bacteriology, 185(4), 1218–1228. https://doi.org/10.1128/JB.185.4.1218-1228.2003

McDonald, L. A., Barbieri, L. R., Carter, G. T., Lenoy, E., Lotvin, J., Petersen, P. J., … Williamson, R. T. (**2002**). Structures of the muraymycins, novel peptidoglycan biosynthesis inhibitors. Journal of the American Chemical Society, 124(35), 10260–10261. https://doi.org/10.1021/ja017748h

Meeske, A. J., Riley, E. P., Robins, W. P., Uehara, T., Mekalanos, J. J., Kahne, D., … Rudner, D. Z. (**2016**). SEDS proteins are a widespread family of bacterial cell wall polymerases. Nature, 537(7622), 634–638. https://doi.org/10.1038/nature19331

Mehlitz, A., Eylert, E., Huber, C., Lindner, B., Vollmuth, N., Karunakaran, K., … Rudel, T. (**2017**). Metabolic adaptation of *Chlamydia trachomatis* to mammalian host cells. Molecular Microbiology, 103(6), 1004–1019. https://doi.org/10.1111/mmi.13603

Mengin-Lecreulx, D., van Heijenoort, J., & Park, J. T. (**1996**). Identification of the *mpl* gene encoding UDP-N-acetylmuramate: L-alanyl-gamma-D-glutamyl-meso-diaminopimelate ligase in *Escherichia coli* and its role in recycling of cell wall peptidoglycan. Journal of Bacteriology, 178(18), 5347–5352. https://doi.org/10.1128/jb.178.18.5347-5352.1996

Menon, S., Timms, P., Allan, J. A., Alexander, K., Rombauts, L., Horner, P., … Huston, W. M. (**2015**). Human and pathogen factors associated with *Chlamydia trachomatis*-related infertility in women. Clinical Microbiology Reviews, 28(4), 969–985. https://doi.org/10.1128/CMR.00035-15

Miller, J. H. (**1972**). Experiments in Molecular Genetics. Cold Spring Harbor Laboratory, Cold Spring Harbor, N.Y.

Miura, K., Inouye, S., Sakai, K., Takaoka, H., Kishi, F., Tabuchi, M., … Nakazawa, A. (**2001**). Cloning and characterization of adenylate kinase from *Chlamydia pneumoniae*. The Journal of Biological Chemistry, 276(16), 13490–13498. https://doi.org/10.1074/jbc.M009461200

Molle, V., Nakaura, Y., Shivers, R. P., Yamaguchi, H., Losick, R., Fujita, Y., & Sonenshein, A. L. (**2003**). Additional targets of the Bacillus subtilis global regulator CodY identified by chromatin immunoprecipitation and genome-wide transcript analysis. Journal of Bacteriology, 185(6), 1911–1922. https://doi.org/10.1128/JB.185.6.1911-1922.2003

Morgenstein, R. M., Bratton, B. P., Nguyen, J. P., Ouzounov, N., Shaevitz, J. W., & Gitai, Z. (**2015**). RodZ links MreB to cell wall synthesis to mediate MreB rotation and robust morphogenesis. Proceedings of the National Academy of Sciences of the United States of America, 112(40), 12510–12515. https://doi.org/10.1073/pnas.1509610112

Morlot, C., Uehara, T., Marquis, K. A., Bernhardt, T. G., & Rudner, D. Z. (**2010**). A highly coordinated cell wall degradation machine governs spore morphogenesis in *Bacillus subtilis*. Genes & Development, 24(4), 411–422. https://doi.org/10.1101/gad.1878110

Moulder, J. W., Novosel, D. L., & Officer, J. E. (**1963**). Inhibition of the growth of agents of the *Psittacosis* group by D-cycloserine and its specific reversal by D-alanine. Journal of Bacteriology, 85(3), 707–711. https://doi.org/10.1128/jb.85.3.707-711.1963

Moulder, J. W. (**1966**). The relation of the psittacosis group (*Chlamydiae*) to bacteria and viruses. Annual Review of Microbiology, 20, 107–130. https://doi.org/10.1146/annurev.mi.20.100166.000543

Moulder, J. W. (**1991**). Interaction of chlamydiae and host cells in vitro. Microbiological Reviews, 55(1), 143–190. https://doi.org/10.1128/mr.55.1.143-190.1991

Moulder, J. W. (**1993**). Why is Chlamydia sensitive to penicillin in the absence of peptidoglycan? Infectious Agents and Disease, 2(2), 87–99.

Mueller, E. A., Iken, A. G., Ali Öztürk, M., Winkle, M., Schmitz, M., Vollmer, W., … Levin, P. A. (**2021**). The active repertoire of *Escherichia coli* peptidoglycan amidases varies with physiochemical environment. Molecular Microbiology, 116(1), 311–328. https://doi.org/10.1111/mmi.14711

Mullis, K., Faloona, F., Scharf, S., Saiki, R., Horn, G., & Erlich, H. (**1986**). Specific enzymatic amplification of DNA *in vitro*: the polymerase chain reaction. Cold Spring

Harbor Symposia on Quantitative Biology, 51 Pt 1, 263–273. https://doi.org/10.1101/sqb.1986.051.01.032

Newhall, W. J. (**1987**). Biosynthesis and disulfide cross-linking of outer membrane components during the growth cycle of *Chlamydia trachomatis*. Infection and Immunity, 55(1), 162–168. https://doi.org/10.1128/iai.55.1.162-168.1987

Neyen, C., **& Lemaitre**, B. (**2016**). Sensing Gram-negative bacteria: a phylogenetic perspective. Current Opinion in Immunology, 38, 8–17. https://doi.org/10.1016/j.coi.2015.10.007

Nicholson, T. L., Olinger, L., Chong, K., Schoolnik, G., & Stephens, R. S. (**2003**). Global stage-specific gene regulation during the developmental cycle of *Chlamydia trachomatis*. Journal of Bacteriology, 185(10), 3179–3189. https://doi.org/10.1128/JB.185.10.3179-3189.2003

Nielsen, H. (**2017**). Predicting secretory proteins with SignalP. Methods in Molecular Biology (Clifton, N.J.), 1611, 59–73. https://doi.org/10.1007/978-1-4939-7015-5_6

Ohnishi, R., Ishikawa, S., & Sekiguchi, J. (**1999**). Peptidoglycan hydrolase LytF plays a role in cell separation with CwlF during vegetative growth of *Bacillus subtilis*. Journal of Bacteriology, 181(10), 3178–3184. https://doi.org/10.1128/JB.181.10.3178-3184.1999

Omsland, A., Sixt, B. S., Horn, M., & Hackstadt, T. (**2014**). Chlamydial metabolism revisited: interspecies metabolic variability and developmental stage-specific physiologic activities. FEMS Microbiology Reviews, 38(4), 779–801. https://doi.org/10.1111/1574-6976.12059

Osaka, I., **& Hefty**, P. S. (**2013**). Simple resazurin-based microplate assay for measuring *Chlamydia* infections. Antimicrobial Agents and Chemotherapy, 57(6), 2838–2840. https://doi.org/10.1128/AAC.00056-13

Oshida, T., Sugai, M., Komatsuzawa, H., Hong, Y. M., Suginaka, H., & Tomasz, A. (**1995**). A *Staphylococcus aureus* autolysin that has an N-acetylmuramoyl-L-alanine amidase domain and an endo-beta-N-acetylglucosaminidase domain: cloning, sequence analysis, and characterization. Proceedings of the National Academy of Sciences of the United States of America, 92(1), 285–289. https://doi.org/10.1073/pnas.92.1.285

Otten, C., De Benedetti, S., Gaballah, A., Bühl, H., Klöckner, A., Brauner, J., … Henrichfreise, B. (**2015**). Co-solvents as stabilizing agents during heterologous overexpression in *Escherichia coli* - application to chlamydial penicillin-binding protein 6. PloS One, 10(4), e0122110–e0122110. https://doi.org/10.1371/journal.pone.0122110

Otten, C., Brilli, M., Vollmer, W., Viollier, P. H., & Salje, J. (**2018**). Peptidoglycan in obligate intracellular bacteria. Molecular Microbiology, 107(2), 142–163. https://doi.org/10.1111/mmi.13880

Ouellette, S. P., Karimova, G., Subtil, A., & Ladant, D. (**2012**). *Chlamydia* co-opts the rod shape-determining proteins MreB and Pbp2 for cell division. Molecular Microbiology, 85(1), 164–178. https://doi.org/10.1111/j.1365-2958.2012.08100.x

Ouellette, S. P., Rueden, K. J., Gauliard, E., Persons, L., de Boer, P. A., & Ladant, D. (**2014**). Analysis of MreB interactors in *Chlamydia* reveals a RodZ homolog but fails to detect an interaction with MraY. Frontiers in Microbiology, 5, 279. https://doi.org/10.3389/fmicb.2014.00279

Ouellette, S. P., Lee, J., & Cox, J. V. (**2020**). Division without Binary Fission: Cell Division in the FtsZ-Less *Chlamydia*. Journal of Bacteriology, 202(17). https://doi.org/10.1128/JB.00252-20

Packiam, M., Weinrick, B., Jacobs Jr, W. R., & Maurelli, A. T. (**2015**). Structural characterization of muropeptides from *Chlamydia trachomatis* peptidoglycan by mass spectrometry resolves “chlamydial anomaly.” Proceedings of the National Academy of Sciences of the United States of America, 112(37), 11660–11665. https://doi.org/10.1073/pnas.1514026112

Panzetta, M. E., Valdivia, R. H., & Saka, H. A. (**2018**). *Chlamydia* Persistence: A survival strategy to evade antimicrobial effects *in-vitro* and *in-vivo*. Frontiers in Microbiology, 9, 3101. https://doi.org/10.3389/fmicb.2018.03101

Park, J. T. (**1993**). Turnover and recycling of the murein sacculus in oligopeptide permease-negative strains of *Escherichia coli*: indirect evidence for an alternative permease system and for a monolayered sacculus. Journal of Bacteriology, 175(1), 7–11. https://doi.org/10.1128/jb.175.1.7-11.1993

Park, J. T. (**1995**). Why does *Escherichia coli* recycle its cell wall peptides? Molecular Microbiology, 17(3), 421–426. https://doi.org/10.1111/j.1365-2958.1995.mmi_17030421.x

Park, J. T., Raychaudhuri, D., Li, H., Normark, S., & Mengin-Lecreulx, D. (**1998**). MppA, a periplasmic binding protein essential for import of the bacterial cell wall peptide L-alanyl-gamma-D-glutamyl-meso-diaminopimelate. Journal of Bacteriology, 180(5), 1215–1223. https://doi.org/10.1128/JB.180.5.1215-1223.1998

Park, J. T., **& Uehara**, T. (**2008**). How bacteria consume their own exoskeletons (turnover and recycling of cell wall peptidoglycan). Microbiology and Molecular Biology Reviews : MMBR, 72(2), 211–227, table of contents. https://doi.org/10.1128/MMBR.00027-07

Patin, D., Bostock, J., Blanot, D., Mengin-Lecreulx, D., & Chopra, I. (**2009**). Functional and biochemical analysis of the *Chlamydia trachomatis* ligase MurE. Journal of Bacteriology, 191(24), 7430–7435. https://doi.org/10.1128/JB.01029-09

Patin, D., Bostock, J., Chopra, I., Mengin-Lecreulx, D., & Blanot, D. (**2012**). Biochemical characterisation of the chlamydial MurF ligase, and possible sequence of the chlamydial peptidoglycan pentapeptide stem. Archives of Microbiology, 194(6), 505–512. https://doi.org/10.1007/s00203-011-0784-8

Peters, N. T., Dinh, T., & Bernhardt, T. G. (**2011**). A fail-safe mechanism in the septal ring assembly pathway generated by the sequential recruitment of cell separation amidases and their activators. Journal of Bacteriology, 193(18), 4973–4983. https://doi.org/10.1128/JB.00316-11

Peters, N. T., Morlot, C., Yang, D. C., Uehara, T., Vernet, T., & Bernhardt, T. G. (**2013**). Structure-function analysis of the LytM domain of EnvC, an activator of cell wall remodelling at the *Escherichia coli* division site. Molecular Microbiology, 89(4), 690–701. https://doi.org/10.1111/mmi.12304

Pettersen, E. F., Goddard, T. D., Huang, C. C., Couch, G. S., Greenblatt, D. M., Meng, E. C., & Ferrin, T. E. (**2004**). UCSF Chimera--a visualization system for exploratory research and analysis. Journal of Computational Chemistry, 25(13), 1605–1612. https://doi.org/10.1002/jcc.20084

Phillips-Campbell, R., Kintner, J., & Schoborg, R. V. (**2014**). Induction of the *Chlamydia muridarum* stress/persistence response increases azithromycin treatment failure in a murine model of infection. Antimicrobial Agents and Chemotherapy, 58(3), 1782–1784. https://doi.org/10.1128/AAC.02097-13

Pilhofer, M., Rappl, K., Eckl, C., Bauer, A. P., Ludwig, W., Schleifer, K.-H., & Petroni, G. (**2008**). Characterization and evolution of cell division and cell wall synthesis genes in the bacterial phyla *Verrucomicrobia*, *Lentisphaerae*, *Chlamydiae*, and *Planctomycetes* and phylogenetic comparison with rRNA genes. Journal of Bacteriology, 190(9), 3192–3202. https://doi.org/10.1128/JB.01797-07

Pilhofer, M., Aistleitner, K., Biboy, J., Gray, J., Kuru, E., Hall, E., … Jensen, G. J. (**2013**). Discovery of chlamydial peptidoglycan reveals bacteria with murein sacculi but without FtsZ. Nature Communications, 4, 2856. https://doi.org/10.1038/ncomms3856

Pillai, B., Cherney, M. M., Diaper, C. M., Sutherland, A., Blanchard, J. S., Vederas, J. C., & James, M. N. G. (**2006**). Structural insights into stereochemical inversion by diaminopimelate epimerase: an antibacterial drug target. Proceedings of the National Academy of Sciences of the United States of America, 103(23), 8668–8673. https://doi.org/10.1073/pnas.0602537103

Pinheiro, J., Biboy, J., Vollmer, W., Hirt, R. P., Keown, J. R., Artuyants, A., … Simoes-Barbosa, A. (**2018**). The protozoan *Trichomonas vaginalis* targets bacteria with laterally acquired NlpC/P60 peptidoglycan hydrolases. MBio, 9(6). https://doi.org/10.1128/mBio.01784-18

Pospischil, A., Borel, N., Chowdhury, E. H., & Guscetti, F. (**2009**). Aberrant chlamydial developmental forms in the gastrointestinal tract of pigs spontaneously and experimentally infected with *Chlamydia suis*. Veterinary Microbiology, 135(1–2), 147–156. https://doi.org/10.1016/j.vetmic.2008.09.035

Price, N. P. J., & Tsvetanova, B. (**2007**). Biosynthesis of the tunicamycins: a review. The Journal of Antibiotics, 60(8), 485–491. https://doi.org/10.1038/ja.2007.62

Price, M. J., Ades, A. E., De Angelis, D., Welton, N. J., Macleod, J., Soldan, K., … Horner, P. J. (**2013**). Risk of pelvic inflammatory disease following *Chlamydia trachomatis* infection: analysis of prospective studies with a multistate model. American Journal of Epidemiology, 178(3), 484–492. https://doi.org/10.1093/aje/kws583

Raetz, C. R. H., Reynolds, C. M., Trent, M. S., & Bishop, R. E. (**2007**). Lipid A modification systems in gram-negative bacteria. Annual Review of Biochemistry, 76, 295–329. https://doi.org/10.1146/annurev.biochem.76.010307.145803

Rajeeve, K., Vollmuth, N., Janaki-Raman, S., Wulff, T. F., Baluapuri, A., Dejure, F. R., … Rudel, T. (**2020**). Reprogramming of host glutamine metabolism during *Chlamydia trachomatis* infection and its key role in peptidoglycan synthesis. Nature Microbiology, 5(11), 1390–1402. https://doi.org/10.1038/s41564-020-0762-5

Ranjit, D. K., Liechti, G. W., & Maurelli, A. T. (**2020**). Chlamydial MreB directs cell division and peptidoglycan synthesis in *Escherichia coli* in the absence of FtsZ activity. MBio, 11(1), e03222-19. https://doi.org/10.1128/mBio.03222-19

Rick, P. D., Hubbard, G. L., Kitaoka, M., Nagaki, H., Kinoshita, T., Dowd, S., … Ho, C. (**1998**). Characterization of the lipid-carrier involved in the synthesis of enterobacterial common antigen (ECA) and identification of a novel phosphoglyceride in a mutant of *Salmonella typhimurium* defective in ECA synthesis. Glycobiology, 8(6), 557–567. https://doi.org/10.1093/glycob/8.6.557

Rigden, D. J., Jedrzejas, M. J., & Galperin, M. Y. (**2003**). Amidase domains from bacterial and phage autolysins define a family of gamma-D,L-glutamate-specific amidohydrolases. Trends in Biochemical Sciences, 28(5), 230–234. https://doi.org/10.1016/s0968-0004(03)00062-8

Riley, M., Abe, T., Arnaud, M. B., Berlyn, M. K. B., Blattner, F. R., Chaudhuri, R. R., … Wanner, B. L. (**2006**). *Escherichia coli* K-12: a cooperatively developed annotation snapshot--2005. Nucleic Acids Research, 34(1), 1–9. https://doi.org/10.1093/nar/gkj405

Rivas-Marín, E., **& Devos**, D. P. (**2018**). The Paradigms They Are a-Changin': past, present and future of PVC bacteria research. Antonie van Leeuwenhoek, 111(6), 785–799. https://doi.org/10.1007/s10482-017-0962-z

Rocaboy, M., Herman, R., Sauvage, E., Remaut, H., Moonens, K., Terrak, M., … Kerff, F. (**2013**). The crystal structure of the cell division amidase AmiC reveals the fold of the AMIN domain, a new peptidoglycan binding domain. Molecular Microbiology, 90(2), 267–277. https://doi.org/10.1111/mmi.12361

Rours, G. I. J. G., Duijts, L., Moll, H. A., Arends, L. R., de Groot, R., Jaddoe, V. W., … Verbrugh, H. A. (**2011**). *Chlamydia trachomatis* infection during pregnancy associated with preterm delivery: a population-based prospective cohort study. European Journal of Epidemiology, 26(6), 493–502. https://doi.org/10.1007/s10654-011-9586-1

Rowley, J., Vander Hoorn, S., Korenromp, E., Low, N., Unemo, M., Abu-Raddad, L. J., … Taylor, M. M. (**2019**). Chlamydia, gonorrhoea, trichomoniasis and syphilis: global prevalence and incidence estimates, 2016. Bulletin of the World Health Organization, 97(8), 548-562P. https://doi.org/10.2471/BLT.18.228486

Ruggiero, A., Marasco, D., Squeglia, F., Soldini, S., Pedone, E., Pedone, C., & Berisio, R. (**2010**). Structure and functional regulation of RipA, a mycobacterial

enzyme essential for daughter cell separation. Structure (London, England : 1993), 18(9), 1184–1190. https://doi.org/10.1016/j.str.2010.06.007

Rund, S., Lindner, B., Brade, H., & Holst, O. (**1999**). Structural analysis of the lipopolysaccharide from *Chlamydia trachomatis* serotype L2. The Journal of Biological Chemistry, 274(24), 16819–16824. https://doi.org/10.1074/jbc.274.24.16819

Savaris, R. F., Fuhrich, D. G., Duarte, R. V, Franik, S., & Ross, J. (**2017**). Antibiotic therapy for pelvic inflammatory disease. The Cochrane Database of Systematic Reviews, 4(4), CD010285. https://doi.org/10.1002/14651858.CD010285.pub2

Scheffers, D.-J., **& Pinho**, M. G. (**2005**). Bacterial cell wall synthesis: new insights from localization studies. Microbiology and Molecular Biology Reviews : MMBR, 69(4), 585–607. https://doi.org/10.1128/MMBR.69.4.585-607.2005

Scherler, A., Jacquier, N., Kebbi-Beghdadi, C., & Greub, G. (**2020**). Diverse stress-inducing treatments cause distinct aberrant body morphologies in the *Chlamydia*-related bacterium, *Waddlia chondrophila*. Microorganisms, 8(1), 89. https://doi.org/10.3390/microorganisms8010089

Schilit, S. L. P. (**2019**). Recent advances and future opportunities to diagnose male infertility. Current Sexual Health Reports, 11(4), 331–341. https://doi.org/10.1007/s11930-019-00225-8

Schleifer, K. H., **& Kandler**, O. (**1972**). Peptidoglycan types of bacterial cell walls and their taxonomic implications. Bacteriological Reviews, 36(4), 407–477. https://doi.org/10.1128/br.36.4.407-477.1972

Schmidt, D. M., Hubbard, B. K., & Gerlt, J. A. (**2001**). Evolution of enzymatic activities in the enolase superfamily: functional assignment of unknown proteins in *Bacillus subtilis* and *Escherichia coli* as L-Ala-D/L-Glu epimerases. Biochemistry, 40(51), 15707–15715. https://doi.org/10.1021/bi011640x

Schmidt, K. L., Peterson, N. D., Kustusch, R. J., Wissel, M. C., Graham, B., Phillips, G. J., & Weiss, D. S. (**2004**). A predicted ABC transporter, FtsEX, is needed for cell division in *Escherichia coli.* Journal of Bacteriology, 186(3), 785–793. https://doi.org/10.1128/JB.186.3.785-793.2004

Schneider, T., Gries, K., Josten, M., Wiedemann, I., Pelzer, S., Labischinski, H., & Sahl, H.-G. (**2009**). The lipopeptide antibiotic Friulimicin B inhibits cell wall biosynthesis through complex formation with bactoprenol phosphate. Antimicrobial Agents and Chemotherapy, 53(4), 1610–1618. https://doi.org/10.1128/AAC.01040-08

Schuurman-Wolters, G. K., **& Poolman**, B. (**2005**). Substrate specificity and ionic regulation of GlnPQ from *Lactococcus lactis*. An ATP-binding cassette transporter with four extracytoplasmic substrate-binding domains. The Journal of Biological Chemistry, 280(25), 23785–23790. https://doi.org/10.1074/jbc.M500522200

Schwöppe, C., Winkler, H. H., & Neuhaus, H. E. (**2002**). Properties of the glucose-6-phosphate transporter from *Chlamydia pneumoniae* (HPTcp) and the glucose-6-phosphate sensor from *Escherichia coli* (UhpC). Journal of Bacteriology, 184(8), 2108–2115. https://doi.org/10.1128/JB.184.8.2108-2115.2002

Sham, L.-T., Butler, E. K., Lebar, M. D., Kahne, D., Bernhardt, T. G., & Ruiz, N. (**2014**). Bacterial cell wall. MurJ is the flippase of lipid-linked precursors for peptidoglycan biogenesis. Science (New York, N.Y.), 345(6193), 220–222. https://doi.org/10.1126/science.1254522

Shimada, K., Chen, S., Dempsey, P. W., Sorrentino, R., Alsabeh, R., Slepenkin, A. V, … Arditi, M. (**2009**). The NOD/RIP2 pathway is essential for host defenses against *Chlamydophila pneumoniae* lung infection. PLoS Pathogens, 5(4), e1000379. https://doi.org/10.1371/journal.ppat.1000379

Shimada, T., Yamazaki, K., & Ishihama, A. (**2013**). Novel regulator PgrR for switch control of peptidoglycan recycling in *Escherichia coli*. Genes to Cells: Devoted to Molecular & Cellular Mechanisms, 18(2), 123–134. https://doi.org/10.1111/gtc.12026

Sievers, F., Wilm, A., Dineen, D., Gibson, T. J., Karplus, K., Li, W., … Higgins, D. G. (**2011**). Fast, scalable generation of high-quality protein multiple sequence alignments using Clustal Omega. Molecular Systems Biology, 7, 539. https://doi.org/10.1038/msb.2011.75

Singh, S. K., SaiSree, L., Amrutha, R. N., & Reddy, M. (**2012**). Three redundant murein endopeptidases catalyse an essential cleavage step in peptidoglycan synthesis of *Escherichia coli* K12. Molecular Microbiology, 86(5), 1036–1051. https://doi.org/10.1111/mmi.12058

Singh, S. K., Parveen, S., SaiSree, L., & Reddy, M. (**2015**). Regulated proteolysis of a cross-link-specific peptidoglycan hydrolase contributes to bacterial morphogenesis. Proceedings of the National Academy of Sciences of the United States of America, 112(35), 10956–10961. https://doi.org/10.1073/pnas.1507760112

Singh, R., Liechti, G., Slade, J. A., & Maurelli, A. T. (**2020**). *Chlamydia trachomatis* oligopeptide transporter performs dual functions of oligopeptide transport and peptidoglycan recycling. Infection and Immunity, 88(5), e00086-20. https://doi.org/10.1128/IAI.00086-20

Skaletz-Rorowski, A., Potthoff, A., Nambiar, S., Wach, J., Kayser, A., Kasper, A., & Brockmeyer, N. H. (**2021**). Sexual behaviour, STI knowledge and *Chlamydia trachomatis* (CT) and *Neisseria gonorrhoeae* (NG) prevalence in an asymptomatic cohort in Ruhr-area, Germany: PreYoungGo study. Journal of the European Academy of Dermatology and Venereology : JEADV, 35(1), 241–246. https://doi.org/10.1111/jdv.16913

Skilton, R. J., Cutcliffen, L. T., Barlow, D., Wang, Y., Salim, O., Lambden, P. R., & Clarke, I. N. (**2009**). Penicillin induced persistence in *Chlamydia trachomatis:* high quality time lapse video analysis of the developmental cycle. PloS One, 4(11), e7723–e7723. https://doi.org/10.1371/journal.pone.0007723

Skipp, P., Robinson, J., O'Connor, C. D., & Clarke, I. N. (**2005**). Shotgun proteomic analysis of *Chlamydia trachomatis*. Proteomics, 5(6), 1558–1573. https://doi.org/10.1002/pmic.200401044

Slade, J. A., Brockett, M., Singh, R., Liechti, G. W., & Maurelli, A. T. (**2019**). Fosmidomycin, an inhibitor of isoprenoid synthesis, induces persistence in

Chlamydia by inhibiting peptidoglycan assembly. PLoS Pathogens, 15(10), e1008078. https://doi.org/10.1371/journal.ppat.1008078

Smith, T. J., & Foster, S. J. (**1995**). Characterization of the involvement of two compensatory autolysins in mother cell lysis during sporulation of *Bacillus subtilis* 168. Journal of Bacteriology, 177(13), 3855–3862. https://doi.org/10.1128/jb.177.13.3855-3862.1995

Smith, T. J., Blackman, S. A., & Foster, S. J. (**2000**). Autolysins of *Bacillus subtilis*: multiple enzymes with multiple functions. Microbiology (Reading, England), 146 (Pt 2, 249–262. https://doi.org/10.1099/00221287-146-2-249

Stamm, W. E. (**1999**). *Chlamydia trachomatis* infections: progress and problems. The Journal of Infectious Diseases, 179 Suppl, S380-3. https://doi.org/10.1086/513844

Stephens, R. S., Kalman, S., Lammel, C., Fan, J., Marathe, R., Aravind, L., … Davis, R. W. (**1998**). Genome sequence of an obligate intracellular pathogen of humans: *Chlamydia trachomatis*. Science (New York, N.Y.), 282(5389), 754–759. https://doi.org/10.1126/science.282.5389.754

Stock, C., Guillén-Grima, F., Prüfer-Krämer, L., Serrano-Monzo, I., Marin-Fernandez, B., Aguinaga-Ontoso, I., & Krämer, A. (**2001**). Sexual behavior and the prevalence of *Chlamydia trachomatis* infection in asymptomatic students in Germany and Spain. European Journal of Epidemiology, 17(4), 385–390. https://doi.org/10.1023/a:1012713813161

Storey, C., **& Chopra**, I. (**2001**). Affinities of beta-lactams for penicillin binding proteins of *Chlamydia trachomatis* and their antichlamydial activities. Antimicrobial Agents and Chemotherapy, 45(1), 303–305. https://doi.org/10.1128/AAC.45.1.303-305.2001

Studier, F. W. (**2005**). Protein production by auto-induction in high density shaking cultures. Protein Expression and Purification, 41(1), 207–234. https://doi.org/10.1016/j.pep.2005.01.016

Subtil, A., Collingro, A., & Horn, M. (**2014**). Tracing the primordial *Chlamydiae*: extinct parasites of plants ? Trends in Plant Science, 19(1), 36–43. https://doi.org/10.1016/j.tplants.2013.10.005

Suchland, R. J., Geisler, W. M., & Stamm, W. E. (**2003**). Methodologies and cell lines used for antimicrobial susceptibility testing of *Chlamydia* spp. Antimicrobial Agents and Chemotherapy, 47(2), 636–642. https://doi.org/10.1128/AAC.47.2.636-642.2003

Suchland, R. J., Dimond, Z. E., Putman, T. E., & Rockey, D. D. (**2017**). Demonstration of persistent infections and genome stability by whole-genome sequencing of repeat-positive, same-serovar *Chlamydia trachomatis* collected from the female genital tract. The Journal of Infectious Diseases, 215(11), 1657–1665. https://doi.org/10.1093/infdis/jix155

Suchland, R. J., Carrell, S. J., Wang, Y., Hybiske, K., Kim, D. B., Dimond, Z. E., … Rockey, D. D. (**2019**). Chromosomal recombination targets in *Chlamydia* interspecies lateral gene transfer. Journal of Bacteriology, 201(23). https://doi.org/10.1128/JB.00365-19

Sukhithasri, V., Nisha, N., Biswas, L., Anil Kumar, V., & Biswas, R. (**2013**). Innate immune recognition of microbial cell wall components and microbial strategies to evade such recognitions. Microbiological Research, 168(7), 396–406. https://doi.org/10.1016/j.micres.2013.02.005

Sweet, C. R., Lin, S., Cotter, R. J., & Raetz, C. R. (**2001**). A *Chlamydia trachomatis* UDP-N-acetylglucosamine acyltransferase selective for myristoyl-acyl carrier protein. Expression in *Escherichia coli* and formation of hybrid lipid A species. The Journal of Biological Chemistry, 276(22), 19565–19574. https://doi.org/10.1074/jbc.M101868200

Taguchi, A., Welsh, M. A., Marmont, L. S., Lee, W., Sjodt, M., Kruse, A. C., … Walker, S. (**2019**). FtsW is a peptidoglycan polymerase that is functional only in complex with its cognate penicillin-binding protein. Nature Microbiology, 4(4), 587–594. https://doi.org/10.1038/s41564-018-0345-x

Tamura, A., **& Manire**, G. P. (**1968**). Effect of penicillin on the multiplication of meningopneumonitis organisms (*Chlamydia psittaci*). Journal of Bacteriology, 96(4), 875–880. https://doi.org/10.1128/jb.96.4.875-880.1968

Tanino, T., Al-Dabbagh, B., Mengin-Lecreulx, D., Bouhss, A., Oyama, H., Ichikawa, S., & Matsuda, A. (**2011**). Mechanistic analysis of muraymycin analogues: a guide to the design of MraY inhibitors. Journal of Medicinal Chemistry, 54(24), 8421–8439. https://doi.org/10.1021/jm200906r

Tartoff, K. D., **& Hobbs**, C. A. (**1987**). Improved Media for Growing Plasmid and Cosmid Clones. Bethesda Research Laboratories Focus, 9(12).

Taylor-Brown, A., Vaughan, L., Greub, G., Timms, P., & Polkinghorne, A. (**2015**). Twenty years of research into *Chlamydia*-like organisms: a revolution in our understanding of the biology and pathogenicity of members of the phylum Chlamydiae. Pathogens and Disease, 73(1), 1–15. https://doi.org/10.1093/femspd/ftu009

Taylor-Brown, A., Madden, D., & Polkinghorne, A. (**2018**). Culture-independent approaches to chlamydial genomics. Microbial Genomics, 4(2), e000145. https://doi.org/10.1099/mgen.0.000145

Tekniepe, B. L., Schmidt, J. M., & Starr, P. (**1981**). Life cycle of a budding and appendaged bacterium belonging to morphotype IV of the *Blastocaulis-Planctomyces* group. Current Microbiology, 5(1), 1–6. https://doi.org/10.1007/BF01566588

Thomas, V., Casson, N., & Greub, G. (**2006**). *Criblamydia sequanensis*, a new intracellular *Chlamydiales* isolated from Seine river water using amoebal co-culture. Environmental Microbiology, 8(12), 2125–2135. https://doi.org/10.1111/j.1462-2920.2006.01094.x

Turner, K. A., Rambhatla, A., Schon, S., Agarwal, A., Krawetz, S. A., Dupree, J. M., & Avidor-Reiss, T. (**2020**). Male infertility is a women's health issue - Research and clinical evaluation of male infertility is needed. Cells, 9(4). https://doi.org/10.3390/cells9040990

Uehara, T., **& Bernhardt**, T. G. (**2011**). More than just lysins: peptidoglycan hydrolases tailor the cell wall. Current Opinion in Microbiology, 14(6), 698–703. https://doi.org/10.1016/j.mib.2011.10.003

Uehara, T., Dinh, T., & Bernhardt, T. G. (**2009**). LytM-domain factors are required for daughter cell separation and rapid ampicillin-induced lysis in *Escherichia coli.* Journal of Bacteriology, 191(16), 5094–5107. https://doi.org/10.1128/JB.00505-09

Uehara, T., **& Park**, J. T. (**2003**). Identification of MpaA, an amidase in *Escherichia coli* that hydrolyzes the gamma-D-glutamyl-meso-diaminopimelate bond in murein peptides. Journal of Bacteriology, 185(2), 679–682. https://doi.org/10.1128/JB.185.2.679-682.2003

Uehara, T., Parzych, K. R., Dinh, T., & Bernhardt, T. G. (**2010**). Daughter cell separation is controlled by cytokinetic ring-activated cell wall hydrolysis. The EMBO Journal, 29(8), 1412–1422. https://doi.org/10.1038/emboj.2010.36

Vacheron, M., Guinand, M., Françon, A., & Michel, G. (**1979**). Characterisation of a new endopeptidase from sporulating *Bacillus sphaericus* which is specific for the y-D-Glutamyl-L-lysine and y-D-Glutamyl-(L)meso-diaminopimelate linkages of peptidoglycan substrates. European Journal of Biochemistry, 100(1), 189–196. https://doi.org/10.1111/j.1432-1033.1979.tb02048.x

van Heijenoort, J. (**2001**). Recent advances in the formation of the bacterial peptidoglycan monomer unit. Natural Product Reports, 18(5), 503–519. https://doi.org/10.1039/a804532a

van Niftrik, L., & Devos, D. P. (**2017**). Editorial: *Planctomycetes-Verrucomicrobia-Chlamydiae* Bacterial Superphylum: New model organisms for evolutionary cell biology. Frontiers in Microbiology. https://doi.org/10.3389/fmicb.2017.01458

van Teeseling, M. C. F., Mesman, R. J., Kuru, E., Espaillat, A., Cava, F., Brun, Y. V, … van Niftrik, L. (**2015**). Anammox *Planctomycetes* have a peptidoglycan cell wall. Nature Communications, 6, 6878. https://doi.org/10.1038/ncomms7878

Viala, J., Chaput, C., Boneca, I. G., Cardona, A., Girardin, S. E., Moran, A. P., … Ferrero, R. L. (**2004**). Nod1 responds to peptidoglycan delivered by the *Helicobacter pylori cag* pathogenicity island. Nature Immunology, 5(11), 1166–1174. https://doi.org/10.1038/ni1131

Vollmer, W., Blanot, D., & de Pedro, M. A. (**2008a**). Peptidoglycan structure and architecture. FEMS Microbiology Reviews, 32(2), 149–167. https://doi.org/10.1111/j.1574-6976.2007.00094.x

Vollmer, W., Joris, B., Charlier, P., & Foster, S. (**2008b**). Bacterial peptidoglycan (murein) hydrolases. FEMS Microbiology Reviews, 32(2), 259–286. https://doi.org/10.1111/j.1574-6976.2007.00099.x

Von Prowazek, S., & **Halberstädter**, L. (**1907**). Zur Aetiologie des Trachoms. DMW - Deutsche Medizinische Wochenschrift, 33(32), 1285–1287. https://doi.org/10.1055/s-0029-1188920

Vouga, M., Baud, D., & Greub, G. (**2017a**). *Simkania negevensis* may produce long-lasting infections in human pneumocytes and endometrial cells. Pathogens and Disease, 75(1). https://doi.org/10.1093/femspd/ftw115

Vouga, M., Baud, D., & Greub, G. (**2017b**). *Simkania negevensis*, an example of the diversity of the antimicrobial susceptibility pattern among *Chlamydiales*. Antimicrobial Agents and Chemotherapy, 61(8). https://doi.org/10.1128/AAC.00638-17

Wagner, M., **& Horn**, M. (**2006**). The *Planctomycetes*, *Verrucomicrobia*, *Chlamydiae* and sister phyla comprise a superphylum with biotechnological and medical relevance. Current Opinion in Biotechnology, 17(3), 241–249. https://doi.org/10.1016/j.copbio.2006.05.005

Wagner, S., Klepsch, M. M., Schlegel, S., Appel, A., Draheim, R., Tarry, M., … de Gier, J.-W. (**2008**). Tuning *Escherichia coli* for membrane protein overexpression. Proceedings of the National Academy of Sciences of the United States of America, 105(38), 14371–14376. https://doi.org/10.1073/pnas.0804090105

Walter, A., Friz, S., & Mayer, C. (**2021**). Chitin, chitin oligosaccharide, and chitin disaccharide metabolism of *Escherichia coli* revisited: Reassignment of the roles of ChiA, ChbR, ChbF, and ChbG. Microbial Physiology, 31(2), 178–194. https://doi.org/10.1159/000515178

Wang, Z.-M., Li, X., Cocklin, R. R., Wang, M., Wang, M., Fukase, K., … Dziarski, R. (**2003**). Human peptidoglycan recognition protein-L is an N-acetylmuramoyl-L-alanine amidase. The Journal of Biological Chemistry, 278(49), 49044–49052. https://doi.org/10.1074/jbc.M307758200

Wardrop, S., Fowler, A., O'Callaghan, P., Giffard, P., & Timms, P. (**1999**). Characterization of the koala biovar of *Chlamydia pneumoniae* at four gene loci--*ompAVD4*, *ompB,* 16S rRNA, *groESL* spacer region. Systematic and Applied Microbiology, 22(1), 22–27. https://doi.org/10.1016/S0723-2020(99)80024-1

Weatherspoon-Griffin, N., Zhao, G., Kong, W., Kong, Y., Morigen, Andrews-Polymenis, H., … Shi, Y. (**2011**). The CpxR/CpxA two-component system up-regulates two Tat-dependent peptidoglycan amidases to confer bacterial resistance to antimicrobial peptide. The Journal of Biological Chemistry, 286(7), 5529–5539. https://doi.org/10.1074/jbc.M110.200352

Webley, W. C., & Hahn, D. L. (**2017**). Infection-mediated asthma: etiology, mechanisms and treatment options, with focus on *Chlamydia pneumoniae* and macrolides. Respiratory Research, 18(1), 98. https://doi.org/10.1186/s12931-017-0584-z

Weiss, D. S. (**2004**). Bacterial cell division and the septal ring. Molecular Microbiology, 54(3), 588–597. https://doi.org/10.1111/j.1365-2958.2004.04283.x

Wiesenfeld, H. C., Hillier, S. L., Meyn, L. A., Amortegui, A. J., & Sweet, R. L. (**2012**). Subclinical pelvic inflammatory disease and infertility. Obstetrics and Gynecology, 120(1), 37–43. https://doi.org/10.1097/AOG.0b013e31825a6bc9

Wilmes, M., Meier, K., Schiefer, A., Josten, M., Otten, C. F., Klöckner, A., … Pfarr, K. (**2017**). AmiD Is a novel peptidoglycan amidase in *Wolbachia* endosymbionts of

Drosophila melanogaster. Frontiers in Cellular and Infection Microbiology, 7, 353. https://doi.org/10.3389/fcimb.2017.00353

Wolf, A. J., **& Underhill**, D. M. (**2018**). Peptidoglycan recognition by the innate immune system. Nature Reviews. Immunology, 18(4), 243–254. https://doi.org/10.1038/nri.2017.136

Workowski, K. A., Bachmann, L. H., Chan, P. A., Johnston, C. M., Muzny, C. A., Park, I., … Bolan, G. A. (**2021**). Sexually transmitted infections treatment guidelines, 2021. MMWR. Recommendations and reports : Morbidity and mortality weekly report. Recommendations and reports (Vol. 70). https://doi.org/10.15585/mmwr.rr7004a1

World Health Organization. (**2020**). WHO alliance for the global elimination of trachoma by 2020: progress report, 2019. Weekly Epidemiological Record, 95(30), 349–360. Retrieved from https://pesquisa.bvsalud.org/portal/resource/en/mdl-20203426091

Xia, Q., Wang, T., Xian, J., Song, J., Qiao, Y., Mu, Z., … Sun, Z. (**2020**). Relation of *Chlamydia trachomatis* infections to ectopic pregnancy: A meta-analysis and systematic review. Medicine, 99(1), e18489–e18489. https://doi.org/10.1097/MD.0000000000018489

Xu, Q., Abdubek, P., Astakhova, T., Axelrod, H. L., Bakolitsa, C., Cai, X., … Wilson, I. A. (**2010**). Structure of the γ-D-glutamyl-L-diamino acid endopeptidase YkfC from *Bacillus cereus* in complex with L-Ala-γ-D-Glu: insights into substrate recognition by NlpC/P60 cysteine peptidases. Acta Crystallographica. Section F, Structural Biology and Crystallization Communications, 66(Pt 10), 1354–1364. https://doi.org/10.1107/S1744309110021214

Xu, Q., Chiu, H.-J., Farr, C. L., Jaroszewski, L., Knuth, M. W., Miller, M. D., … Wilson, I. A. (**2014**). Structures of a bifunctional cell wall hydrolase CwlT containing a novel bacterial lysozyme and an NlpC/P60 DL-endopeptidase. Journal of Molecular Biology, 426(1), 169–184. https://doi.org/10.1016/j.jmb.2013.09.011

Xu, Q., Mengin-Lecreulx, D., Liu, X. W., Patin, D., Farr, C. L., Grant, J. C., … Wilson, I. A. (**2015**). Insights into substrate specificity of NlpC/P60 cell wall hydrolases containing bacterial SH3 domains. MBio, 6(5), e02327. https://doi.org/10.1128/mBio.02327-14

Xu, Q., Sudek, S., McMullan, D., Miller, M. D., Geierstanger, B., Jones, D. H., … Wilson, I. A. (**2009**). Structural basis of murein peptide specificity of a gamma-D-glutamyl-l-diamino acid endopeptidase. Structure (London, England : 1993), 17(2), 303–313. https://doi.org/10.1016/j.str.2008.12.008

Yakhnina, A. A., McManus, H. R., & Bernhardt, T. G. (**2015**). The cell wall amidase AmiB is essential for *Pseudomonas aeruginosa* cell division, drug resistance and viability. Molecular Microbiology, 97(5), 957–973. https://doi.org/10.1111/mmi.13077

Yamashita, A., Norton, E., Petersen, P. J., Rasmussen, B. A., Singh, G., Yang, Y., … Ho, D. M. (**2003**). Muraymycins, novel peptidoglycan biosynthesis inhibitors: synthesis and SAR of their analogues. Bioorganic & Medicinal Chemistry Letters, 13(19), 3345–3350. https://doi.org/10.1016/s0960-894x(03)00671-1

Yang, D. C., Peters, N. T., Parzych, K. R., Uehara, T., Markovski, M., & Bernhardt, T. G. (**2011**). An ATP-binding cassette transporter-like complex governs cell-wall hydrolysis at the bacterial cytokinetic ring. Proceedings of the National Academy of Sciences of the United States of America, 108(45), E1052-60. https://doi.org/10.1073/pnas.1107780108

Yang, D. C., Tan, K., Joachimiak, A., & Bernhardt, T. G. (**2012**). A conformational switch controls cell wall-remodelling enzymes required for bacterial cell division. Molecular Microbiology, 85(4), 768–781. https://doi.org/10.1111/j.1365-2958.2012.08138.x

Yang, C., Briones, M., Chiou, J., Lei, L., Patton, M. J., Ma, L., … Caldwell, H. D. (**2019**). *Chlamydia trachomatis* lipopolysaccharide evades the canonical and noncanonical inflammatory pathways to subvert innate immunity. MBio, 10(2). https://doi.org/10.1128/mBio.00595-19

Yeruva, L., Spencer, N., Bowlin, A. K., Wang, Y., & Rank, R. G. (**2013**). Chlamydial infection of the gastrointestinal tract: a reservoir for persistent infection. Pathogens and Disease, 68(3), 88–95. https://doi.org/10.1111/2049-632X.12052eee

Danksagung

Zuallererst meinen herzlichen Dank an Prof. Dr. Tanja Schneider für die Aufnahme in ihre Arbeitsgruppe, die fachliche Betreuung meiner Doktorarbeit, die langjährige gute Zusammenarbeit und den wertvollen wissenschaftlichen Austausch.

Mein besonderer Dank gilt den Mitgliedern meiner Promotionskommission, Priv.-Doz. Dr. Christiane Dahl, Prof. Dr. Lukas Schreiber und Prof. Dr. Ulrich Kubitscheck, für ihre Zeit und ihr Interesse an meiner Arbeit. Priv.-Doz. Dr. Christiane Dahl möchte ich zudem dafür danken, dass sie während meiner Bachelorarbeit meine Begeisterung für die Mikrobiologie geweckt hat.

Ich bedanke mich herzlich bei Dr. Beate Henrichfreise dafür, dass sie während der gesamten Zeit meiner Promotion jederzeit ein offenes Ohr für meine Fragen hatte und bereit war, mich mit ihren Ideen, ihrem Wissen und ihrem Enthusiasmus für das Thema zu unterstützen und voranzubringen.

Ich danke unseren Kooperationspartnern, Prof. Dr. Christoph Mayer und Robert Kluj, Prof. Dr. Gilbert Greub, Dr. Nicolas Jacquier und Sébastien Aeby, Prof. Dr. Scot Ouellette und Dr. Junghoon Lee, Prof. Dr. Dominique Mengin-Lecreulx sowie Prof. Dr. Waldemar Vollmer und Dr. Federico Corona für die engagierte Zusammenarbeit und die freundliche Unterstützung beim YkfC Projekt.

Der AG von Prof. Dr. Satoshi Ichikawa danke ich für die Bereitstellung von Muraymycin und Caprazamycin Derivaten und der AG von Priv.-Doz. Dr. Sabine Amslinger für die Bereitstellung der α-X-Chalkone.

Ebenso danke ich der AG von Prof. Dr. Johannes Hegemann für die Bereitstellung der genomischen DNA von *C. pneumoniae.*

Ich danke der Jürgen-Manchot-Stiftung für das Promotionsstipendium, welches mir den Abschluss meiner wissenschaftlichen Ausbildung ermöglicht hat.

Ich danke der gesamten AG Schneider, den „Chlamydien“ und den „Staphylokokken“. Besonderen Dank an Henrike Bühl, Anna Klöckner und Christian Otten, von denen ich so viel im Labor lernen konnte und an Sebastian Krannich, Iris Löckener und Julia Dannenberg. Vielen lieben Dank, Julia Deisinger, Thomas Franke, Fabian Grein, Stefania De Benedetti, Anna Müller, Marvin Rausch, Kevin Ludwig, Nils Jelden, Benjamin Winnerling, Melina Arts, Vanessa Becker, Lisa Fritz, Jan-Samuel Puls, Claudia Wagner, Isabel Bodenstein und Prof Dr. Hans-Georg Sahl!

Vielen Dank auch an alle AGs des IfmBs und an die AG Bierbaum für die gute Zusammenarbeit und die Bereitschaft jederzeit Wissen und Geräten zu teilen.

Vielen lieben Dank an Melanie Brunke für ihre Hilfe und alle wertvollen Diskussionen.

Zu guter Letzt meinen riesengroßen Dank an meine Freund*innen und Familie, die mich während dieser Arbeit unterstützt und ermutigt haben. Danke an Chris, Miri, Corinna, Lene, Lea, Frida, die Mimis und die Vargas-Alschers.

Tausend Dank vor allem an Melli, Julia, Malin, Kristin, Uwe und Jonathan - ohne euch wäre diese Arbeit nicht möglich gewesen.